The Anatomy, Taxonomy and Systematics of Middle Triassic–Early Jurassic Ichthyosaurs (Reptilia: Ichthyopterygia) and the Phylogeny of Ichthyopterygia

Andrzej Stefan Wolniewicz

St Edmund Hall

Department of Earth Sciences

University of Oxford

A thesis submitted for the degree of

Doctor of Philosophy

Trinity 2017

DECLARATION

This dissertation is the result of my own work and includes nothing which is the outcome of work done in collaboration except where specifically stated in the text.

Andrzej Stefan Wolniewicz

ACKNOWLEDGEMENTS

First and foremost, I thank my supervisor, Roger Benson, for giving me the opportunity to pursue a doctoral degree under his guidance. His feedback has greatly improved the thoroughness of my research and the clarity of my reasoning and written work. Apart from his invaluable help in developing my research skills, Roger also provided support during the difficult moments of my DPhil studies and encouraged me to always try to give my best, no matter how hard life got, so that the potential he saw in me would not go to waste. For all his advice, help and support I am eternally grateful.

My doctoral studies were supported by a Natural Environment Research Council studentship (NE/L50/530/1). In addition, I have also received Postgraduate College Grants and a Graduate Writing-Up Grant from St Edmund Hall and the Doris O. and Samuel P. Welles Research Grant from the UCMP.

The successful completion of this doctoral thesis would not have been possible if it were not for the assistance of numerous curators, researchers and staff members in museums and institutions worldwide, who provided access to specimens in their care. I thank Bill Simpson (FMNH), Sandra Chapman (NHMUK), Christian Klug (PIMUZ), Kevin Seymour, Brian Iwama and Ian Morrison (ROM), Brandon Strilisky (TMP) and Pat Holroyd (UCMP), for providing access and information on fossil specimens which were the primary focus of this thesis. I also thank Da-yong Jiang and Zuo-yu Sun (GMPKU), Qinghua Shang (IVPP), Sali Underwood (NSM), Eliza Howlett and Hilary Ketchum (OUMNH), Erin Maxwell (SMNS) and Long Cheng (SPCV) for providing access to additional comparative material cited in this thesis.

For discussions on ichthyosaur anatomy, systematics and phylogeny and for sharing information on unpublished fossil specimens, I thank Ryosuke Motani, Don Brinkman, Donald Henderson, Valentin Fischer, Nadia Fröbisch, Neil Kelley, Erin Maxwell, Martin Sander and Lars Schmitz. I also thank my examiners, Erin Saupe and Richard Butler, for their constructive feedback, which significantly improved the quality of my thesis.

The palaeontological community at the University of Oxford is also thanked for their continued assistance and support throughout my DPhil studies. I particularly thank Matt Friedman, John Clarke,

Sam Giles and Laura Soul for their advice and support during the first few months of my doctoral studies; Serjoischa Evers, David Ford and James Neenan for help and numerous fruitful discussions over a beer; and Gemma Benevento, César Espinoza-Campuzano, David Legg and Felipe de la Parra for their friendship. I also thank members of the entire student community at the Department of Earth Sciences, especially Tyler Ambrose, Joshua Combs, Sean Hopkins, †Danielle Kondla, Tom Lamont, Lawrence Percival, Marisa Storm, Tim Sweere and Owen Weller, for their help, support and numerous shared moments.

Many people have given me hospitality during my trips abroad. In particular I thank Kentaro Chiba, Kirstin Brink, Thomas Cullen, Derek Larson, Mateusz Wosik and other members of the Department of Paleontology at the ROM, who made me feel like a member of their own research group every time I visited. I also thank Matteo Fabbri, Guillermo Navalón and Jasmina Wiemann for their company during the Society of Vertebrate Paleontology Annual Meetings. I also thank members of the Polish palaeontological community, namely Tomasz Sulej, Grzegorz Niedźwiedzki, Mateusz Tałanda and Łukasz Czepiński for inviting me to participate in their fieldwork, numerous fruitful discussions and plenty of fun at student conferences in Poland.

I also thank my friends from the Polish community at the University of Oxford, namely Krzysztof Bar, Marcin Bieliński, Tomasz Dobrzycki, Maciej Marówka, Przemysław Pobrotyn and Michał Przykucki for their friendship, support and numerous, long and meaningful conversations in our mother tongue. I also thank people I have met at the Oxford University Catholic Chaplaincy, especially Claudia Azevedo and Fr. Keith McMillan, for their friendship and support. Grzegorz Lorek and the entire community of Secondary Grammar School no 1 in Leszno are thanked for their continued support during my time at Oxford.

I thank my parents, Maria and Stefan, and my sister Katarzyna for their love and unconditional support throughout my DPhil studies. Finally, thanks go to Katarzyna Nowak, whose love and support have made it a lot easier for me to cope with the stresses of the academic and non-academic sides of my doctoral studies and for making especially the last few months of my Oxford experience more exciting than ever.

ABSTRACT

Ichthyosaurs were a successful group of Mesozoic marine reptiles spanning a time interval of nearly 160 million years, from the Early Triassic to the early Late Cretaceous. Although ichthyosaurs have a long history of research, dating back to the early 18th century, significant controversies still surround their anatomy, taxonomy and evolution.

The revision of the cranial anatomy of the basal ichthyosaur *Cymbospondylus* from the Middle Triassic (Anisian) resolves a 100-year controversy surrounding the arrangement its skull bones. Comparisons with the recently discovered colossal, predatory ichthyosaur *Thalattoarchon* result in the identification of shared synapomorphies, which provide evidence for a close relationship between the two taxa. Together with other, recent discoveries from China, this demonstrates the rapid ecomorphological diversification of ichthyosaurs in the early Middle Triassic.

The incompletely sampled Late Triassic marine fossil record hinders our understanding of ichthyosaur evolution across the Triassic-Jurassic boundary. A new genus and species of large-bodied, early parvipelvian (fish-shaped) ichthyosaur from the Late Triassic (upper Norian) of British Columbia, Canada, is described. The new taxon is characterized by the possession of labiolingually flattened, bicarinate tooth crowns. Its co-occurrence with other small- to medium-sized parvipelvians, representing different ecomorphologies, demonstrates that parvipelvian ichthyosaurs were already ecomorphologically diverse at the beginning of their evolutionary history and maintained high ecological diversity throughout the Late Triassic.

The ichthyosaur diversity of the Lower Jurassic (Hettangian–Pliensbachian) of the United Kingdom is still poorly understood, due to the lack of detailed studies of ichthyosaur anatomy. Here, I describe a new genus and species of ichthyosaur, defined by the possession of five autapomorphies and a unique combination of both plesiomorphic and derived characters. Phylogenetic analysis recovers the new taxon as an early-diverging parvipelvian, providing evidence of a temporally staggered, rather than catastrophic, ichthyosaur turnover at the Triassic-Jurassic boundary.

EXTENDED ABSTRACT

Ichthyosaurs (Reptilia: Ichthyopterygia) were a diverse clade of Mesozoic marine reptiles spanning nearly 160 million years, from the Early Triassic to the early Late Cretaceous. Ichthyosaurs possessed distinct skeletal, sensory and locomotory adaptations and provide an excellent opportunity to study the pattern and process of morphological evolution in a long-lived, secondarily aquatic tetrapod clade. Because ichthyosaur evolution was influenced by sea level change and climate fluctuations, they also provide an excellent example of how changes in the Earth's system shape evolutionary pathways. However, despite having a long history of research, dating back to the early 18th century, significant gaps in our understanding of ichthyosaur anatomy, taxonomy and phylogeny still exist.

Cymbospondylus is an iconic ichthyosaur genus that provides valuable information on the anatomy of basal members of the clade. Well preserved material of *Cymbospondylus*, including complete and partially complete skulls, has been known for over a century from the Middle Triassic of Nevada, USA and southern Switzerland. However, there is still a lack of consensus regarding the cranial anatomy of *Cymbospondylus*, with different authors presenting markedly different interpretations of the circumorbital, temporal and skull roof regions. This lack of consensus hinders our understanding of early ichthyosaur evolution and obscures character polarity at the base of the ichthyopterygian phylogenetic tree. First hand examination of all well-preserved skull material referred to *Cymbospondylus* worldwide clarifies previous controversies surrounding its cranial anatomy (Chapter 4). Important identified anatomical characters include: a lacrimal with a smooth lateral surface, lacking neurovascular foramina or an opening for the nasolacrimal duct; an anteroposteriorly elongated prefrontal which excludes the postfrontal from contributing to the dorsal orbital margin; a dorsoventrally broad, triangular posterodorsal process of the postorbital; a posterior process of the jugal; an internasal suture forming a sharp crest posteriorly; and a postfrontal with an anteroposteriorly elongated and mediolaterally broad groove running along the dorsal surface of its anteromedial process. These new observations have implications for the taxonomy and phylogeny of Cymbospondylidae. Personal examination of the holotype skull of *Cy. 'nicholllsi'* indicates that all discrete character states proposed as autapomorphies for this taxon have arisen from misinterpretation of the cranial anatomy

and no differences in discrete character states are found between well-preserved skulls of *Cy. piscosus* (type species) and *Cy. 'nichollsi'*, which is here considered as the junior synonym of *Cy. piscosus*. The cranial autapomorphies that have been proposed to distinguish *Cy. buchseri* from the Middle Triassic of Switzerland from *Cy. piscosus* have also been identified as invalid. However, features of the postcranial anatomy of *Cy. buchseri* are considered different enough from the anatomy of *Cy. piscosus*, that *Cy. buchseri* is maintained as a distinct species. First hand examination of the type skull of *Thalattoarchon saurophagis*, a colossal ichthyosaur which co-occurs with *Cymbospondylus* in the Middle Triassic of Nevada, USA, has revealed that *T. saurophagis* shares many synapomorphies with *Cymbospondylus*, including four features shared only between the two taxa, to the exclusion of all other ichthyopterygians: the presence of an internasal crest, a parietal plateau, a lateral groove on the postfrontal and a prefrontal contributing to the entire dorsal orbital margin. This provides additional evidence to support the recently proposed, but weakly supported, cymbospondylid affinity for *T. saurophagis*. Cymbospondylidae thus includes durophagous (*Xinminosaurus*) and macropredatory (*Cymbospondylus*, *Thalattoarchon*) forms, and indicates rapid diversification of the clade in the first part of the Middle Triassic (Chapter 5).

A key episode in the evolutionary history of ichthyosaurs was the emergence of the clade Parvipelvia in the Late Triassic (Norian). Parvipelvian ichthyosaurs were characterized by a reduced pelvic girdle and a streamlined, fish-shaped body plan. These anatomical innovations were related to the evolution of an oscillatory mode of swimming, hydrodynamically more efficient than the undulatory-based locomotion of more basal ichthyosaurs, enabling parvipelvians to adapt to life in the pelagic realm. This transition between non-parvipelvian and parvipelvian ichthyosaurs is poorly understood due to the incomplete sampling of the global marine Late Triassic fossil record. However, an abundant ichthyosaur fauna from the Pardonet Formation (Late Triassic) of Williston Lake and nearby localities in British Columbia, Canada, documents this transition very well. A new taxon of early parvipelvian ichthyosaur from Williston Lake is described in Chapter 3. Represented by a single specimen collected by Royal Ontario Museum crews in 1991, it is the most complete ichthyosaur specimen known from the upper Norian and provides valuable information on the ecomorphological

diversity of Parvipelvia in the latest Triassic. The specimen consists of a partial rostrum with numerous teeth, partial forefins, a partial pelvic girdle and partial hindfin. The size of the available material indicates a large animal, approaching 7 m in fork length, similar in size to the large predatory ichthyosaur *Temnodontosaurus* from the Early Jurassic of Europe. The teeth of the new taxon are set in a dental groove, without distinct alveoli, like in other parvipelvian ichthyosaurs, and have large, labiolingually flattened, bicarinate crowns. This tooth morphology indicates the new ichthyosaur was an apex predator, feeding on large-bodied prey items. The forefin of the new ichthyosaur has four primary digits and only a single, reduced accessory digit, with notching occurring along the entire anterior margin of the forefin. A small, circular foramen enclosed by the contiguous shafts of the epipodials, shared with some other basal parvipelvians, is also present. The ischium of the new taxon is plate-like, but longer mediolaterally than anteroposteriorly, resembling ischia of some other basal parvipelvians, and is markedly different from the anteroposteriorly broad ischia of more basal Triassic ichthyosaurs. The pubis of the new taxon is styloidal, like in other parvipelvians. There are only two proximal tarsals in the hindfin of the new taxon, similar to the condition in more basal ichthyosaurs such as *Mixosaurus*. This is in contrast to euichthyosaurs, where the number of elements in the distal tarsal row increases to three. A phylogenetic analysis (Chapter 5) recovers the new taxon as an early-diverging parvipelvian. Because other currently known basal parvipelvians from the Norian are small- to medium-sized ichthyosaurs, representing different ecomorphologies, this indicates that the clade was already ecologically diverse at the very beginning of their evolutionary history. Fragmentary remains from the middle Norian indicate that similar, apex-predator parvipelvians were already present in the middle Norian and challenge the hypotheses of diminishing ichthyosaur morphological diversity near the end of the Triassic.

The Blue Lias Formation (Lower Jurassic) of the United Kingdom documents the first diverse ichthyosaur fauna post-dating the end-Triassic extinction event. To date, six ichthyosaur genera have been recognized, represented by as many as 15 species. However, even though this fauna is represented by numerous ichthyosaur specimens, the lack of comprehensive anatomical descriptions of these taxa hinders our understanding of the true diversity of ichthyosaurs from the Early Jurassic of the United

Kingdom. In Chapter 2, a new genus and species of ichthyosaur from the Blue Lias Formation (Hettangian–Sinemurian) is described. The new taxon is represented by two specimens, which had previously been referred to the genus *Ichthyosaurus*. The type specimen is a nearly complete, three-dimensionally preserved skull from Stockton, Warwickshire, whereas a partial specimen consisting of a partial cranium, a few centra and the humerus is designated as a referred specimen. The new taxon can be distinguished by the following autapomorphies: (1) overbite comprising 24% of preorbital (=rostrum) length with a mediolaterally broad and dorsally rounded cross-section; (2) jugal bifurcating posterodorsally into a broad anterior posterodorsal process and a narrow posterior posterodorsal process; (3) posterior process of postorbital overlapped by the anterior posterodorsal process of the jugal laterally and overlapping the posterior posterodorsal process of the jugal laterally; (4) an elongated retroarticular process, comprising 9% of the mandibular ramus length; (5) a reduced anterior flange of the humerus, forming a thickened and rounded anterior margin. The new taxon also possesses at least two plesiomorphic features: (1) the posterior process of the jugal, otherwise seen only in some Triassic ichthyosaurs, and (2) an anterior terrace of the supratemporal fenestra, otherwise seen only in non-parvipelvian ichthyosaurs and the basal parvipelvian *Macgowania janiceps*. This unique combination of characters clearly differentiates this new taxon from other ichthyosaur taxa from the Early Jurassic of the UK, encouraging further descriptive studies of ichthyosaur anatomy, in order to obtain a better understanding of their taxonomic diversity. A phylogenetic analysis (Chapter 5) recovers this taxon as an early-diverging parvipelvian, whereas all other ichthyosaur taxa from the Early Jurassic of the UK are placed within a monophyletic Neoichthyosauria. This suggests a temporally staggered, rather than the recently proposed catastrophic, turnover of ichthyosaurs across the Triassic–Jurassic boundary.

CONTENTS

INSTITUTIONAL ABBREVIATIONS

ANSP, Academy of National Sciences of Drexel University, Philadelphia, PA, USA;

BGS, British Geological Survey London Centre, Natural History Museum, London, England, UK;

BRSMG, City of Bristol Museum and Art Gallery, Bristol, England, UK;

CM, Carnegie Museum of Natural History, Pittsburgh, PA, USA;

FMNH, The Field Museum, Chicago, IL, USA;

GMPKU, Geological Museum of Peking University, Beijing, China;

IVPP, Institute of Vertebrate Paleontology and Paleoanthropology, Beijing, China;

MHN, Museon, The Hague, Netherlands;

NHMUK, Natural History Museum, London, England, UK;

NSM, Nevada State Museum, Las Vegas, NV, USA;

OUMNH, Oxford University Museum of Natural History, Oxford, England, UK;

PIMUZ, Palaeontological Institute and Museum, University of Zurich, Switzerland;

ROM, Royal Ontario Museum, Toronto, ON, Canada;

SMNS, State Museum of Natural History, Stuttgart, Germany;

SPCV, Wuhan Centre of China Geological Survey, Wuhan, China;

TMP, Royal Tyrrell Museum of Palaeontology, Drumheller, AB, Canada;

UCMP, University of California Museum of Paleontology, Berkeley, CA, USA.

CHAPTER 1: INTRODUCTION

SYSTEMATICS, PHYLOGENY AND EVOLUTION OF ICHTHYOSAURS.

Ichthyosaurs (Ichthyopterygia sensu Motani 1999a) were a long-lived and globally distributed clade of Mesozoic marine reptiles that were important predators in marine ecosystems for ~160 million years, from the late Early Triassic until the early Late Cretaceous (McGowan and Motani, 2003; Motani, 2005a). Ichthyosaurs (meaning "fish lizards" in Greek) are named after the fish-shaped body plan of their derived members (Parvipelvia; see below), with limbs modified into flippers, a well demarcated dorsal fluke and a crescent-shaped caudal fluke (Fig. 1.1). Other anatomical features, in general characteristic of ichthyosaurs, include: an elongate, slender snout with numerous, conical teeth; large orbits with well-developed sclerotic rings; amphicoelous vertebrae; and hyperphalangy and hyperdactyly of the forefins (Motani, 2005a). Ichthyosaurs are widely considered as members of Diapsida (but see Maisch, 1997), but their exact phylogenetic position relative to other diapsid clades remains unresolved (Callaway, 1989; Massare and Callaway, 1990; Caldwell, 1996; Motani et al., 1998, 2015a; Chen et al., 2014; Scheyer et al., 2017). However, most phylogenetic analyses recover them near the base of the Sauria, as either nested within the clade (e.g. Caldwell, 1996) or lying outside (e.g. Massare and Callaway, 1990; Motani et al., 1998; Chen et al., 2014; Motani et al., 2015a). The sister group of ichthyosaurs is the recently described Nasorostra, represented by small, short-snouted, likely suction-feeding and semi-aquatic reptiles from the earliest Triassic (Olenekian) of South China (Motani et al., 2015a; Jiang et al., 2016). Ichthyopterygia and Nasorostra comprise the Ichthyosauriformes (Motani et al., 2015a), and a growing number of evidence suggests that Ichthyosauriformes are the sister taxon of Hupehsuchia, another clade of Early Triassic (Olenekian) marine reptiles from South China (Carroll and Dong, 1991; Motani, 1999a; Chen et al., 2014; Motani et al. 2015a).

The first ichthyopterygians appeared in the late Early Triassic (Olenekian), in the early stages of marine ecosystem recovery after the end-Permian mass extinction event (Motani et al., 2017). *Chaohusaurus* from South China is the stratigraphically oldest and phylogenetically most basal ichthyopterygian (Motani et al., 2014, 2015a, 2015b, 2015c), but other early-diverging ichthyopterygians, representing the clade Grippioidea, are known from slightly younger geological

horizons from North America, Spitzbergen and Japan (Fig. 1.2; Ji et al., 2016). Basal ichthyopterygians were small- to medium-sized animals (body length of ~1–3 m), had a relatively small skull, an elongate trunk with ~40 vertebrae lying anterior to the pelvic girdle (presacral vertebrae), a short tail and limbs modified into flippers (Motani et al., 1996). Their overall body plan resembled that of modern scyliorhinid sharks, and suggests these ichthyosaurs were anguilliform swimmers, generating propulsion through lateral movements of the trunk and tail (Motani et al., 1996). It was recently demonstrated that basal ichthyopterygians were live-bearing, but birth occurred head-first, like in terrestrial animals, in contrast to the tail-first birth in derived ichthyosaurs (Motani et al., 2014). This challenges the traditional view that viviparity evolved as an aquatic adaptation in ichthyosaurs, and suggests that viviparity was already present in the terrestrial ancestors of ichthyosaurs.

Ichthyosauria is a major ichthyosaur clade nested within Ichthyopterygia, and comprises all ichthyosaurs, to the exclusion of Grippioidea and *Chaohusaurus*. Five major clades can be distinguished within Ichthyosauria, namely: Cymbospondylidae, Mixosauridae, Shastasauridae, Toretocnemidae and Parvipelvia (Fig. 1.2). Cymbospondylidae are widely regarded as the most basal ichthyosaurian clade (e.g. Ji et al., 2016). Until recently, cymbospondylids were represented by only a few species of the genus *Cymbospondylus* – a giant (body length of ~9 m) ichthyosaur, with a relatively small head and an elongate trunk (65 presacral vertebrae), from the Middle Triassic (Anisian) of North America and Europe (Fig 1.2; e.g. Merriam, 1908; Sander, 1989; Fröbisch et al., 2006). However, recent findings from the Middle Triassic of China and North America indicate that the clade was ecomorphologically diverse, and was also represented by small, durophagous forms, as well as colossal apex predators (Jiang et al., 2008; Fröbisch et al., 2013; Ji et al., 2016; chapters 4 and 5 of this work).

Mixosauridae are one of the better-known clades of ichthyosaurians, due to the numerous, complete and well-preserved specimens known from the Middle Triassic (Anisian–Ladinian) of North America, Europe and China (Fig. 1.2; e.g. Brinkmann, 1998; Motani, 1999b; Nicholls et al., 1999; Schmitz et al., 2004; Jiang et al., 2006; Liu et al., 2013). Mixosaurids were small-bodied ichthyosaurians (body length ~1–2 m) with a body plan somewhat intermediate between the basal ichthyopterygians and the more derived Parvipelvia – they had proportionally large heads and ~50 presacral vertebrae. Some mixosaurids had broad, rounded dentition at the back of their jaws, indicating durophagy (e.g.

Motani, 2005b). The tails of Mixosaurids were unique among ichthyosaurs, in that the dorsoventral height of the caudal centra was greatest in the central caudal region, which indicates a high capability for rapid acceleration (Motani, 1998).

Shastasauridae are another well-known clade of ichthyosaurians, with a temporal range extending from the Middle–Late Triassic of North America, Europe and South China (Fig. 1.2; e.g. Merriam, 1902; Camp, 1980; Dal Sasso and Pinna, 1996; Fischer et al., 2014a; Ji et al., 2016). Shastasaurids were in general large-bodied ichthyosaurs, characterised by extremely high vertebral counts (reaching ~90 presacral and ~100 caudal vertebrae; Sander et al., 2011). Some shastasaurids attained a colossal body size (~20 m in total body length), and were the largest marine reptiles ever to have evolved (Nicholls and Manabe, 2004). Shastasaurids were ecologically diverse and included specialized, short-snouted ram-feeders (Sander et al., 2011; Motani et al., 2013), and colossal apex predators (Motani et al., 1999a). Shastasaurids were also the first ichthyosaurs to evolve a tailbend – a downturned distal part of the caudal region which supported a bilobed caudal fluke, but the extent of this caudal fluke remains unknown (Motani, 2008; Ji et al., 2011).

Toretocnemidae are the sister group to Parvipelvia and are known from the Middle–Late Triassic of North America and South China (Fig. 1.2; e.g. Merriam, 1908; Li, 1999; Yang et al., 2013). Toretocnemids were small-bodied ichthyosaurs and had a dorsoventrally deep trunk, similar to mixosaurids and parvipelvians, but their caudal fluke was intermediate between that of both clades (Motani, 2008).

Parvipelvia are the most well-known clade of ichthyosaurs, ranging from the Late Triassic (Norian) to the early Late Cretaceous (Fig. 1.2; e.g. McGowan, 1997; Fischer et al., 2016). Parvipelvians evolved a fish-shaped body plan with a streamlined, dorsoventrally deep trunk, a well-demarcated dorsal fin and a lunate caudal fluke, which is clearly demonstrated by fossil specimens preserving approximate body outlines (e.g. Hauff and Hauff, 1981). The name Parvipelvia means “the ones with a small pelvis” in Greek, and indicates that the size of the pelvic girdle of these ichthyosaurs was reduced in comparison to more basal forms. This is similar to modern cetaceans, in which the caudal muscles are attached to the trunk, instead of the pelvic bones, which allows for a swimming mode relying on oscillatory movements of the tail, rather than on undulatory movements of the entire body (Motani,

2005a). A large body of evidence suggests that parvipelvian ichthyosaurs were likely fast-moving, active, marine predators able to maintain constant, high body temperatures and were well adapted to life in the pelagic realm (Motani et al. 1999b; Motani 2002a, 2002b, 2010; Bernard et al. 2010). Parvipelvians were live-bearing, like all other ichthyosaurs, but in contrast to basal ichthyopterygians, in which birth occurred head-first, birth in parvipelvians occurred tail-first. This is similar to modern cetaceans and indicates that tail-first birth was an aquatic adaptation, which evolved in order to reduce the risk of suffocation during parturition (Motani et al., 2014).

As a long-lived clade of secondarily marine tetrapods with distinct skeletal, locomotory and sensory adaptations, ichthyosaurs provide an opportunity to explore morphological evolution in a marine group spanning a long time interval. Motani et al. (1996) were the first to use a quantitative approach in order to study the evolution of ichthyosaur swimming. In their study, Motani et al. (1996) quantified various aspects of the body outlines of ichthyosaurs from different stages of their evolutionary history, and compared them with similar measurements obtained from modern sharks. The results obtained by Motani et al. (1996) indicate that the body proportions of basal ichthyopterygians were most similar to those of modern scyliorhinid sharks, which are angulliform (eel-like) swimmers, whereas the body plan of parvipelvian ichthtyosaurs was most similar to that of lamnid sharks, which are thunniform swimmers. This demonstrates that the evolution of ichthyosaur swimming proceeded, in general, in the direction of increasing ability of efficient cruising. Because large-bodied, thunniform swimmers are under stringent physical constraints, Motani (2002a) was able to estimate the swimming speed of the parvipelvian *Stenopterygius* using the principles of fluid mechanics. By using parameters such as body length and the dorsoventral span of the caudal fluke obtained from exceptionally preserved fossils with preserved body outlines, Motani (2002a) concluded that the optimal speed of *Stenopterygius* was lower than that of cetaceans of similar size, but was comparable to that of tunas of approximately equal body size.

Motani (2002b) developed an alternative method of calculating the optimal swimming speed of *Stenopterygius*, which assumed that during steady swimming, the energy consumption equals drag power to overcome plus the energy needed for the maintenance of basic metabolism (Massare, 1988). By assuming three different metabolic rates known in extant swimming vertebrates (average

ectothermic, elevated ectothermic, endothermic), Motani (2002b) was able to provide three different optimal swimming speed estimates for *Stenopterygius*. One of these estimates (optimal swimming speed ~1 m/s), obtained assuming the elevated ectothermic metabolic rate, was in accordance with the speed estimate obtained by Motani (2002a). These results indicated that derived parvipelvian ichthyosaurs were likely capable of sustaining elevated, constant body temperatures, like modern tunas. This hypothesis was later supported by Bernard et al. (2010), who studied the isotopic composition if ichthyosaur teeth, and concluded that ichthyosaur metabolic rates were higher than those of ectothermic fish known from the same environments.

Ichthyosaur physiology has also been studied in the context of their ability of deep diving. Motani et al. (1999b) used principles of optical physics to calculate the visual sensitivity of ichthyosaurian eyes and compared them with that of modern animals. Their results indicate that early-diverging ichthyosaurians had a visual sensitivity similar to that of modern diurnal animals, including humans, whereas parvipelvian ichthyosaurs had a visual sensitivity comparable to that of nocturnal animals. This indicates the ability of derived ichthyosaurs to locate prey in low light conditions. Motani et al. (1999b) also studied the frequency of pathologies related to decompression syndrome present in ichthyosaur limb bones and determined that the frequency of pathological elements observed in derived parvieplvians was much higher than that observed in more basal ichthyosaurs. Together, this evidence indicates a trend of increased adaptation to a pelagic lifestyle and the ability of deep diving throughout ichthyosaur evolution.

In the last 10 years, numerous studies have focused on the interactions between ichthyosaur evolution and changes in the Earth System. In particular, they focused on three key episodes in ichthyosaur evolution: their emergence in the late Early Triassic (Motani et al., 2017), ichthyosaur turnover across the Triassic–Jurassic boundary (Motani, 2008; Benson and Butler, 2011; Thorne et al., 2011; Kelley et al., 2014; Dick and Maxwell, 2015), and the extinction of ichthyosaurs in the early Late Cretaceous (Fischer et al., 2016). Motani et al. (2017) determined that the rates of morphological evolution in ichthyosaurs were non-homogenous, and were highest at the beginning of their evolutionary history, gradually decreasing over time. It was argued that the use of the lower evolutionary rates in divergence time estimates can bias the results towards older estimated divergence

times. By using the initial, fast evolutionary rates, Motani et al. (2017) were able to obtain a divergence time estimate for ichthyosaurs that was in accordance with that obtained from an independent method based on high-resolution stratigraphic confidence intervals, and suggested a divergence time in the late Early Triassic. These results indicate that ichthyosaurs did not evolve prior to the end-Permian mass extinction, but most likely invaded marine habitats in the early stages of the recovery phase after the Permian–Triassic extinction event.

The Triassic–Jurassic extinction event is thought to have had a profound effect on ichthyosaur evolution, causing a great decline in ichthyosaur taxonomic diversity and morphological disparity. Thorne et al. (2011) attributed this to a mass extinction event which occurred at, or very close to, the Triassic–Jurassic boundary. However, the Late Triassic time bin used by Thorne et al. (2011) was very broad, consisting of the Carnian, Norian and Rhaetian, with a total duration of ~26 million years. Because of the incompletely sampled marine fossil record of the latest Triassic (Norian–Rhaetian; e.g. Benson et al., 2010), it is difficult to establish the exact timing of the extinction of ichthyosaur lineages throughout the Late Triassic, and it is likely that these extinctions occurred over a prolonged period of time. Motani (2008) was the first to suggest that the Triassic extinctions of some ichthyosaur lineages, adapted to shallow-water environments (e.g. durophagous forms), were likely related to falling sea levels, which reduced the availability of near-shore environments which these ichthyosaurs inhabited. Derived (parvipelvian) ichthyosaurs, adapted to life in the open ocean, remained unaffected by these changes in sea level. This hypothesis was later supported by Benson and Butler (2011) and Kelley et al. (2014), who quantitatively determined that the diversity of shallow-marine tetrapods in the Late Triassic was largely determined by changes in sea level. Thorne et al. (2011) and Dick and Maxwell (2015) presented different models describing ichthyosaur turnover across the Triassic–Jurassic boundary, but these models did not take into consideration the likely effect of environmental change on ichthyosaur evolution.

Fischer et al. (2016) performed a rigorous, quantitative analysis of the taxonomic and ecomorphological diversity of Cretaceous ichthyosaurs. They determined that ichthyosaur diversity in the Cretaceous was higher than previously thought, but that Cretaceous ichthyosaurs were characterised by lower rates of morphological evolution (consistent with the results of Motani et al., 2017), which

likely contributed to their final extinction. Furthermore, Fischer et al. (2016) determined that ichthyosaur extinction in the Cenomanian occurred in at least two steps – one, at the beginning of the Cenomanian and one at, or close to, the Cenomanian–Turonian boundary. Therefore, it seems that both the emergence of ichthyosaurs in the late Early Triassic, and their extinction in the early Late Cretaceous, occurred in periods of profound climatic perturbation, characterized by very high global temperatures (Motani, 2016).

HISTORICAL BACKGROUND.

Fragmentary ichthyosaur remains have been reported in the literature since the turn of the eighteenth century, but they were initially identified as the remains of fishes or of humans drowned in the Noachian flood (Delair, 1969; Callaway, 1997). The first scientifically important ichthyosaur discovery was made by the famous English fossil collector Mary Anning and her brother Joseph in Lyme Regis, Dorset, in 1811 (Lang, 1959). It was a complete ichthyosaur skull (NHMUK PV R1158, now referred to *Temnodontosaurus platyodon*), which became the first ichthyosaur specimen to be scientifically described (Home, 1814). Soon after this initial discovery, numerous complete ichthyosaur skeletons were excavated from Early Jurassic rocks in Lyme Regis, Dorset, and Street, Somerset, in southern England (Delair, 1969). These fossil specimens enabled early nineteenth century naturalists to obtain comprehensive knowledge of ichthyosaur anatomy (De la Beche and Conybeare, 1821; Conybeare, 1822; Hawkins, 1834; Owen, 1840, 1851, 1881, 1849-84). These early ichthyosaur discoveries also had a huge influence on the shaping of early ideas about the history of life on Earth, partly contributing to the formulation of Darwin's evolutionary theory a few decades later (McGowan, 2001).

Numerous other ichthyosaur fossil localities, spanning their entire stratigraphic range, were discovered worldwide at the end of the nineteenth and the beginning of the twentieth century. The most important ones include: the Sticky Keep Formation (Olenekian, Early Triassic) of the Svalbard Archipelago, Norway (e.g. Wiman, 1910); the Grenzbitumen-Zone of Monte San Giorgio (Anisian–Ladinian, Middle Triassic) on the border of Switzerland and Italy (e.g. Bassani, 1886); the Muschelkalk (Anisian–Ladinian, Middle Triassic) of Germany (e.g. Huene, 1916); the Prida Formation (Anisian,

Middle Triassic) of Nevada, USA (e.g. Merriam, 1908); the Hosselkus Limestone (Carnian, Late Triassic) of California, USA (e.g. Merriam, 1908); the Posidonienschiefer (Toarcian, Early Jurassic) of Holzmaden, Germany (e.g. Fraas, 1891; Huene, 1922); the Oxford Clay (Callovian–Oxfordian, Middle–Late Jurassic) of England (e.g. Andrews, 1910); the Sundance Formation (Callovian–Oxfordian, Middle–Late Jurassic) of Wyoming, USA (e.g. Gilmore, 1905); and Early–Late Cretaceous (Albian–Cenomanian) localities in Cambridgeshire, England (e.g. Carter, 1886a, 1886b). However, after initial description, the ichthyosaur material discovered from these localities has not received much scientific attention throughout the twentieth century, with the exception of the Jurassic ichthyosaurs from the United Kingdom and Germany (e.g. Appleby 1956, 1979; McGowan 1973, 1974a, 1974b, 1979).

Ichthyosaurs started to regain the interest of palaeontologists in the 1980s, at the same time when cladistics was becoming the most widely used method of phylogenetic inference (Hull, 2010). The first phylogenetic hypotheses of ichthyosaur relationships were limited in scope and incorporated only a small number of characters and taxa, but were of great importance, as they challenged some of the well-established, historical ideas about ichthyosaur evolution (Mazin, 1982; Kirton, 1983; Godefroit, 1993; Nicholls et al., 1999). Callaway (1989) produced the first phylogenetic hypothesis of ichthyosaur interrelationships based on a small character-taxon matrix (9 taxa scored for 33 characters). The first comprehensive phylogenetic hypotheses for ichthyosaurs, based on extensive character-taxon matrices, were published by Motani (1999a), Sander (2000) and Maisch and Matzke (2000a). The analysis of Motani (1999a) was particularly important for our understanding of ichthyosaur evolution, as it not only introduced a modern scheme of ichthyosaur systematics, but also provided a robust phylogenetic framework for testing hypotheses of ichthyosaur morphological evolution (see above).

During the last 20 years, abundant ichthyosaur fossils have been discovered from the Triassic of North America and South China, as well as the Middle Jurassic–Late Cretaceous of North and South America, Europe, the Middle East and Australia (reviewed in Ji et al., 2016). These findings have helped to fill in significant gaps in our understanding of ichthyosaur evolution, but important questions remain unanswered.

AIMS OF THE THESIS.

The ichthyosaur fauna from the Early Jurassic (Hettangian-Sinemurian) of the United Kingdom represents the first well-known ichthyosaur fauna post-dating the Late Triassic extinction event. Numerous ichthyosaur fossils, ranging from isolated elements to complete skeletons, have been uncovered from the Early Jurassic (Hettangian – Sinemurian) rocks of England in the 19th and early 20th centuries (e.g. Benton and Spencer, 1995). The latest comprehensive taxonomic revision of this fauna suggested the presence of three genera – *Temnodontosaurus*, *Leptonectes* and *Ichthyosaurus* – represented by a few ecomorphologically disparate species (e.g. McGowan and Motani, 2003). The great majority of Early Jurassic ichthyosaur specimens from the United Kingdom have been customarily assigned to one of these three genera. However, because no comprehensive anatomical descriptions of these taxa have been provided to date and the latest diagnoses for these taxa were based heavily on continuous morphological characters of the cranium (McGowan, 1974a, b; McGowan, 1989), the assignment of numerous partial ichthyosaur specimens to one of these three genera remains controversial. Recent detailed studies of ichthyosaur skull roof anatomy have demonstrated that the morphology of some ichthyosaur specimens from the Early Jurassic of England, previously assigned to *Ichthyosaurus*, shows plesiomorphic character states and differs significantly from the skull roof morphologies of the other well-established ichthyosaur genera (McGowan and Motani, 2002; Motani, 2005). This suggests that the currently recognized diversity of ichthyosaurs from the Lower Jurassic of England is underestimated. Understanding the breadth of taxonomic and phylogenetic diversity of Early Jurassic ichthyosaurs from England is important for determining whether ichthyosaurs underwent a diversification event in the aftermath of the Triassic-Jurassic extinction event, or whether ichthyosaur turnover across the Triassic-Jurassic boundary was more mosaic.

Our understanding of ichthyosaur evolution across the Triassic-Jurassic boundary is also limited due to the incompletely sampled Late Triassic fossil record (e.g. Benson et al., 2010). Although diverse ichthyosaur faunas are known from the Carnian of the United States (Merriam, 1895, 1902, 1903, 1908) and China (e.g. Li, 1999; Yin et al., 2000; Li and You, 2002; Chen and Cheng, 2003; Maisch et al., 2006; Chen et al., 2007; Shang and Li, 2009; Sander et al., 2011; Ji et al., 2013) and the lower–middle Norian of Canada (e.g. McGowan, 1997; Nicholls and Manabe, 2001, 2004), only

isolated ichthyosaur remains are known from latest Triassic bonebeds of Europe, which are dominated by remains of large-bodied shastasaurid ichthyosaurs (e.g. Storrs, 1994; Fischer et al., 2014a). The stratigraphically oldest and phylogenetically most basal parvipelvian ichthyosaurs are known from the lower–middle Norian of the Pardonet Formation, British Columbia, Canada (e.g. McGowan, 1995a, 1996, 1997; Motani, 1999a) and are represented by small- to medium-sized forms. This suggests that the ecological and taxonomic diversity of Parvipelvia was low early in their evolutionary history, and other groups of non-parvipelvian ichthyosaurs were more abundant and ecologically diverse throughout the latest Triassic (e.g. Thorne et al., 2011). However, a gap of nearly 20 million years separates the oldest parvipelvian ichthyosaurs of the Pardonet Formation from the diverse ichthyosaur fauna of the Lower Jurassic of the United Kingdom (e.g. McGowan and Motani, 2003), which hinders our understanding of ichthyosaur evolution in the latest Triassic. Numerous ichthyosaur specimens were collected from Pardonet Formation outcrops of Williston Lake by ROM field crews in the 1990's. At least one of these specimens is upper Norian in age and represents a previously undescribed, large-bodied parvipelvian (McGowan, 1997). A detailed understanding of the anatomy and phylogenetic position of this new parvipelvian taxon is crucial to obtain a better understanding of ichthyosaur evolution at the end of the Triassic.

The Middle Triassic is another interesting, but poorly studied interval in ichthyosaur evolution. Ichthyosaurs were already ecologically diverse by the Anisian, and were represented by the well-known, diverse clade of small-bodied mixosaurids and the large-bodied *Cymbospondylus*. The anatomy of mixosaurid ichthyosaurs has been the subject of detailed re-examination in recent years (e.g. Motani, 1999c; Nicholls et al., 1999; Maisch and Matzke, 2001; Schmitz et al., 2004; Jiang et al., 2006), but the anatomy of *Cymbospondylus* is still poorly understood, with different authors presenting markedly different interpretations of its cranial morphology (e.g. Merriam, 1908; Sander, 1989; Motani, 1999b; Maisch and Matzke, 2004; Fröbisch et al., 2006). Furthermore, three currently recognized species of *Cymbospondylus* have been reported to differ significantly in their cranial anatomy, exhibiting remarkable variation within an ichthyosaur genus (Merriam, 1908; Sander, 1989; Fröbisch et al., 2006). These controversies surrounding the cranial anatomy of *Cymbospondylus* hinder our understanding of

early ichthyosaur evolution. Furthermore, the recently discovered durophagous ichthyosaur *Xinminosaurus catactes* from the Anisian of South China (Jiang et al., 2008) and the colossal apex predator *Thalattoarchon saurophagis* from the Anisian of Nevada, USA (Fröbisch et al., 2013) have been recovered in a clade with *Cymbospondylus* in a recent phylogenetic analysis (Ji et al., 2016), but nodal support for this clade was weak. A thorough reassessment of the cranial anatomy of *Cymbospondylus* is crucial to evaluate this hypothesis of an ecomorphologically disparate Cymbospondylidae and to better understand the evolutionary dynamics of ichthyosaurs in the Anisian, during a time of marine ecosystem recovery in the aftermath of the end-Permian mass extinction.

The aims of this thesis are:

- to provide a comprehensive description of a new genus and species of parvipelvian ichthyosaur from the Lower Jurassic of the United Kingdom and to provide detailed comparisons of its anatomy with that of other Lower Jurassic ichthyosaurs (Chapter 2);
- to provide a comprehensive description of a new genus and species of parvipelvian ichthyosaur from the Late Triassic of Williston Lake, British Columbia, Canada and discuss its implications for our understanding of early parvipelvian evolution (Chapter 3);
- to provide a comprehensive re-description of the cranial anatomy of *Cymbospondylus* and reassess the taxonomy of the genus (Chapter 4);
- to incorporate the new information on ichthyosaur anatomy into a phylogenetic hypothesis for ichthyosaurs, and discuss its implications on ichthyosaur evolution in the Middle Triassic and across the Triassic-Jurassic boundary (Chapter 5).

FIGURES

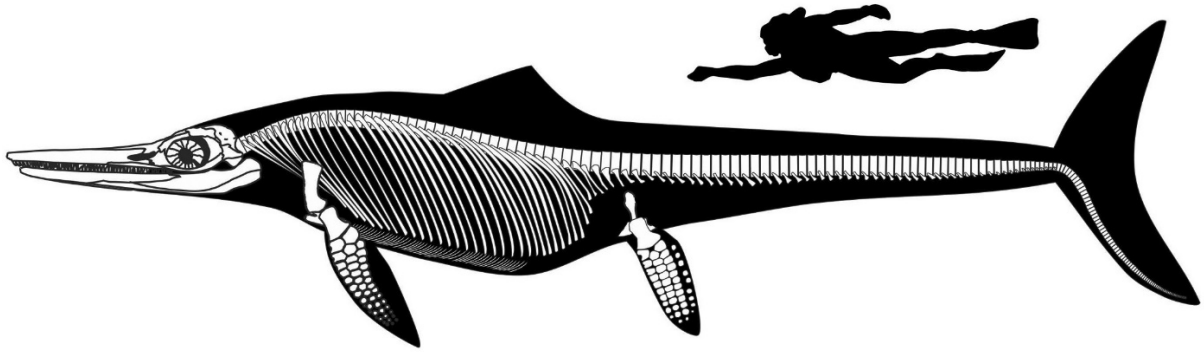

FIGURE 1.1. *Temnodontosaurus platyodon*, a parvipelvian ichthyosaur from the Lower Jurassic (Hettangian–Sinemurian) of the United Kingdom, exemplifying the characteristic, fish-shaped body plan of derived ichthyosaurs, with limbs modified into flippers, a well-demarcated dorsal fluke and crescent-shaped caudal fluke. Human for scale. Image courtesy R. Motani.

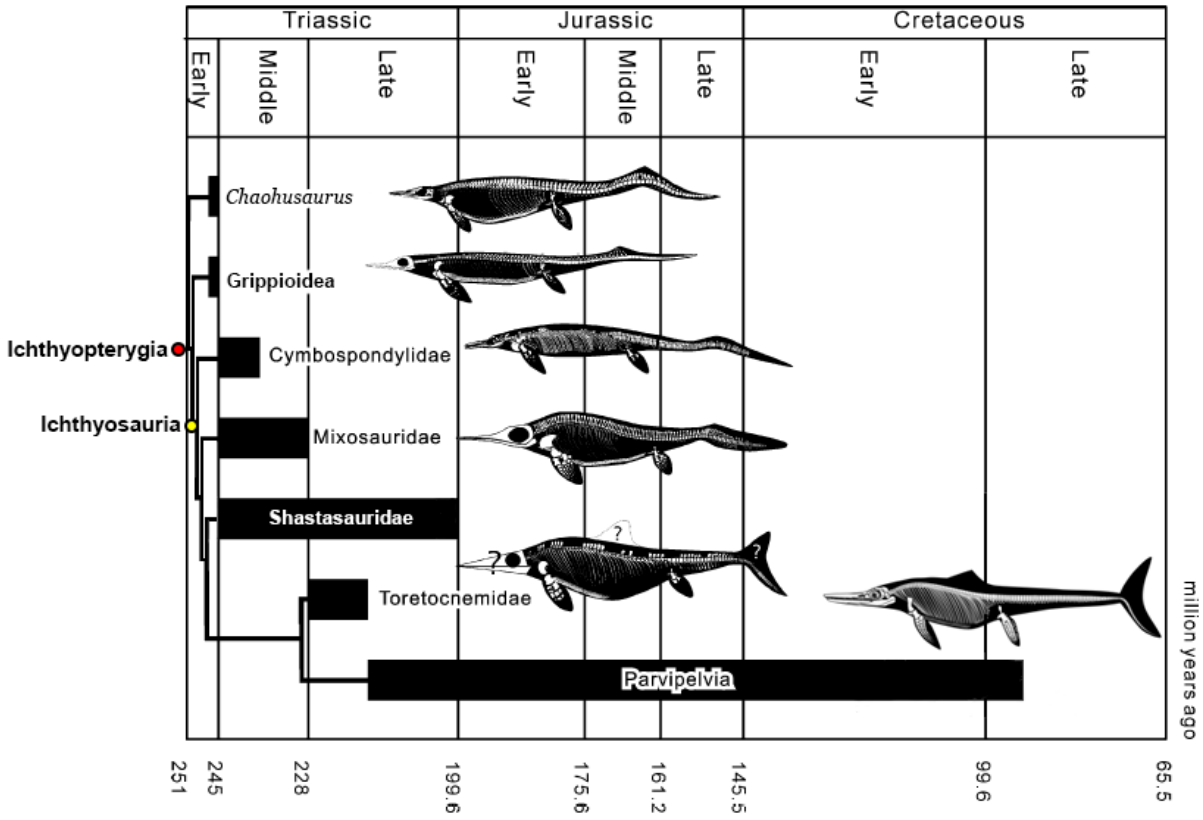

FIGURE 1.2. Simplified phylogeny of the Ichthyopterygia, highlighting the major clades, their divergent body plans and stratigraphic distribution (modified from Motani, 2009).

CHAPTER 2: A NEW PARVIPELVIAN ICHTHYOSAUR (REPTILIA: ICHTHYOPTERYGIA) FROM THE BLUE LIAS FORMATION (LOWER JURASSIC, HETTANGIAN–SINEMURIAN) OF THE UNITED KINGDOM.

INTRODUCTION

Ichthyosaurs were a group of secondarily aquatic amniotes that were important components of Mesozoic marine faunas for approximately 160 million years, from the Early Triassic until the early Late Cretaceous (e.g. Motani, 2005a; Motani, 2009; Benson, 2013). Ichthyosaurs were characterized by a set of unique skeletal, sensory and locomotory adaptations, including a fish-shaped body plan with a well demarcated caudal fluke and limbs modified into flippers, an elongated snout and large eyeballs (e.g. Motani et al., 1996; Motani et al., 1999b; Motani, 2005a). The exact phylogenetic position of ichthyosaurs within amniotes is still a matter of debate (e.g. Caldwell, 1996; Motani et al., 1998), but recent cladistic analyses have provided strong evidence for a close relationship between ichthyosaurs and thalattosaurs, hupehsuchians and nasorostrans (e.g. Motani et al., 2015a; Jiang et al., 2016; but see Neenan et al., 2013, 2015a). Early ichthyosaurs from the Early and Middle Triassic (e.g. McGowan and Motani, 2003) had body proportions that still resembled those of their terrestrial ancestors and they were likely anguilliform swimmers, using lateral undulations of the trunk and tail to generate propulsion (Motani et al., 1996). A key episode in ichthyosaur evolution occurred in the Late Triassic (Norian), when the first representatives of the clade Parvipelvia – ichthyosaurs with a reduced pelvic girdle – appeared (McGowan, 1995a, 1996, 1997). The small size of the pelvic girdle and hind limb indicates that in parvipelvians the caudal muscle series were most likely connected to the trunk musculature and enabled a thunniform mode of swimming, in which propulsion was generated by oscillations of the posterior caudal region (Motani et al., 1996; Motani, 2002a). This represents a major innovation in ichthyosaur evolution that allowed parvipelvians to adapt to life in the pelagic realm, where they functioned as active predators (Motani, 2002b; Bernard et al., 2010). Parvipelvians were the only major clade of ichthyosaurs to continue diversifying after the end-Triassic extinction event (e.g. Motani,

2005a; Fischer et al., 2014a) until their extinction at the Cenomanian–Turonian boundary (Bardet, 1994; Fischer et al., 2016).

The anatomy, evolution and biology of derived parvipelvian ichthyosaurs has been extensively studied (e.g. McGowan and Motani, 2003; Motani, 2005a). However, the early evolutionary history of the clade is poorly known. The stratigraphically oldest and phylogenetically most basal members of Parvipelvia are known exclusively from the Late Triassic (Norian) of the Pardonet Formation, British Columbia, Canada (McGowan, 1991, 1995a, 1996, 1997). They include the small-bodied *Hudsonelpidia brevirostris* (body length ~1 m; McGowan, 1995a, 1997), the medium-sized *Macgowania janiceps* (body length ~3m; McGowan, 1996, 1997; Motani, 1999a; Henderson, 2015) and an undescribed, large-bodied form (body length ~7 m; McGowan, 1997; see Chapter 3). Unfortunately, all of these basal parvipelvian taxa are known only from partial remains, which are often poorly preserved. This, in combination with the incomplete sampling of the global Late Triassic (Norian and Rhaetian) fossil record of marine tetrapods (e.g. Benson et al., 2010), hinders our understanding of early parvipelvian evolution.

By the Early Jurassic, as much as 20 million years after their first appearance in the fossil record, parvipelvians were already taxonomically and ecologically diverse. This is evidenced by the ichthyosaur fauna of the lower part of the Lias Group ("Lower Lias") of the United Kingdom, which is the first known ichthyosaur fauna post-dating the end-Triassic extinction event (McGowan and Motani, 2003). The lower part of the Lias Group stretches from Yorkshire, in the northeast of England, to Dorset in the south and exposes rocks of Hettangian to Pliensbachian age (Benton and Spencer, 1995). Extensive quarrying in the 19th and early 20th centuries uncovered numerous ichthyosaur fossils, ranging from isolated elements to complete, articulated specimens, from at least 40 localities spread along the entire length of the outcrop (Benton and Spencer, 1995).

The latest taxonomic reviews (McGowan and Motani, 2003; Maisch, 2010) recognized 4 genera and as many as 10 species of ichthyosaurs from the lower part of the Lias Group as valid. These include: the basal neoichthyosaurian *Temnodontosaurus*, comprising *T. platyodon* (Conybeare, 1822) and *T. eurycephalus* (McGowan, 1974a); the leptonectids *Leptonectes*, comprising *L. tenuirostris* (Conybeare,

1822), *L. solei* (McGowan, 1993) and *L. moorei* (McGowan and Milner, 1999) and *Excalibosaurus costini* (McGowan, 1986, 2003); and the basal thunnosaurian *Ichthyosaurus*, comprising *I. communis* (De la Beche and Conybeare, 1821), *I. breviceps* (Owen, 1881), *I. conybeari* (Lydekker, 1888) and *I. intermedius* (Conybeare, 1822; considered valid by Maisch, 2010; contra McGowan and Motani, 2003 and Massare and Lomax, 2017). Recently, an ongoing review of Lower Jurassic ichthyosaurs from the United Kingdom has resulted in the erection of four new taxa: new species within the genus *Ichthyosaurus – I. anningae* (Lomax and Massare, 2015), *I. larkini* and *I. somersetensis* (Lomax and Massare, 2016), and a new genus and species of leptonectid ichthyosaur – *Wahlisaurus massarae* (Lomax, 2016). Furthermore, this systematic review of 'Lower Lias' ichthyosaurs has also resulted in the resurrection of the genus *Protoichthyosaurus* (Appleby, 1979; considered invalid by Maisch and Matzke, 2000a and McGowan and Motani, 2003), represented by two species: *P. prostaxalis* and *P. appelbeyi* (Lomax et al., 2017). These new discoveries bring the total number of currently recognized Early Jurassic ichthyosaurs from the United Kingdom to six genera, represented by as many as 16 species. The latest phylogenetic hypotheses proposed for parvipelvian ichthyosaurs (Ji et al., 2016; Fischer et al., 2016) place all Jurassic and Cretaceous ichthyosaurs, including those from the Early Jurassic Lias Group, in a monophyletic group (Neoichthyosauria, the last common ancestor of *Temnodontosaurus platyodon* and *Ichthyosaurus*, and all its descendants; Sander, 2000:22). This suggests that all other non-neoichthyosaurians (including basal parvipelvians) became extinct at the Triassic–Jurassic boundary, with neoichthyosaurians experiencing a radiation in the aftermath of the end-Triassic extinction.

The genus *Ichthyosaurus* is by far the most well represented ichthyosaur taxon from the lower part of the Lias Group. However, since its initial description in the early 19th century, *Ichthyosaurus* has become a "waste-basket" taxon. Ichthyosaur fossils that lack the autapomorphic rostrum, flipper and girdle morphology of *Temnodontosaurus* and *Leptonectes* have been customarily assigned to *Ichthyosaurus* (Motani, 2005c). However, Motani (2005c) noted that multiple isolated skulls from the lower part of the Lias Group which have been assigned to *Ichthyosaurus* demonstrate a skull roof configuration different to that of well-studied representatives of the genus. As a consequence, Motani

(2005c) concluded that at least one additional, undescribed genus of ichthyosaur was present in the Lower Lias ichthyosaur fauna, but refrained from more detailed taxonomic conclusions pending the discovery of more complete material.

Here, I describe a new genus and species of ichthyosaur from the lower part of the Lias Group of the United Kingdom, previously assigned to *Ichthyosaurus* sp., based on two specimens comprising both cranial and postcranial material. The new genus is defined on the basis of well-defined, discrete apomorphies, that clearly differentiate it from all other ichthyosaur genera known from the lower part of the Lias Group.

SYSTEMATIC PALAEONTOLOGY

ICHTHYOPTERYGIA Owen, 1840

ICHTHYOSAURIA Blainville, 1835

HUENEOSAURIA Maisch and Matzke, 2000a

MERRIAMOSAURIA Motani, 1999a

EUICHTHYOSAURIA Motani, 1999a

PARVIPELVIA Motani, 1999a

Gen. et sp. nov. A.

Figs 2.2–2.16

Ichthyosaurus sp. Motani, 1999c:32, fig. 3N

Leptonectidae (=Eurhinosauria) indet. Motani et al., 1999a:SI1

Ichthyosauria indet. McGowan and Motani 2002:86A

Ichthyosaurus communis McGowan and Motani, 2003:31, fig. 44A

Ichthyosauria indet. McGowan and Motani, 2003:50, fig. 69

Ichthyosauria indet. Motani, 2005c:342

Holotype. NHMUK PV R3000 (Figs 2.2–2.6, 2.14–2.16), an almost complete, three-dimensionally preserved skull with mandible in occlusion. The skull is only slightly deformed posterodorsally, as the right temporal region is crushed dorsoventrally and all of its constituting bones are broken. NHMUK PV R3000 was prepared mechanically and much of the bone surface is broken, obscuring anatomical details of the surface. The rostrum has been broken into three segments but the breaks have been subsequently reconstructed in plaster. NHMUK PV R3000 was presented to the NHMUK by the Kayes Cement Works company in 1902.

Referred specimen. ROM 28964 (Figs 2.7–2.14, 2.16), a partial skeleton, comprising a partial articulated left side of the skull and mandible, a disarticulated right nasal, right quadratojugal, left quadrate, multiple disarticulated teeth, two cervical and one dorsal centra, an intercentrum, multiple partial neural arches, one complete and multiple fragmentary caudal ribs and the right humerus. The specimen was donated to the ROM by Richard Vogel in 1975. It was subject to acid preparation, and most of the surface anatomy, including most cranial sutures, is clearly evident. However, the specimen has suffered some damage, which resulted in the breakage of the rostrum and mandible anteriorly and the breakage of bone surfaces on the skull roof and in the temporal region.

Occurrence. The holotype (NHMUK PV R3000) was discovered in Kayes Cement Works Quarry, Stockton, Warwickshire, UK (Fig. 2.1B), one of the many now inactive cement quarries in the region, exposing rocks of the Rugby Limestone Member (upper Hettangian–lower Sinemurian) of the Blue Lias Formation in the lower part of the Lias Group (Fig. 2.1D; Benton and Spencer, 1995; Ambrose, 2001). However, no biostratigraphically relevant fossils were found associated with the specimen and its exact horizon of origin was not recorded. The referred specimen (ROM 28964) was found in Lyme Regis, Dorset, UK (Fig. 2.1C). Ammonite fossils identified as cf. *Schlotheimia* (M. Munt, pers. comm.) were found associated with ROM 28964, which indicates origin from the *angulata* zone of the Hettangian (Fig. 2.1D; Cope et al., 1980; Benton and Spencer, 1995).

Diagnosis. Medium to large-sized parvipelvian ichthyosaur (skull length of holotype 715 mm, measured from the tip of rostrum to the posterior part of the articular surface of quadrate), with four autapomorphies: (1) overbite comprising 24% of preorbital (=rostrum) length with a mediolaterally broad and dorsally rounded cross-section, unlike the mediolaterally narrow rostra of *Excalibosaurus* (McGowan, 1986, 2003) and *Eurhinosaurus* (e.g. Fischer et al., 2011a) – the only other ichthyosaurs with extensive overbites; (2) jugal bifurcating posterodorsally into a broad anterior posterodorsal process and a narrow posterior posterodorsal process; (3) posterior process of postorbital overlapped by the anterior posterodorsal process of the jugal laterally and overlapping the posterior posterodorsal process of the jugal laterally; (4) an elongated retroarticular process, comprising 9% of the mandibular ramus length. *Gen et sp. nov. A* also possesses at least two plesiomorphic features: (1) the posteroventral process of the jugal, otherwise seen only in some non-parvipelvian ichthyosaurs (e.g. Liu et al., 2011), and (2) an anterior terrace of the supratemporal fenestra, otherwise seen only in non-parvipelvian ichthyosaurs (e.g. Ji et al., 2016: character 36) and the basal parvipelvian *Macgowania* (TMP 2009.121.1; Henderson, 2015). As in *Macgowania*, the anterior terrace of the supratemporal fenestra is restricted to the postfrontal in *Gen. et sp. nov. A*; in non-parvipelvians it also extends onto the frontal, parietal, and sometimes the nasal (e.g. Ji et al., 2016). Furthermore, *Gen. et sp. nov. A* also posseses: a mediolaterally narrow and anteroposteriorly short frontal exposure, shared with many Early Jurassic parvipelvians (Ji et al., 2016: character 22:1), but different from *Ichthyosaurus* (Motani, 2005c) and *Hauffiopteryx* (Marek et al., 2015) where the dorsal exposure of the frontal is anteroposteriorly and mediolaterally broader; and a parietal ridge, shared with non-ophthalmosaurid parvipelvians (e.g. Ji et al., 2016: character 33:1). *Gen. et sp. nov. A* also possesses: a postorbital posteroventral process, shared with some specimens of *Ichthyosaurus communis* (e.g. NHMUK PV R3372; Maisch and Matzke, 2000b); a large and triangular squamosal, shared with some other parvipelvian ichthyosaurs (e.g. Ji et al., 2016: characters 24:1, 32:2), but different from *Ichthyosaurus*, where the squamosal is reduced in size (e.g. Motani, 2005c); and a basisphenoid with a single foramen for the internal carotid artery, similar to *Ichthyosaurus* (e.g. NHMUK PV R6697), *Stenopterygius* (e.g. NHMUK PV R33157) and other thunnosaurs, but different from the non-thunnosaurian parvipelvians *Macgowania* (TMP 2009.121.1) and *Temnodontosaurus* spp. (e.g. SMNS 50000), where two foramina are present.

DESCRIPTION

Maturity. Many criteria for assessing the osteological maturity of ichthyosaurs have been proposed to date. Johnson (1977) was the first to address the issue and determined four size-independent criteria for assessing the relative maturity of ichthyosaurs based on forefin anatomy. Since then, multiple authors have proposed other criteria for assessing the ontogenetic state of ichthyosaur specimens, and these are based on the assessment of the degree of ossification and proportions of certain cranial bones (Kear, 2005; Kear and Zammit, 2014); the relative proportions of the sclerotic ring and orbit (Fernàndez et al., 2005); the degree of ossification and proportions of forefin and pectoral girdle elements (Wade, 1984; Caldwell, 1997; Motani and You, 1998; Kear and Zammit, 2014) and other parts of the skeleton (Kear and Zammit, 2014). However, none of these criteria can be applied to NHMUK PV R3000 because the anatomical parts relevant for assessment of the ontogenetic stage are not preserved. The sclerotic ring proportion criterion of Fernàndez et al. (2005) cannot be applied, because the only preserved sclerotic ring of NHMUK PV R3000 is incompletely exposed from the matrix. However, the skull of NHMUK PV R3000 is large (715 mm measured from tip of rostrum to posterior part of the articular surface of the quadrate), and it is larger than in some of the largest individuals of other ichthyosaurs known from the Lower Lias (e.g. *Leptonectes tenuirostris* [skull length of 620 mm in OUM J.10319 with a total body length of ~2,800 mm] and *Ichthyosaurus communis* [skull length of 500 mm in NHMUK PV OR2013* with a total body length of ~3,100 mm; measured from photograph]). I therefore consider NHMUK PV R3000 to be an adult individual. ROM 28964 is a slightly smaller individual (postrostral length of 190 mm, compared to 220 mm in NHMUK PV R3000). The orbit:sclerotic ring aperture ratio measured in ROM 28964 is ca. 10%, compared to a ratio of 20% obtained from juvenile parvipelvians (Fernàndez et al., 2005). However, the proximal end of the humerus of ROM 28964 has a slightly flattened appearance in dorsal/ventral view and the dorsal and ventral surfaces of the bone have rugose patches, both of which were considered as features indicating immaturity by Johnson (1977). Based on my observations, I consider ROM 28964 as a subadult, close to reaching full osteological maturity.

Craniofacial anatomy. The skull of NHMUK PV R3000 is 715 mm long (measured from tip of rostrum to the posterior part of the articular surface of the quadrate; Figs 2.2–2.6 and Table 2.1). The temporal

region is transversely broad (320 mm) and the skull tapers anteriorly into a constricted rostrum, as in other ichthyopterygians (Motani et al., 2015a: character 165:1). The preorbital (=rostrum) length (495 mm) accounts for ca. 70% of the total skull length. The orbits are large (136.2 mm in anteroposterior length, 98.8 mm in dorsoventral height), with a large sclerotic ring filling almost the entire orbit, like in other ichthyopterygians (Motani et al., 2015a: character 172:1). The external nares are retracted posteriorly and situated anteriorly to the orbits. The external naris is anteroposteriorly longer (54.9 mm) than dorsoventrally tall (18.3 mm). It has a dorsoventrally broad, rounded posterior margin and tapers anteriorly into a sharp apex. The postorbital length (84 mm, 12% of skull length) is much shorter than the preorbital length, like in other ichthyopterygians (Motani et al., 2015a: character 166:1). The overbite in NHMUK PV R3000 measures 120 mm, which accounts for 24% of the preorbital (=rostrum) length. The retroarticular process of NHMUK PV R3000 is elongated and measures 61 mm, which corresponds to 9% of the mandibular ramus length. The temporal fenestrae are roughly circular in shape and are longer anteroposteriorly (74.3 mm) than mediolaterally (58.5 mm). The pineal foramen is small (21.1 mm in anteroposterior length, 14.5 mm in mediolateral width), teardrop-shaped and tapers posteriorly.

Premaxilla. Both premaxillae are preserved in NHMUK PV R3000. They are almost complete. The left premaxilla is broken along its posterodorsal margin and the supranarial process is broken off (Figs 2.2, 2.4), while the right premaxilla is broken along its dorsal margin (Figs 2.3–2.4). Mechanical preparation has extensively damaged the surfaces of the premaxillae and major breaks were reconstructed in plaster. In ROM 28964, the anterior portion of the left premaxilla is broken, but the posterior part is complete and its relationships with other bones of the skull are clearly visible (Figs 2.7, 2.14B).

The premaxilla is an anteroposteriorly long and dorsoventrally narrow bone that forms most of the rostrum. The dorsoventral height of the premaxilla tapers anteriorly, and the dorsal surface of the premaxilla curves ventrally abruptly at the tip of the rostrum (Figs 2.2, 2.14A). The lateral wall of the premaxilla is slightly convex. Anteriorly, the dorsolateral wall of the premaxilla bears anteroposteriorly oriented striations (Fig. 2.14A), similar to those seen in *Temnodontosaurus platyodon* (NHMUK PV

R2003; McGowan, 1974a). Because mechanical preparation has damaged the exposed surfaces of the premaxillae, it is not possible to determine whether a premaxillary fossa was present in any form in NHMUK PV R3000. The preserved portion of the premaxilla of ROM 28964 indicates that a premaxillary fossa was absent at least in the posterior part of the premaxilla (Fig. 2.7).

The premaxillae form a straight median suture that extends for approximately two-thirds of the anteroposterior length of the snout (Fig. 2.4). This proportion is significantly higher than in *Temnodontosaurus platyodon*, where the suture between the premaxillae extends for only approximately 36% of the preorbital (=snout) length (NHMUK PV R2003, R1158), but it is similar to *Ichthyosaurus communis*, where the suture between the premaxillae extends for approximately 58% of the preorbital length (e.g. OUM J.13799). Posterodorsally, the medial wall of the premaxilla inserts into a facet on the nasal (Fig. 2.8A, B) and forms an oblique suture with the dorsal exposure of the nasal (Fig. 2.4). Ventrally, the premaxilla contacts the maxilla with a straight suture (Figs 2.2, 2.7, 2.15B). Posteriorly, the premaxilla bifurcates into two processes – the supranarial process and the subnarial process (Figs 2.2, 2.3, 2.7, 2.14B). The supranarial process forms the anterodorsal margin of the external naris and extends along half of its anteroposterior length. This condition is similar to that in many other Early Jurassic parvipelvians (e.g. Ji et al., 2016: character 1:1), *Macgowania janiceps* (TMP 2009.121.1; Henderson, 2015) and *Mikadocephalus gracilirostris* (PIMUZ T 4376), but different from the condition seen in *Cymbospondylus piscosus* (e.g. UCMP 9950) and *Guizhouichthyosaurus tangae* (e.g. IVPP V11865), where the supranarial process extends posteriorly beyond the posterior margin of the external naris (e.g. Ji et al., 2016: character 1:0). The subnarial process of the premaxilla forms the anterior part of the ventral border of the external naris, overlaps the anterior part of the lateral surface of the lacrimal laterally and extends to approximately the posterior margin of the external naris. This is similar to many other Early Jurassic parvipelvians (e.g. Ji et al., 2016: character 2:0) and *Macgowania janiceps* (TMP 2009.121.1; Henderson, 2015), but different from *Cymbospondylus piscosus* (e.g. UCMP 9950) and *Guizhouichthyosaurus tangae* (e.g. IVPP V 11865), where the subnarial process of the premaxilla is largely reduced (e.g. Ji et al. 2016: character 2:1).

In NHMUK PV R3000 the premaxillae extend 120 mm anterior to the tip of the mandibular symphysis, forming an overbite that comprises approximately 24% of the snout length (495 mm; Fig. 2.14A). This overbite is significantly larger than the well documented, but slight overbites present in *Leptonectes tenuirostris* (McGowan, 1989) and *Pervushovisaurus campylodon* (Fischer, 2016). Only two other ichthyosaur taxa possess extensive overbites: *Excalibosaurus costini* (McGowan, 1986, 2003) and *Eurhinosaurus longirostris* (e.g. McGowan, 1979). In *Excalibosaurus costini* (ROM 47697), the overbite comprises approximately 45% of preorbital (=rostrum) length, while in *Eurhinosaurus longirostris* (SMNS 14931) the overbite forms approximately 60% of the preorbital length. Furthermore, in *Excalibosaurus* and *Eurhinosaurus*, the premaxilla is mediolaterally and dorsoventrally narrow and has a parabolic outline dorsally (e.g. Fischer et al., 2011a). This is in contrast to the condition in NHMUK PV R3000, where the overbite is mediolaterally broad and dorsally rounded.

A cross-section of a broken fragment of the rostrum of ROM 28964 (Fig. 2.11D, E) demonstrates the presence of a dental groove in the premaxilla. The dental groove is formed from alveoli remnants, where the transverse septa separating the posterior and anterior surfaces of successive tooth bases are reduced into dorsoventrally oriented ridges on the inner surfaces of the labial and lingual walls of the dental groove. These ridges demarcate dorsoventrally oriented furrows on both the medial and lateral walls of the dental groove that enclose the tooth bases.

Several historical specimens of Early Jurassic ichthyosaurs from the United Kingdom have been shown to have been manipulated with and assembled into composites (e.g. McGowan, 1990; Massare and Lomax, 2016a). Because the rostrum of NHMUK PV R3000 has been broken in multiple places, and the breaks have subsequently been filled in with plaster (Figs 2.2–2.4), this raises a question of whether the unusual and autapomorphic overbite of NHMUK PV R3000 represents actual anatomy or the result of manipulation. In fact, I believe that NHMUK PV R3000 has not been manipulated with, and present the following lines of evidence to support my view: 1) the major breakages in both the rostrum and mandible are adjacent to each other and the total lengths of the plastered areas are not very different between the upper and lower jaws, so it is very unlikely that the plaster reconstruction affects the relative lengths of the two; 2) the anterior tips of both mandibular rami gently taper anteriorly, and

even though the tip of the mandible is obscured by matrix, no broken bone surfaces are present, which would indicate damage to the anterior tips of the dentaries (Fig. 2.14A); 3) the matrix associated with the anterior portion of the premaxillae contains only premaxillary teeth – I would expect to have at least some dentary teeth preserved in the matrix if the extent of the dentary bones was similar to the premaxillae.

Maxilla. Both maxillae are almost completely preserved in NHMUK PV R3000, except for their most anterior portions, which have been badly damaged and reconstructed in plaster (Figs 2.2–2.3). In ROM 28964 the left maxilla is complete, and acid preparation has revealed many details of its morphology (Figs 2.7, 2.14B). The maxilla is an anteroposteriorly elongated and dorsoventrally narrow bone that forms the posteroventral part of the rostrum. It achieves its greatest dorsoventral height approximately midway along its anteroposterior length and is approximately triangular in lateral view.

The anterior process of the maxilla forms a straight suture with the premaxilla dorsally. The anterior process extends well anterior to the external naris, but does not extend anteriorly beyond the dorsal exposure of the nasals, similar to other Early Jurassic parvipelvians (e.g. Ji et al., 2016: character 3:1), but unlike in *Temnodontosaurus platyodon*, where the anterior process of the maxilla extends anteriorly as far as the dorsal exposure of the nasals (NHMUK PV R1158). Dorsally, the maxilla contacts the lacrimal. Posteriorly, the maxilla possesses a shallow facet for insertion of the anterior process of the jugal (Fig. 14B). The premaxilla excludes the maxilla from participation in the ventral border of the external naris, like in *Ichthyosaurus* and *Temnodontosaurus trigonodon*, but unlike *Macgowania janiceps* (TMP 2009.121.1) and all other Early Jurassic neoichthyosaurians, where the maxilla contributes to the ventral border of the external naris (e.g. Fischer et al., 2016: char. 11:0). A series of anteroposteriorly elongated grooves is located on the lateral surface of the maxilla dorsally in its central part (Fig. 2.14B). A similar set of grooves is present on the lateral surface of the maxilla in *Guizhouichthyosaurus tangae* (e.g. IVPP V11869). However, in this taxon, the grooves are much deeper and end with large, oval neurovascular foramina perforating the lateral surface of the maxilla. In contrast to *G. tangae*, the lateral surface of the maxilla of *Gen. et sp. nov. A* does not bear any foramina.

Lacrimal. The left lacrimal of NHMUK PV R3000 is well preserved (Fig. 2.2), while the right lacrimal is still heavily obscured by matrix (Fig. 2.3). In ROM 28964 the left lacrimal is well preserved and its surface anatomy and relationships with adjacent bones are clearly visible (Figs 2.7, 2.14B).

The lacrimal comprises an anterior process, a dorsally ascending process and a posteroventral process. The anterior process of the lacrimal is overlapped by the subnarial process of the premaxilla laterally and forms the posterior part of the ventral margin of the external naris. The ascending process is anteroposteriorly broad and approximately fan-shaped. Dorsally, it contacts the nasal with an interdigitating suture. Posteriorly it contacts the prefrontal. The posteroventral process of the lacrimal forms a sharp crest posteriorly that forms the anteroventral margin of the orbit. Ventrally, the lacrimal contacts the maxilla anteriorly and is slightly overlapped laterally by the anterior process of the jugal posteriorly. A single, large, centrally placed anterior opening for the nasolacrimal duct is present on the lateral surface of the lacrimal, immediately posterior to the subnarial process of the premaxilla (Fig. 2.14B). The central part of the lateral surface of the lacrimal also bears a depression which is perforated by numerous small to minute neurovascular foramina (Fig. 2.14B). This condition is similar to that observed in other Early Jurassic parvipelvians (e.g. *Temnodontosaurus platyodon* [NHMUK PV R1158], *Ichthyosaurus communis* [e.g. NHMUK PV R39492] and *Stenopterygius quadriscissus* [e.g. OUM JZ 163]). Neurovascular foramina are also present on the lateral surface of the lacrimal in *Shastasaurus pacificus* (UCMP 9017; Sander et al., 2011) and *Guanlingsaurus liangae* (SPCV 03107; Sander et al., 2011) but the foramina of these taxa are larger and far less numerous.

Nasal. The nasals of NHMUK PV R3000 are well preserved in articulation with adjacent bones of the rostrum and skull roof (Figs 2.2–2.4). Part of the lateral surface dorsal to the external naris of both nasals has been broken off and an anteroposteriorly narrow part of the nasals located anterior to the external nares has been reconstructed in plaster. In ROM 28964 both nasals are well preserved, the left nasal in articulation with the rest of the cranium and the right disarticulated (Figs 2.7–2.8).

The nasal forms the posterior part of the rostrum dorsally and contributes to the anterior part of the skull roof. The nasals form a straight, median suture (Fig. 2.4). Anterolaterally, the nasal is overlapped by the premaxilla, as indicated by the presence of an anteroposteriorly elongated and

mediolaterally broad facet clearly visible in the right nasal of ROM 28964 (Fig. 2.8) and partially exposed along the dorsal border of the left external naris in NHMUK PV R3000 (Fig. 2.2). As a result, the dorsal exposure of the nasal is approximately triangular in shape. Anteromedially to the external naris, the dorsal surface of the nasal becomes slightly convex. The internasal depression is located immediately posterior to this convexity, posteromedially to the external naris (Figs 2.7–2.8). The internasal depression is also present in other parvipelvian ichthyosaurs (e.g. Maisch and Matzke, 2000a: character 16:1), *Guanlingsaurus liangae* (SPCV 03107) and '*Callawayia*' *wolonggangense* (SPCV 10305) but it is absent in *Cymbospondylus piscosus* (UCMP 9950) and mixosaurids (e.g. *Mixosaurus panxianensis*, GMPKU-P-1065). The dorsal surface of the internasal depression is perforated by numerous neurovascular foramina (Fig. 2.8). Laterally, immediately posterior to the supranarial process of the premaxilla, the nasal forms part of the dorsal margin of the external naris. The nasal produces a small descending process immediately posterior to the external naris (Fig. 2.8). Posterolaterally, the nasal contacts the lacrimal anteriorly and the prefrontal posteriorly (Fig. 2.8). The posterior part of the nasal is transversely broad, overlaps the anterior portion of the frontal medially, and inserts into a dedicated facet on the anterodorsal surface of the postfrontal laterally (Fig. 2.4). The nasal possibly contacts the parietal posteriorly, although this is only visible on the right side of the skull and it is difficult to determine whether this difference is a preservational artefact or reflects actual anatomy (see Frontal).

Prefrontal. Both prefrontals are preserved in NHMUK PV R3000, but their supraorbital crests have been broken off (Figs 2.2–2.3). The left prefrontal is completely preserved in ROM 28964 (Figs 2.7, 2.14B).

The prefrontal forms the anterodorsal margin of the orbit. Anteriorly, it forms a suture with the lacrimal, but the exact shape of this suture is difficult to determine as the antorbital region in NHMUK PV R3000 has been slightly damaged during preparation (left side) or is obscured by matrix (right side) and the prefrontal/lacrimal contact is also damaged in ROM 28964 (Fig. 2.14B). Dorsally, the prefrontal contacts the nasal anteriorly and the postfrontal posteriorly. A sharp, dorsoventrally thin supraorbital crest projects laterally along the entire length of the prefrontal (Fig. 2.14B). Medially, the prefrontal is

excluded from contact with the frontal by the nasal (Fig. 2.4). This also occurs in *Macgowania janiceps* (TMP 2009.121.1), *Temnodontosaurus platyodon* (NHMUK PV R2003, R1158) and *Leptonectes tenuirostris* (NHMUK PV R498) but differs from *Ichthyosaurus*, *Stenopterygius* (Motani, 2005c) and *Hauffiopteryx* (Marek et al., 2015) in which a medial extension of the prefrontal contacts the frontal laterally.

Frontal. The paired frontals are exposed on the anterior part of the skull roof, and are clearly visible in NHMUK PV R3000 (Figs 2.4, 2.15B). Anteriorly, the frontals are overlapped by the posterior portion of the nasals. It is not clear whether the parietal excludes the frontal from the postfrontal. On the right side, the frontal is clearly excluded from the postfrontal by the parietal, but the skull has been slightly crushed dorsoventrally in this region, which obscures the relationships of bones forming the skull roof. On the left side, the frontal contacts the postfrontal through an anteroposteriorly short suture, but the anterior portion of the parietal is broken off, so the true anterior extent of the parietal cannot be determined (Fig. 2.15B). Posteriorly, the frontals contact the parietals through an oblique suture. The frontals form an anteroposteriorly very short, median suture anteriorly and almost fully enclose the pineal foramen posteriorly (Fig. 2.15B). Because the anterior portions of the parietals are poorly preserved, it is not possible to determine whether the parietals clearly contribute to the posterior margin of the pineal foramen, like in *Temnodontosaurus platyodon* (NHMUK PV R1158), *Leptonectes tenuirostris* (NHMUK PV R498), *Eurhinosaurus longirostris* (SMNS R4085) and *Suevoleviathan disinteger* (SMNS 15390), or whether it is more reminiscent of the condition seen in some specimens of *Ichthyosaurus* (McGowan, 1973) and *Hauffiopteryx* (Marek et al., 2015), where the contribution of the parietals to the margin of the pineal foramen is minimal or absent. The dorsal exposure of the frontals is anteroposteriorly very short and mediolaterally very narrow, which is similar to many other Early Jurassic parvipelvians (e.g. Ji et al., 2016: character 22:1), but differs from *Ichthyosaurus* (Motani, 2005b) and *Hauffiopteryx* (Marek et al., 2015), where the frontals occupy a proportionally much greater area of the skull roof.

Postfrontal. In NHMUK PV R3000 both postfrontals are well preserved and only slightly damaged. The dorsal surface of the left postfrontal is broken posterolaterally and the left postfrontal is also

partially broken along its ventral rim (Figs 2.2, 2.4). Because the right temporal region of NHMUK PV R3000 is dorsoventrally crushed, the posterior part of the right postfrontal is ventrally displaced (Fig. 2.3). The medial margins of both postfrontals are also slightly broken (Fig. 2.4). In ROM 28964, the left postfrontal is only partially preserved, missing most of its medial portion (Fig. 2.7).

The postfrontal can be divided into a medial process, which occupies the anterolateral part of the skull roof, and a posterolateral process which forms the dorsal margin of the orbit (Figs 2.2, 2.4, 2.15). The anterior part of the medial process is offset ventrally from the plane of the skull roof by an angle of approximately 135° and bears a facet into which the posterior portion of the nasal inserts (Figs 2.2, 2.4, 2.15). Anterolaterally, the medial process of the postfrontal contacts the prefrontal (Fig. 2.4). The posterior part of the medial process contacts the parietal laterally. It is not clear whether the medial process of the postfrontal contacts the frontal (see Frontal). Posteriorly, the medial process of the postfrontal forms the anterior margin of the supratemporal fenestra. The posterolateral process of the postfrontal contacts the postorbital posteroventrally and the squamosal posteriorly (Figs 2.2, 2.16). The dorsal surface of the medial process of the postfrontal is transversely divided by a raised, parabolic ridge (Figs 2.4, 2.15B). The surface of the postfrontal lying posterior to this ridge forms the ‘anterior terrace’ of the supratemporal fenestra (Motani, 1999a). The ‘anterior terrace’ is a plesiomorphic character that is present in all Triassic ichthyosaurs known from well preserved cranial material, unlike in post-Triassic ichthyosaurs, where the dorsal surface of the medial process of the postfrontal is not divided by a raised ridge (Motani, 1999a; Maisch and Matzke, 2000a; Ji et al., 2016). However, the ‘anterior terrace’ is formed by the postfrontal, frontal, parietal and sometimes nasal in almost all Triassic ichthyosaurs (Motani, 1999a; Maisch and Matzke, 2000a; Ji et al., 2016), while in *Gen. et sp. nov. A* it is restricted to the postfrontal only. The only other ichthyosaur in which the ‘anterior terrace’ of the supratemporal fenestra is restricted to the postfrontal is the basal parvipelvian *Macgowania janiceps* (TMP 2009.121.1; Henderson, 2015).

Jugal. The left jugal is almost completely preserved in NHMUK PV R3000 (Fig. 2.2), while the right jugal is broken anteriorly and dorsoventrally crushed posteriorly (Fig. 2.3). The jugal is almost completely preserved in ROM 28964, except for its most anterior part, which has been broken off (Figs

2.7, 2.14B). The jugal is a dorsally recurved, anteroposteriorly long and dorsoventrally very narrow bone, situated in the ventral part of the circumorbital region, and forming the ventral margin of the orbit. Anteriorly, the jugal slightly overlaps the lacrimal and the maxilla and terminates posterior to the anterior extent of the lacrimal (Figs 2.2, 2.3). Posterodorsally, the jugal bifurcates into two autapomorphic posterodorsal processes: an anteroposteriorly broad anterior process and an anteroposteriorly narrow posterior process (Fig. 2.15A). Anterodorsally, the ascending portion of the jugal contacts the postorbital and the anterior posterodorsal process of the jugal overlaps the posteroventral process of the postorbital (Fig. 2.15A). It is not clear whether the postorbital excludes the jugal from the quadratojugal in lateral view, as this region is damaged and partially obscured by matrix in NHMUK PV R3000 and the suture lines are not clearly demarcated in this region in ROM 28964. Posteriorly, the jugal forms the anterior portion of the lower temporal arch. Posteroventrally, the jugal forms a posteroventral process (Fig. 2.15A), which is a plesiomorphic character shared only with *Parvinatator wapitiensis* (TMP 89.127.8; Nicholls and Brinkmann, 1995), *Cymbospondylus piscosus* (e.g. UCMP 9950) and *Mixosaurus panxianensis* (e.g. GMPKU-P-1033; Jiang et al., 2006). A series of anteroposteriorly elongated striations is located anteroventral to the posteroventral process in both NHMUK PV R3000 and ROM 28964 and could indicate the presence of a membranous lower temporal bar in *Gen. et sp. nov. A*. The presence of a similar bar has been hypothesised for some primitive ichthyosaurians (Liu et al., 2011).

Postorbital. The left postorbital is completely preserved in NHMUK PV R3000 (Fig. 2.2), while the right postorbital is badly crushed (Fig. 2.3). The left postorbital is well preserved in ROM 28964, but the sutures it forms with adjacent bones of the temporal region are not well demarcated (Fig. 2.7). The postorbital forms the anterodorsal part of the temporal region and the posterior margin of the orbit (Fig. 2.15A). Anterodorsally, the postorbital contacts the postfrontal, but the nature of this contact is not clear, because the bone surface in this region is broken in NHMUK PV R3000 and the postfrontal-postorbital suture is not well demarcated in ROM 28964. Posterodorsally, the postorbital contacts the squamosal. Ventrally, the postorbital forms a parabolic contact with the jugal (Fig. 2.15B). *Gen. et sp. nov. A* possesses a posteroventral process of the postorbital, a feature it shares with some specimens of

Ichthyosaurus communis (e.g. NHMUK PV R3372; Maisch and Matzke, 2000b). The lateral surface of the posteroventral process is overlapped by the anterior part of the posterodorsal process of the jugal. Posteriorly, the posteroventral process of the postorbital overlaps the anterior part of the lateral surface of the posterior posterodorsal process of the jugal. The posterior margin of the posteroventral process of the postorbital contacts the quadratojugal.

Parietal. The paired parietals form the central and posterior part of the skull roof and are well preserved in NHMUK PV R3000, except for the dorsal surfaces, which have been broken off (Figs 2.4, 2.15). The parietal can be divided into an anterior process and a posterolateral process. The posterolateral process is laterally offset from the anterior process at an angle of approximately 135°. The parietals form a straight, median suture. The dorsal surfaces of the parietals are inclined medially and form an anteroposteriorly oriented, longitudinal ridge, which is elevated slightly beyond the plane of the skull roof in lateral view (Figs 2.2, 2.15A), and forms the 'sagittal eminence' (Motani, 1999a). A similar, low parietal eminence is also present in some shastasaurids (e.g. *Guizhouichthyosaurus tangae* [IVPP V11865], '*Callawayia*' *wolonggangense* [SPCV 10306], *Guanlingsaurus liangae* [SPCV 03107] and *Shastasaurus pacificus* [UCMP 9017]), *Callawayia neoscapularis* (TMP 94.380.11; Nicholls and Manabe, 2001), *Qianichthyosaurus zhoui* (Maisch et al., 2008), and some parvipelvian ichthyosaurs (e.g. Ji et al., 2016: character 21). This is in contrast to the tall sagittal eminence in *Cymbospondylus piscosus* (e.g. UCMP 9950) and mixosaurids (Ji et al., 2016: character 21:2). Anteriorly, the parietals form a fork of around 60°. The parietal fork contacts the frontals for most of its length, and possibly contributes to the posterior margin of the pineal foramen, although the preservation of the anterior portion of the parietals does not allow for an accurate assessment (see Frontal; Fig. 2.15B). Similarly, it is difficult to determine whether the parietal contacts the nasal anteriorly, as this contact is only visible on the right side of the skull (see Nasal). Laterally, the parietal contacts the medial portion of the postfrontal anteriorly and forms the medial margin of the supratemporal fenestra posteriorly. The posterolateral process of the parietal contacts the anteromedial process of the supratemporal along an interdigitating suture (Figs 2.4, 2.15B). The anterolateral margin of the posterolateral process is elevated into a longitudinal ridge ('parietal ridge' of Motani [1999a]), a feature shared with mixosaurids (e.g. Ji

et al., 2016: character 33), *Callawayia neoscapularis* (TMP 94.380.11; Nicholls and Manabe, 2001) and many Early Jurassic parvipelvians (e.g. Ji et al., 2016: character 33).

Supratemporal. Both supratemporals are preserved in NHMUK PV R3000, but most of the anterolateral process of the left supratemporal is broken off (Fig. 2.4) and the right supratemporal is badly crushed (Figs 2.3, 2.6). As in many other ichthyosaurs (e.g. *Ichthyosaurus* [McGowan, 1973]), the supratemporal is a triradiate bone located in the posterior part of the temporal region (Fig. 2.6). The supratemporal is divided into an anterolateral process, an anteromedial process and a descending process. The anterolateral process of the supratemporal forms the posterolateral margin of the supratemporal fenestra and its lateral surface is overlapped by the postorbital anteriorly and squamosal posteriorly. The anteromedial process is short, forms the posteromedial margin of the supratemporal fenestra and contacts the posterolateral process of the parietal with an interdigitating suture. The ventral process of the supratemporal contacts the medial surface of the quadrate dorsally.

Squamosal. The left squamosal is well preserved in NHMUK PV R3000, but its dorsal margin is broken off (Figs 2.2, 2.15A). The squamosal is a small bone in the shape of an isosceles triangle, situated in the posterodorsal corner of the temporal region. The squamosal overlaps the lateral surface of the posterolateral process of the postfrontal anterorodorsally, overlaps the lateral surface of the anteromedial process of the supratemporal posterodorsally and extensively overlaps the anterior part of the lateral surface of the quadratojugal (Fig. 2.9A). This is in contrast to *Ichthyosaurus* (e.g. Motani, 2005c), in which the squamosal is small and most of the lateral surface of the quadratojugal is clearly exposed. Anteriorly, the squamosal contacts the postorbital. The triangular shape of the squamosal is a character shared by *Gen. et sp. nov. A* with other Early Jurassic parvipelvians, including *Ichthyosaurus* (Motani, 2005c), and is in contrast to the irregular shape of the squamosal seen in more basal ichthyosaurs (e.g. Ji et al., 2016: character 24).

Quadratojugal. The left quadratojugal is well preserved in articulation with adjacent bones of the temporal region in NHMUK PV R3000 (Figs 2.2, 2.4, 2.15A). In ROM 28964, the left quadratojugal is also preserved in articulation (Fig. 2.7), whereas the right one is completely disarticulated (Fig. 2.9). The main body of the quadratojugal has the form of an anteroposteriorly and dorsoventrally broad sheet

of bone, slightly recurved laterally. Its lateral surface is extensively covered by small pits and striations (Fig. 2.9A), which mark the position of facets for the reception of the squamosal and postorbital. Posteroventrally, the quadratojugal forms a transversely broad and dorsomedially inclined quadrate process, for reception of the quadrate condyle. The articular surface of the quadrate process is sub-oval in posterior view (Fig. 2.9B), concave and covered in pits and ridges, suggesting extensive cartilage covering. The ventral margin of the quadratojugal is concave and forms the posterior portion of the lower temporal arch. Because the ventral part of the temporal region is not well preserved in NHMUK PV R3000 and ROM 28964 it is not possible to determine whether the jugal contacted the quadratojugal slightly or whether this contact was absent. Because of the extensive overlap by the squamosal and postorbital, only a small, dorsoventrally tall and anteroposteriorly narrow exposure of the quadratojugal is visible in lateral view. This condition is shared with *Ichthyosaurus*, *Stenopterygius*, *Aegirosaurus* and *Ophthalmosaurus* (Maisch and Matzke, 2000a) and indicates an anteroposteriorly shortened postorbital region, in comparison to an elongated postorbital region reported from many basal ichthyosaurs (e.g. Ji et al., 2016: character 31).

Quadrate. Both quadrates are preserved in articulation in NHMUK PV R3000, although the right quadrate is dorsoventrally crushed and its surfaces are heavily abraded (Figs 2.2–2.3, 2.6). A disarticulated left quadrate is preserved in ROM 28964 (Fig. 2.10). The quadrate is located in the posterior part of the temporal region and forms the cranial component of the cranio-mandibular joint. The main body of the quadrate is anteroposteriorly and dorsoventrally broad and slightly recurved medially. The dorsal margin of the quadrate is convex and possesses a longitudinal groove, as in *Ichthyosaurus* (McGowan, 1973; Fig. 2.10A, C). Like in other ichthyosaurs the quadrate becomes mediolaterally thick ventrally and forms the articular condyle. A deep, longitudinal groove runs along the anteroposterior length of the condyle ventrally (Fig. 2.10B, D). Posterolaterally, the condyle bears an articular surface for the articular. The lateral surface of the quadrate is slightly concave. A low, anteroventrally oriented ridge extends from the posterior margin of the quadrate anteriorly, and terminates roughly halfway along the quadrate's anteroposterior length (Fig. 2.10C, D). An ovate area for articulation with the quadrate process of the quadratojugal is present on the lateral surface of the

quadrate, immediately dorsally to the articular surface of the condyle (Fig. 2.10C, D). The medial surface of the quadrate is slightly convex, but its surface is heavily abraded in ROM 28964, obscuring anatomical details. However, it is clearly visible in NHMUK PV R3000, that the medial surface of the quadrate contacted the lateral surface of the descending process of the supratemporal dorsally, the distal part of the stapes at roughly mid-anteroposterior height, and the posterolateral process of the pterygoid, ventrally (Fig. 2.6).

Vomer. The paired vomers are visible in ventral view in NHMUK PV R3000 (Fig. 2.5) and form the anteromedial part of the palate. The vomers are dorsoventrally compressed, sheet-like bones that taper anteriorly and are roughly triangular in shape, with the obtuse angle located posteromedially. The vomers form a straight, median suture. Anterolaterally, the vomer forms a straight suture with the premaxilla and forms the medial margin of the internal naris immediately posterior to this contact. Posterolaterally, the vomer overlaps the anterior portion of the palatine. Posteriorly, the vomer forms an anteromedially oriented, straight suture with the horizontal plate of the pterygoid.

Palatine. The palatines are visible in palatal view in NHMUK PV R3000 (Fig. 2.5) and form the lateral parts of the palate. Like the vomers, the palatines are dorsoventrally compressed, plate-like bones, similar to the ones in *Ichthyosaurus* (McGowan, 1973) and *Stenopterygius* (Owen, 1881). The palatine tapers anterolaterally into an anteroposteriorly elongated and mediolaterally narrow process, which forms the anterolateral border of the palate. Medially, the anterolateral process contacts the premaxilla via a straight suture anteriorly and forms the lateral margin of the internal naris immediately posterior to this. Anteromedially, the palatine is overlapped by the posterior portion of the vomer. Posteromedially, the palatine is slightly overlapped by the transverse plate of the pterygoid.

Pterygoid. The paired pterygoids are well preserved in NHMUK PV R3000. As in other ichthyosaurs, they form the major part of the palate (Fig. 2.5) and are similar in morphology to pterygoids described for *Ichthyosaurus* (McGowan, 1973). Posteriorly, the pterygoid forms a posterolateral process, a posteromedial process and an ascending process (Fig. 2.6). The posteromedial process is dorsoventrally compressed, tapers slightly medially and is oriented slightly ventromedially. The posterolateral process of the pterygoid is dorsoventrally compressed, oriented slightly ventrolaterally and contacts the medial

surface of the quadrate, dorsally. The ascending process of the pterygoid is mediolaterally compressed and also contacts the medial surface of the quadrate. Anteriorly to the three processes, the pterygoid becomes mediolaterally constricted. Anterior to this constriction, the pterygoid forms an anteroposteriorly elongated and anteriorly tapering horizontal plate, which is slightly inclined dorsomedially. Posteriorly, the medial margin of the horizontal plate is concave and forms the lateral margin of the interpterygoid vacuity (Figs 2.5, 2.16C). The basisphenoid contacts the pterygoid along the lateral margins of this vacuity. More anteriorly, the horizontal plates of both pterygoids form a straight, median suture. The parabasisphenoid contacts the pterygoids immediately posterior to this suture. Anterolaterally, the horizontal plate of the pterygoid contacts the posterior portion of the vomer via a straight, posterolaterally oriented suture. Laterally, the horizontal plate of the pterygoid slightly underlaps the medial portion of the palatine, with which it forms a slightly laterally recurved suture.

Epipterygoid. Only the distal part of the left epipterygoid is partially exposed in the interpterygoid vacuity in NHMUK PV R3000 (Figs 2.5, 2.16C). The epipterygoid is preserved in articulation and is still heavily covered in matrix, which obscures anatomical details. Nevertheless, it is likely that the morphology of the epipterygoid was similar to that described for *Ichthyosaurus* (McGowan, 1973).

Basisphenoid and parabasisphenoid. The basisphenoid is well preserved in NHMUK PV R3000, but it is still heavily obscured by matrix so that it is only exposed in palatal and posterodorsal views (Figs 2.5–2.6, 2.16C). The morphology of the basisphenoid is very similar to that described for *Ichthyosaurus* (McGowan, 1973). The basisphenoid forms part of the ventral wall of the braincase and its ventral surface occupies the posterior part of the interpterygoid vacuity (Fig. 2.16C). In posterior view, the rugose, anterodorsally inclined posterior surface of the basisphenoid is partially exposed (Fig. 2.6). A deep, median furrow for reception of the basioccipital peg of the basioccipital is clearly visible along the posterior surface. In palatal view, the paired, anterolaterally oriented and ventrally inclined basipterygoid processes are clearly visible (Figs 2.5, 2.15C). The basipterygoid processes are short, similar to those in other Early Jurassic parvipelvians, but unlike the laterally expanded basipterygoid processes of ophthalmosaurids (Fischer et al., 2011b: character 18). The basipterygoid processes contact the medial margins of the horizontal plates of the pterygoids, posteriorly. A large, single, oval foramen

for the internal carotid artery is clearly visible in the posterior part of the ventral surface of the basisphenoid (Figs 2.5, 2.16C). A single foramen for the internal carotid artery is also present in some other Early Jurassic parvipelvians, such as *Ichthyosaurus* (McGowan, 1973) and *Stenopterygius* (NHMUK PV R 33157; Owen, 1881), but unlike in *Temnodontosaurus* sp. (e.g. *T. trigonodon* [SMNS 50000], *T. azerguensis* [Martin et al., 2012]) and the basal parvipelvian *Macgowania janiceps* (TMP 2009.121.1).

The parabasisphenoid is an anteroposteriorly elongated, rod-like bone, which is well co-ossified with the basisphenoid and extends anteriorly from its anteroventral part along the ventral midline of the skull (Figs 2.5, 2.16C). Anteriorly, the parabasisphenoid contacts the horizontal plates of the paired pterygoids, immediately posterior to the interpterygoid median suture.

(?) Opisthotic. Partially exposed bones are preserved medially to the descending process of the supratemporal and dorsally to the stapes on both sides of NHMUK PV R3000 (Fig. 2.6). These bones are similar in position and proportions to the opisthotics described for *Ichthyosaurus* (McGowan, 1973). However, because the bone surfaces of these elements are entirely broken and the elements are heavily obscured by matrix, their exact identity and morphology cannot be determined with confidence.

Stapes. The left stapes is preserved in NHMUK PV R3000 (Fig. 2.6). However, its surfaces are heavily damaged, so it is not possible to describe its precise morphology. The proximal and distal ends of the stapes are comparable in size, similar to other Early Jurassic parvipelvians, but different from ophthalmosaurids, where the proximal stapedial head is greatly expanded (Fischer et al., 2013: character 24). The distal end of the stapes contacts the medial surface of the quadrate at approximately half of its dorsoventral height. Ventrally, the stapes contacts the dorsal surface of the posterolateral process of the pterygoid, but this is most likely a preservational artefact (the stapes does not contact the pterygoid in three-dimensionally preserved specimens of *Ichthyosaurus*; McGowan, 1973). A putative opisthotic is located anterodorsally to the stapes, but it is not clear whether there is any contact between these two bones.

Dentary. Only the anterior portion of the left dentary is preserved in NHMUK PV R3000 (Fig. 2.2). Its posterior part is broken and partially reconstructed in plaster. The right dentary of NHMUK PV R3000 is also incomplete, with its anterior and middle portions damaged and reconstructed in plaster (Fig. 2.3). The left dentary is partially preserved in ROM 28964, with its anterior portion broken off (Fig. 2.7). The dentary is an anteroposteriorly elongated bone which forms the lateral surface of the anterior part of the mandibular ramus. The dorsoventral height of the dentary remains approximately constant anteriorly, but decreases gradually posterior to the level of the external naris. Posteriorly, the dentary extends to the mid-orbital region. The lateral wall of the dentary is convex, and the dentary is slightly recurved laterally, which is clearly visible in ventral view (Fig. 2.5). The dentary overlaps the anterior portion of the surangular laterally. Anteroventrally and medially, the dentary forms a laterally recurved suture with the splenial. A shallow, dorsoventrally narrow dentary fossa is present throughout the entire length of the preserved portion of the dentary in ROM 28964 (Fig. 2.7). Similar to the premaxilla, a dental groove (see Premaxilla) is also present in the dentary, as evidenced by a broken rostrum fragment of ROM 28964 (Fig. 2.11D, E).

Splenial. Both splenials are well preserved in NHMUK PV R3000, but have been damaged in the posterior part of the mandibular symphysis and have been subsequently reconstructed in plaster (Fig. 2.6). The posteroventral surface of the right splenial in NHMUK PV R3000 is broken off. In ROM 28964, only the posterior portion of the left splenial is preserved (Fig. 2.7). The splenial is a thin, anteroposteriorly elongated, sheet-like bone which forms the ventral and medial surfaces of the mandibular ramus. Anteriorly, the splenials reach the tip of the mandibular ramus and are united along the ventral midline of the skull to form the mandibular symphysis. The mandibular symphysis is ca. 220 mm in anteroposterior length, which accounts to approximately 33% of mandibular ramus length (660 mm). Posteriorly, the splenial becomes laterally recurved and extends along the ventromedial surface of the mandibular ramus, overlapping the medial surface of the angular. Posterodorsally, the splenial forms a short contact with the prearticular.

Surangular. Both surangulars are well preserved in NHMUK PV R3000 (Figs 2.2–2.3, 2.5). In ROM 28964, the left surangular is well preserved, but its posterior part is slightly broken (Fig. 2.7). The

surangular forms the lateral surface of the posterior part of the mandibular ramus. It is overlapped by the dentary anterodorsally. Ventrally, it forms a posterodorsally oriented, parabolic suture with the angular along its entire anteroposterior length. Posteriorly, the lateral surface of the articular attaches to the medial surface of the surangular. A deep, anteroposteriorly short surangular fossa is clearly present on the lateral surface of the surangular. It is located ventral to the posterior part of the orbit and forms the posterior extension of the dentary fossa (Figs 2.2, 2.7). The surangular also forms a low coronoid process, which can be observed on the left lateral side of NHMUK PV R3000, posteroventrally to the posterior process of the jugal (Fig. 2.14A). An anteroposteriorly elongated, ovoid depression is present dorsally on the posterolateral surface of the surangular. This depression is rugose and bordered ventrally by a prominent ridge and most likely marks the main insertion for *musculus depressor mandibulae* (McGowan, 1973). Anteroventrally to this depression, the surangular is perforated by numerous minute neurovascular foramina.

Angular. Both angulars are well preserved in NHMUK PV R3000 (Figs 2.2–2.3, 2.5). In ROM 28964 only the left angular is partially preserved, with its posterior margin slightly broken (Fig. 2.7). The angular forms the posteroventral part of the lateral and medial surfaces of the mandibular ramus. The lateral exposure of the angular is dorsoventrally narrow anteriorly, but becomes dorsoventrally broader posteriorly. However, the maximum dorsoventral height of the angular is smaller than the maximum dorsoventral height of the surangular. A similar condition is present in many Triassic ichthyosaurs, and in *Ichthyosaurus* and *Stenopterygius*. This is in contrast to the condition seen in some other Early Jurassic parvipelvians and ophthalmosaurids, where the lateral exposures of the surangular and angular are of roughly equal dorsoventral dimensions (e.g. Ji et al., 2016: character 47). Dorsally, the angular forms a posterodorsally oriented, parabolic suture with the surangular, along its entire anteroposterior length. Medially, the angular is overlapped by the splenial anteriorly and forms a posterodorsally oriented, parabolic suture with it.

Prearticular. The prearticulars are preserved in NHMUK PV R3000 (Figs 2.6, 2.16A). The prearticular is an anteroposteriorly elongated, dorsoventrally narrow, mediolaterally compressed, splint-like bone, located in the posterodorsal part of the medial surface of the mandibular ramus. Anteriorly, the

prearticular is overlapped by the splenial. Ventrally, it is overlapped by the angular. Posterodorsally, it contacts the articular.

Articular. Both articulars are well preserved in articulation in NHMUK PV R3000, but the medial surface of the left articular is slightly broken (Figs 2.6, 2.16A). The articular forms the mandibular glenoid and the dorsomedial surface of the retroarticular process. As in other ichthyosaurs, the articular is a small, mediolaterally compressed element which attaches to the medial surface of the posterior part of the surangular. Anteriorly, the articular has an anteromedially oriented articular surface for reception of the quadrate condyle. A dorsoventrally oriented ridge separates the articular surface from the concave, medial surface. The retroarticular process of the mandibular ramus is elongated in comparison to other ichthyosaurs and comprises 9% of the mandibular ramus length – an autapomorphy of *Gen. et sp. nov. A.*

The elongated retroarticular processes could potentially be a preservational artefact, as the mandible could have been displaced from the cranium during diagenesis. I believe this not to be the case, as: 1) the quadrates are preserved in articulation with the articular bones (Fig. 2.6); and 2) the dentition is preserved in life position - if the mandible was diagenetically displaced from the cranium, I would expect the articular and quadrate not to be in articulation and the teeth to be displaced.

Scleral/sclerotic ring. The complete left scleral/sclerotic ring is preserved in NHMUK PV R3000, but it is slightly crushed dorsoventrally and its outer margin is heavily obscured by matrix (Fig. 2.2). In ROM 28964, the complete left scleral ring is preserved in three dimensions, but the external surfaces of many ossicles are crushed and/or broken (Figs 2.7, 2.16D). The morphology of the scleral ossicles is similar to that seen in other ichthyosaurs. Each comprises a flat, trapezoidal lateral surface and a peripheral surface set off from the lateral surface at an obtuse angle. The contiguous and outer margins of the ossicles have crenulated/denticulated margins. The scleral ring of NHMUK PV R3000 comprises 13 ossicles. This is within the range recorded for the majority of parvipelvian ichthyosaurs (e.g. 13 in *Temnodontosaurus platyodon* [ROM 7972], 12-16 in *Ichthyosaurus* [McGowan, 1973], 14 in *Ophthalmosaurus natans* [CM 878], 13-14 in *Platypterygius australis* [Kear, 2005]) and is smaller than the number of scleral ossicles in more basal ichthyosaurs, such as cymbospondylids (e.g. 16 in

Xinminosaurus catactes [GMPKU-P-1206]), mixosaurids (up to 19 [McGowan and Motani, 2003]), and shastasaurids (e.g. ~15 in *Guizhouichthyosaurus tangae* [IVPPV 11869]).

Teeth. Many teeth are preserved in situ in NHMUK PV R3000, but most of them are damaged and/or are partially obscured by matrix. Numerous teeth are preserved in situ or disarticulated in ROM 28964, but the dentition preserved in situ is partially obscured by matrix and many of the disarticulated teeth are badly damaged. The teeth of *Gen. et sp. nov. A* are dorsoventrally elongated and recurved lingually, as in other ichthyosaurs. The most complete, disarticulated tooth of ROM 28964 (Fig. 2.11A–C) measures 42.8 mm in apicobasal height, of which 16.5 mm (ca. 40%) is the crown height. The crown is conical, sub-circular in cross-section, with a pointed apex. Fine, apicobasal ridges cover the surface of the crown and these ridges are separated by fine, apicobasal grooves (Fig. 2.16B). The tooth base is sub-circular in cross-section and covered in relatively mediolaterally broad, longitudinal ridges, which are separated by mediolaterally narrow, deep grooves. Many isolated teeth of ROM 28964 have resorption pits located lingually at the bases of the roots and numerous replacement teeth are also preserved in the form of enamel cones displaced from replacement alveoli. In NHMUK PV R3000, the largest teeth are located in the posterior part of the dentary and decrease in size both anteriorly and posteriorly. Because the dentition is only partially preserved in both known specimens of *Gen. et sp. nov. A*, it is not possible to give an accurate tooth count.

Centra. Three centra are preserved in ROM 28964. One centrum (labelled ‘V3’; Fig. 2.12A–E) is well preserved, with slightly abraded bone surfaces on its left side. It is roughly pentagonal in anterior/posterior view and its apophyses are weakly developed. The dorsoventrally elongated, roughly ovoid, dorsolaterally oriented diapophyses are confluent with the hourglass-shaped floor of the neural canal, which indicates this centrum was located in the anterior cervical region (McGowan and Motani, 2003). The second centrum (labelled ‘V2’; Fig. 2.12F–J) is not as well preserved as the first one, with its right side heavily distorted and broken. This centrum is also roughly pentagonal in anterior/posterior view, and its diapophyses are also confluent with the floor of the neural canal, which indicates its origin from the posterior cervical/anterior dorsal series. Furthermore, because the dimensions of this centrum are slightly greater than those of the ‘V3’ centrum, this centrum was most likely located posterior to the

‘V3’ centrum in the cervical series. The third centrum (‘V1’; Fig. 2.12K–O) is heavily distorted with badly damaged surfaces. However, the prominent, well developed apophyses located in the dorsal half of the centrum and facets for the neural arch, which are slightly raised above the floor of the neural canal, indicate that centrum ‘V1’ was part of the anterior dorsal series.

Atlantal intercentrum. An atlantal intercentrum is preserved in ROM 28964. The atlantal intercentrum is mediolaterally broader than it is anteroposteriorly long and is roughly triangular in dorsal/ventral view (Fig. 2.12P–Q). The ventral surface of the atlantal intercentrum is markedly convex (Fig. 2.12R), with its posterior slope anteroposteriorly longer than the anterior slope. The atlantal intercentrum has an anterodorsally oriented facet for articulation with the basioccipital condyle. Posterodorsally, the atlantal intercentrum forms a facet for the ventral portion of the atlantal centrum.

Neural arches. Many partially preserved neural arches are associated with ROM 28964 (Fig. 2.12S–V). As in other ichthyosaurs, the pedicels of the neural arches form anteroposteriorly elongated, mediolaterally broad, roughly ovoid articular surfaces. These contact corresponding facets on both sides of the floor of the neural canal on the dorsal surface of the vertebral centra. The prezygapophyses have anterodorsally oriented, unpaired facets. The postzygapophyseal facets face posteroventrally. The neural spines are mediolaterally compressed, as in most ichthyosaurs, but different from the neural spines of shastasaurids (e.g. Merriam, 1908), which are circular in cross-section.

Ribs. Many partial anterior caudal ribs are preserved in ROM 28964. Like in other ichthyosaurs, the anterior caudal ribs are dorsoventrally elongated and slightly anteroposteriorly compressed distally. They achieve their greatest anteroposterior length proximally. The dorsal surfaces of the anterior caudal rib heads possess two depressions for articulation with the rib facets on corresponding vertebral centra. The anterior caudal rib heads also possess a median constriction, which gives them an 8-shape in dorsal view. One posterior caudal rib is also preserved in ROM 28964. As in other ichthyosaurs, the proximal surface of the rib head is slightly concave and roughly circular in dorsal view. The anteroposterior length of this rib increases ventrally. The posterior caudal rib is mediolaterally compressed and possesses a small process extending from its medial surface.

Humerus. The right humerus is well preserved in ROM 28964 (Fig. 2.13), with only the posterior part of the distal end broken off. The humerus is proximodistally longer than anteroposteriorly wide (proximodistal length:anteroposterior width ratio of 1.68). Its proximal and distal ends have roughly equal anteroposterior lengths, as in *Ichthyosaurus*, but in contrast to all other Early Jurassic parvipelvians (e.g. Ji et al., 2016: character 85). The humerus possesses a low dorsal process protruding from its proximodorsal surface, and a low deltopectoral crest extending anteroventrally from its proximoventral surface. The low dorsal process and low deltopectoral crest are similar to those seen in many other Early Jurassic parvipelvians, but are markedly different from the protruding dorsal process and deltopectoral crest seen in ophthalmosaurids (Motani, 1999a: character 56; Fischer et al., 2011b: character 31, respectively). Anteriorly, the humerus possesses a reduced anterior flange (Ji et al., 2016: character 82), which forms a dorsoventrally thickened, rounded anterior margin, separated from the rest of the humeral shaft by a proximodistally elongated depression (Fig. 2.13A–D). A similar reduced anterior flange of the humerus is also present in *Ichthyosaurus* (Motani, 1999c). The anterodistal margin of the humerus forms a convexity, which is also present in *Temnodontosaurus* spp., leptonectids, *Stenopterygius* and *Hauffiopteryx*, but is absent in *Suevoleviathan* and *Ichthyosaurus*, where the anterodistal part of the humerus forms an acute angle in dorsal/ventral view (Fischer et al., 2013: character 44). In *Gen. et sp. nov. A* the mediolateral width of this anterodistal convexity decreases anteriorly, but it is difficult to compare this character state with that of other Early Jurassic ichthyosaurs, due to their mostly two-dimensional preservation, with the humeri often embedded within the rock matrix. The posterior margin of the humerus is concave and has the form of a sharp crest (Fig. 2.13E). A roughly round-shaped tubercle is present on the ventral surface of the humerus, immediately distal to the distal extent of the deltopectoral crest (Fig. 2.13C–E). Two shallow, concave facets are present in the distal part of the humerus, the anterior one for the radius and the posterior one for the ulna. They are both roughly equal in anteroposterior length and dorsoventral width.

DISCUSSION

Comparison with the genus *Ichthyosaurus*. Both the holotype (NHMUK PV R3000) and referred specimen (ROM 28964) of *Gen. et sp. nov. A* were previously referred to the genus *Ichthyosaurus*.

However, *Gen. et sp. nov. A* possesses four autapomorphies (see Diagnosis) and the following discrete characters are clearly present in at least one specimen of *Gen. et sp. nov. A*, but are not present in *Ichthyosaurus*: 1) the posteroventral process of the jugal (e.g. McGowan, 1973); 2) the anterior terrace of the supratemporal fenestra (e.g. Motani, 2005c). Furthermore, *Gen. et sp. nov. A* possesses an anteroposteriorly short and mediolaterally narrow dorsal exposure of the frontal - this exposure is more extensive in *Ichthyosaurus* (e.g. McGowan, 1973; Motani, 2005c); and the squamosal of *Gen. et sp. nov. A* is large, whereas the squamosal is greatly reduced in size in *Ichthyosaurus*, exposing the lateral surface of the supratemporal (e.g. NHMUK PV R10021). In addition to these observations, a phylogenetic analysis, using the Jiang et al. (2016) data matrix (Chapter 5), does not find *Gen. et sp. nov. A* as the sister taxon of *Ichthyosaurus*. Together, these findings provide strong evidence for the generic separation of *Gen. et sp. nov. A* and *Ichthyosaurus*.

Comparison with other ichthyosaurs from the Lower Lias of the United Kingdom. In addition to possessing four discrete autapomorphies (see Diagnosis) and two plesiomorphies that have not been observed in any other Early Jurassic ichthyosaur (see Diagnosis), *Gen. et sp. nov. A* differs from representatives of Leptonectidae (the genera *Leptonectes* and *Excalibosaurus*; see McGowan, 1986, 1989, 2003) by the possession of: 1) a laterally oriented temporal region, compared with the posteriorly oriented temporal region of leptonectids (e.g. Motani, 1999a:character 25); 2) a mediolaterally broad rostrum, compared to the mediolaterally narrow and elongated rostrum of leptonectids (e.g. Fischer et al., 2011a); 3) large teeth with crown striations, as opposed to small dentition with smooth crowns in leptonectids (e.g. Druckenmiller and Maxwell, 2010: character 25); and 4) a humerus in which the distal and proximal extremities are approximately equal in anteroposterior length – in leptonectids the anteroposterior length of the distal part of the humerus is much greater than that of the proximal region (e.g. McGowan, 1989).

Gen. et sp. nov. A also differs from *Temnodontosaurus* by the possession of: 1) an anteroposteriorly longer premaxillary suture (66% of preorbital length, compared with 36% in *Temnodontosaurus* [e.g. NHMUK PV R1158, 2003]); 2) maxilla anterior process reduced, compared with an anteriorly elongated maxilla anterior process, which extends anteriorly to the posterior end of

the premaxillary suture in *Temnodontosaurus* (e.g. NHMUK PV R1158, 2003); and 3) a humerus in which the distal and proximal extremities are approximately equal in anteroposterior length – in *Temnodontosaurus* the anteroposterior length of the distal part of the humerus is much greater than that of the proximal region (NHMUK PV R2003).

Palaeoecology of *Gen. et sp. nov. A*. A quantitative analysis of the palaeoecology of *Gen. et sp. nov. A*, and a comparative analysis of the palaeoecology of the Lower Lias ichthyosaur fauna in general, is beyond the scope of the present contribution. However, some conclusions can be drawn from the qualitative anatomical observations presented here. The dental morphology of *Gen. et sp. nov. A*, with robust, conical crowns and a rounded tooth apex, suggests it represents the smash feeding guild of Massare (1987) with a diet most likely consisting of dibranchiate cephalopods and fish. Other than the enlarged retroarticular process, the muscle scars and origin/insertion points on the mandible of *Gen. et sp. nov. A* are comparable to those described for *Ichthyosaurus* (McGowan, 1973). However, the most peculiar feature of *Gen. et sp. nov. A* – its overbite – is unique amongst ichthyosaurs. *Gen. et sp. nov. A* represents the only ichthyosaur lineage except for leptonectids which evolved a moderate to large overbite. Predatory (McGowan, 1979) and sensory (Riess, 1986) functions have been previously suggested for the overbites of leptonectids. However, the rostrum of *Gen. et sp. nov. A* has the proportions of a 'typical' ichthyosaur snout and is quite robust and mediolaterally broad, rather than slender and mediolaterally narrow, like in leptonectids. This makes it unlikely that the overbite in *Gen. et sp. nov. A* functioned like those of leptonectids. Fischer (2016) described slight overbites in *Pervushovisaurus campylodon*, a Late Cretaceous platypterygiine ichthyosaur. However, the extent of this overbite is much smaller than the one observed in *Gen. et sp. nov. A* and its ecological significance remains unknown.

It is possible that the overbite played an important function in the feeding ecology of *Gen. et sp. nov. A* and the elongated retroarticular processes could have evolved to accommodate jaw function with the extensive overbite. Unfortunately, because of the lack of fossil or extant marine analogs possessing a similar overbite and mandibular anatomy, it is not possible to determine how the overbite functioned during prey capture and manipulation.

Taxonomic diversity of ichthyosaurs from the Lower Lias of the United Kingdom. The recognition of *Gen. et sp. nov. A* as a distinct genus confirms the preliminary findings of Motani (2005c) of unrecognized generic diversity within the Lower Lias ichthyosaur fauna. Our findings, together with other recent work (see Introduction), show that the generic diversity of ichthyosaurs from the Lower Jurassic of the United Kingdom had been underestimated.

Earlier taxonomic revisions of Lower Lias ichthyosaurs were based mostly on continuous characters of the skull, the ranges of which would frequently overlap between taxa, leaving ambiguity when assigning specimens to particular taxa (e.g. McGowan 1974a, 1974b, 1989; McGowan and Motani, 2003). Our work on *Gen. et sp. nov. A*, together with the recent revision of *Ichthyosaurus conybeari* (Massare and Lomax, 2016) and the erection of new species of *Ichthyosaurus – I. anningae* (Lomax and Massare, 2015), *I. larkini* and *I. somersetensis* (Lomax and Massare, 2016), indicate that taxonomically informative, and previously unrecognized, variation in discrete morphological characters is present among Lower Lias ichthyosaurs. This finding necessitates further study and revision of the Lower Jurassic ichthyosaur fauna of the United Kingdom to achieve a better understanding of ichthyosaur diversity and evolution in this time period.

FIGURES AND TABLES

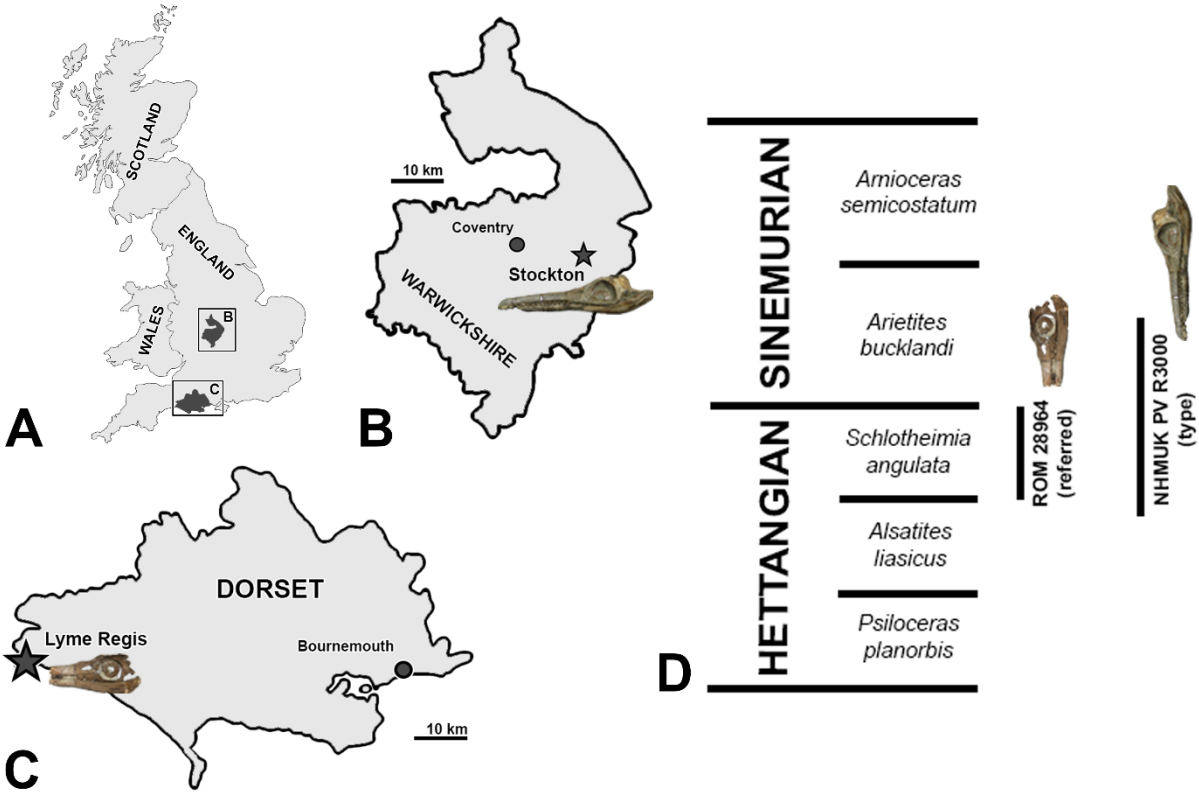

FIGURE 2.1. Occurrence and stratigraphic distribution of *Gen. et sp. nov. A.* (**A**) Outline of the United Kingdom (excluding Northern Ireland), showing the geographic positions of the type (**B**) and referred specimen (**C**) localities. (**B**) Outline map of Warwickshire, UK, with star indicating the position of Stockton, the type locality (NHMUK PV R3000) for *Gen et sp. nov. A.* (**C**) Outline map of Dorset, UK, with star indicating the position of Lyme Regis, the locality for the referred specimen (ROM 28964) of *Gen et sp. nov. A.* (**D**) Simplified stratigraphy of the earliest Jurassic of the United Kingdom (based on Ambrose, 2001) showing the stratigraphic range for the type (Rugby Limestone Member; upper Hettangian–lower Sinemurian) and referred (*angulata* zone; upper Hettangian) specimens of *Gen et sp. nov. A.*

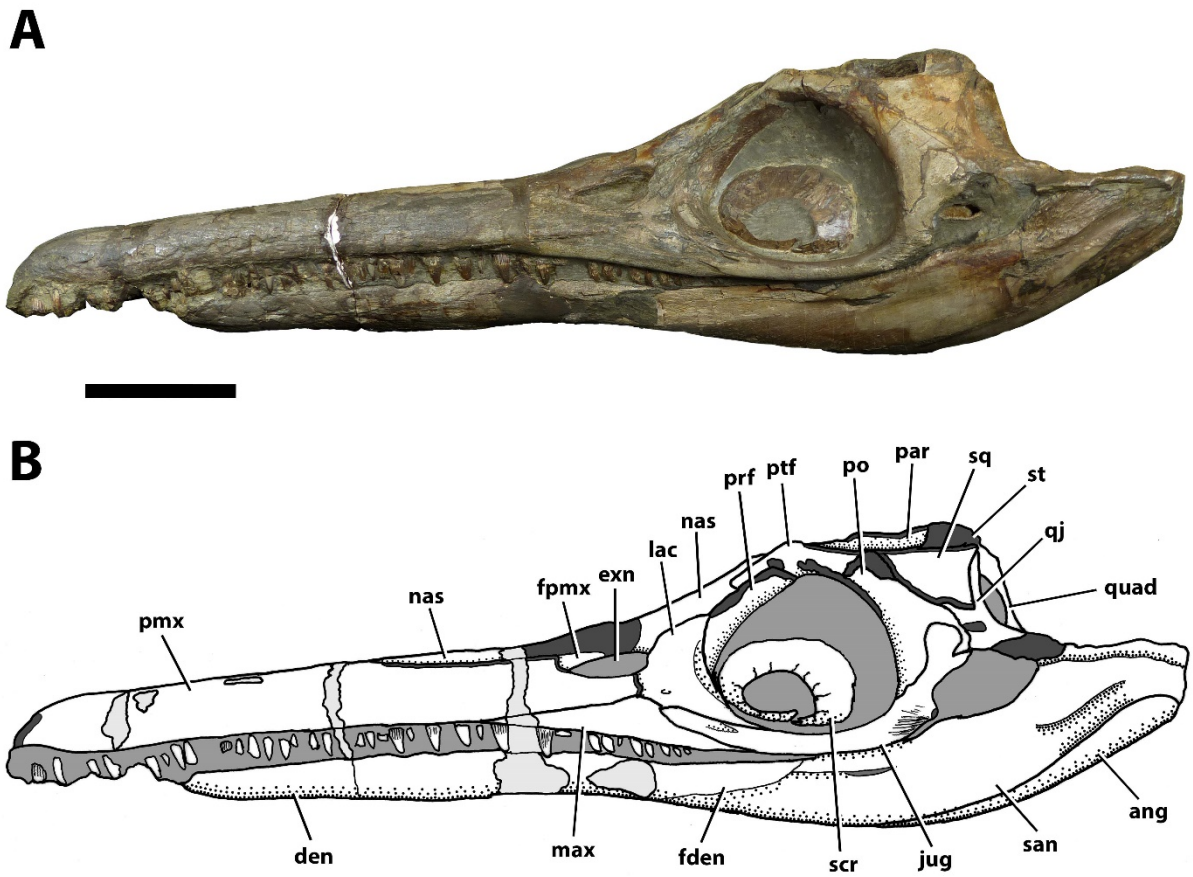

FIGURE 2.2. Holotype skull (NHMUK PV R3000) of *Gen et sp. nov. A*, in left lateral view (**A**). In line drawing (**B**), light-grey indicates portions of the skull that were reconstructed in plaster, mid-grey indicates rock matrix, and dark-grey indicates broken bone surface. Abbreviations: **ang**, angular; **den**, dentary; **exn**, external naris; **fden**, facet for dentary; **fpmx**, facet for premaxilla; **jug**, jugal; **lac**, lacrimal; **max**, maxilla; **nas**, nasal; **par**, parietal; **pmx**, premaxilla; **po**, postorbital; **prf**, prefrontal; **ptf**, postfrontal; **qj**, quadratojugal; **quad**, quadrate; **san**, surangular; **scr**, sclerotic ring; **sq**, squamosal; **st**, supratemporal. Scale bar equals 10 cm.

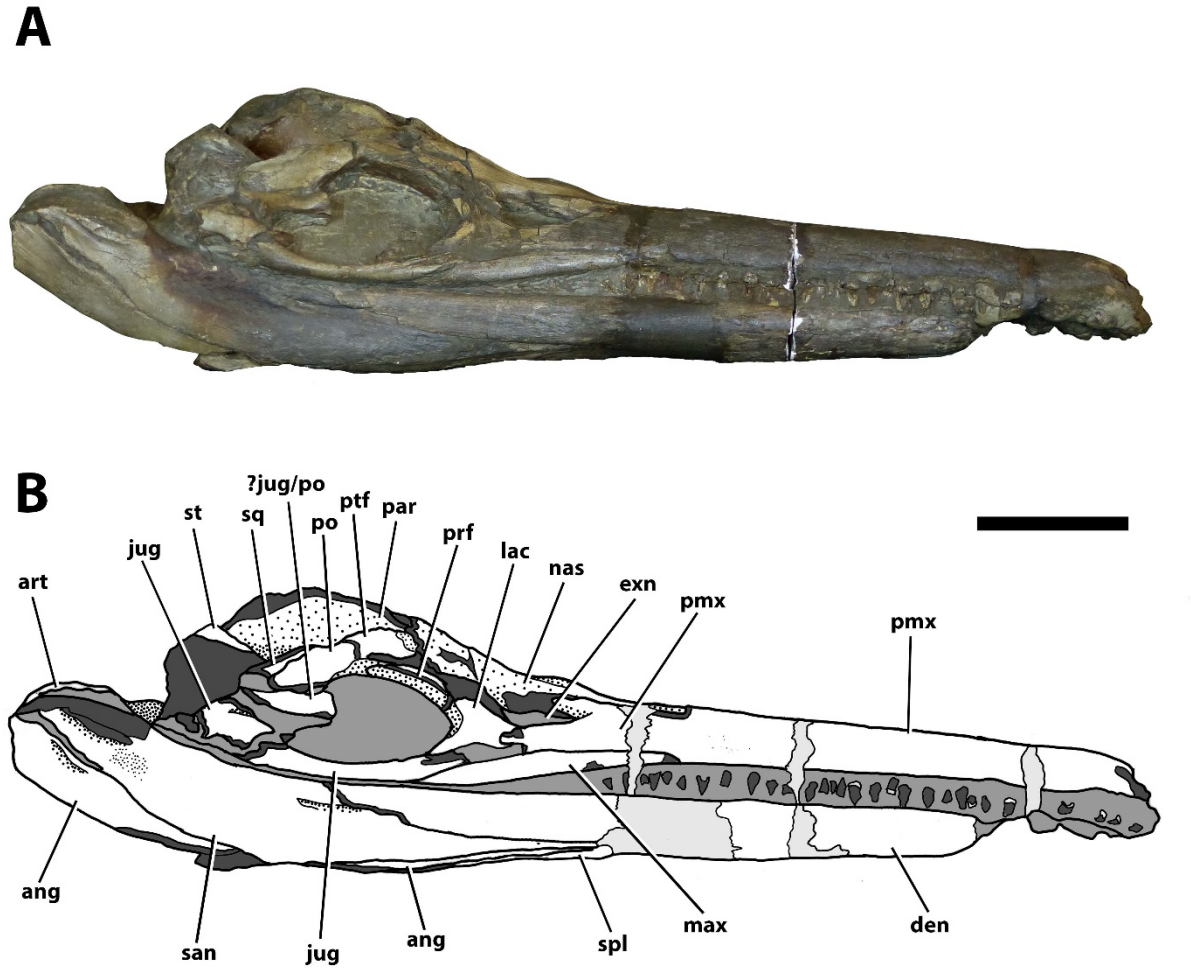

FIGURE 2.3. Holotype skull (NHMUK PV R3000) of *Gen. et sp. nov. A*, in right lateral view (**A**). In line drawing (**B**), light-grey indicates portions of the skull that were reconstructed in plaster, mid-grey indicates rock matrix, and dark-grey indicates broken bone surface. Abbreviations: **?jug/po**, ?jugal/postorbital; **ang**, angular; **art**, articular; **den**, dentary; **exn**, external naris; **jug**, jugal; **lac**, lacrimal; **max**, maxilla; **nas**, nasal; **par**, parietal; **pmx**, premaxilla; **po**, postorbital; **prf**, prefrontal; **ptf**, postfrontal; **san**, surangular; **spl**, splenial; **sq**, squamosal; **st**, supratemporal. Scale bar equals 10 cm.

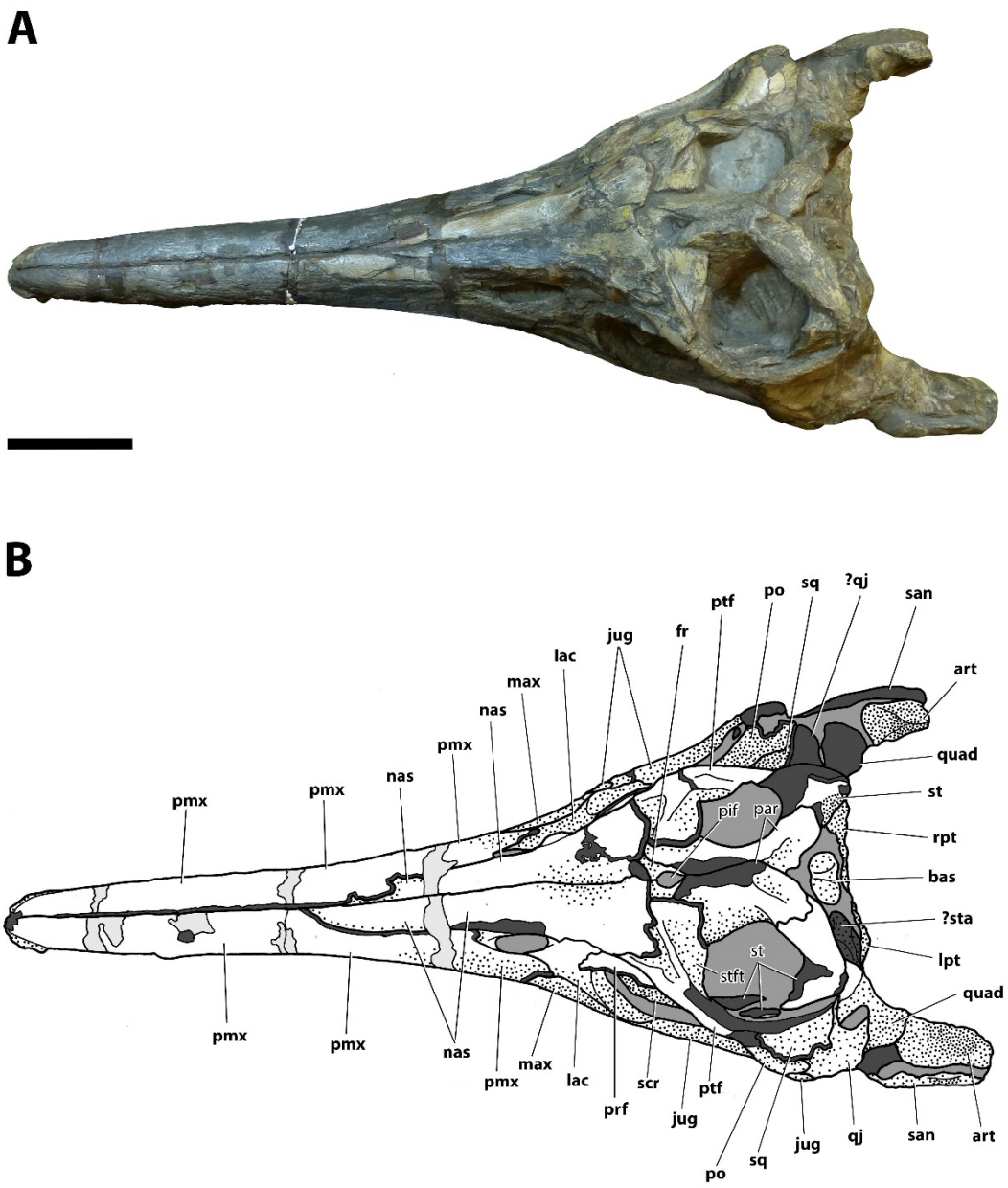

FIGURE 2.4. Holotype skull (NHMUK PV R3000) of *Gen. et sp. nov. A*, in dorsal view (**A**). In line drawing (**B**), light-grey indicates portions of the skull that were reconstructed in plaster, mid-grey indicates rock matrix, and dark-grey indicates broken bone surface. Abbreviations: **?qj**, ?quadratojugal; **?sta**, ?stapes; **art**, articular; **bas**, basisphenoid; **fr**, frontal; **jug**, jugal; **lac**, lacrimal; **lpt**, left pterygoid; **max**, maxilla; **nas**, nasal; **par**, parietal; **pif**, pineal foramen; **pmx**, premaxilla; **po**, postorbital; **ptf**, postfrontal; **qj**, quadratojugal; **quad**, quadrate; **rpt**, right pterygoid; **san**, surangular; **scr**, sclerotic ring; **sq**, squamosal; **st**, supratemporal; **utft**, anterior terrace of supratemporal fenestra. Scale bar equals 10 cm.

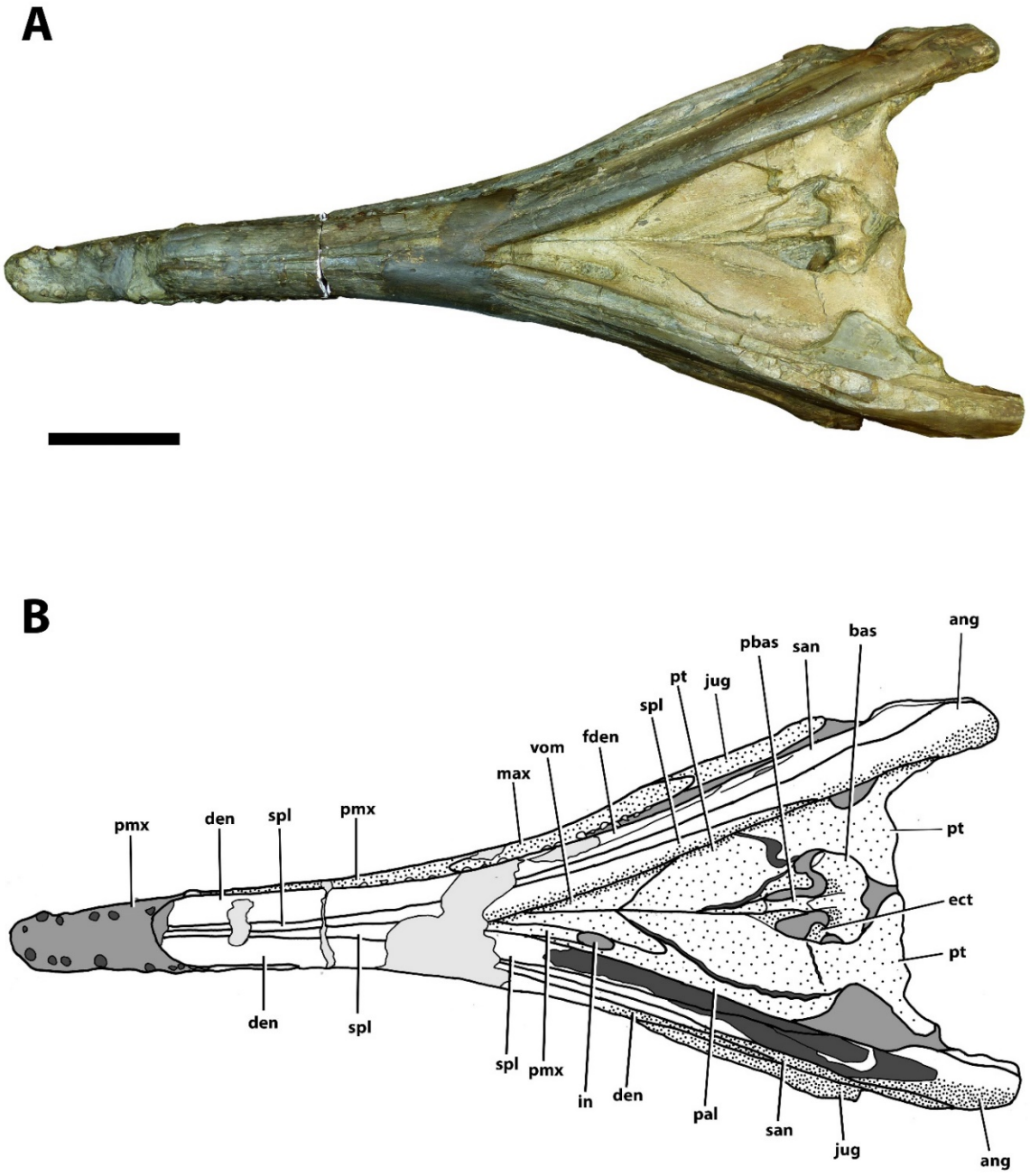

FIGURE 2.5. Holotype skull (NHMUK PV R3000) of *Gen. et sp. nov. A*, in ventral view (**A**). In line drawing (**B**), light-grey indicates portions of the skull that were reconstructed in plaster, mid-grey indicates rock matrix, and dark-grey indicates broken bone surface. Abbreviations: **ang**, angular; **bas**, basisphenoid; **den**, dentary; **ect**, ectopterygoid; **fden**, facet for dentary; **in**, internal naris; **jug**, jugal; **max**, maxilla; **pal**, palatine; **pbas**, parabasisphenoid; **pmx**, premaxilla; **pt**, pterygoid; **san**, surangular; **spl**, splenial; **vom**, vomer. Scale bar equals 10 cm.

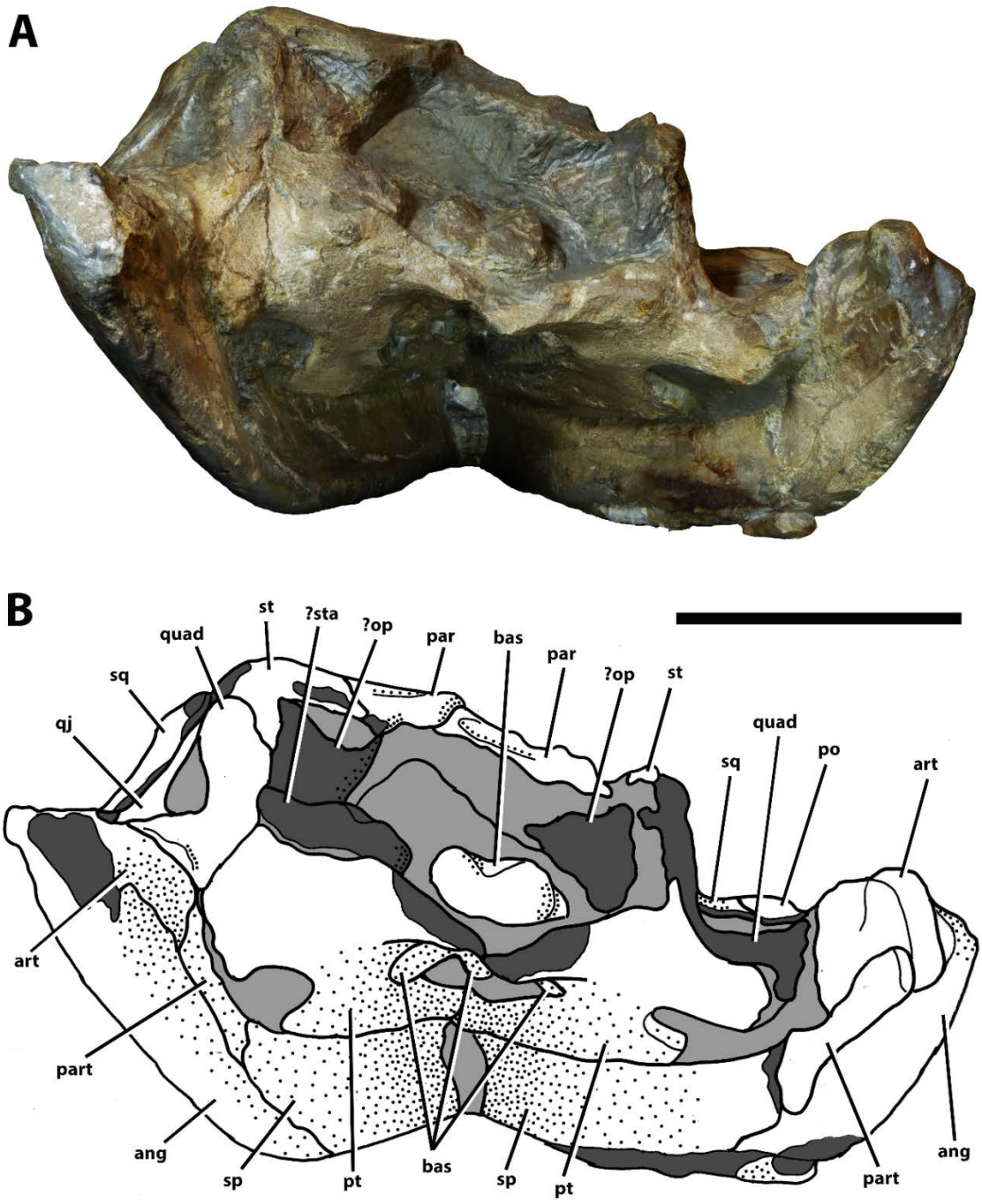

FIGURE 2.6. Holotype skull (NHMUK PV R3000) of *Gen. et sp. nov. A*, in posterior view (**A**). In line drawing (**B**), light-grey indicates portions of the skull that were reconstructed in plaster, mid-grey indicates rock matrix, and dark-grey indicates broken bone surface. Abbreviations: **?op**, ?opisthotic; **?sta**, ?stapes; **ang**, angular; **art**, articular; **bas**, basisphenoid; **par**, parietal; **part**, prearticular; **po**, postorbital; **pt**, pterygoid; **qj**, quadratojugal; **quad**, quadrate; **sp**, splenial; **sq**, squamosal; **st**, supratemporal. Scale bar equals 10 cm.

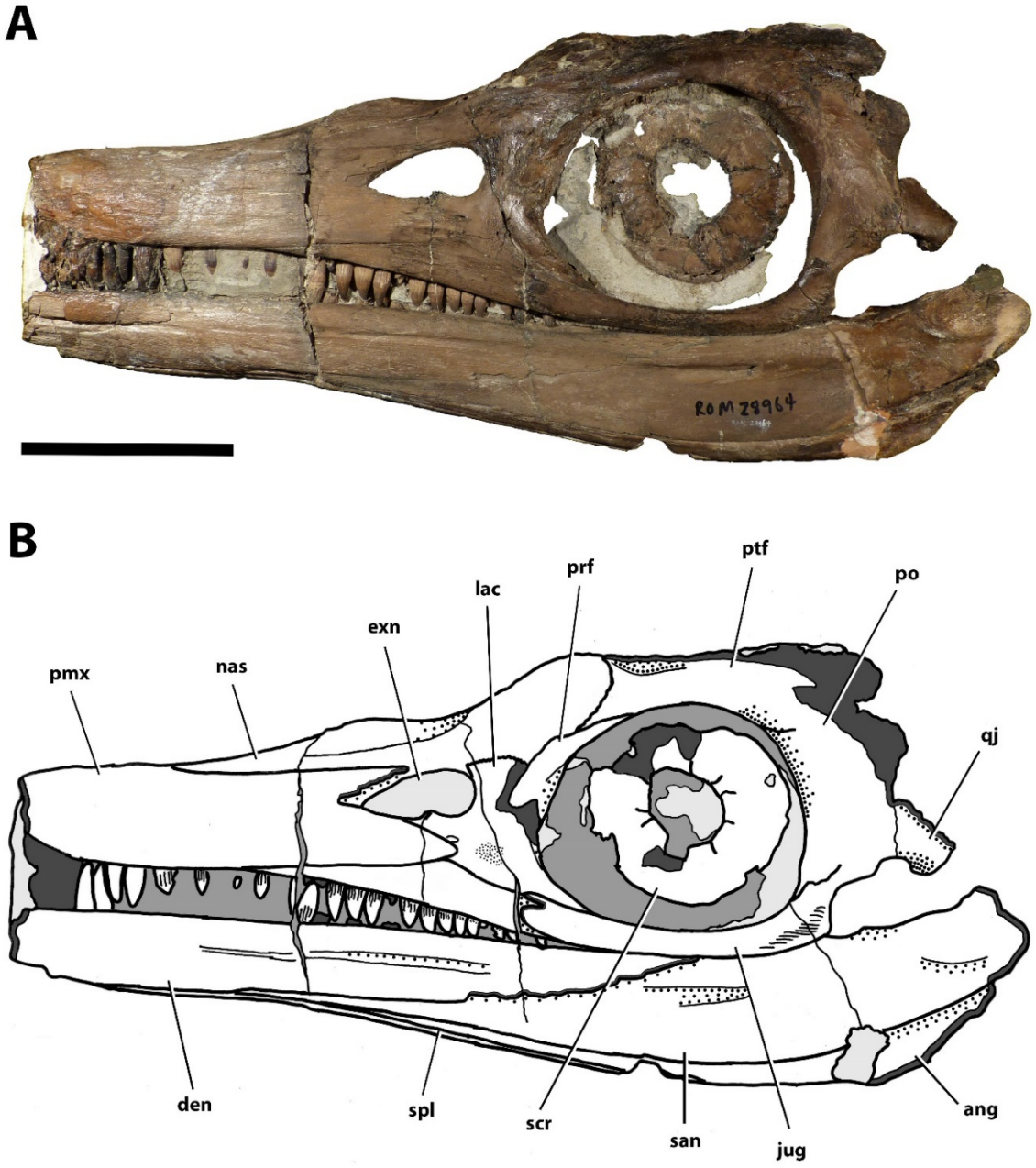

FIGURE 2.7. Skull of the referred specimen (ROM 28964) of *Gen. et sp. nov. A*, in left lateral view (**A**). In line drawing (**B**), light-grey indicates portions of the skull that were reconstructed in plaster, mid-grey indicates rock matrix, and dark-grey indicates broken bone surface. Abbreviations: **ang**, angular; **den**, dentary; **exn**, external naris; **jug**, jugal; **lac**, lacrimal; **nas**, nasal; **pmx**, premaxilla; **po**, postorbital; **prf**, prefrontal; **ptf**, postfrontal; **qj**, quadratojugal; **san**, surangular; **scr**, sclerotic ring; **spl**, splenial. Scale bar equals 10 cm.

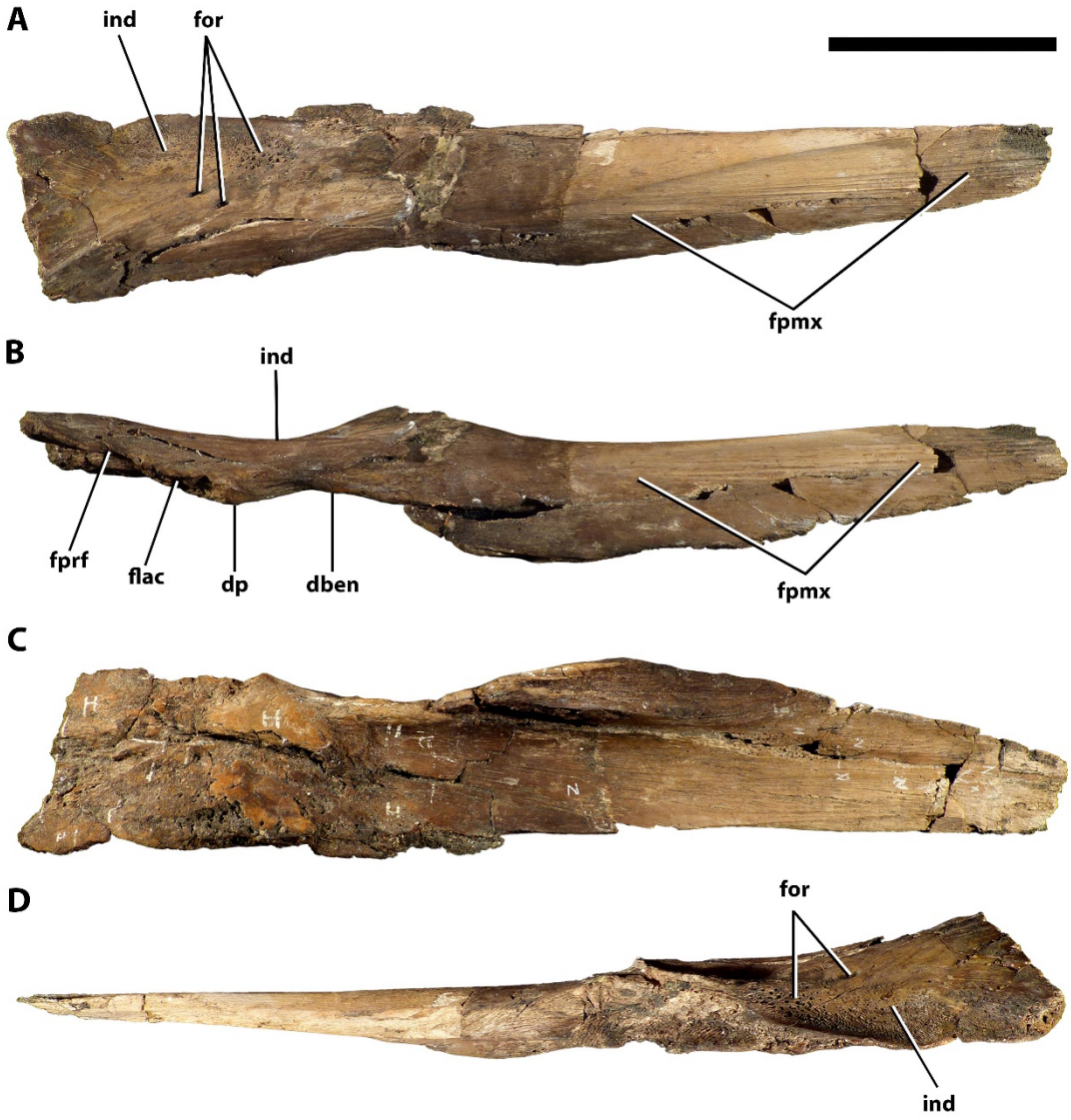

FIGURE 2.8. Right nasal of referred skull (ROM 28964) of *Gen. et sp. nov. A*, in dorsal (**A**), lateral (**B**), ventral (**C**) and medial (**D**) views. Abbreviations: **dben**, dorsal border of external naris; **dp**, descending process; **flac**, facet for lacrimal; **for**, neurovascular foramina; **fpmx**, facet for premaxilla; **fprf**, facet for prefrontal; **ind**, internasal depression. Scale bar equals 5 cm.

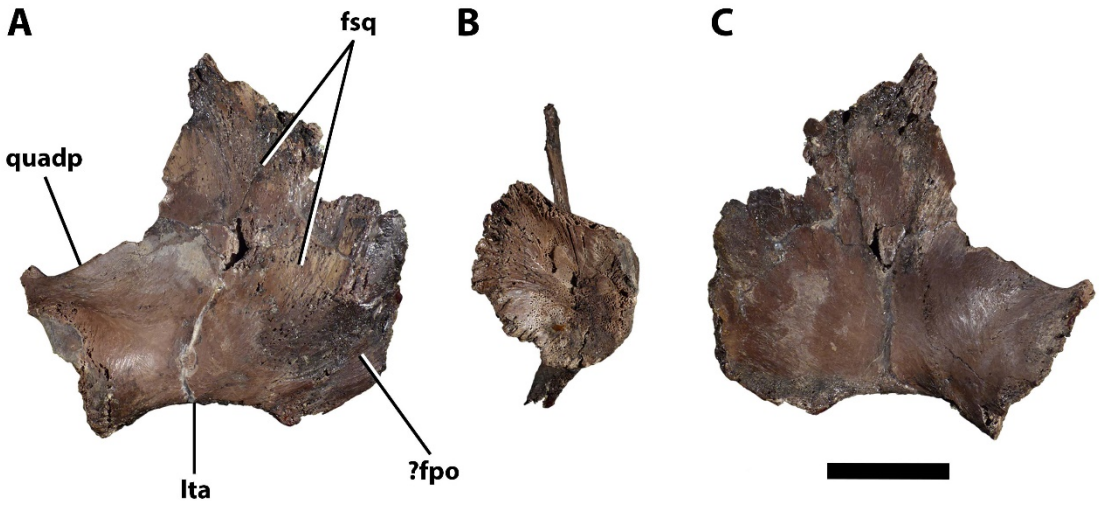

FIGURE 2.9. Right quadratojugal of referred skull (ROM 28964) of *Gen. et sp. nov. A*, in lateral (**A**), posterior (**B**) and medial (**C**) views. Abbreviations: **?fpo**, facet for postorbital; **fsq**, facet for squamosal; **lta**, quadratojugal portion of lower temporal arch; **quadp**, quadrate process. Scale bar equals 2 cm.

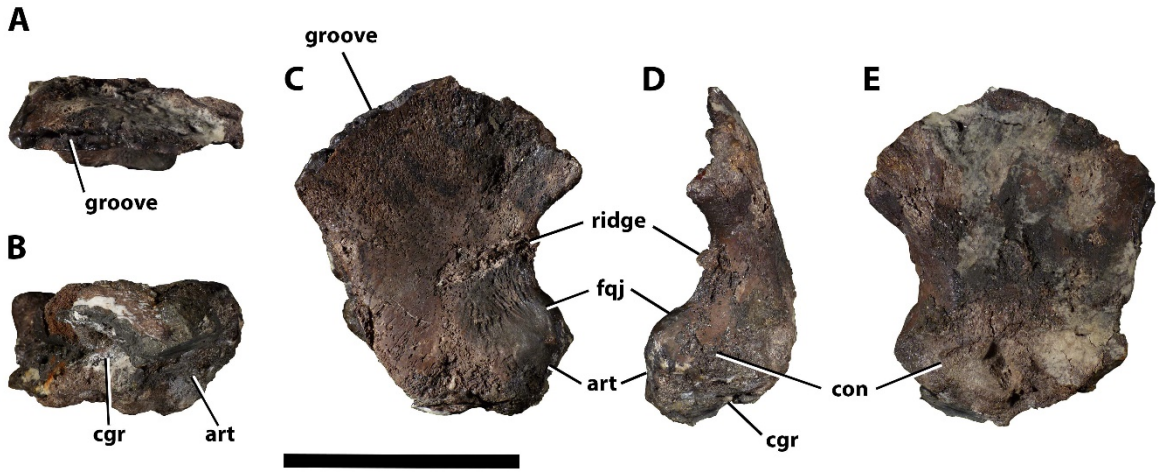

FIGURE 2.10. Left quadrate of referred skull (ROM 28964) of *Gen. et sp. nov. A*, in dorsal (**A**), ventral (**B**), lateral (**C**), posterior (**D**), and medial (**E**) views. Abbreviations: **art**, facet for articular; **cgr**, condylar groove; **con**, articular condyle; **fqj**, facet for quadratojugal. Scale bar equals 5 cm.

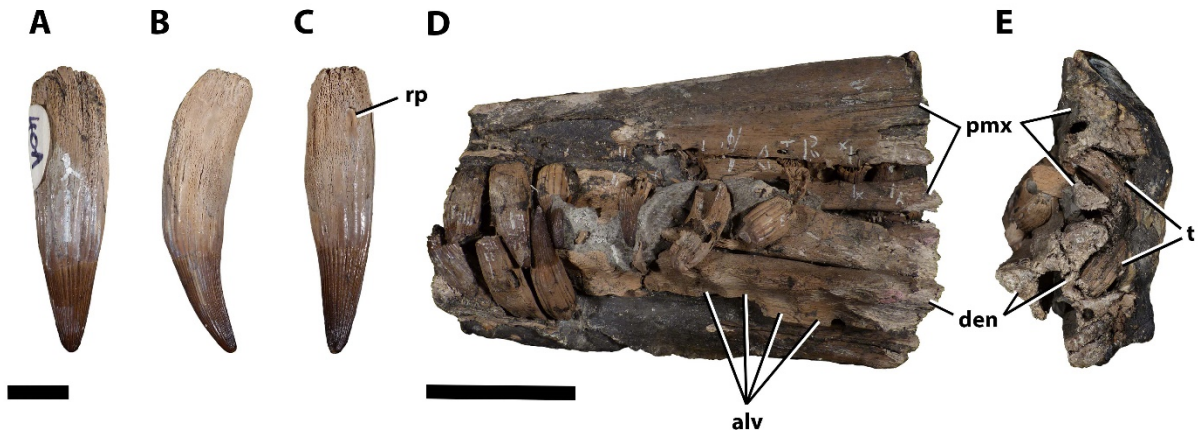

FIGURE 2.11. Dentition of referred skull (ROM 28964) of *Gen. et sp. nov. A*. Disarticulated tooth in labial (**A**), anterior/posterior (**B**), and lingual (**C**) views; broken portion of snout in medial (**D**) and posterior (**E**) views. Abbreviations: **alv**, alveolar remnants; **den**, dentary; **pmx**, premaxilla; **rp**, resorption pit; **t**, teeth. Scale bar equals 1 cm in (**A–D**) and 5 cm in (**E**).

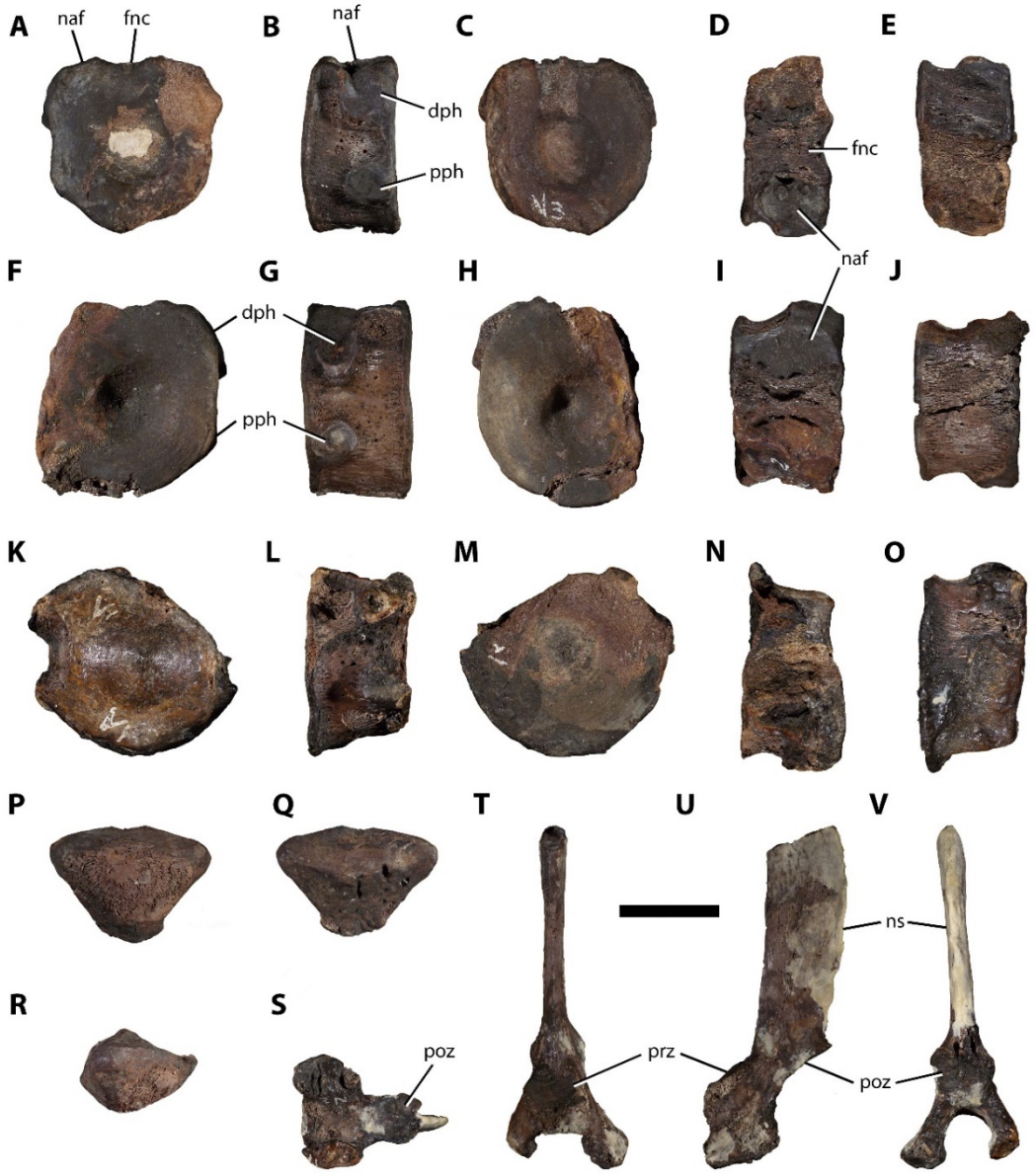

FIGURE 2.12. Axial skeleton elements of referred specimen (ROM 28964) of *Gen et sp. nov. A* Anterior cervical centrum in anterior (**A**), left lateral (**B**), posterior (**C**), dorsal (**D**) and ventral (**E**) views; posterior cervical centrum in anterior (**F**), right lateral (**G**), posterior (**H**), dorsal (**I**) and ventral (**J**) views; anterior dorsal centrum in anterior (**K**), left lateral (**L**), posterior (**M**), dorsal (**N**) and ventral (**O**) views; atlantal intercentrum in ventral (**P**), dorsal (**Q**) and left lateral (**R**) views; dorsal neural arch in ventral (**S**), anterior (**T**), left lateral (**U**) and posterior (**V**) views. Abbreviations: **dph**, diapophysis; **fnc**, floor of neural canal; **naf**, facet for neural arch; **ns**, neural spine; **poz**, postzygapophysis; **pph**, parapophysis; **prz**, prezygapophysis. Scale bar equals 2 cm.

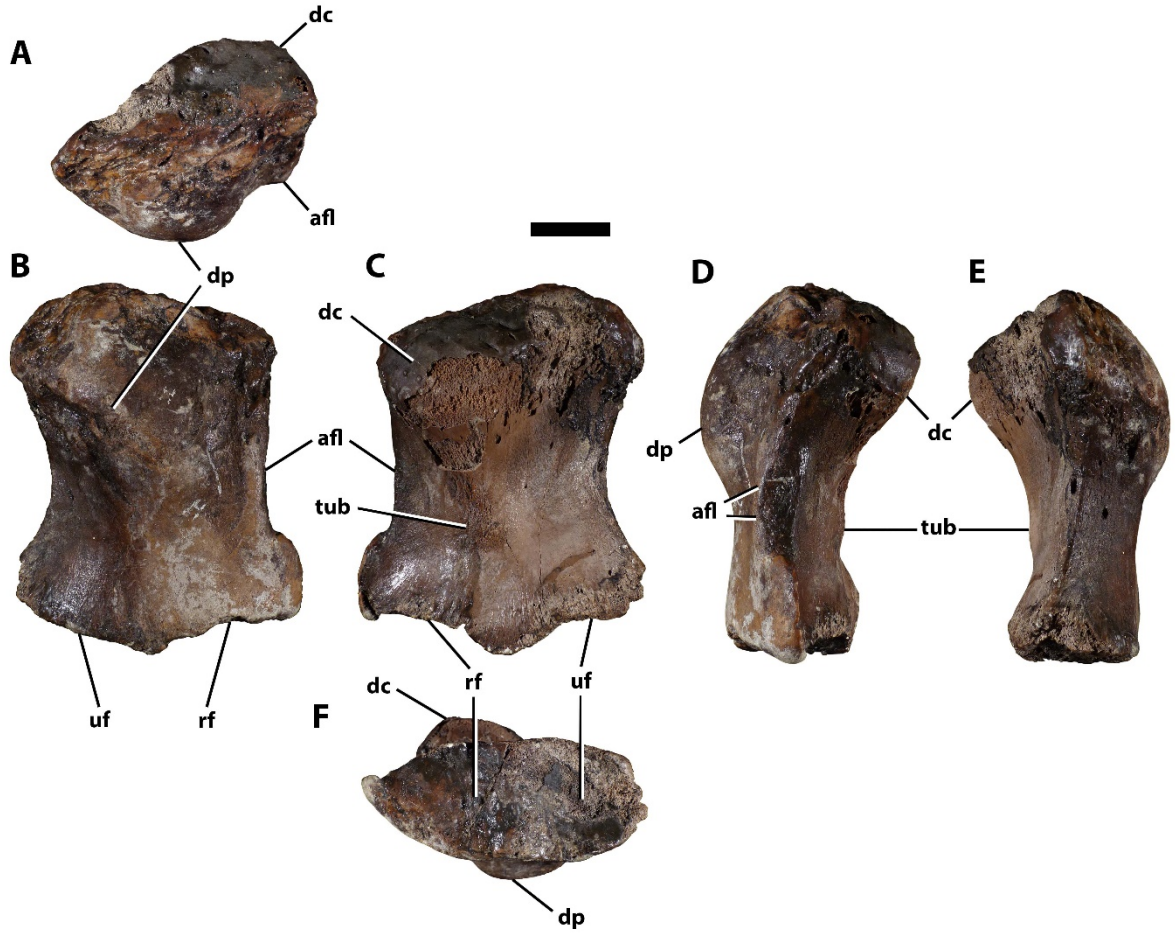

FIGURE 2.13. Right humerus of referred specimen (ROM 28964) of *Gen. et sp. nov. A*, in proximal (**A**), dorsal (**B**), ventral (**C**), anterior (**D**), posterior (**E**), and distal (**F**) views. Abbreviations: **afl**, anterior flange; **dc**, deltopectoral crest; **dp**, dorsal process; **rf**, radial facet; **tub**, tuberosity; **uf**, ulnar facet. Scale bar equals 2 cm.

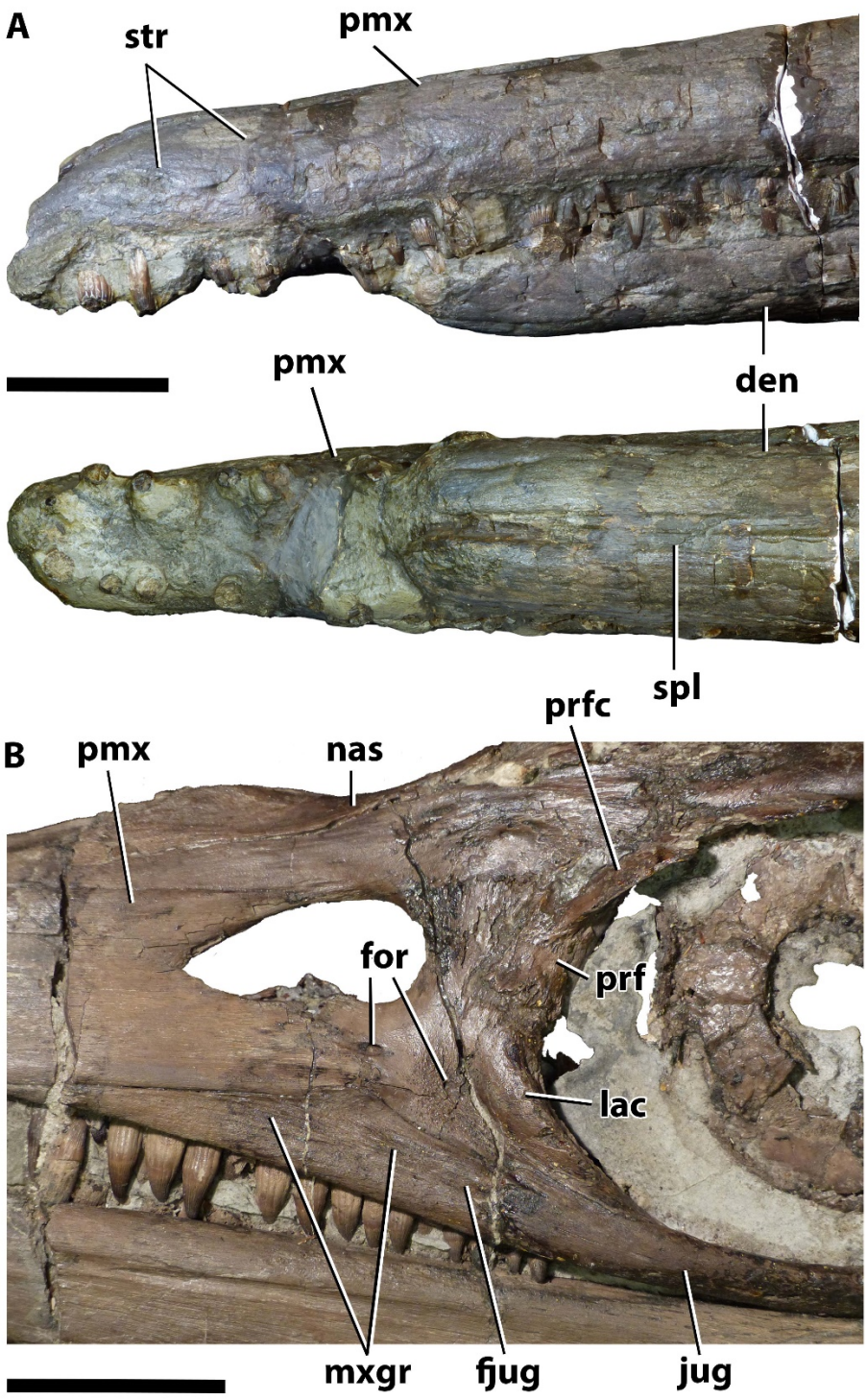

FIGURE 2.14. Close-ups of the skull of *Gen. et sp. nov. A*, in left lateral view. (**A**) Overbite of the holotype skull (NHMUK PV R3000), (**B**) antorbital and circumnarial regions of referred skull (ROM 28964). Abbreviations: **den**, dentary; **fjug**, facet for jugal; **for**, neurovascular foramina; **jug**, jugal; **lac**, lacrimal; **mxgr**, maxillary grooves; **nas**, nasal; **pmx**, premaxilla; **prf**, prefrontal; **prfc**, prefrontal crest; **spl**, splenial, **str**, striations. Scale bar equals 5 cm.

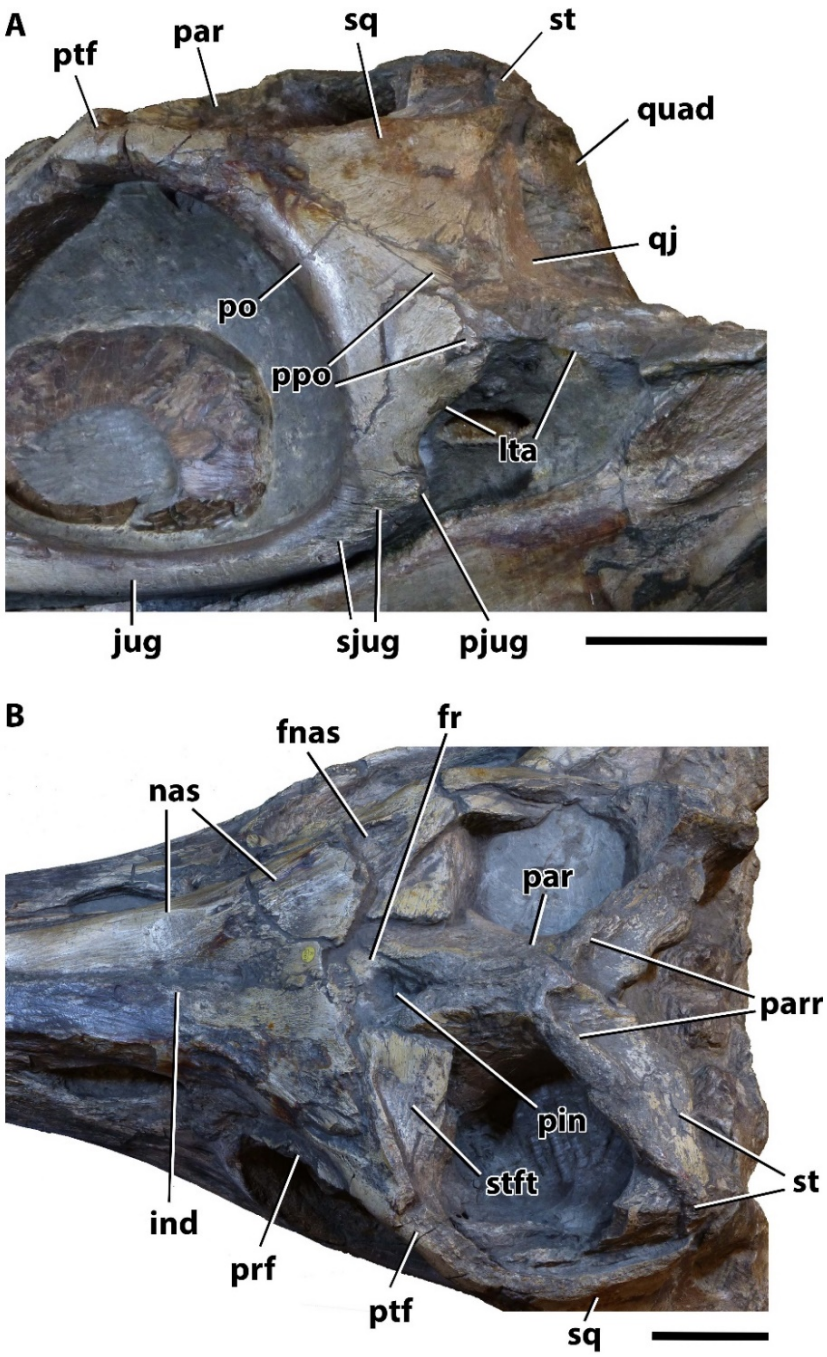

FIGURE 2.15. Close-ups of holotype skull (NHMUK PV R3000) of *Gen. et sp. nov. A,* (**A**) temporal region in left lateral view, (**B**) skull roof in dorsal view. Abbreviations: **fnas**, facet for nasal; **fr**, frontal; **ind**, internasal depression; **jug**, jugal; **lta**, lower temporal arch; **nas**, nasal; **par**, parietal; **parr**, parietal ridge; **pin**, pineal foramen; **pjug**, posteroventral process of jugal; **po**, postorbital; **ppo**, posteroventral process of postrorbital; **prf**, prefrontal; **ptf**, postfrontal; **qj**, quadratojugal; **quad**, quadrate; **sjug**, striations of jugal; **sq**, squamosal; **st**, supratemporal; **stft**, supatemporal fenestra anterior terrace. Scale bar equals 2 cm.

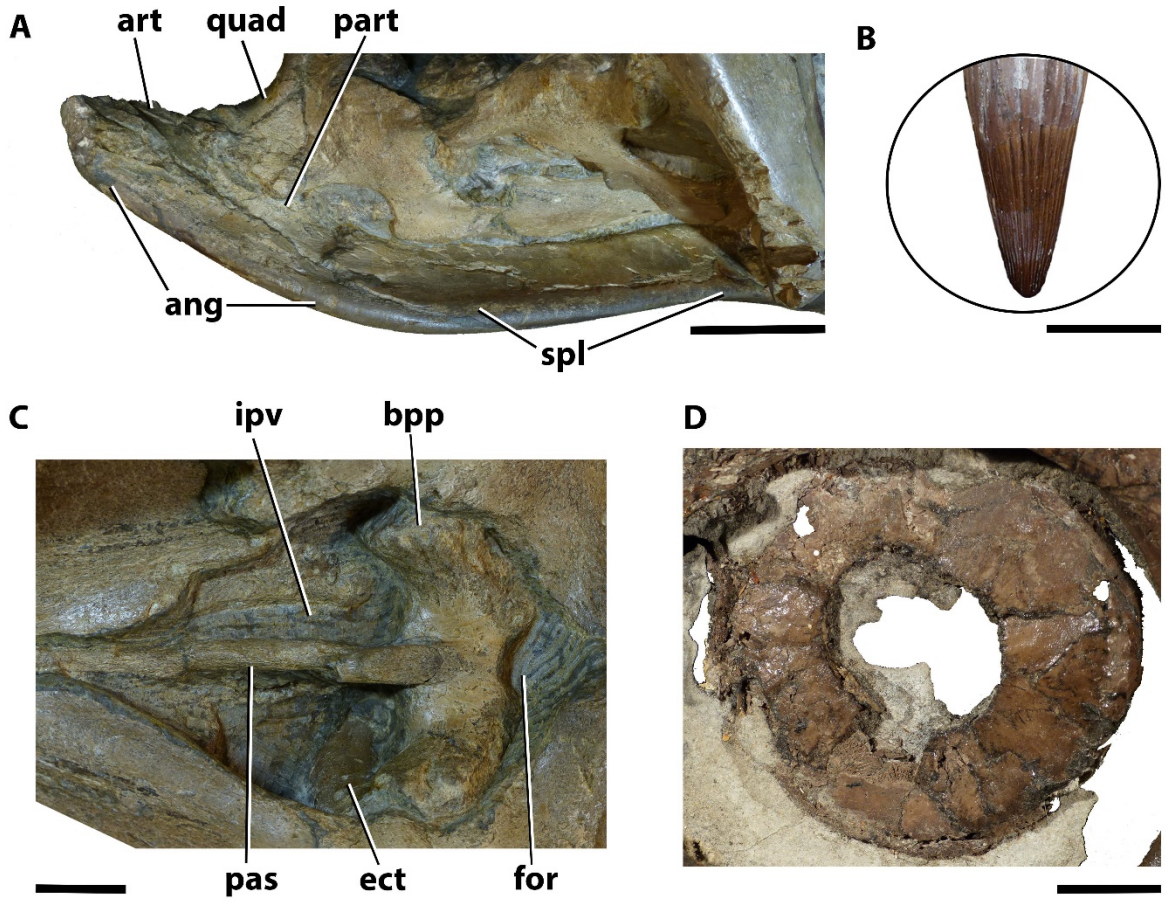

FIGURE 2.16. Close-ups of holotype (NHMUK PV R3000; **A**, **C**) and referred (ROM 28964; **B**, **D**) skulls of *Gen. et sp. nov. A*. **A**, left mandibular ramus in medial view; **B**, tooth crown; **C**, interpterygoid vacuity; **D**, scleral/sclerotic ring. Abbreviations: **ang**, angular; **art**, articular; **bpp**, basipterygoid process; **ect**, ectopterygoid; **for**, foramen for internal carotid artery; **ipv**, interpterygoid vacuity; **part**, prearticular; **pas**, parabasisphenoid; **quad**, quadrate; **spl**, splenial. Scale bars equal 5 cm in (**A**), 1 cm in (**B**), 2 cm in (**C**) and (**D**).

	NHMUK PV R3000	ROM 28964
Skull length	715 (l), 710 (r)	435i
Mandibular length	660 (l), 640 (r)	475i
Preorbital (=rostrum) length	495 (l), 492 (r)	245i
Premaxillary length	350 (l), 365 (r)	110i
Prenarial length	420 (l), 420 (l)	165i
Postorbital length	82 (l), 90 (r)	70
Mandibular width	320	-
Orbit maximum ap length	136.2 (l), 130.8 (r)	122.2
Orbit maximum dv height	98.8 (l), 76.3 (r)	101.1
Sclerotic ring maximum ap length	88.8	92.5
Sclerotic ring maximum dv height	56.9	82.1
Sclerotic ring aperture maximum ap length	46.9	37.3
Sclerotic ring aperture maximum dv height	26.6	33.2
No of sclerotic ossicles	13	~11
External naris maximum ap length	54.9 (l), 55.4 (r)	54.6
External naris maximum ml width	18.3 (l), 23.0 (r)	22.7
Pineal foramen maximum ap length	21.1	-
Pineal foramen maximum ml width	14.5	-
Supratemporal fenestra maximum ap length	74.3 (l), 71.7 (r)	-
Supratemporal fenestra maximum ml width	58.5 (l), 60.0 (r)	-
Humerus maximum pd length	-	84.3
Humerus maximum proximal ap length	-	63.0
Humerus maximum distal ap length	-	67.8i
Humerus minimum ap length	-	50.0
Radial facet maximum ap length	-	31.7
Radial facet maximum dv thickness	-	27.5
Ulnar facet maximum ap length	-	34.2
Ulnar facet maximum dv thickness	-	29.0
Centrum ‘V3’ maximum ap length	-	18.7
Centrum ‘V3’ maximum dv height	-	37.5
Centrum ‘V3’ maximum ml width	-	39.9
Centrum ‘V2’ maximum ap length	-	21.3
Centrum ‘V2’ maximum dv height	-	40.1
Centrum ‘V2’ maximum ml width	-	35.7

TABLE 2.1. Selected cranial and postcranial measurements of the type (NHMUK PV R3000) and referred (ROM 28964) specimens of *Gen. et sp. nov. A* All measurements are given in mm. Abbreviations: **ap**, anteroposterior; **dv**, dorsoventral; **i**, incomplete; **l**, left; **ml**, mediolateral; **pd**, proximodistal; **r**, right.

CHAPTER 3: A NEW PARVIPELVIAN ICHTHYOSAUR (REPTILIA; ICHTHYOPTERYGIA) FROM THE PARDONET FORMATION (UPPER NORIAN, LATE TRIASSIC) OF WILLISTON LAKE, BRITISH COLUMBIA, CANADA.

INTRODUCTION

Ichthyosaurs were a group of secondarily aquatic Mesozoic diapsids of uncertain phylogenetic affinities (e.g. Caldwell, 1996; Motani et al., 1998; Motani et al., 2015a; Jiang et al., 2016). They were important components of Mesozoic marine faunas from their first appearance in the Early Triassic (Olenekian) up to their extinction in the early Late Cretaceous (Cenomanian; e.g. McGowan and Motani, 2003; Motani, 2005a). Derived members of the clade, such as the Early Jurassic *Ichthyosaurus* and *Stenopterygius*, were active pelagic predators (Motani 2002a, b; Bernard et al., 2010) characterized by the possession of a streamlined, 'fish-shaped' body plan with a well demarcated caudal fluke which enabled a thunniform ('tuna-like') mode of swimming (Motani et al., 1996). However, more basal ichthyosaurs possessed a markedly different body plan, with an elongated trunk and tail with only a weakly developed caudal fluke and exhibited an anguilliform ('eel-like') mode of swimming (Motani et al., 1996). The evolutionary transition between these two body plans occurred through the Late Triassic (Norian; see below), and was marked by the appearance of the first representatives of the clade Parvipelvia (Motani, 1999a), characterized by a reduced pelvic girdle. Like in modern cetaceans, the caudal muscle series of parvipelvian ichthyosaurs was probably not connected to the pelvic bones, but to the trunk musculature instead, which allowed for a more oscillatory, rather than undulatory, mode of swimming. Parvipelvian ichthyosaurs were the only ichthyosaur group that survived the Late Triassic extinction event, which caused a catastrophic drop in ichthyosaur diversity and disparity, leading to the extinction of all non-parvipelvian ichthyosaur lineages adapted to life in near-shore environments (Bardet, 1994; Benson and Butler, 2011; Thorne et al., 2011; Kelley et al., 2014; Fischer et al., 2014a). The Late Triassic origins of Parvipelvia were therefore instrumental to ichthyosaur survival of the Late Triassic extinction event, and studying their early evolution is crucial for a better understanding of the

evolutionary assembly of key anatomical features that ultimately led to their later evolutionary success. However, our knowledge of the early evolution of Parvipelvia, and Late Triassic ichthyosaurs in general, is very limited due to the incomplete sampling of the global marine Late Triassic (Norian and Rhaetian) fossil record (e.g. Benson et al., 2010).

Williston Lake, located in the northwestern part of British Columbia, Canada (Fig. 3.1A), is one of only a few localities in the world that document the evolutionary transition between non-parvipelvian and parvipelvian ichthyosaurs (McGowan, 1997). Williston Lake is a huge artificial body of water that was formed after the W. A. C. Bennett Dam was built across the Peace River in 1968 (McGowan, 1997). The shores of Williston Lake reveal exposures of the Pardonet Formation, a marine horizon of Late Triassic age (late Carnian–Rhaetian; Orchard and Tozer, 1997). Fieldwork carried out by the Department of Palaeontology, Royal Ontario Museum, ON, Canada (ROM), at Williston Lake between 1987–1994 resulted in the discovery of a diverse Late Triassic marine vertebrate fauna, including ichthyosaurs, thalattosaurs and fish, with specimens originating from different horizons spanning the entire Norian section (McGowan, 1997). Ichthyosaur remains were the most abundant, with 45 specimens of varying levels of completeness, ranging from isolated elements to complete skeletons, discovered by 1994 (McGowan, 1997; note that fieldwork conducted by the ROM at Williston Lake continued until the early 2000's, and numerous additional specimens had been collected by then [I. Morrison, pers. comm., December 2015]).

The ichthyosaur fauna from Williston Lake represents a wide range of their phylogenetic and ecological diversity and includes: giant shastasaurids (e.g. ROM 44661) from the middle Norian; *Callawayia neoscapularis* (McGowan, 1994) from the lower Norian, recovered in phylogenetic analyses as either a shastasaurid (Nicholls and Manabe, 2001) or a basal euichthyosaurian (Maisch and Matzke, 2000; Ji et al., 2016); and the stratigraphically oldest and phylogenetically most basal parvipelvians: the medium-sized *Macgowania janiceps* (body length ~3 m; McGowan, 1996, 1997; Motani, 1999a) from the middle Norian and the small-bodied *Hudsonelpidia brevirostris* (body length ~1 m; McGowan, 1995a, 1997; Motani, 1999a) from the lower Norian (Fig. 3.1D).

Unfortunately, most ichthyosaur specimens collected from Williston Lake by the ROM crews are incompletely preserved, hindering our understanding of their anatomy and phylogenetic position. However, fieldwork carried out by crews from the Royal Tyrrell Museum of Palaeontology, Drumheller, AB, Canada (TMP) since the 1990's in the Pink Mountain region of British Columbia (approx. 100 km north of Williston Lake; Nicholls and Manabe, 2001) has significantly expanded our knowledge of the transitional ichthyosaur fauna found at Williston Lake. This fieldwork has yielded additional specimens of giant shastasaurids, including the colossal type specimen of *Shonisaurus sikanniensis* (Nicholls and Manabe, 2004), as well as additional specimens of *Callawayia neoscapularis* (Nicholls and Manabe, 2001, 2004) and *Macgowania janiceps* (Nicholls and Manabe, 2004; Henderson, 2015). These discoveries have helped to better understand the important anatomical changes which occurred during the transition from non-parvipelvian to parvipelvian ichthyosaurs in the middle and upper Norian.

Despite all these ichthyosaur discoveries, the basal parvipelvians *Macgowania janiceps* and *Hudsonelpidia brevirostris*, are currently our only source of information on parvipelvian evolution in the Late Triassic. A gap in the fossil record of around 15 million years separates *Macgowania janiceps*, the phylogenetically most basal parvipelvian recovered from the Pardonet Formation, from the taxonomically and ecologically diverse parvipelvian ichthyosaur fauna of the Lower Jurassic (Hettangian–Pliensbachian, approx. 201–183 mya) of the United Kingdom, which is the first diverse ichthyosaur fauna post-dating the end-Triassic extinction event (e.g. McGowan and Motani, 2003). However, numerous ichthyosaur specimens collected by ROM crews from middle and upper Norian horizons at Williston Lake clearly represent previously undescribed parvipelvian morphologies and indicate that the diversity of parvipelvian ichthyosaurs currently known from Williston Lake is underestimated. Furthermore, the upper Norian age of some of these specimens indicates that they have great potential to provide new, important insights into parvipelvian evolution at the end of the Triassic, during a period of profound changes to the Earth system, and help us better understand the origins of Early Jurassic parvipelvian diversity.

Here, I describe a new genus and species of parvipelvian ichthyosaur from Williston Lake, based on a specimen collected by ROM crews during the 1991 field season. I provide a detailed osteological description of the preserved elements of the new taxon, and compare its anatomy with other Late Triassic and Early Jurassic parvipelvian ichthyosaurs and non-parivpelvian ichthyosaurs of the Late Triassic.

SYSTEMATIC PALAEONTOLOGY

ICHTHYOPTERYGIA Owen, 1840

ICHTHYOSAURIA Blainville, 1835

HUENEOSAURIA Maisch and Matzke, 2000

MERRIAMOSAURIA Motani, 1999a

EUICHTHYOSAURIA Motani, 1999a

PARVIPELVIA Motani, 1999a

Gen. et sp. nov. B.

Figs 3.2–3.7

Ichthyosauria indet. McGowan, 1997:69

Ichthyosauria indet. Motani, 1997:16

Holotype and only specimen. ROM 44295, a partial skeleton comprising a partially preserved rostrum and associated dentition; a partially preserved, but unprepared, vertebral column; fragmentary ribs; a fragmentary pectoral girdle; the proximal portion of one forefin, and the distal portion of the other forefin; and an almost completely preserved pelvic girdle and hindfin. A preliminary description of ROM 44295 was given by McGowan (1997). This account was very brief and was published before the preparation of the forefin, hindfin and pelvic girdle material had been completed. The morphology of

the notched elements in the leading edge of the forefin of ROM 44295 was also briefly discussed by Motani (1997).

Occurrence. The type specimen (ROM 44295) was collected from the base of Pardonet Hill in the Peace Reach of Williston Lake (Fig. 3.1B). It was preserved in a series of large blocks which had weathered out from the western slope of the hill (Fig. 3.1C), but it was not possible to determine the exact horizon of origin of these blocks. However, numerous invertebrate fossils are preserved on the block surfaces. These include calcite-filled replacements of the upper Norian spherical spongiomorph *Heterastridium* (e.g. Stanley and Senowbari-Daryan, 1999) and impressions of the upper Norian bivalve *Monotis* (e.g. McRoberts, 2011). In addition, conodont microfossil analysis (performed by M. Orchard of the Canada Geological Survey; I. Morrison, pers. comm., 2015) on the block matrix indicates origin from the upper Norian *Epigondolella bidentata* conodont biozone (Orchard and Tozer, 1997; Fig. 3.1D). Together, the available invertebrate and microfossil evidence suggests an upper Norian age for ROM 44295.

Diagnosis. *Gen. et sp. nov. B* is characterized by the following combination of characters: mediolaterally flattened tooth crowns with mesial and distal carinae, similar in morphology to those in *Thalattoarchon saurophagis* (FMNH PR 3032; Fröbisch et al., 2013), *Himalayasaurus tibetensis* (Motani et al., 1999a) and some teeth of *Temnodontosaurus platyodon* (e.g. ROM 7972; McGowan, 1995b), but the crown is not enlarged (in contrast to *H. tibetensis*) and its surface is smooth or ornamented by subtle, apicobasally oriented ridges (crown surface ridges also occur in *H. tibetensis* and *Te. platyodon*, but in *Th. saurophagis* the crown surfaces are entirely smooth); an anterodistal tuberosity of the humerus, similar to *Hudsonelpidia brevirostris* (ROM 44629; McGowan, 1995a) and many Early Jurassic parvipelvians (e.g. Fischer et al., 2016: character 63:1), but different from some specimens of *Ichthyosaurus* sp. (e.g. Lomax and Massare, 2015, 2016) and *Stenopterygius* sp. (e.g. Johnson, 1977), where the anterodistal extremity of the humerus forms an acute angle; a small radio-ulnar foramen, circular in outline, similar to that in *Macgowania janiceps* (ROM 41992; McGowan, 1996) and *Leptonectes tenuirostris* (e.g. OUMNH J.10319; McGowan, 1989); manus with four primary digits (II-

V) comprised of tightly packed, polygonal phalanges, like in other euichthyosaurians (e.g. Motani, 1999c) and with only one posterior accessory digit, comprised of small phalanges that are circular in outline, similar to the condition present in *Macgowania janiceps* (ROM 41992; McGowan, 1996); notching along the entire anterior margin of the forefin, similar to *Macgowania janiceps* (ROM 41992; McGowan, 1996) and some specimens of *Temnodontosaurus trigonodon* (e.g. SMNS 50000; Motani, 1999c); anteroposteriorly narrow pelvic bones, like in other parvipelvian ichthyosaurs (e.g. Motani, 1999a); only two elements in the distal tarsal row, similar to the condition in basal ichthyosaurs, but different from the condition in toretocnemids and other parvipelvians, where the distal tarsal row increases to three elements (e.g. Ji et al., 2016: character 141); notching along the entire anterior margin of the hindfin, similar to the condition in *Temnodontosaurus trigonodon* (e.g. SMNS 15950).

DESCRIPTION

Rostrum and mandible (Fig. 3.2)**.** The distal portions of the dentigerous parts of the rostrum and mandibular rami are preserved in ROM 44295, but they are badly broken and their surfaces are heavily weathered so it is not possible to give a detailed account of their morphology. However, because the dentigerous region of ichthyosaurs is formed extensively by the premaxilla (cranium) and dentary (mandibular ramus; e.g. McGowan and Motani, 2003) it is very likely that most of the preserved bone fragments are parts of these bones. The maximum anteroposterior length of the preserved part of the rostrum measures 1080 mm. A dentigerous bone, which is ventrally displaced from the main portion of the rostrum, was interpreted by McGowan (1997) as a mandibular ramus. An anteroposteriorly elongate and dorsoventrally narrow bone fragment, which lies dorsally to the main portion of this dentigerous bone, resembles the splenial, but because the rostrum is badly broken and weathered it cannot be ruled out that this bone fragment represents a broken off, dorsal portion of the premaxilla or ventral portion of the dentary. A longitudinal row of anteroposteriorly elongate, ellipsoidal foramina is present anteriorly on the exposed surface of this dentigerous bone. However, because such foramina have been described from the lateral surfaces of ichthyosaur premaxillae and both the lateral and medial surfaces

of ichthyosaur dentaries (e.g. Nicholls and Manabe, 2001), it is not possible to determine the exact identity of the preserved tooth-bearing bone.

Dentition (Fig. 3.3)**.** Numerous teeth are preserved in ROM 44295 in articulation or closely associated with the rostrum and mandible. However, none of the preserved teeth are complete. The majority of the teeth are severely broken and/or weathered and are preserved as oblique or transverse sections, although a few teeth are preserved as approximately parasagittal sections. The most complete of these parasagittal sections is located in the anterior part of the ventrally displaced dentigerous bone (Fig. 3.3A) and measures 73.0 mm in apicobasal length. The apicobasal length of the crown of this tooth measures approx. 21.0 mm, and the mesiodistal width of the crown measures 20.8 mm at its base. However, because the tooth is preserved as a parasagittal section, the given measurements should be treated as an approximation. A partially preserved tooth crown measuring approx. 40.0 mm in apicobasal height indicates the maximum size of the dentition was approximately 50% greater than the complete, measured tooth.

Only a few partial tooth crowns are preserved (Fig. 3.3B, C, D). The largest preserved crown, located in the posterior part of the preserved portion of the rostrum/mandible, measures 40.0 mm in apicobasal height and 25.0 mm in anteroposterior width at its base. The tooth crowns bear mesial and distal carinae (Fig. 3.3C); this feature is most evident in some of the preserved crown cross-sections. Bicarinate teeth are also present in *Cymbospondylus petrinus* (UCMP 9950, UCMP 9913; feature more pronounced in some teeth than in others), *Thalattoarchon saurophagis* (FMNH PR 3032; Fröbisch et al., 2013), *Himalayasaurus tibetensis* (Motani et al., 1999a) and *Temnodontosaurus platyodon* (feature present only in some of the teeth; e.g. ROM 7972; McGowan, 1995b). Because all the preserved crowns are bicarinate, this feature was most likely present in all teeth, similar to the situation in *Thalattoarchon saurophagis* (FMNH PR 3032; Fröbisch et al., 2013), but in contrast to *Cymbospondylus petrinus* (UCMP 9950, UCMP 9913) and *Temnodontosaurus platyodon* (e.g. ROM 7972; McGowan, 1995b), in which only some of the crowns bear carinae. The best preserved crown surface in ROM 44295 (Fig. 3.3D) bears subtle apicobasally oriented ridges, but other preserved crowns have a smooth surface. Smooth crown surfaces also occur in *Thalattoarchon saurophagis* (FMNH PR 3032; Fröbisch et al.,

2013), and leptonectid ichthyosaurs (e.g. Maisch and Matzke, 2000), while the bicarinate crowns of *Temnodontosaurus platyodon* bear subtle ridges (ROM 7972). The crowns of ROM 44295 differ from the crowns of *Cymbospondylus petrinus* (UCMP 9950, UCMP 9913), *Himalayasaurus tibetensis* (Motani et al., 1999a), and *Suevoleviathan disinteger* (SMNS 15390; Maisch, 1998), in which the crowns are ornamented by prominent apicobasal ridges. The relative size of the tooth crowns is similar to those of most other ichthyosaurs, but contrasts with those of *Himalayasaurus tibetensis*, which has enlarged crowns (Motani et al., 1999a). The preserved parts of the tooth bases indicate that they were roughly circular in cross section, and their surface was ornamented by prominent, longitudinal striations, like in some other Late Triassic and Early Jurassic parvipelvians, such as *Macgowania janiceps, Suevoleviathan disinteger* and *Temnodontosaurus platyodon* (e.g. Ji et al., 2016: character 63). The largest preserved cross-section through a tooth base measures 31.5 mm in diameter.

A few preserved cross-sections through the tooth bases of ROM 44295 demonstrate that strongly folded dentine – plicidentine – was present (Fig. 3.3E). Each dentine fold is transversely narrow towards the pulp cavity and becomes transversely broader towards the periphery of the tooth base. The dentine folds are of roughly equal dimensions and are evenly spaced along the entire circumference of the tooth base. A similar arrangement of dentine folds was reported in *Eurhinosaurus* and *Temnodontosaurus* by Fraas (1891). The layer of cementum enveloping the outer surface of the tooth base is not preserved, but osteocementum is present between the dentine folds and penetrates the pulp cavity, as in other Early Jurassic ichthyosaurs (Fraas, 1891; Besmer, 1947).

The teeth of ROM 44295 are tightly packed, with adjacent tooth bases contacting each other basally (Fig. 3.3A), and there is no indication of a bony septum separating individual alveoli. ROM 44295 shares the absence of alveoli with parvipelvian ichthyosaurs, but is in contrast to almost all non-parvipelvian ichthyosaurs, where distinct sockets are present at least anteriorly in the jaws (e.g. Ji et al., 2016: char. 59).

Axial skeleton. McGowan (1997) reported that several articulated vertebral series, comprising 67 vertebrae in total, were preserved in ROM 44295. However, when ROM 44295 was personally examined for the purpose of this study in December 2015, only one block containing an articulated

series of ca. 10 vertebral centra could be located. Multiple rib and possible gastral basket elements are also preserved in ROM 44295 and lie in close association with one of the preserved forefins. Unfortunately, the vertebral centra, as well as the ribs and potential gastral basket elements, are poorly preserved as badly weathered, oblique or parasagittal sections and it is not possible to describe their morphology in detail.

Pectoral girdle. Possible pectoral girdle elements are preserved in ROM 44295, in close association with the proximal end of the only preserved humerus. However, these elements are preserved as badly weathered sections and it is not possible to establish their identity, nor provide a detailed description of their morphology.

Forefin. Both forefins are partially preserved in ROM 44295. One of the forefins comprises a badly weathered humerus and epipodials and a well preserved manus, missing only the distal phalanges (Fig. 3.4). The other forefin comprises the epipodials and a complete manus, with the distal phalanges disarticulated (Fig. 3.5). Determining the correct orientation of ichthyosaur forefins is largely based on examination of surface anatomy features of the proximal part of the humerus (e.g. McGowan and Motani, 2003). However, because the only preserved humerus of ROM 44295 is badly weathered proximally and none of the relevant surface anatomy features are preserved, it is not possible to determine which of the forefins is the right one and which one is the left one.

The only humerus of ROM 44295 is preserved as a badly weathered, paracoronal section (Fig. 3.4). Its proximal end is anteroposteriorly shorter than the distal end (85.0 mm and 165.0 mm, respectively), like in *Hudsonelpidia brevirostris* (ROM 41993; McGowan, 1995a), *Temnodontosaurus* spp. (e.g. *T. trigonodon*, SMNS 15950; *T. platyodon*, NHMUK PV R2003), Leptonectidae (e.g. *Leptonectes tenuirostris*, OUM J.10319; *Eurhinosaurus longirostris*, SMNS 14931), *Stenopterygius* sp. (e.g. Johnson, 1977; Maisch, 2008) and *Hauffiopteryx typicus* (e.g. SMNS 51552), but different from *Macgowania janiceps* (ROM 41991; McGowan, 1991), *Gen. et sp. nov A* (ROM 28964; Chapter 2), *Suevoleviathan disinteger* (SMNS 15390; Maisch, 1998), *Ichthyosaurus* spp. (e.g. Lomax and Massare, 2016) and *Malawania anachronus* (Fischer et al., 2013), where the distal and proximal ends of the

humerus are of roughly equal anteroposterior length. The distal end of the humerus possesses an anteroproximal tuberosity, as in many Late Triassic and Early Jurassic parvipelvians (Fischer et al., 2016: char. 63:1), but is different from the condition in cf. *Macgowania janiceps* (ROM 41991; McGowan, 1996), some specimens of *Ichthyosaurus* (e.g. Lomax and Massare, 2016) and *Malawania anachronus* (Fischer et al., 2013), where the anteroproximal end of the humerus forms an acute angle with the radial facet. The distal end of the humerus bears two, distally facing facets – an anterior one for the radius and a posterior one for the ulna. The radial facet is anteroposteriorly longer than the ulnar facet (95.0 mm and 75.0 mm, respectively), like in some specimens of *Temnodontosaurus trigonodon* (e.g. SMNS 15950). However, because the humerus is preserved as a paracoronal section, the apparent difference in length between the distal humeral facets could also be explained as a preservational/orientation artefact.

Both radii are preserved in ROM 44295. The dorsal/ventral surface of the radius associated with the proximally complete forefin is weathered proximally and posteriorly and the same radius is broken distally along a transverse plane (Fig. 3.4). Only the anteriodistal part of the radius associated with the distally complete forefin is preserved, and its surface is heavily eroded (Fig. 3.5). The radius contacts the humerus proximally, the ulna posteriorly, the radiale distally and the intermedium posterodistally. It is pentagonal in dorsal/ventral outline, like in many other parvipelvian ichthyosaurs (e.g. Motani, 1999c). Its maximum proximodistal length equals its anteroposterior width (115.0 mm), similar to *Macgowania janiceps* (ROM 41993; McGowan, 1991) but in contrast to all other Early Jurassic parvipelvians, where the anteroposterior width of the radius is greater than its proximodistal length (e.g. Motani, 1999c). The radius bears a notch in its anterior margin, like in *Macgowania janiceps* (ROM 41992; McGowan, 1996) and many other Early Jurassic parvipelvians (e.g. Motani, 1999c). The radius also bears a notch in its posterior margin, like in *Macgowania janiceps* (ROM 41992; McGowan, 1996) and *Leptonectes tenuirostris* (e.g. McGowan, 1989).

A partial ulna of ROM 44295 is associated with the proximally complete forefin (Fig. 3.4). It is preserved as a badly weathered, paracoronal section. The ulna contacts the humerus proximally, the radius anteriorly, the intermedium anterodistally and the ulnare posterodistally. The anterior margin of the ulna bears a notch, which together with the notch on the posterior margin on the radius, forms a

small, circular interepipodial foramen. A similar interepipodial foramen is also present in *Macgowania janiceps* (ROM 41992; McGowan, 1996) and *Leptonectes tenuirostris* (e.g. McGowan, 1989).

The morphology of the carpals and metacarpals is similar to that of other parvipelvian ichthyosaurs (Motani, 1999c). The proximal carpals are almost completely preserved in the proximally complete forefin (Fig. 3.4), while only a badly weathered radiale is preserved in the distally complete forefin (Fig. 3.5). The radiale is roughly pentagonal in dorsal/ventral outline, has a concave dorsal/ventral surface and bears a notch in its anterior margin. The radiale contacts the radius proximally, the intermedium proximally and posteriorly, distal carpal 3 distally and posteriorly, and distal carpal 2 distally. The intermedium is broken at roughly mid-proximodistal height along a transverse plane, and its proximal and posterior surfaces are eroded; an intermedium is not preserved in the distally complete forefin. The intermedium is hexagonal in shape and roughly equal in size to the radiale. Its dorsal/ventral surface is also concave. The intermedium contacts the radius proximally and anteriorly, the ulna proximally, the radiale distally and anteriorly, the ulnare posteriorly, distal carpal 3 distally and distal carpal 4 distally and posteriorly. The ulnare is only partially preserved as a paracoronal section in the proximally complete forefin, while it is not preserved in the distally complete one. It contacts the ulna proximally, the intermedium anteriorly and distal carpal 4 distally.

The distal carpals and metacarpals are preserved in both forefins. Their dorsal or ventral surfaces are completely preserved in the proximally complete forefin (Fig. 3.4), while the surfaces of these bones are heavily eroded in the distally complete forefin (Fig. 3.5). Three distal carpals (2-4) are preserved distal to the corresponding proximal carpals in the proximally complete forefin (Fig. 3.4); only two distal carpals (2-3) are preserved in the distally complete forefin (Fig. 3.5). Distal carpal 2 bears a notch in its anterior margin and is roughly pentagonal in outline, while distal carpals 3 and 4 are roughly hexagonal in outline. Their dorsal/ventral surfaces are slightly concave. Metcarpals ii – iv are preserved distally to the distal carpals in both forefins (Figs 3.4–3.5). Metacarpal ii is roughly pentagonal in outline, whereas the other preserved metacarpals are roughly hexagonal in outline. Metacarpal v is not preserved in any of the forefins in ROM 44295, but the absence of metacarpal v could be a preservational artefact, especially since metacarpal v is present in forefins of some other parvipelvian ichthyosaurs, including *Macgowania janiceps* (e.g. Motani, 1999c).

The manus is well preserved in both forefins of ROM 44295. In one of the forefins, the manus is incomplete distally (Fig. 3.4), but the other forefin preserves the most distal phalanges (Fig. 3.5). In general, the morphology of the manus resembles that of *Macgowania janiceps* and Early Jurassic parvipelvians (e.g. Motani, 1999c). The manus has 5 digits – four primary digits (II-IV) and one postaxial accessory digit. Phalanges forming digits II-IV are rectangular to hexagonal in dorsal/ventral outline, have a concave dorsal/ventral surface and are anteroposteriorly wider than proximodistally long. The phalanges of digit V also have a slightly concave dorsal/ventral surface, but they are rectangular or circular in outline, often proximodistally longer than anteroposteriorly wide. The proximal phalanges are tightly packed proximally, like in most other parvipelvians (e.g. Motani, 1999c), but unlike in some specimens of *Leptonectes tenuirostris* (e.g. IGS 51236), *Leptonectes solei* (McGowan, 1993), and *Eurhinosaurus longirostris* (e.g. SMNS 14931), where the proximal phalanges are more loosely packed. The distal phalanges of ROM 44295 are more loosely arranged, as evidenced by the disarticulated mass of phalanges at the distal end of the distally complete forefin. All of the phalangeal elements forming digit II bear a notch on their anterior margin. A postaxial accessory digit, comprised of small, circular phalanges, is well preserved in the proximally complete forefin of ROM 44295. A similar postaxial accessory digit is also present in *Macgowania janiceps* (ROM 41992; McGowan, 1996) and some specimens of *Stenopterygius* (e.g. Motani, 1999c). The high number of well-ossified phalanges in the longest manual digit (ca. 12 in the distally complete forefin; Fig. 3.5) and the well-ossified accessory digit (Fig. 3.4) indicate osteological maturity of ROM 44295 (Motani, 1999c).

Pelvic girdle (Figs 3.6–3.7)**.** A partial pelvic girdle is preserved in ROM 44295, closely associated with the preserved hindfin. An unidentified element lying in close association with the proximal ends of the pubis and ischium is likely the proximal portion of the ilium (Fig. 3.7). However, the surfaces of this element are damaged and its identity cannot be established with confidence. The ischium is almost complete, with only its distal end incompletely preserved (Figs 3.6–3.7). The ischium is proximodistally longer than anteroposteriorly wide, with a slight median constriction. Its proximal and distal ends are of roughly equal anteroposterior width, but the proximal end has a greater dorsoventral thickness than

the distal end. A similar ischium morphology is present in some Early Jurassic parvipelvian ichthyosaurs (e.g. Ji et al., 2016: character 118:1), but is in contrast to the plate-like, anteroposteriorly broad ischia of more basal, Triassic ichthyosaurs (Ji et al., 2016: character 118:0) and the styloidal ischia of *Leptonectes tenuirostris*, *Ichthyosaurus* and *Hauffiopteryx* (Ji et al., 2016: character 118:2). The pubis is completely preserved. It is proximodistally longer than anteroposteriorly broad and more styloidal than plate-like, similar to the pubis of parvipelvian ichthyosaurs, and in contrast to the plate-like pubis of more basal, Triassic ichthyosaurs (Ji et al., 2016: character 116). The distal end of the pubis is broader anteroposteriorly than its proximal end, as in basal parvipelvians and basal neoichthyosaurs (e.g. McGowan and Motani, 2003), and its proximal end is dorsoventrally thicker than its distal end. The pubis and ischium are roughly equal in size, and enclose an elliptical, mediolaterally broad thyroid fenestra, similar to that of parvipelvian ichthyosaurs (Ji et al., 2016: character 122:2), but different from the roughly trapezoidal, median thyroid fenestra of Triassic ichthyosaurs (Ji et al., 2016: character 122:1). The proximal ends of the pubis and ischium are still partially obscured by matrix, so it is not possible to determine whether the bones were separated from each other or fused proximally, like in some specimens of *Leptonectes* and *Ichthyosaurus* (e.g. McGowan and Motani, 2003). Even though the distal part of the ischium is not preserved, the distal part of the pubis is completely preserved and there is no indication that the two pelvic elements were fused distally, as in some specimens of *Temnodontosaurus* (e.g. SMNS 15950; McGowan, 1979) and *Leptonectes* (McGowan and Motani, 2003).

Hindfin (Figs 3.6–3.7)**.** An almost complete hindfin is preserved in ROM 44295, in close association with the pelvic girdle. Only the distal phalanges and the proximal part of the femur are missing, and the posterior margins of the fibula and calcaneum are slightly damaged. Because determining the correct orientation of the hindfin relies on examination of anatomical features present in the proximal part of the femur (Maxwell et al., 2012a), it is not possible to determine whether the preserved hindfin is the left, or the right one. The femur forms a prominent anterodistal extension, a condition similar to that in mixosaurids (e.g. *Mixosaurus cornalianus*; PIMUZ T 4848), shastasaurids (e.g. *Shonisaurus popularis*, NSM uncatalogued; Camp 1980), *Californosaurus perrini* (UCMP 9119; Merriam, 1908),

toretocnemids (e.g. *Toretocnemus californicus*, UCMP 8100; Merriam, 1905) and basal neoichthyosaurs (e.g. McGowan and Motani, 2003), but different from thunnosaurs (e.g. McGowan and Motani, 2003), in which the femur lacks an anterodistal extension. The tibial and fibular facets are slightly concave and the tibial facet has a greater anteroposterior length than the fibular facet.

The tibia is roughly rectangular in dorsal/ventral outline, with its anterior margin greater in proximodistal length than the posterior margin. The tibia contacts the femur proximally. Its proximal margin is straight and inclined anterodistally. The distal margin of the tibia is slightly convex and is roughly equal in anteroposterior length to the proximal margin. The distal end of the tibia contacts distal tarsals 2 and 3 anteriorly, and the astragalus posteriorly. The anterior margin of the tibia bears a deep notch, roughly at half of its proximodistal length. Proximally to this notch, the tibia forms a rectangular extremity, a feature shared only with *Californosaurus perrini* (UCMP 9119; Merriam, 1908), *Callawayia neoscapularis* (TMP 94.380.11; Nicholls and Manabe, 2001) and toretocnemids (e.g. *Toretocnemus californicus*; UCMP 8100; Merriam, 1905). A shallow notch is also present on the posterior margin of the tibia.

The fibula is roughly equal in size to the tibia and lies in close association to it. It is rectangular in dorsal/ventral outline, with its anterior margin much smaller than the posterior margin in proximodistal length and is strikingly similar to the fibula of *Callawayia neoscapularis* (TMP 94.380.11; Nicholls and Manabe, 2001) in this respect. The proximal end of the fibula is straight, inclined posteroproximally and contacts the femur. The distal end is roughly equal to the proximal end in anteroposterior length and is inclined anterodistally. The distal end of the fibula contacts the astragalus anteriorly and the calcaneum posteriorly. The posterior margin of the fibula is straight, while its anterior margin bears a shallow notch. The notches present on the contiguous margins of the hindfin epipodials form a clearly demarcated spatium interosseum (Fischer et al., 2013:character 64), which is also present in all Triassic ichthyosaurs, as well as basal neoichthyosaurs (with the exception of *Suevoleviathan disinteger*; SMNS 15390), but in contrast to thunnosaurs, where the structure is absent (Ji et al., 2016: character 137).

The proximal tarsal row in ROM 44295 is comprised of two elements, the astragalus and calcaneum. A similar condition is also present in basal ichthyopterygians (e.g. *Chaohusaurus*

geishanensis; GMPKU-P-1118), cymbospondylids (e.g. *Xinminosaurus catactes*; GMPKU-P-1206), mixosaurids (e.g. *Mixosaurus cornalianus*; PIMUZ T 4848), and shastasaurids (e.g. *Guizhouichthyosaurus tangae*; IVPP V11853). By contrast, in euichthyosaurs the proximal tarsal row is comprised of three elements (e.g. Ji et al., 2016: character 141). The astragalus is anteroposteriorly wider than proximodistally long and is roughly pentagonal in outline in dorsal/ventral view. Anteriorly, the astragalus contacts the tibia, distally it contacts distal tarsals 3 and 4, posteriorly it contacts the calcaneum, and proximally it contacts the fibula. The calcaneum is smaller than the astragalus and is roughly rectangular in outline. However, because the posterior margin of the hindfin has eroded away, the apparently rectangular outline of the calcaneum could be a preservational artefact. The calcaneum contacts the fibula proximally, the astragalus anteriorly and distal tarsal 4 and metatarsal V, distally. The distal tarsal row is comprised of four elements. The first of these, distal tarsal 2, is roughly rectangular in outline and bears a deep notch on its anterior margin. Distal tarsals 3 and 4 are roughly pentagonal in outline, with their proximodistal length shorter than their anteroposterior width. Metatarsals ii–iv are roughly rectangular in outline, with their anteroposterior length greater than their proximodistal width. Metatarsal v, in contrast, is roughly oval in outline, with its proximodistal length longer than its anteroposterior width.

Four primary digits (2–5) are present in the pes of ROM 44295. It is not possible to determine whether an accessory digit was present or absent, because the phalanges comprising the accessory digits in ichthyosaurs are more loosely associated with the hindfin than the phalanges comprising the primary digits, and they could have been easily lost and/or damaged during excavation and preparation. The digits are comprised of 8–9 discernable phalanges, but many small, disarticulated phalanges are preserved in the distal part of the hindfin, so the total number of phalanges in each digit was higher than the given phalangeal count. The phalanges comprising primary digit 2 are roughly rectangular in shape and all bear a deep notch on their anterior margin. The phalanges forming primary digits 3 and 4 are rectangular to hexagonal in shape. Digit 5 is comprised of elliptical elements, which are smaller than the elements forming the other phalanges. The tightly packed phalanges in the pes of ROM 44295 are reminiscent of the tightly packed phalanges present in *Ichthyosaurus* (e.g. OUM J.13799) and *Suevoleviathan disinteger* (SMNS 15390), but different from the more loosely associated phalanges in

Temnodontosaurus platyodon (e.g. NHMUK PV R2003) and *Leptonectes tenuirostris* (NHMUK PV R498).

The hindfin of ROM 44295 was most likely only slightly smaller than the forefin (humerus distal anteroposterior length 165.0 mm vs femur distal anteroposterior length 117.8 mm), as in *Suevoleviathan disinteger* (SMNS 15390; Maisch, 1998) and *Temnodontosaurus* spp. (e.g. *T. trigonodon*, SMNS 15950), and in contrast to *Leptonectes tenurostris* (e.g. NHMUK PV R498) and *Ichthyosaurus* (e.g. NHMUK PV R2013; Lomax and Massare, 2016), where the hindfin is much smaller than the forefin. Commencing from the epipodials, all of the elements comprising the anterior margin of the hindfin in ROM 44295 bear notches, as in *Temnodontosaurus trigonodon* (e.g. SMNS 15950).

DISCUSSION

Parvipelvian affinities of *Gen. et sp. nov. B.* Comparisons of the anatomy of ROM 44295 with other Triassic and Early Jurassic ichthyosaurs indicate the presence of many anatomical features characteristic for Parvipelvia, particularly in the anatomy of the forefin and pelvic girdle. The parvipelvian affinities of ROM 44295 are confirmed in a phylogenetic analysis (Chapter 5). ROM 44295 possess two of the four unambiguous synapomorphies of Parvipelvia: 1) ulna contiguous shaft – absent or notch (character 104:1) and the presence of only one postaxial accessory digit in the forefin (character 123:1). The two other unambiguous synapomorphies of Parvipelvia, namely the presence of the scapular antero-proximal extension towards clavicle (character 83:1) and the absence of the posterior extension of the scapula (character 85:1) could not be confirmed because of the poor preservation of the pectoral girdle. Within Parvipelvia, ROM 44295 is recovered as the sister taxon of a clade comprising (*Hudsonelpidia*, (*Malawania*, Neoichthyosauria)) (node B, Fig. 5.2). This clade is supported by a single unambiguous synapomorphy – humerus distal:proximal width ratio – distal wider (character 96:1).

The high number of phalanges in the longest digit and the well-ossified accessory digit in the forefin suggest osteological maturity of ROM 44295 (Motani, 1999b), making it comparable in body size to the Early Jurassic parvipelvian *Temnodontosaurus* and, therefore, one of the largest parvipelvian ichthyosaurs currently known. The dentition of ROM 44295 indicates even more advanced adaptation

to an apex predator lifestyle, with the entire dentition comprised of mediolaterally flattened, bicarinate crowns, in contrast to the dentition of *Temnodontosaurus*, in which only part of the teeth possess carinae. The palaeoecology of ROM 44295 is further explored in the Discussion of Chapter 5.

FIGURES

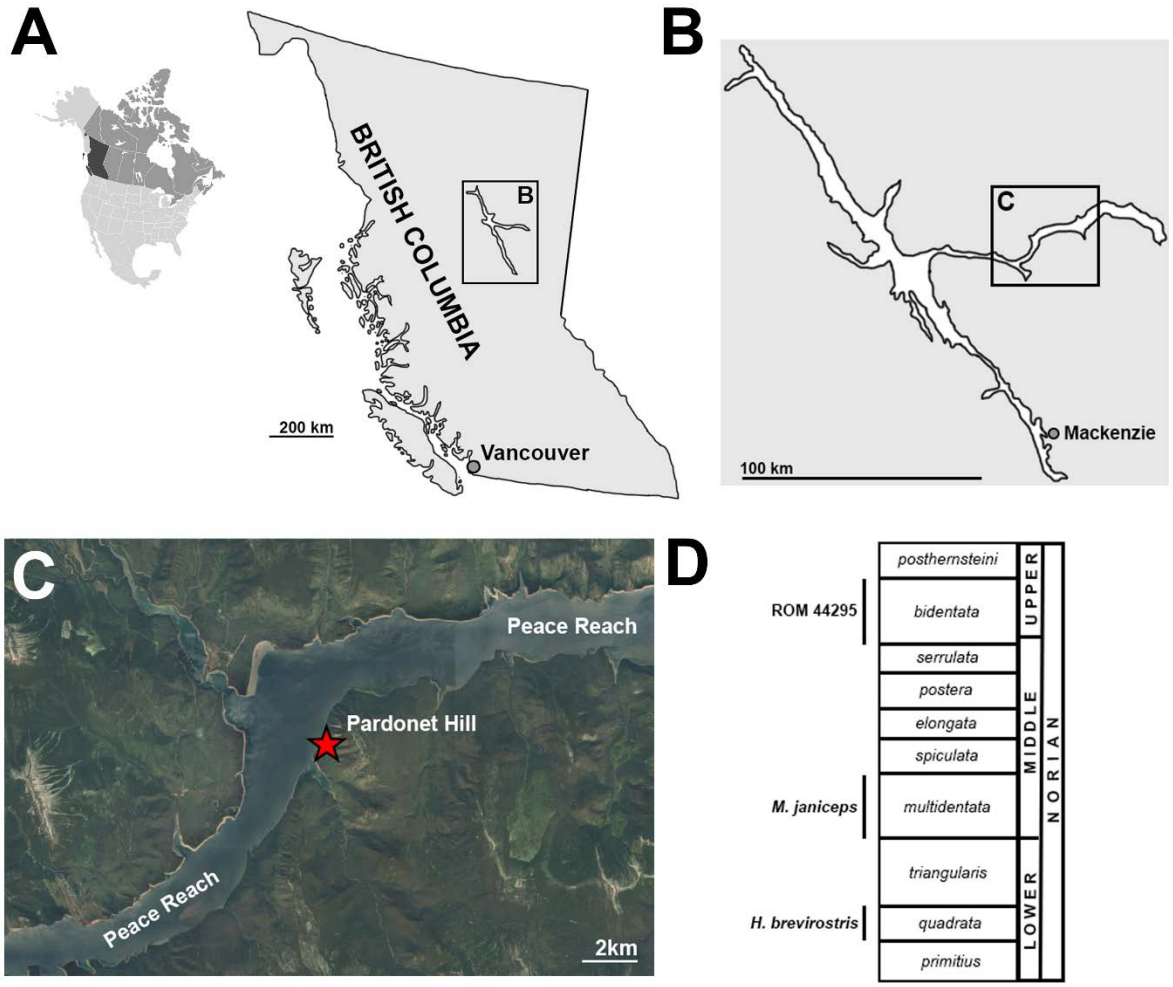

FIGURE 3.1. Pardonet Hill, Williston Lake, British Columbia, Canada – the type (ROM 44295) locality of *Gen et sp. nov. B* (**A**–**C**) and stratigraphic distribution of parvipelvian ichthyosaurs from the Norian of Williston Lake, British Columbia, Canada (**D**). (**A**) Outline map of British Columbia, Canada, showing the geographic position of Williston Lake. (**B**) Outline map of Williston Lake, showing the geographic position of the Peace Reach and Pardonet Hill. (**C**) Pardonet Hill, with star marking the approximate position of ROM 44295 when it was found in the field in 1991. Conodont zones in (**D**) follow Orchard and Tozer (1997).

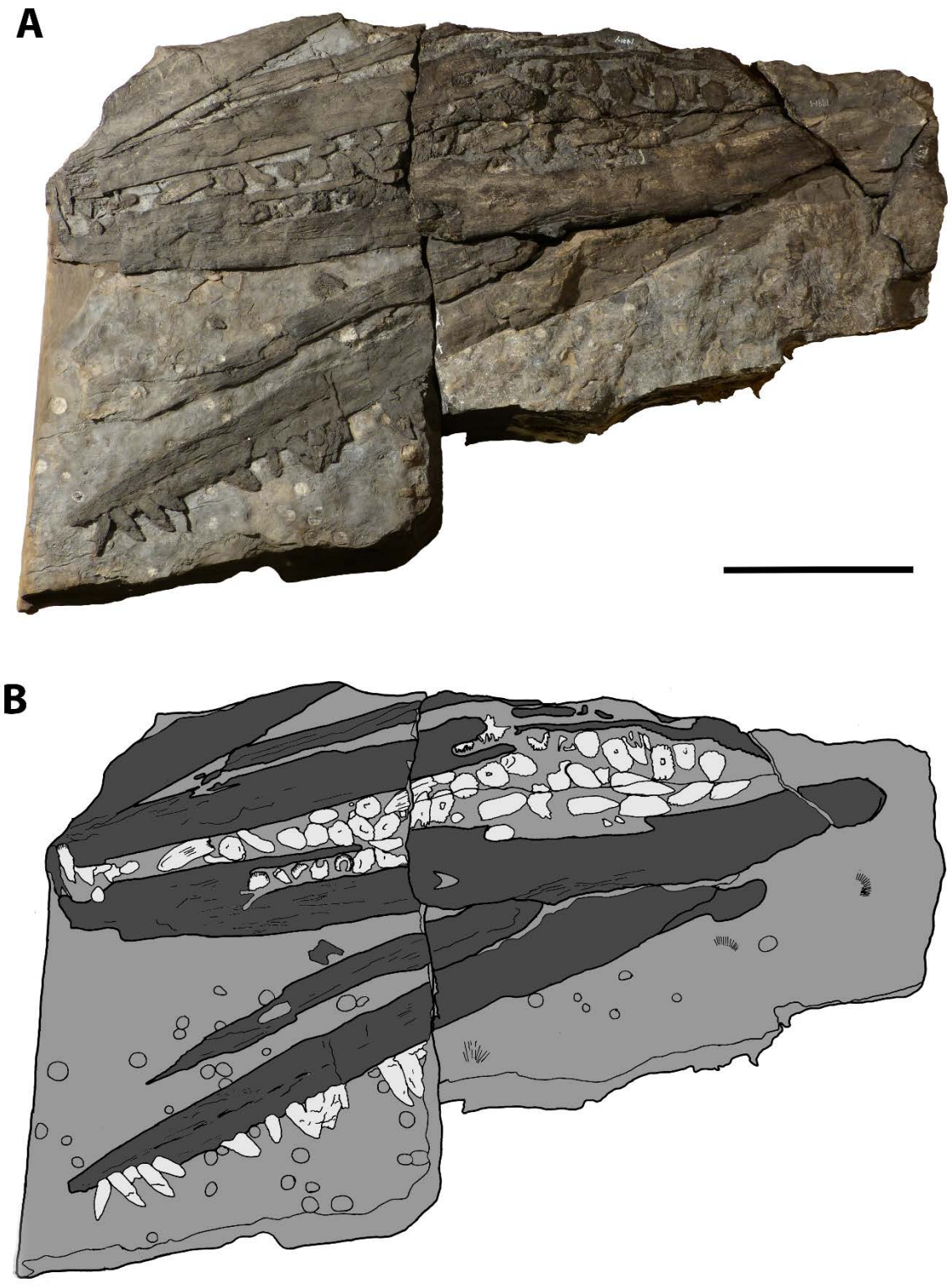

FIGURE 3.2. Partially preserved rostrum, mandible and dentition of the holotype (ROM 44295) of *Gen. et sp. nov. B* (**A**). In line drawing (**B**), grey color indicates block matrix, dark grey indicates broken bone surface, light grey indicates dentition. Round and ellipsoidal outlines indicate calcite-filled replacements of the spongiomorph *Heterastridium*. Scale bar equals 250 mm.

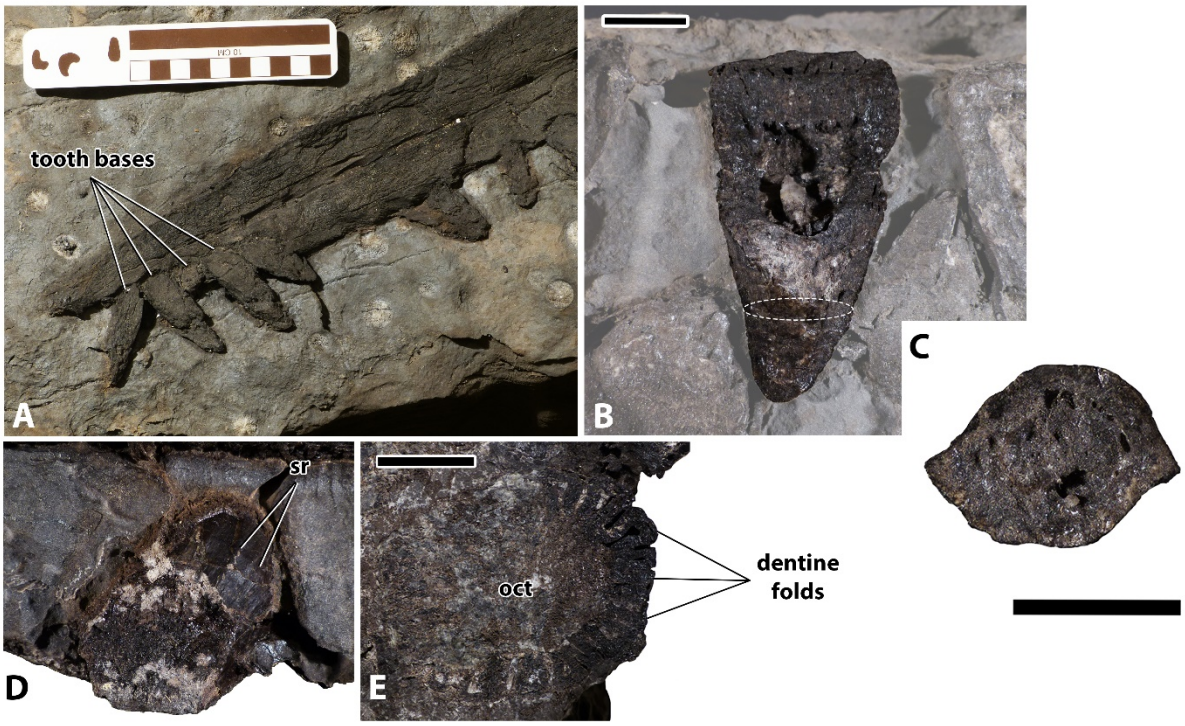

FIGURE 3.3. Dentition of the holotype (ROM 44295) of *Gen. et sp. nov. B.* (**A**) Anterior part of dentigerous bone (premaxilla or dentary) in lateral or medial view, showing preserved tooth sections. Note the adjacent tooth bases contacting each other basally, indicating the absence of distinct alveoli. (**B**) A partially preserved tooth in labial or lingual view, with the tooth base and base of the tooth crown heavily damaged. White elipse indicates approximate position of transverse section in (**C**). (**C**) A preserved transverse section through a tooth crown, clearly showing mesial and distal carinae. (**D**) A partially preserved tooth crown, showing subtle abipcobasally oriented ridges ornamenting its surface. (**E**) A preserved transverse section through a tooth base, showing dentine folds, and osteocementum filling the pulp cavity. Abbreviations: **oct**, osteocementum; **sr**, subtle ridges. Scale bar in A equals 100 mm, all other scale bars equal 10 mm.

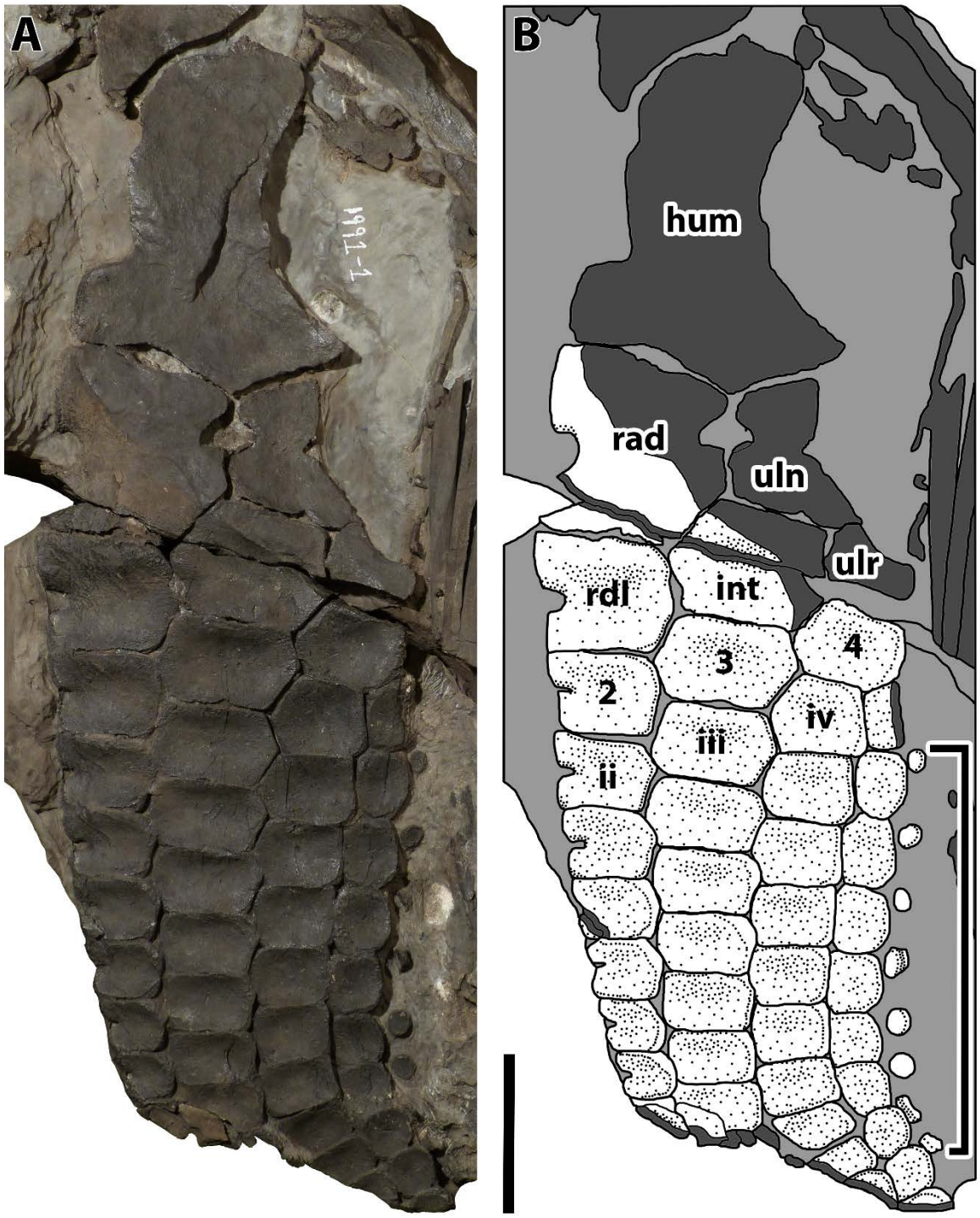

FIGURE 3.4. Proximally complete forefin of holotype (ROM 44295) of *Gen. et sp. nov. B* (**A**). In line drawing (**B**), grey indicates block matrix and dark grey indicates broken bone surface. Abbreviations: **hum**, humerus; **int**, intermedium; **rad**, radius; **rdl**, radiale; **uln**, ulna; **ulr**, ulnare. Arabic numerals indicate distal carpals, roman numerals indicate metacarpals. Square bracket indicates accessory digit. Scale bar equals 100 mm.

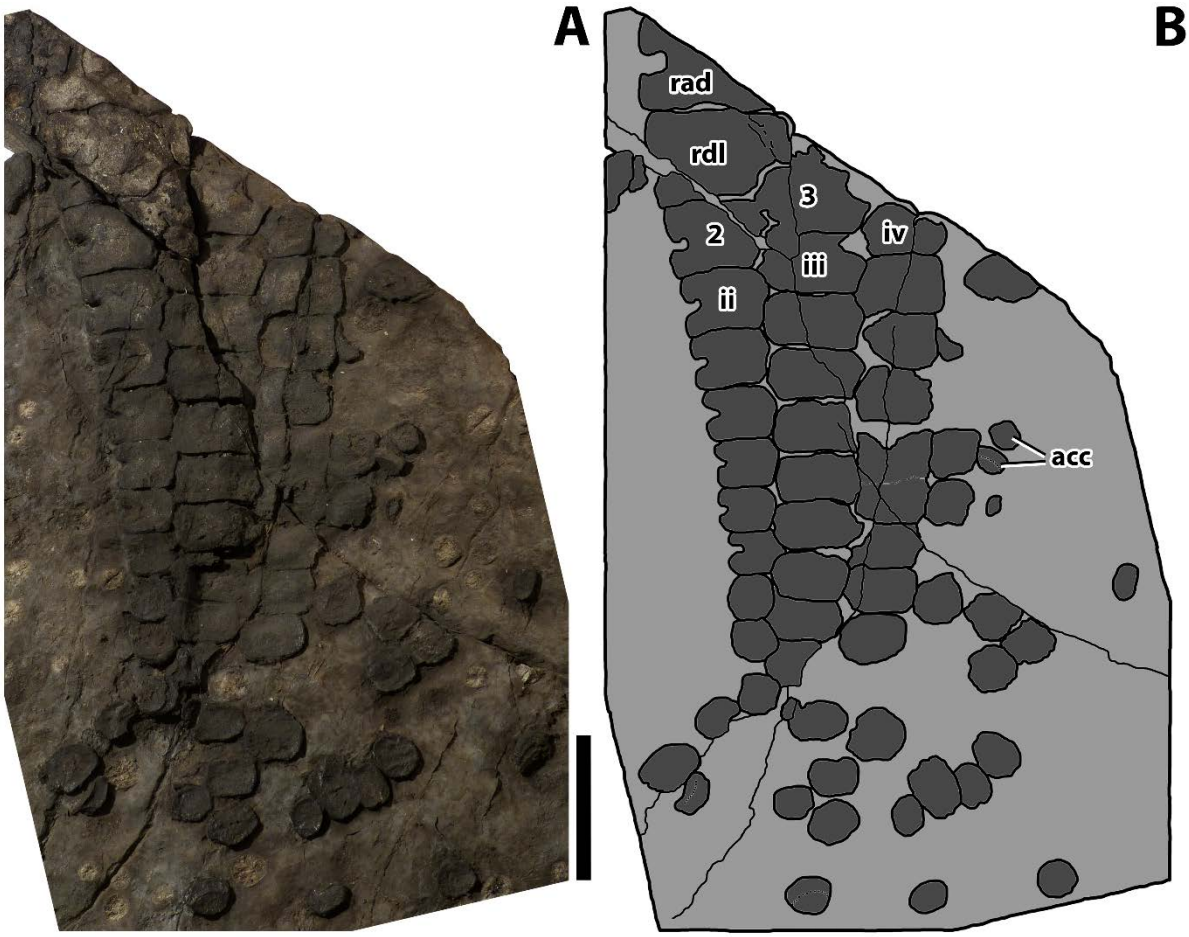

FIGURE 3.5. Distally complete forefin of holotype (ROM 44295) of *Gen. et sp. nov. B* (**A**). In line drawing (**B**), grey indicates block matrix and dark grey indicates broken bone surface. Abbreviations: **acc**, phalanges of accessory digit; **rad**, radius; **rdl**, radiale. Arabic numerals indicate distal carpals, roman numerals indicate metacarpals. Scale bar equals 100 mm.

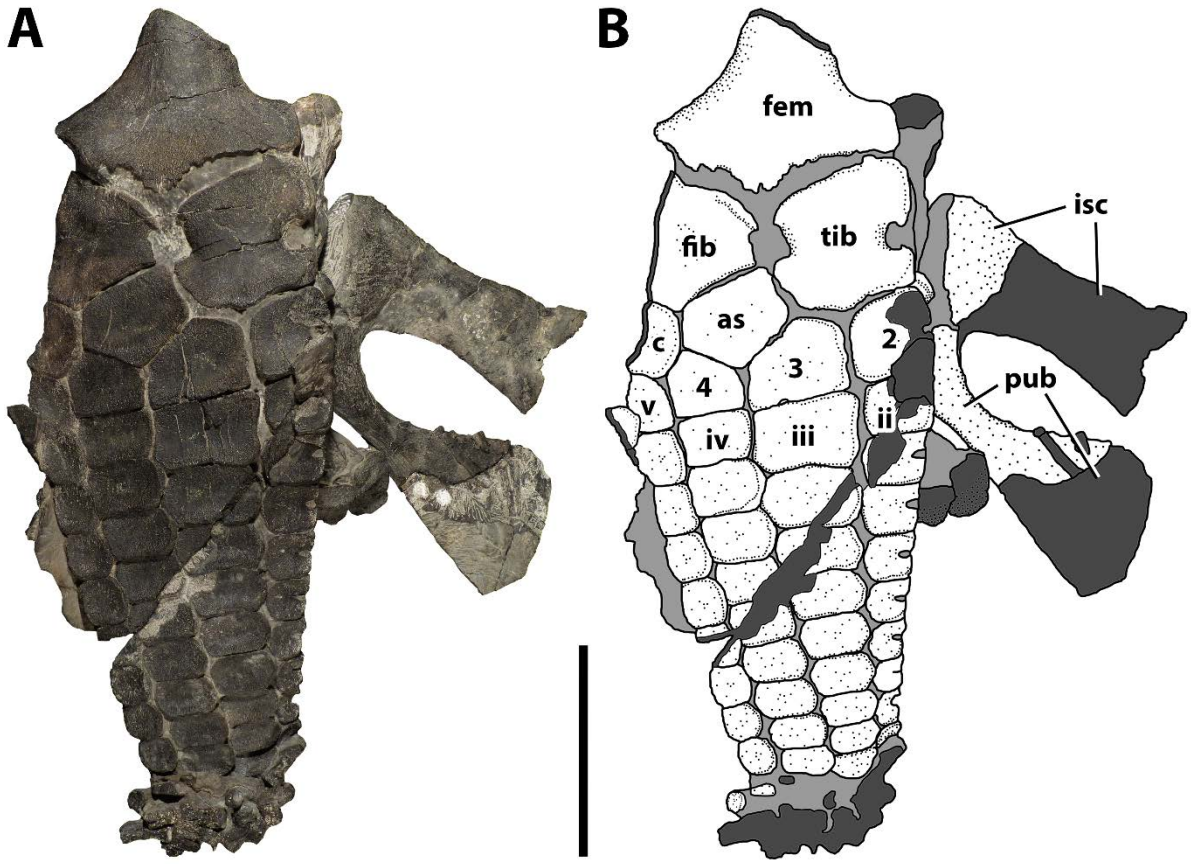

FIGURE 3.6. Pelvic girdle of holotype (ROM 44295) of *Gen. et sp. nov B* in dorsal or ventral view (**A**). In line drawing (B), grey indicates rock matrix and dark grey indicates broken bone surface. Abbreviations: **as**, astragalus; **c**, calcaneum; **fem**, femur; **fib**, fibula; **isc**, ischium; **pub**, pubis; **tib**, tibia. Arabic numerals indicate distal tarsals, roman numerals indicate metatarsals. Scale bar equals 100 mm.

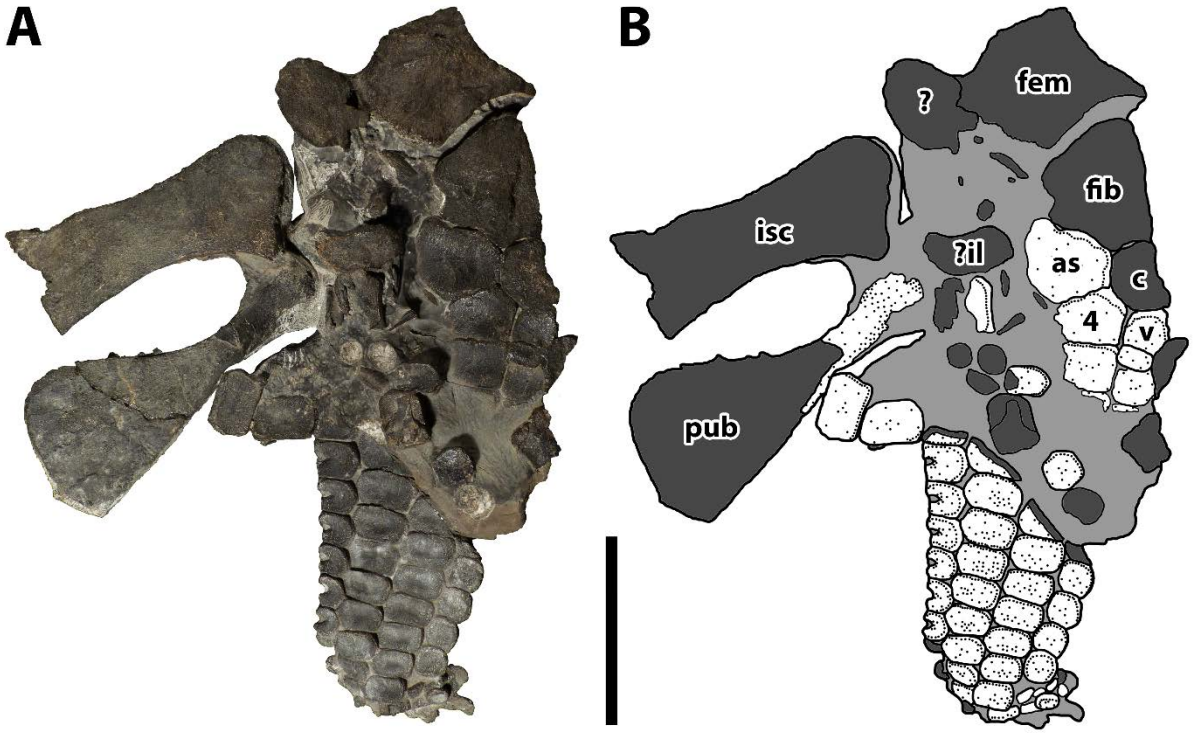

FIGURE 3.7. Pelvic girdle of holotype (ROM 44295) of *Gen. et sp. nov B* in dorsal or ventral view (**A**). In line drawing (B), grey indicates rock matrix and dark grey indicates broken bone surface. Abbreviations: **?il**, possible ilium; **as**, astragalus; **c**, calcaneum; **fem**, femur; **fib**, fibula; **isc**, ischium; **pub**, pubis; **tib**, tibia. Arabic numerals indicate distal tarsals, roman numerals indicate metatarsals. Scale bar equals 100 mm.

CHAPTER 4: A RE-ASSESSMENT OF THE CRANIAL OSTEOLOGY OF *CYMBOSPONDYLUS* LEIDY, 1868 AND A REVISED TAXONOMY OF THE GENUS

INTRODUCTION

Ichthyosaurs (Ichthyopterygia; Owen, 1840) were a successful clade of secondarily aquatic diapsids spanning from the Early Triassic to the early Late Cretaceous (e.g. McGowan and Motani, 2003; Motani, 2005a). Derived members of the clade (Parvipelvia; Motani, 1999a) were characterized by a streamlined, 'fish-like' body plan similar to that of extant lamniform sharks and scombrids, with a well demarcated dorsal fluke and a crescent-shaped caudal fluke. The anatomy of parvipelvians is well known from abundant fossil material from the Jurassic of Europe, especially the Early Jurassic of England (Hettangian–Pliensbachian; e.g. Benton and Spencer, 1995) and Southern Germany (Toarcian; e.g. Hauff and Hauff, 1981), and the Middle–Late Jurassic of England (Callovian–Oxfordian; e.g. Andrews, 1910; Appleby, 1956; Kirton, 1983). Numerous complete, articulated skeletons, some with preserved soft tissues and gut contents (e.g. Owen, 1881; Hauff and Hauff, 1981; Martill, 1995) have helped to gain a thorough understanding of parvipelvian diets (e.g. Pollard, 1968; Keller, 1976; Böttcher, 1989), reproductive biology (e.g. Woodward, 1906; Böttcher, 1990; Deeming et al., 1993), swimming mechanics (e.g. Motani, 2002a), visual sensitivity (Motani et al., 1999b) and even basal metabolic rate (Motani, 2002b; Bernard et al., 2010). However, despite the abundance of exceptionally preserved Jurassic ichthyosaurs, much less is known of the anatomy and evolution of earlier, Triassic ichthyosaurs.

The phylogenetically most basal and stratigraphically oldest ichthyosaurs are known from the Early Triassic (Olenekian) of the Northern Hemisphere (e.g. Wiman, 1929; Young and Dong, 1972; Shikama et al., 1978; Nicholls and Brinkman, 1995; Cuthbertson et al., 2013). These ichthyosaurs exhibit plesiomorphic anatomical states (Motani, 1999a) and are important for our understanding of the early evolution of ichthyosaurs and the phylogenetic relationships between ichthyosaurs and other diapsids (e.g. Motani et al., 1998; Chen et al., 2014a). Unfortunately, most specimens are incomplete,

hindering our understanding of the early evolution of ichthyosaurs. Nevertheless, the anatomy and phylogeny of early ichthyosaurs has been the subject of extensive work in the last 20 years (e.g. Motani, 1996, 1997a, 1997b, 1998b, 2000; Cuthbertson et al., 2013a, 2013b, 2014) and abundant, well-preserved early ichthyosaurs from South East China (Chen et al., 2014b; Motani et al., 2014; Motani et al., 2015b; Motani et al., 2015c) will undoubtedly yield new, important insights.

Historically, knowledge of the early evolutionary history of ichthyosaurs was based almost entirely on fossil material collected from the Middle Triassic (Anisian–Ladinian) of the Grenzbitumen-Zone of Monte San Giorgio in Switzerland and Italy (e.g. Bassani, 1886), the Muschelkalk of Germany (e.g. Huene, 1916) and the Prida Formation of Nevada, USA (e.g. Merriam, 1905, 1908, 1910). Diagnostic specimens from these localities are dominated by representatives of three genera: the small-bodied (body length of 1-2 m) mixosaurids *Mixosaurus* and *Phalarodon*, and the large-bodied (body length ~9 m) cymbospondylid *Cymbospondylus*. Historically-collected specimens of mixosaurids have undergone detailed revision (e.g. Brinkmann, 1998, 2004; Motani, 1999b; Maisch and Matzke, 2001; Schmitz, 2005). Together with new discoveries from North America and China, this has provided important insights into their anatomy, systematics and biogeography, making the Mixosauridae one of the best-known clades of ichthyosaurs (e.g. Nicholls et al., 1999; Schmitz et al., 2004; Jiang et al., 2006, 2007; Liu et al., 2013). *Cymbospondylus*, on the other hand, remains poorly known, despite the existence of well-preserved material and a long history of research.

Cymbospondylus was originally erected based on fragmentary axial material from the West Humboldt Range and New Pass Range of the Middle Triassic (Anisian) Prida Formation, northern Nevada, USA (Leidy, 1868). Two species, *Cy. piscosus* and *Cy. petrinus*, were described, but no type species was designated. Merriam (1902) designated *Cy. piscosus* as the type species, as was discussed first by Leidy (1868), and he synonymized a third genus described by Leidy (1868), *Chonespondylus grandis*, with *Cymbospondylus*, resulting in the new combination: *Cymbospondylus* (?) *grandis*. Subsequently, more complete cranial and postcranial material assigned to *Cy. petrinus* (Merriam, 1905, 1908) allowed Merriam (1908) to synonymize *Cy.* (?) *grandis* with *Cy. petrinus*. However, the main diagnostic feature Merriam (1902, 1908) used to distinguish *Cy. piscosus* from *Cy. petrinus* - the shape of the amphicoelus concavities of vertebral centra - was considered undiagnostic by McGowan and

Motani (2003:66), who suggested the synonymy of *Cy. piscosus* and *Cy. petrinus*. I agree with their conclusions and refer all substantially complete *Cymbospondylus* specimens described by Merriam (1902, 1905, 1908) to *Cy. piscosus*.

The well-preserved specimens, extensively documented by Merriam (1905, 1908), have allowed a detailed understanding of the anatomy of *Cymbospondylus* (see Diagnosis). The plesiomorphic anatomy of *Cymbospondylus* reflects its phylogenetic position within Ichthyopterygia – *Cymbospondylus* is recovered at the base of the Ichthyosauria, a clade comprising all ichthyosaurs, to the exclusion of the Early Triassic ichthyopterygians *Chaohusaurus* and Grippioidea (Motani, 1999a; Ji et al., 2016; but see Maisch and Matzke, 2000, who found *Cymbospondylus* as the outgroup of a clade comprising a paraphyletic Shastasauridae and Parvipelvia).

Merriam (1908) described the skull of *Cymbospondylus piscosus* based primarily on UCMP 9950. For several decades after its initial description, *Cymbospondylus* remained the most complete and well-preserved skull of an early ichthyosaur. It was therefore the subject of many comparative studies, and its cranial anatomy was re-interpreted by multiple authors (von Huene, 1916; Romer, 1968; Camp, 1980; Massare & Callaway, 1990; Motani, 1999a; Maisch & Matzke, 2000, 2004; Ji et al., 2016). These accounts vary considerably in the interpretation of the circumorbital, temporal and skull roof regions, hindering our understanding of the cranial anatomy of *Cymbospondylus*.

Two additional species of *Cymbospondylus*, represented by highly complete and well-preserved material, were described since the publication of Merriam's (1905, 1908) work (numerous fragmentary specimens from North America and Europe have also been referred to *Cymbospondylus*; see McGowan and Motani, 2003, and Fröbisch et al., 2006, for recent reviews). A third species - *Cymbospondylus buchseri* - was erected on the basis of a well-preserved, partial skeleton from the Middle Triassic Grenzbitumen-Zone (Anisian–Ladinian) of Cava Tre Fontane, Monte San Giorgio, Switzerland (Sander, 1989). It differs from *Cy. piscosus* by its smaller size (estimated length of ~6 m, compared to an estimated length of ~9 m for *Cy. piscosus* [Merriam, 1908]), the possession of a proportionally larger orbit and shorter postorbital region (Sander, 1989:fig. 4), and forefin elements which are proximodistally shorter and anteroposteriorly wider than those described for *Cy. piscosus* (Sander, 1989:fig. 8). A fourth species, *Cymbospondylus nichollsi*, was described by Fröbisch et al. (2006). The

type specimen was excavated from the Fossil Hill Member (Anisian) of the Middle Triassic Favret Formation of the Augusta Mountains, Nevada, USA, and consists of a partially preserved skull, pectoral girdle and vertebral column. Although the postcranial anatomy of *Cy. nichollsi* greatly resembles that described for *Cy. piscosus* (Merriam, 1908), the described cranial anatomy is remarkably different from that of *Cy. piscosus* and *Cy. buchseri* (Fröbisch et al., 2006:fig. 11). For example, *Cy. nichollsi* was interpreted to have the cranial component of the cranio-mandibular joint formed by the squamosal, not quadratojugal, a condition different from every other ichthyosaur known from mostly complete cranial material. Furthermore, a neomorphic element posterior to the parietal was also proposed to be present in *Cy. nichollsi* and the genus as a whole.

The lack of consensus regarding the cranial anatomy of *Cymbposondylus piscosus*, and the proposed high interspecific variation in cranial anatomy of *Cymbospondylus*, hinder our understanding of the early evolution of ichthyosaurs, obscuring character polarity at the base of the ichthyosaurian phylogenetic tree. Furthermore, two recently described ichthyosaurian taxa – the durophagous *Xinminosaurus catactes* from the Middle Triassic of China (Jiang et al., 2008) and the colossal predator *Thalattoarchon saurophagis* (Fröbisch et al., 2013), which co-occurs with *Cymbospondylus nichollsi* in the Anisian of the Fossil Hill Member of the Favret Formation, Nevada, have recently been recovered in a clade together with *Cymbospondylus* (Ji et al., 2016). However, the nodal support recovered for this clade was weak, and the characters supporting cymbospondylid affinities for *Xinminosaurus* and *Thalattoarchon* are based mostly on postcranial anatomy – the presence of a coracoid foramen in *Xinminosaurus* (Ji et al., 2016) and similar morphology of pelvic and hindfin elements in *Thalattoarchon* (Fröbisch et al., 2013). A potential affinity of *Xinminosaurus* and *Thalattoarchon* with cymbospondylids is interesting, as it suggests the rapid evolution of an ecologically-disparate clade of marine reptiles in the aftermath of the end-Permian extinction event. Therefore, reconstructing the phylogenetic relationships between these Middle Triassic ichthyosaurs can provide new information on the pattern and process of ecosystem recovery in the Early and Middle Triassic (Scheyer et al., 2014).

The main objectives of the present contribution are as follows: 1) to provide a comprehensive re-description of the cranial anatomy of *Cymbospondylus*, based on personal examination of all available, well-preserved specimens, in order to provide a reliable source of data for comparative studies

of Early and Middle Triassic ichthyosaurs; 2) to identify synapomorphies which may help resolve the phylogenetic affinities of Middle Triassic ichthyosaurs; and 3) for use in phylogenetic studies of Ichthyopterygia.

SYSTEMATIC PALAEONTOLOGY

ICHTHYOPTERYGIA Owen, 1840

ICHTHYOSAURIA Blainville, 1835

CYMBOSPONDYLIDAE Huene, 1948

CYMBOSPONDYLUS Leidy, 1868

Revised diagnosis. Large-bodied ichthyosaurian, reaching ~9 m in total length in the largest individuals, possessing the following combination of characters: posterodorsal process of premaxilla extending posterior to external naris; posteroventral process of premaxilla extremely reduced or absent; maxilla posterodorsal process present; postfrontal lateral groove present; postfrontal excluded from posterodorsal orbital margin by prefrontal; nasal crest in posterior part of internasal suture present; anterior processes of parietals form parietal fork; frontal contribution to anterior margin of pineal foramen present; frontal contribution to anterior margin of supratemporal fenestra; parietal plateau present; prominent sagittal eminence present, with contributions from the parietal, anteriorly, and supratemporal, posteriorly; parietal posterolateral process elongate; supratemporal anteromedial process elongate; postorbital posterodorsal process broad; concave articular surface of the basioccipital condyle; an elongated trunk with more than 55, and most likely ~65 presacral vertebrae; an emargination of the anterior margin of the fan-shaped scapula; a humerus with a concave anterior flange; a coracoid perforated by a single, large coracoid foramen; clavicle with anterodorsal flange; carpals circular in outline; metacarpals retaining a distinct shaft, at least partially; probable pentadactyly; diapophyses reaching anterior margin of vertebral centra; and a pronounced deepening of the amphicoelous excavation of vertebral centra near their centre.

Cymbospondylus piscosus Leidy, 1868

Cymbospondylus piscosus Leidy, 1868:178

Cymbospondylus petrinus Leidy, 1868:178

Chonespondylus grandis Leidy, 1868:178

Cymbospondylus(?) *grandis* Merriam, 1902:106

Cymbospondylus nichollsi, Fröbisch et al., 2006:517.

Holotype. ANSP uncatalogued (Leidy, 1868), a series of two mostly complete and two fragmentary vertebral centra. This specimen is now presumed to be lost (R. Motani, pers. comm., Nov 2016); see McGowan and Motani (2003:66) for remarks regarding assignment of a neotype.

Referred specimens. UCMP 9950 (Figs 4.1–4.2); UCMP 9913 (Figs 4.3–4.4); UCMP 9154; UCMP 9947; FMNH PR 2251 (Figs 4.5–4.6).

Occurrence. Prida Formation (Anisian, Middle Triassic), West Humboldt Range and New Pass Range, Nevada, USA (ANSP and UCMP specimens); Fossil Hill Member, Favret Formation (Anisian, Middle Triassic), Augusta Mountains, Pershing County, Nevada, USA (exact locality on file at FMNH; Fröbisch et al., 2006).

Revised diagnosis. *Cymbospondylus* with proximodistally elongate (proximodistal length:distal anteroposterior width = 1.62) and anteroposteriorly narrow (proximodistal length:minimum anteroposterior width = 2.44) humerus shaft (Sander, 1989).

Cymbospondylus buchseri Sander, 1989

Holotype. PIMUZ T 4351, partial skull and anterior half of skeleton (Sander, 1989:fig. 7).

Occurrence. Grenzbitumenzone beds (Anisian–Ladinian boundary, Middle Triassic), Cava tre Fontane, Monte San Giorgio, Ticino (Tessin), Switzerland.

Revised diagnosis. *Cymbospondylus* with humerus almost as proximodistally long as anteroposteriorly broad (proximodistal length:distal anteroposterior width = 1.16; proximodistal length:minimum anteroposterior width = 1.37; Sander, 1989).

DESCRIPTION

Remarks. During the preparation of this study (2014-2017), restricted access to UCMP 9950 and UCMP 9913 did not allow for detailed examination of the palate and the medial surfaces of the mandibular rami of these specimens. However, examination of FMNH PR 2251 revealed that the anatomy of the palate and medial surfaces of the mandibular rami of this specimen have been correctly interpreted and comprehensively described by Fröbisch et al. (2006) and were in accordance with the description and figures of these anatomical regions published by Merriam (1908). As a result, the palate and medial wall of the mandibular ramus were not re-described in the present study. The anatomy of the lateral surface of the mandibular ramus of all of the specimens examined in this study was found to be in accordance with previously published accounts and was also not re-described. The teeth and relevant jaw fragments, on which Merriam (1908) based his original description of the dentition of *Cymbospondylus*, could not be located in the collections of the UCMP during the preparation of this study, so re-description of the dentition was also omitted from the present study. The reader is directed to Merriam (1908), Sander (1989) and Fröbisch et al. (2006), for information on the morphology of the dentition, mandibular ramus and palate of *Cymbospondylus*.

The only complete, articulated braincase of *Cymbospondylus* (UCMP 9950) is incompletely prepared and many of the exposed bone surfaces have been damaged by mechanical preparation. Additionally, the lack of well-preserved, comparative braincase material of basal ichthyopterygians, hinders the correct identification and interpretation of the braincase anatomy of *Cymbospondylus*. Because of this, the braincase anatomy is also not re-described and the reader is asked to consult Merriam (1908) and Maisch and Matzke (2004) for currently available interpretations of the braincase anatomy of *Cymbospondylus*.

Craniofacial anatomy. The general craniofacial anatomy of *Cymbospondylus* is best exemplified by a complete, three-dimensionally preserved skull of *Cymbospondylus petrinus* (UCMP 9950; Figs 4.1–4.2). This skull suffers from slight deformation, as indicated by the rostrum, which is slightly bent ventrally and towards the right, but is otherwise well preserved, with many of the sutures clearly visible.

However, because the skull was subject to mechanical preparation, its surface anatomy, especially of the rostrum, is obscured by numerous small cracks, most of which have subsequently been filled in with plaster. A second, partially complete (right side heavily eroded) and three-dimensionally preserved skull of *Cy. petrinus* (UCMP 9913; Figs 4.3–4.4) is slightly crushed mediolaterally in the postorbital region, as indicated by the proportionally narrow transverse width of the posterior part of the skull, temporal fenestrae, and mandible (Table 4.1). This skull preserves the surface anatomy and the sutures well, but was extensively damaged and has been heavily reconstructed in plaster. The type skull of *Cy. nichollsi* (FMNH PR 2251; Figs 4.5–4.6), is also three-dimensionally preserved and undistorted, but misses the preorbital region, and its bone surfaces are covered in numerous cracks, which can be easily confused with sutural lines. The type skull of *Cy. buchseri* (PIMUZ T 4351; Fig. 4.7) is exposed in left lateral view only, with the preorbital region poorly preserved and only a few distinguishable sutures present in the circumorbital and temporal regions.

The skull of *Cymbospondylus* is large (skull length = 1110 mm in UCMP 9950, 1200 mm in UCMP 9913; measured from tip of snout to posterior edge of articular surface of quadrate), but it is proportionally small in comparison to the rest of the body (12% of total estimated body length [Merriam, 1908]), like in basal ichthyopterygians (McGowan and Motani, 2003). This is in contrast to the proportionally larger skulls of more derived ichthyosaurians (e.g. 20% in the mixosaurid *Mixosaurus cornalianus* [PIMUZ T 4376], 16% in the shastasaurid *Guizhouichthyosaurus tangae* [IVPP V11853; Shang and Li, 2009], and 23% in the parvipelvian *Temnodontosaurus platyodon* [NHMUK PV R2003; McGowan, 1974a). The skull is transversely broad posteriorly (470 mm in UCMP 9950) and tapers anteriorly into a mediolaterally constricted snout, like in other ichthyopterygians (Motani et al., 2015a: char. 165:1). The preorbital (=rostrum) length is 730 mm (UCMP 9950) and accounts for approximately 66% of the skull length. The orbits are large (190 mm in anteroposterior length, and 98 mm in dorsoventral height; measured on the left side of UCMP 9950), with well-developed sclerotic rings (UCMP 9913, FMNH PR 2251, PIMUZ T 4351), like in other ichthyopterygians (Motani et al., 2015a: char.172:1). The external nares are retracted posteriorly as in other ichthyosaurs, and oriented laterally, like in other ichthyosaurians, but in contrast to basal ichthyopterygians, where the external nares are oriented more dorsally (e.g. Ji et al., 2016: char. 7). The size and shape of the external naris is difficult

to determine, as in UCMP 9950 it is obscured by plaster and matrix, and the circumnarial region is badly damaged in UCMP 9913. Nonetheless, the incompletely preserved, posterior portions of the external nares in FMNH PR 2251 suggest that the external nares were anteroposteriorly elongate and dorsoventrally narrow, and roughly ellipsoidal in outline. The postorbital length (= 190 mm in UCMP 9950) is much shorter than the preorbital region, like in other ichthyopterygians (Motani et al., 2015a: char. 166:1). However, in comparison with other ichthyosaurs, the postorbital region is relatively broad anteroposteriorly, like in some basal ichthyopterygians, some mixosaurids and some shastasaurids, but in contrast to parvipelvian ichthyosaurs, where the relative postorbital length is anteroposteriorly narrow (e.g. Ji et al., 2016: char. 31). The temporal fenestrae are large, anteroposteriorly longer than mediolaterally broad (200 mm and 125 mm, respectively; left side of UCMP 9950). They are mediolaterally widest anteriorly, with a convex anterior margin, and taper posteriorly into a sharp apex. The skull of *Cymbospondylus* bears a dorsoventrally tall sagittal crest, although its relative height differs between specimens. In UCMP 9913 and FMNH PR 2251, this crest is dorsoventrally short, whereas it is dorsoventrally taller in UCMP 9950 (because the skull roof is severely broken in PIMUZ T 4351 the relative height of the sagittal crest cannot be assessed in this specimen). The sagittal crest is a feature shared by *Cymbospondylus* with mixosaurid ichthyosaurs (e.g. Jiang et al., 2006). However, in contrast to mixosaurids, where the sagittal crest is formed by the nasals anteriorly, parietals and supratemporals posteriorly, the sagittal crest in *Cymbospondylus* is formed by the parietals and supratemporals only. The pineal foramen is circular or oval in outline, slightly longer anteroposteriorly than mediolaterally, but its exact shape and dimensions are difficult to establish because they are highly dependent on the degree of preparation of the matrix filling it. In FMNH PR 2251, two, small, suboval foramina, formed within the incompletely co-ossified interparietal suture, are located posterior to the pineal foramen. A single, small, interparietal foramen is also present in *Thalattoarchon saurophagis* (FMNH PR 3032). The dorsal surfaces of the parietals are not well preserved in UCMP 9950, UCMP 9913 and PIMUZ T 4351, so the presence or absence of similar foramina cannot be confirmed. In dorsal view, the posterior margin of the skull roof forms a deep indentation in *Cymbospondylus*, similar to *Thalattoarchon saurophagis* (FMNH PR 3032), basal ichthyopterygians and some shastasaurids, but in contrast to

parvipelvian ichthyosaurs, where the posterior margin of the skull forms only a shallow indentation (Maisch and Matzke, 2000: char. 27).

Premaxilla. The premaxillae are completely preserved in UCMP 9950, but because the skull was mechanically prepared, the surface of the left premaxilla contains multiple breakages and cracks, most of which have subsequently been filled in with plaster (Figs 4.1–4.2). The surface anatomy of the right premaxilla of UCMP 9950 is partially obscured by incomplete preparation and reconstruction in plaster. Both premaxillae are well preserved in UCMP 9913, clearly showing the surface anatomy, but their posterior parts have been reconstructed in plaster, due to a large break in the circumnarial region (Figs 4.3–4.4). In PIMUZ T 4351, only fragments of the anterior parts of the premaxillae are preserved, and in FMNH PR 2251 only small, weathered fragments of the premaxillae are preserved dorsally to the external nares (Figs 4.5–4.6).

Like in most other ichthyosaurs, the premaxilla is an anteroposteriorly elongated and dorsoventrally narrow bone, which forms the main part of the rostrum and bears most of the teeth. In lateral view, the premaxilla forms an acute apex, and its dorsoventral height increases posteriorly until its acme at approximately half of its anteroposterior length. The dorsoventral height of the premaxilla begins to decrease posteriorly to this point. The premaxillae are united along the dorsal midline of the skull and form a straight suture which extends for approximately 50% of the preorbital length. The posterior part of the premaxilla overlaps the ventrolateral part of the nasal, as in other ichthyosaurs, and the external contact between the two bones has the form of a straight suture. Posteroventrally, the premaxilla contacts the anterior process of the maxilla along a straight, obliquely oriented suture. Posteriorly, the premaxilla forms a prominent supranarial process, which extends posteriorly beyond the posterior margin of the external naris. A similar, prominent supranarial process of the premaxilla is also present in the shastasaurid ichthyosaurs *Guizhouichthyosaurus tangae* (IVPP V11865, 11869), *Callawayia wolonggangense* (SPCV 10306) and *Shonisaurus* sp. (UCMP 27141–46; described as *Shastasaurus altispinax* by Callaway and Massare, 1989, but referred to *Shonisaurus* sp. by Motani, 1999a), but differs from the condition in mixosaurids and euichthyosaurs, in which the supranarial process is reduced (e.g. Ji et al., 2016: char. 1:1). The subnarial process of the premaxilla is completely

reduced, similar to basal ichthyopterygians, mixosaurids, shastasaurids and toretocnemids (e.g. Ji et al., 2016: char. 2:1), but in contrast to parvipelvian ichthyosaurs, in which the subnarial process extends as far posteriorly as the posterior margin of the external naris (e.g. Ji et al., 2016: char. 2:0). In UCMP 9950 and UCMP 9913, the ventral margin of the supranarial process contributes to the dorsal margin of the external naris. In FMNH PR 2251 the premaxilla is excluded from the external naris by the nasal. However, the posterior extremities of the supranarial processes are poorly preserved in FMNH PR 2251, and a prominent facet for the supranarial process of the premaxilla is clearly visible on the lateral surface of the nasal, along the dorsal margin of the external naris. Anteroposteriorly elongate, dorsoventrally very narrow and mediolaterally shallow furrows of the dental fossa run along the lateral surface of the premaxilla, clearly seen in UCMP 9913 (Fig. 4.3).

Maxilla. The maxillae are well preserved in UCMP 9950 (Figs 4.1–4.2). In UCMP 9913, the posterior part of the anterior process of the left maxilla is damaged and reconstructed in plaster (Figs 4.3–4.4), whereas the right maxilla is badly weathered. In FMNH PR 2251 only the posterodorsal and posterior processes of both maxillae are preserved (Figs 4.5–4.6). In PIMUZ T 4351, only the posterior process of the left maxilla is well preserved, while the anterior and posterodorsal processes are heavily damaged and partially reconstructed in plaster (Fig. 4.7).

Like in other ichthyosaurs, the maxilla forms the posteroventral part of the rostrum. The maxilla is an anteroposteriorly elongate, triradiate bone, which forms an anterior process, a posterodorsal process and a posterior process. The anterior process of the maxilla bears the maxillary dentition. It forms a straight suture with the premaxilla dorsally. In dorsolateral view, the anterior process of the maxilla extends as far anteriorly as the anterior part of the dorsal exposure of the nasals. Similar elongation of the anterior process of the maxilla is also present in basal ichthyopterygians, mixosaurids, shastasaurids and *Temnodonotosaurus* (e.g. Ji et al., 2016: char. 3:1), whereas in the majority of parvipelvian ichthyosaurs the anterior process of the maxilla is reduced and does not extend as far anteriorly as the nasal (e.g. Ji et al., 2016: char. 3:0). The posterodorsal process of the maxilla (“maxilla dorsal lamina” of Motani, 1999a), which is an ichthyopterygian plesiomorphy (e.g. Ji et al., 2016: char. 4), contributes to the ventral margin of the external naris and contacts the descending process of the

nasal dorsally, and the lacrimal posteriorly. The posterior process of the maxilla contacts the posteroventral process of the lacrimal anteriorly. The posterior process of the maxilla forms approximately the anterior third of the ventral part of the suborbital bar, but is excluded from the ventral orbital margin by the jugal, as evidenced by FMNH PR 2251 (Fig. 5; the contact between the maxilla and jugal is not well preserved in UCMP 9950, UCMP 9913 and PIMUZ T 4351). The lateral surface of the anterior process of the maxilla is smooth in UCMP 9950 and UCMP 9913, in contrast to *Thalattoarchon saurophagis* (FMNH PR 3032), *Grippia longisrostris* (Motani, 2000), and some mixosaurids (e.g. Brinkmann, 2004; Schmitz et al., 2004), in which the lateral surface of the maxilla bears a series of foramina.

Nasal. The nasals are completely preserved in UCMP 9950 (Figs 4.1–4.2). In FMNH PR 2251, only the anterior parts of the dorsal exposures of the nasals are missing (Figs 4.5–4.6), whereas in UCMP 9913, the dorsal exposures of the nasals are heavily damaged and reconstructed in plaster (Figs 4.3–4.4). In PIMUZ T 4351, the posterior parts of the nasals are poorly preserved, and are partially reconstructed in plaster (Fig. 4.7).

Like in other ichthyosaurs, the nasals contribute to the posterior part of the dorsal surface of the rostrum and the anterior part of the skull roof. The anterolateral surface of the nasal is overlapped by the premaxilla, so only the dorsal surface and the descending process of the nasal are visible in external view. Anteriorly, the paired nasals extend as far as the anterior process of the maxilla. The dorsal exposure of the nasal is roughly triangular in outline – it forms a pointed apex anteriorly and the mediolateral width of the nasal gradually increases posteriorly. The nasals are united along the dorsal midline of the skull by a straight suture. The dorsal surface of the nasals is flat, like in basal ichthyopterygians and mixosaurids (Ryosuke Motani, pers. comm., August 2017) and the internasal depression/foramen, characteristic for shastasaurid (e.g. *Guizhouichthyosaurus tangae* [IVPPV 11865, *Guanlingsaurus liangae* [SPCV 03107; Sander et al., 2011]) and parvipelvian (e.g. Maisch and Matzke, 2000: character 16:1) ichthyosaurs, is absent. The posterior part of the internasal suture forms a sharp crest, clearly visible in UCMP 9950 and FMNH PR 2252 (Figs 4.2, 4.6), a feature shared only with *Thalattoarchon saurophagis* (FMNH PR 3032; Fröbisch et al., 2013:fig. 1A-B). The nasal forms a

descending process at the level of the anterior orbital margin. The descending process of the nasal contacts the supranarial process of the premaxilla anteriorly, the posterodorsal process of the maxilla ventrally, and the ascending process of the lacrimal posteroventrally. The descending process of the nasal is bordered dorsally by a thickened, anteroposteriorly oriented ridge. The nasal is tightly co-ossified to the postfrontal posterolaterally, and forms a heavily interdigitating suture with the frontals, medially.

Lacrimal. The lacrimals are well preserved in UCMP 9950 (Figs 4.1–4.2) and FMNH PR 2251 (Figs 4.5–4.6). In UCMP 9913 (Figs 4.3–4.4), the lacrimals are partially damaged by a large crack running along the anterior part of the skull roof, and have been reconstructed in plaster. In PIMUZ T 4351 (Fig. 4.7), the left lacrimal is heavily damaged and partially reconstructed in plaster. The lacrimal forms the anterior orbital margin. It contacts the prefrontal posterodorsally, the descending process of the nasal anterodorsally, the posterodorsal process of the maxilla anteriorly, the posterior process of the maxilla anteroventrally and the anterior process of the jugal posteroventrally. As in other ichthyosaurs, a sharp, thickened ridge separates the anterolateral surface of the lacrimal from its posterior surface, which forms the anterior orbital margin (best exemplified by FMNH PR 2251; Fig. 4.5). The anterolateral surface of the lacrimal is smooth and does not bear any neurovascular foramina, similar to *Thalattoarchon saurophagis* (FMNH PR 3032), *Grippia longirostris* (Motani, 2000), and mixosaurids (e.g. Schmitz et al., 2004), but different from some shastasaurids, in which the lacrimal is perforated by neurovascular foramina (e.g. *Shastasaurus pacificus* [UCMP 9017], *Guanlingsaurus liangae* [SPCV 03107; Sander et al., 2011]).

Prefrontal. Both prefrontals are preserved in UCMP 9950; the left prefrontal is broken posteriorly (Figs 4.1–4.2) and the right prefrontal is heavily damaged and extensively reconstructed in plaster (Fig. 4.2). In UCMP 9913, the left prefrontal is damaged both anteriorly and posteriorly, and the anterior break has been reconstructed in plaster, whereas the morphology of the right prefrontal is almost completely obscured by damage resulting from weathering and mechanical preparation (Figs 4.3–4.4). In PIMUZ T 4351 (Fig. 4.7) the left prefrontal is completely preserved posteriorly, but it cannot be distinguished

from other bones of the circumorbital region anteriorly. In FMNH PR 2251, the left prefrontal is extensively damaged, but the right prefrontal is completely preserved and its relationships with other bones of the circumorbital and skull roof regions are clearly visible.

The prefrontal is an anteroposteriorly elongate, dorsoventrally narrow bone that forms the entire dorsal margin of the orbit. The anterior end of the prefrontal forms a pointed apex and contacts the lacrimal anteroventrally and the nasal anterodorsally. Dorsally, the prefrontal forms a straight suture with the postfrontal, and excludes the postfrontal from the dorsal orbital margin. The posterior end of the prefrontal is crenulated in FMNH PR 2251 and overlaps the anterodorsal part of the postorbital. Ventrally, the prefrontal forms the entire dorsal margin of the orbit, a condition which is shared only with one other ichthyopterygian, *Thalattoarchon saurophagis* (FMNH PR 3032). In all other ichthyopterygians, the prefrontal contributes only to the anterodorsal orbital margin, whereas the posterodorsal orbital margin is formed by the frontal and postfrontal (basal ichthyopterygians; e.g. Motani et al., 1998; Motani, 2000; Cuthbertson et al., 2013a) or postfrontal only (all other ichthyosaurians; e.g. McGowan and Motani, 2003).

Frontal. The paired frontals are well preserved in UCMP 9950 (Fig. 4.2), UCMP 9913 (Fig. 4.4) and FMNH PR 2251 (Fig. 4.6), while in PIMUZ T 4351 they are very poorly preserved. The frontals occupy the median part of the skull roof between the orbits and are united along the dorsal midline of the skull with a straight suture. Anteriorly, the medial parts of the frontals form an interdigitating suture with the posterior ends of the nasals (Figs 4.2, 4.4, 4.6). Posteriorly, the medial parts of the frontals become inclined dorsally and extend posteriorly to form the anterior margin of the pineal foramen. The lateral parts of the frontals extend posteriorly to form the anterior margin of the supratemporal fenestra. They contribute to the ‘anterior terrace’ of the supratemporal fenestra (see Postfrontal) and are overlapped by the postfrontal laterally. The medial and lateral exposures of the frontals are partially separated by the anterior processes of the parietals, which overlie the frontals. In *Thalattoarchon saurophagis* (FMNH PR 3032), the anterior processes of the parietals also form a deep parietal fork and partially separate the medial and lateral exposures of the frontals.

Postfrontal. In UCMP 9950 the left postfrontal is completely preserved (Figs 4.1–4.2), whereas the right postfrontal is slightly damaged anteriorly and partially reconstructed in plaster. In UCMP 9913 both postfrontals are well preserved, but the left postfrontal is damaged along the anterolateral margin of the supratemporal fenestra and reconstructed in plaster (Figs 4.3–4.4). In FMNH PR 2251 both postfrontals are well preserved (Figs 4.5–4.6). In PIMUZ T 4351 only the lateral part of the left postfrontal is possibly preserved dorsally to the postorbital (Fig. 4.7).

Like in other ichthyopterygians, the postfrontal forms the lateral border of the skull roof. It is slightly recurved laterally and can be divided into an anteromedial process and a posterolateral process. Anteriorly, the anteromedial process of the postfrontal is well co-ossified to the posterolateral margin of the nasal, so that only a faint, interdigitating suture can be observed between the two bones. A low but prominent, slightly medially recurved ridge separates the anteromedial process of the postfrontal into a medial and lateral parts. This ridge extends posteriorly into a tall crest on the dorsal surface of the anterior part of the posterolateral process, a feature shared with *Thalattoarchon saurophagis* (FMNH PR 3032). A shallow, wide and smooth groove is located laterally to this ridge, on the lateral part of the anteromedial process, and is bordered laterally by another low ridge. *Cymbospondylus* shares both of these features exclusively with *Thalattoarchon saurophagis* (FMNH PR 3032) among ichthyopterygians. The medial part of the anteromedial process of the postfrontal overlaps the frontal laterally and forms the lateral part of the ‘anterior terrace’ of the supratemporal fenestra (Motani, 1999a: char. 14), which in *Cymbospondylus* is also formed by contributions from the frontal and parietal. This is similar to the condition in basal ichthyopterygians and shastasaurids, but different from mixosaurids, in which the ‘anterior terrace’ also has a nasal contribution, and parvipelvians, in which the anterior terrace is limited to the postfrontal or completely absent (e.g. Ji et al., 2016: char. 36; pers. obs.). The posterior border of the anteromedial process of the postfrontal forms the anterior margin of the supratemporal fenestra.

The anteromedial process and the anterior part of the posterolateral process of the postfrontal contact the prefrontal ventrally. Posterior to the contact with the prefrontal, the ventral margin of the posterolateral process is tightly co-ossified to the dorsal border of the postorbital. Posterior to the ventral contact with the postorbital, the posterolateral process contacts the squamosal. Medially, the lateral

process forms the lateral margin of the supratemporal fenestra anteriorly, and overlaps the supratemporal along the posterior two-thirds of its anteroposterior length. The posterolateral process of the postfrontal of *Cymbospondylus* is remarkably long anteroposteriorly. In shastasaurids, where the length of the postorbital region is proportionally long, much like in *Cymbospondylus*, the lateral process of the postfrontal extends only to the posterior orbital region and does not contact the supratemporal, so that the dorsal margin of the postorbital forms part of the lateral margin of the supratemporal fenestra (e.g. *Guizhouichthyosaurus tangae* [IVPP V11865], *Guanlingsaurus liangae* [SPCV 03107; Sander et al., 2011]. A similar, anteroposteriorly elongate posterolateral process of the postfrontal is present in *Thalattoarchon saurophagis* (FMNH PR 3032). In basal ichthyopterygians the lateral process of the postfrontal is also anteroposteriorly elongate, but it does not overlap the supratemporal extensively (e.g. Motani et al., 1998; Motani, 2000; Cuthbertson et al., 2013a). In mixosaurids, the postfrontal-supratemporal contact, if present, is also less extensive than in *Cymbospondylus* and *Thalattoarchon* (e.g. Motani, 1999b; Jiang et al., 2006).

Postorbital. The postorbital is well preserved in all cranial material referred to *Cymbospondylus*. In UCMP 9950, only the posterior margin of the left postorbital is broken (Fig. 4.1), whereas in UCMP 9913 the anterodorsal portion of the postorbital is reconstructed in plaster (Fig. 4.3). In FMNH PR 2251 and PIMUZ T 4351 the postorbital is well co-ossified to the neighbouring bones of the circumorbital, temporal and skull roof regions, so that it is difficult to trace the sutures between them (Figs. 4.4, 4.7). The postorbital attains its greatest anteroposterior width dorsally and its anteroposterior width gradually decreases ventrally, until it forms an acute apex at the level of the ventral orbital margin. The anterior margin of the postorbital is concave and forms the posterior orbital margin. Anterodorsally, the lateral surface of the postorbital is overlapped by the posterior part of the prefrontal. The dorsal margin of the postorbital forms a straight suture with the posterolateral process of the postfrontal, and is therefore excluded from the lateral margin of the supratemporal fenestra, in contrast to basal ichthyopterygians (e.g. Motani et al., 1998) and shastasaurids (e.g. *Guizhouichthyosaurus tangae* [IVPPV 11865], *Guanlingsaurus liangae* [SPCV 03107; Sander et al., 2011], where the postorbital contributes to the lateral margin of the supratemporal fenestra. The posterior margin of the postorbital is tightly co-

ossified to the squamosal posterodorsally and quadratojugal posteroventrally and forms an interdigitating suture with both of these bones. Ventrally, the postorbital extensively overlaps the ascending process of the jugal.

The dorsally wide (anteroposteriorly) postorbital of *Cymbospondylus* is similar to the postorbital of *Thalattoarchon saurophagis* (FMNH PR 3032), basal ichthyopterygians (e.g. Motani et al., 1998; Motani, 2000; Cuthbertson et al., 2013a), mixosaurids (e.g. Motani, 1999b; Schmitz et al., 2004) and shastasaurids (e.g. *Guizhouichthyosaurus tangae* [IVPP V11865], *Guanlingsaurus liangae* [SPCV 03107], *Shastasaurus pacificus* [UCMP 9017]), but different from the postorbital of parvipelvian ichthyosaurs, which is anteroposteriorly narrow and forms an anterodorsally pointed apex (e.g. Maisch and Matzke, 2000a; Ji et al., 2016).

Squamosal. The squamosals are well preserved in UCMP 9950 (Figs 4.1–4.2). In UCMP 9913, only the left squamosal is well preserved (Figs 4.3–4.4), while the right one is badly weathered. In FMNH PR 2251, the right squamosal is well preserved and tightly co-ossified to the postorbital and quadratojugal (Figs 4.5–4.6), whereas the left one is not preserved. In PIMUZ T 4351 the anterior part of the left squamosal is likely preserved, but due to the high degree of co-ossification between the squamosal and surrounding bones of the temporal and circumorbital region, it is not possible to determine this with confidence (Fig. 4.7). The squamosal is a large, sheet-like bone which occupies the dorsal part of the temporal region, and is approximately trapezoidal in outline in lateral view, wider anteroposteriorly than taller dorsoventrally. Anteriorly, the squamosal is overlapped by the postorbital, and the two bones form an interdigitating suture. Dorsally, the squamosal forms a straight suture with the posterolateral process of the postorbital along almost its entire anteroposterior length. Posterior to the contact with the postfrontal, the squamosal forms an anteroposteriorly short, straight contact with the supratemporal. As a result, the squamosal is excluded from participation in the lateral margin of the supratemporal fenestra by the postfrontal and supratemporal. The broken-off, posteroventral corner of the left squamosal in UCMP 9950 (Fig. 4.1) reveals that the squamosal extensively overlaps the dorsal portion of the quadratojugal. The posterior margin of the squamosal is slightly concave and contributes to the dorsal part of the anterolateral margin of the quadrate-quadratojugal foramen.

Jugal. The jugals are best preserved in FMNH PR 2251, where their relationships with other bones of the circumorbital and temporal regions are clearly visible (Fig. 4.5). In UCMP 9950 (Fig. 4.1) the relationships between the jugal and bones of the circumorbital region are difficult to determine, whereas in UCMP 9913 (Fig. 4.3) and PIMUZ T 4351 (Fig. 4.7) the anterior process of the jugal is broken and more or less extensively reconstructed in plaster.

Like in other ichthyopterygians, the jugal can be divided into an anterior process and a posterior, ascending process. The anterior process is anteroposteriorly elongate and dorsoventrally very narrow and forms the suborbital bar. Anteriorly, the anterior process of the jugal tapers to a point and terminates at the level of the anterior orbital margin. The anterior process of the jugal contacts the posterior process of the lacrimal, dorsally, and the posterior process of the maxilla, ventrally. The ascending process of the jugal is extensively overlapped by the postorbital anteriorly, like in *Thalattoarchon saurophagis* (FMNH PR 3032), basal ichthyopterygians (e.g. Motani et al., 1998; Motani, 1997, 2000) and mixosaurids (e.g. Motani, 1999b; Jiang et al., 2006). In UCMP 9950, the ascending process of the jugal contacts the quadratojugal posterodrosally, but this contact is only visible because the postorbital is broken along its posterior margin, and a jugal-quadratojugal contact is not visible in lateral view in any of the other specimens, which preserve a posteriorly complete postorbital. The posterior margin of the ascending process of the jugal is concave and forms the jugal contribution of the lower temporal arch. Posteroventrally, the jugal forms a prominent, posteroventral process. This process is clearly visible in UCMP 9913 (Fig. 4.3) and FMNH PR 2251 (Fig. 4.5). In UCMP 9950, the jugal is broken posteriorly, obscuring this feature (Fig. 4.1). It is not clear whether the posterior process of the jugal is completely absent in PIMUZ T 4351, or whether it is obscured by the overlying postorbital or incompletely freed from the surrounding rock matrix (Fig. 4.7). The posteroventral process of the jugal is also present in some specimens of *Mixosaurus panxianensis* (Jiang et al., 2006), *Gen et sp. nov. A* (Chapter 2) and an undescribed, colossal ichthyosaur from the Middle Triassic of Nevada, USA (P. M. Sander, pers. comm., Aug 2017). A posteroventral process of the jugal has also been reported in some ophthalmosaurid ichthyosaurs (e.g. Moon and Kirton, 2016), but it is significantly less well-developed than the posteroventral process of the taxa listed above.

Quadratojugal. The quadratojugals are well preserved in UCMP 9950 (Figs 4.1–4.2). In UCMP 9913, the left quadratojugal is well preserved (Figs 4.3–4.4), but the right quadratojugal is very poorly preserved. In FMNH PR 2251 (Fig. 4.5), only the right quadratojugal is well preserved, whereas the left one is not preserved. The quadratojugal is not preserved in PIMUZ T 4351 (Fig. 4.7). In lateral view, the quadratojugal forms an anteroposteriorly elongate, dorsoventrally narrow, roughly quadrangular exposure, similar to basal ichthyopterygians (e.g. Motani et al., 1998; Motani, 2000), *Thalattoarchon saurophagis* (FMNH PR 3032), and *Phalarodon atavus* (Motani, 1999b). Anteriorly, the quadratojugal is overlapped by the postorbital and the two bones form a heavily interdigitating suture. Dorsally, the quadratojugal is overlapped by the squamosal. Posteroventrally, the quadratojugal forms a posteromedially oriented quadrate process, which contacts the anterior surface of the articular condyle of the quadrate. The ventral margin of the quadratojugal is concave and forms the quadratojugal contribution of the lower temporal arch, a feature present in many Triassic ichthyosaurs (e.g. Ji et al., 2016: char. 30). The posterior margin of the quadratojugal is slightly concave and contributes to the ventral part of the anterolateral margin of the quadrate-quadratojugal foramen.

Parietal. The parietals are well preserved in UCMP 9950 (Figs 4.1–4.2), UCMP 9913 (Figs 4.3–4.4) and FMNH PR 2251 (Figs 4.5–4.6). In PIMUZ T 4351 (Fig. 4.7), the left parietal is well preserved anteriorly and the posterior part of the right parietal is preserved in medial view. The paired parietals form the central part of the skull roof and contribute to the anterior part of the sagittal eminence. Anteriorly, the parietal forms an anteroposteriorly elongate anterior process, which overlaps the frontal. In UCMP 9950 (Fig. 4.2) the parietals seem to extend far anteriorly and contact the posterior margin of the nasals. In contrast, in UCMP 9913 (Fig. 4.4) the parietals' anterior processes seem to terminate anterior to the posterior margin of the nasals. However, because the parietals are tightly co-ossified with the frontals in both UCMP 9950 and UCMP 9913, and because mechanical preparation has slightly damaged the surfaces of bones on the skull roof, the fronto-parietal suture is not well demarcated. Therefore, the degree of elongation of the anterior processes of the parietals should be interpreted as ambiguous. In FMNH PR 2251, where the sutures on the skull roof are well demarcated (Fig. 4.6), the anterior processes do not extend anteriorly to contact the nasal. In UCMP 9950, the anterior processes

of the parietals seem to bifurcate into two, short, parallel prongs anteriorly, but the presence of these prongs could not be confirmed in any of the other specimens, so this feature could be a preservational/preparational artefact. Anteroposteriorly elongate anterior processes of the parietals are also present in the shastasaurid *Guanlingsaurus liangae* (SPCV 03107; Sander et al., 2011) and *Thalattoarchon saurophagis* (FMNH PR 3032). In *Guanlingsaurus*, the anterior processes of the parietals converge anteriorly so that the frontal is excluded from the anterior margin of the pineal foramen, while in *Thalattoarchon* the anterior processes form a fork and the medial exposure of the frontal forms the anterior margin of the pineal foramen, much like in *Cymbospondylus* (see Frontal). In the shastasaurids *Shastasaurus pacificus* (UCMP 9017) and *Guizhouichthyosaurus tangae* (IVPP V11865) the anterior processes of the parietals are not as anteroposteriorly elongate as in *Cymbospondylus*, so that the frontal exposure is much more extensive medially in these taxa.

Posteriorly, the anterior processes of the parietals become inclined dorsally so that the parietals form the anterior part of the tall, sagittal crest. The parietals contribute to the lateral margins of the pineal foramen and converge posteriorly, also forming its posterior margin. Laterally and posteriorly to the pineal foramen, the dorsal surface of the parietal forms a flattened plateau, much like that in *Thalattoarchon saurophagis* (FMNH PR 3032). The interparietal suture is anteroposteriorly short and straight in UCMP 9950 and UCMP 9913, but in FMNH PR 2251, the interparietal suture is incompletely co-ossified and two, small foramina, located posteriorly to the pineal foramen, can be seen within it. In *Thalattoarchon saurophagis* (FMNH PR 3032), the interparietal suture is similarly not completely co-ossified and contains one, small foramen.

Anteroaterally, the parietal overlaps the lateral exposure of the frontal and laterally it forms the anterior part of the medial margin of the supratemporal fenestra. Medially to the anterior margin of the supratemporal fenestra, the parietal forms a short, lateral process. The parietal also forms an anteroposteriorly long, dorsoventrally tall and mediolaterally narrow posterolateral process, similar to *Thalattoarchon saurophagis* (FMNH PR 3032), basal ichthyopterygians and shastasaurids (e.g. Ji et al., 2016: char. 34). The posterolateral process is laterally overlapped by the supratemporal along almost its entire anteroposterior length. This is in contrast to *Thalattoarchon saurophagis* (FMNH PR 3032), where the posterolateral process is extensively overlapped by the supratemporal only posteriorly.

Supratemporal. The supratemporals are well preserved in UCMP 9950 (Figs 4.1–4.2) and UCMP 9913 (Figs 4.3–4.4), but the anteromedial process of the left supratemporal of UCMP 9913 is slightly damaged dorsally and reconstructed in plaster. In FMNH PR 2251, the morphology of the supratemporals is obscured by extensive breakage of the posterior part of the skull, and in PIMUZ T 4351 the supratemporals are also extensively damaged. Like in other ichthyosaurs, the supratemporal is located in the posterior part of the temporal region. The supratemporal can be divided into an anterolateral process and an anteromedial process; the descending process of the supratemporal is absent, in contrast to mixosaurids, shastasaurids and parvipelvians, where a prominent descending process of the supratemporal is present (Motani, 1999a: char. 22). The anterolateral process of the supratemporal forms the posterior part of the lateral margin of the supratemporal fenestra and is overlapped by the posterolateral process of the postfrontal, laterally. The anteromedial process forms the posterior part of the medial margin of the supratemporal fenestra and is overlapped by the posterolateral process of the parietal, medially. In comparison to other ichthyopterygians, the anteromedial process of the supratemporal is anteroposteriorly elongate, which is an autapomorphy of the genus (Ji et al., 2016: char. 19).

DISCUSSION

Comparison of previously published accounts of the cranial morphology of *Cy. piscosus* (Fig. 4.8). The cranial anatomy of *Cy. piscosus* was investigated by multiple authors since its original description (Merriam, 1908 [Fig. 4.8A]; Huene, 1916 [Fig. 4.8B]; Camp, 1980 [Fig. 4.8C]; Sander, 1989 [Fig. 4.8D]; Massare and Callaway, 1990 [Fig. 4.8E]; Motani, 1999a [reproduced in McGowan and Motani, 2003; fig. 4.8F]; Maisch and Matzke, 2000, 2004 [Fig. 4.8G]; Fröbisch et al., 2006 [Fig. 4.8H]; Ji et al., 2016 [Fig. 4.8I]). Even though some parts of the cranium have been interpreted consistently by all the listed authors, the interpretations of the relationships of bones forming the circumorbital region vary markedly between them. It is not surprising that such discrepancies exist in the literature, as interpretation of the cranial anatomy of *Cy. piscosus* is particularly challenging and is caused by: 1) mechanical preparation performed on UCMP 9950 and UCMP 9913, which has left many of the bone

surfaces broken, obscuring their original morphology; 2) extensive reconstruction in plaster, which has subsequently been painted to color match the color of the original fossils, further obscuring the relationships between the cranial bones; and 3) the lack of well preserved and extensively described cranial material of other basal ichthyosaurs, which prohibits comparison of the morphology of *Cy. piscosus* against a robust, comparative framework. However, the recent re-description and discovery of new, exceptionally preserved cranial material of mixosaurids (e.g. Motani, 1999b; Schmitz et al., 2004; Jiang et al., 2006), the discovery of well preserved, cranial material of Late Triassic (Carnian) shastasaurids from South East China (e.g. Li and You, 2002; Chen et al., 2007; Sander et al., 2011) and the discovery of the well-preserved type skull of *Cy. nichollsi* (FMNH PR 2251; Fröbisch et al., 2006) has provided an extensive, comparative framework, which makes it possible to determine the true configuration of the cranial bones of *Cy. petrinus*.

The morphology of the rostrum, with the extensive supranarial process of the premaxilla and the triradiate maxilla, was consistently interpreted by all authors who provided an interpretive drawing of the preorbital region (Merriam, 1908 [Fig. 4.8A]; Sander, 1989 [Fig. 4.8D]; Massare and Callaway, 1990 [Fig. 4.8E]; Motani, 1999a [Fig. 4.8F]; Maisch and Matzke, 2000, 2004 [Fig. 4.8G]; Fröbisch et al., 2006 [Fig. 4.8H]; Ji et al., 2016 [Fig. 4.8I]) and matches the interpretation presented herein. The morphology of the jugal, quadratojugal and the skull roof was also very consistently, and accurately, interpreted by all authors. The anatomy of the posterior part of the temporal region has proven to be more problematic. Merriam (1908; Fig. 4.8A) interpreted the lateral element occupying the posterodorsal corner of the temporal region as the supratemporal, and the medial element as the squamosal, while Huene (1916; Fig. 4.8B) identified the lateral element as the squamosal and the medial element as supratemporal. After Romer (1968) and McGowan (1973) concluded that ichthyosaurs lacked the supratemporal, all accounts of the cranial anatomy of *Cy. piscosus* published before 1999 indicated the presence of a single, large squamosal, forming the entire posterior part of the temporal region (Camp, 1980 [Fig. 4.8C]; Sander, 1989 [Fig. 4.8D]; Massare and Callaway, 1990 [Fig. 4.8E]). However, after Motani (1999a, c) established the presence of a supratemporal bone in ichthyosaurs, all subsequent reconstructions of the cranial anatomy of *Cy. piscosus* correctly identified the lateral element as the squamosal and the medial element as the supratemporal. However, Motani (1999a; Fig.

4.8F) did not correctly identify the postfrontal-squamosal suture, and Fröbisch et al. (2006; Fig. 4.8H) mistook the postfrontal for the supratemporal, and identified the supratemporal as a supernumerary ossification (see below).

The most profound differences between the published interpretations of the cranial anatomy of *Cy. piscosus* concern the circumorbital region, in particular the morphology of the lateral exposures of the nasal, lacrimal, prefrontal, postfrontal and postorbital. Merriam (1908; Fig. 4.8A) and Huene (1916; Fig. 4.8B) correctly described and figured the lacrimal as contributing to the anterior orbital margin, whereas Camp (1980; Fig. 4.8C) failed to recognize this contribution. However, all subsequent authors correctly identified the position and morphology of the lacrimal, albeit their line drawings differed slightly regarding the details of the posterodorsal, anterior and posteroventral extent of the lacrimal.

Although the anteroposterior extent of the dorsal exposure of the nasals was consistently interpreted in all previous accounts of the cranial morphology of *Cy. piscosus*, the extent of its lateral exposure remained controversial. Merriam (1908; Fig. 4.8A) suggested a possible nasal exposure posterior to the external naris, but because he did not delineate the sutures between the bones of the circumorbital region, the true identity of the bone exposed in this region remained ambiguous. In his drawing of UCMP 9913, Huene (1916; Fig. 4.8B) correctly suggested that this lateral exposure is indeed formed by the nasal. Sander (1989; Fig. 4.8D), Massare and Callaway (1990; Fig. 4.8E), and Motani (1999a; Fig. 4.8F) failed to identify the lateral exposure of the nasal in their interpretative drawings. Maisch and Matzke (2000, 2004; Fig. 4.8G) confirmed the observations of Merriam (1908) and Huene (1916) that the nasal is exposed posteriorly to the supranarial process of the premaxilla, and both Fröbisch et al. (2006; Fig. 4.8H) and Ji et al. (2016; Fig. 4.8I) reached the same conclusions.

The prefrontal is probably the single most controversial element of the cranial anatomy of *Cy. piscosus*, as all previously published accounts differ quite significantly from each other regarding the presented morphology of the prefrontal and its relationships with other cranial bones. Merriam (1908; Fig. 4.8A) suggested that the prefrontal forms the anterodorsal margin of the orbit in UCMP 9950, but refrained from drawing sutural lines between the prefrontal and the surrounding bones, so that the exact morphology of the prefrontal remained unknown. Huene (1916; Fig. 4.8B) confirmed that the prefrontal formed the anterodorsal orbital margin, but also suggested the entire prefrontal is limited to the

anterodorsal orbital margin in *Cy. piscosus*, even though the posterior part of the prefrontal in UCMP 9913 is broken and partially reconstructed in plaster (Fig. 4.3). The interpretation of Huene (1916; Fig. 4.8B) was later followed by Massare and Callaway (1990; Fig. 4.8E). Camp (1980; Fig. 4.8C) correctly identified that the prefrontal forms the entire dorsal margin of the orbit, but because the right prefrontal of UCMP 9950 is obscured by two cracks, which have been filled in with plaster, the true posterior extent of the prefrontal could not be established. Both Sander (1989; Fig. 4.8D) and Motani (1999a; Fig. 4.8F) interpreted the lateral exposure of the nasal as the anteriormost part of the prefrontal. Both authors also concluded that the prefrontal was restricted to the anterodorsal orbital margin, and was excluded from its posterodorsal border by the postorbital and/or postfrontal, although both authors refrained from indicating the sutural contact between the prefrontal and postfrontal. Maisch and Matzke (2000, 2004; Fig. 4.8G) were the first to suggest that the prefrontal forms the entire dorsal margin of the orbit and ends just posteriorly to it, but they also suggested that the prefrontal was dorsoventrally broad anteriorly, mistaking much of the posterodorsal process of the lacrimal for the anterior part of the prefrontal. Fröbisch et al. (2006; Fig. 4.8H) and Ji et al. (2016; Fig. 4.8I) suggested the prefrontal was anteroposteriorly very short and restricted to the anterodorsal margin of the orbit.

The identity of the postfrontal also remained enigmatic. Merriam (1908; Fig. 4.8A) could not identify the suture separating the postfrontal from the prefrontal and refrained from describing the morphology of the anteromedial portion of the postfrontal. However, he correctly identified its anteroposteriorly elongate, posterolateral process. Huene (1916; Fig. 4.8B) also identified the anteroposteriorly elongate posterolateral process of the postfrontal, but, like Merriam (1908; Fig. 4.8A), was not able to describe the detailed morphology of the postfrontal anteriorly and concluded that the postfrontal forms the entire posterodorsal orbital margin (an interpretation followed by Massare and Callaway [1990; Fig. 4.8E]. Camp (1980; Fig. 4.8C) wrongly interpreted the posterodorsal process of the postorbital as the postfrontal. Sander (1989; Fig. 4.8D) was not able to identify the suture between the prefrontal and postfrontal, and concluded that the postfrontal formed the posterodorsal margin of the orbit. Motani (1999a; Fig. 4.8F) also failed to locate the prefrontal-postfrontal suture but noted that the postfrontal was excluded from the posterodorsal orbital margin by the postorbital. Maisch and Matzke (2000, 2004; Fig. 4.8G) were the first to correctly identify the anatomy of the postfrontal and

their observations match the ones presented here. Fröbisch et al. (2006; Fig. 4.8H) interpreted the posterolateral process of the postfrontal as the supratemporal. Ji et al. (2016; Fig. 4.8I) misinterpreted the posterolateral process of the postfrontal as a posterodorsal extension of the posterodorsal process of the postorbital.

The ventral extent of the postorbital of *Cy. piscosus* was correctly identified by all previous authors, but the morphology of its dorsal part remained controversial. Merriam (1908; Fig. 4.8A) and Sander (1989; Fig. 4.8D) refrained from delineating the dorsal extent of the postorbital, while Huene (1916; Fig. 4.8B), Camp (1980; Fig. 4.8C), Massare and Callaway (1990; Fig. 4.8E) and Motani (1999a; Fig. 4.8F) figured a postorbital which was crescent-shaped in outline, with the posterodorsal process completely reduced. Maisch and Matzke (2000, 2004; Fig. 4.8G) and Fröbisch et al. (2006; Fig. 4.8H) presented an accurate representation of the morphology of the postorbital, by figuring a broad, triangular, posterodorsal process. Ji et al. (2016; Fig. 4.8I) also figured a postorbital with a well-developed, posterodorsal process, but in their reconstruction they interpreted the posterolateral part of the postfrontal as forming part of the postorbital.

Maisch and Matzke (2004) and Fröbisch et al. (2006; Fig. 4.8H) introduced two supernumerary bones into the cranial morphology of *Cy. piscosus*. The interparietal was introduced by Maisch and Matzke (2004) as a medial, anteroposteriorly elongate, triangular element, braced between the supratemporals. The exact identity of this element is not possible to determine in UCMP 9950, due to the incomplete preparation of the back of the skull, nor in UCMP 9913, where the bones of the braincase are obscured by the anterior cervicals (Figs 4.3–4.4). Although the hypothesis of a supernumerary interparietal in *Cy. piscosus* cannot be rejected, it is more plausible that this element is the supraoccipital, because the element seems to articulate posteriorly with the dorsal parts of the exoccipitals, like the supraoccipital of all other ichthyosaurs. Furthermore, an isolated basal ichthyopterygian basioccipital, described as *Cymbospondylus germanicus* by Huene (1916:fig. 39) is anteroposteriorly elongate, in contrast to the basioccipitals of mixosaurids and all other, more derived ichthyosaurs and shows that the supraoccipital in basal ichthyopterygians, and possibly *Cymbospondylus*, could have been anteroposteriorly elongate as well. Due to the lack of well preserved,

comparative braincase material of basal ichthyopterygians, the identity of the interparietal element of *Cy. petrinus* must remain ambiguous.

The postparietal of Fröbisch et al. (2006; Fig. 4.8H) has exactly the same morphology, size and position as the bone identified here (and by most other authors) as the supratemporal in UCMP 9950 and UCMP 9913. Therefore, there is currently no definite evidence for the presence of supernumerary ossifications in *Cy. petrinus*, based on currently known specimens.

Taxonomic status of *Cy. nichollsi* (Table 4.2). *Cy. nichollsi* was diagnosed on the basis of the following features (Fröbisch et al., 2006): a longer postorbital region than in *Cy. piscosus* (ratio of postnarial:postorbital region of 1.85 in *Cy. nichollsi* and 2.11 in *Cy. piscosus*); parietal foramen fully enclosed by the parietals; posterior process of the nasal bordering the supratemporal fenestra anterorolaterally; postorbital contributing to the lateral margin of the supratemporal fenestra; an anteroposteriorly long and dorsoventrally narrow supratemporal extending posteriorly beyond the temporal region; quadratojugal not contributing to the craniomandibular joint; squamosal participation in the margin of the lower temporal arch; a robust clavicle; and 8-10 'cervicals' (defined as all vertebrae possessing distinct parapophyses), in comparison to 6 'cervicals' in *Cy. buchseri* and 12 'cervicals' in *Cy. piscosus*.

Comparison of the relative length of the postorbital region between the type of *Cy. nichollsi* (FMNH PR 2251), UCMP 9950 and UCMP 9913 (referred skulls of *Cy. piscosus*) is problematic, because Fröbisch et al. (2006) did not provide a definition of how the postnarial and postorbital length was measured. However, when the postnarial length is defined as the distance between the posterior margin of the posterior naris and the posterior border of the articular surface of the quadrate, and the postorbital length is defined as the distance between the posterior orbital margin and the posterior border of the articular surface of the quadrate, the postnarial:postorbital ratio of the specimens listed above is as follows: 2.58 for UCMP 9950, 2.34 for UCMP 9913 and 2.77 for FMNH PR 2251. However, since the circumnarial region in both UCMP 9950 and UCMP 9913 is damaged to at least a certain extent, and both specimens suffer from preservational deformation to at least some degree, using the postnarial:postorbital ratio for diagnostic purposes is questionable.

Personal examination of the type skull of *Cy. nichollsi* (FMNH PR 2251) performed for this study revealed that all of the discrete characters proposed as diagnostic for *Cy. nichollsi* have arisen through misinterpretation of the actual anatomy. The parietal foramen is bordered by the parietals laterally and posteriorly, but its anterior border is formed by the paired frontals, exposed in the central part of the skull roof, just like in UCMP 9950 and UCMP 9913 (compare Figs 4.2, 4.4, 4.6). The nasal of FMNH PR 2251 does not possess a posterior process; the posterolateral margin of the dorsal exposure of the nasal is tightly co-ossified to the anteromedial part of the postfrontal, so the suture between these bones is not well visible, giving the impression of the nasal extending posteriorly to the level of the supratemporal fenestra (Fig. 4.6). The dorsal margin of the postorbital is tightly co-ossified to the ventral margin of the postfrontal, but the suture between these bones is nonetheless distinguishable, and provides evidence that the postorbital is excluded from the lateral margin of the supratemporal fenestra in FMNH PR 2251 (Fig. 4.5), just like in UCMP 9950 (Fig. 4.1) and UCMP 9913 (Fig. 4.3). The supratemporal described by Fröbisch et al. (2006; Fig. 4.8H) has the same morphology and position as the posterolateral process of the postfrontal in UCMP 9950 and 9913, indicating misidentification of the postfrontal as the supratemporal by Fröbisch et al. (2006;). The suture between the squamosal and quadratojugal is not well visible, due to the high degree of co-ossification of the bones forming the temporal region of FMNH PR 2251 (Fig. 4.5). However, in posterior view, a quadrate process identical in morphology to the quadrate process of the quadratojugal of UCMP 9950 and UCMP 9913 is clearly visible in FMNH PR 2251 (Fig. 4.5). Therefore, it is not necessary to assume that this process is formed by the squamosal, but by the quadratojugal, as in the referred skulls of *Cy. piscosus*. Consequently, the squamosal contribution to the lower temporal arch is also not present in FMNH PR 2251, contra Fröbisch et al. (2006).

A robust clavicle was also proposed as a diagnostic feature of *Cy. nichollsi* (Fröbisch et al., 2006). The robustness of the clavicles between the three species of *Cymbospondylus* cannot be compared, because the clavicle of PIMUZ T 4351 is partially embedded in matrix and its anterior portion was already badly broken off when the specimen was examined during the preparation of this study (March–August 2016). The clavicle of UCMP 9950 is also partially embedded in matrix and it was not possible to relocate the only three-dimensionally preserved clavicle of *Cy. petrinus* (UCMP

9154) for comparison in the UCMP collections when this study was being prepared. Therefore, the robustness of the clavicle, without providing any quantitative definition, is not considered a good diagnostic character.

The number of cervicals was also proposed as an important diagnostic character for differentiating between species of *Cymbospondylus*. Sander (1989) first defined the cervical vertebrae of *Cy. buchseri* as all those possessing parapophyses, giving a number of 6 cervicals. This definition was then followed by Fröbisch et al. (2006), which resulted in a cervical count of 8-10 in FMNH PR 2251 (exact number was not possible to determine due to pectoral girdle elements obscuring the anatomy of posterior cervicals). Sander (1989) noted the number of cervicals in PIMUZ T 4351 was different from *Cy. piscosus*, for which a number of 11 cervicals was given by Merriam (1908:112). However, Merriam (1908:112) defined cervicals as all vertebrae lying anterior to the pectoral girdle, not those possessing parapophyses. Because of the different definitions of cervicals given by both authors, their number cannot be reliably compared. Sander (1989:168-9) also stated that a number of 6 cervicals with clearly developed parapophyses was also given by Merriam (1908:113) for a specimen of *Cy. piscosus* (UCMP 9154). However, Merriam (1908:113) in fact noted that the number of cervical vertebrae bearing parapophyses was variable in different specimens he referred to *Cy. piscosus*, ranging between six (UCMP 9154) and 13 (UCMP 9943). Because the number of vertebrae with well-developed parapophyses is the only difference between the otherwise very similar cranial and postcranial material assigned to *Cy. piscosus* by Merriam (1908; pers. obs.), I conclude that this variability is most likely due to intraspecific variation and/or ontogeny, especially since the individual with the lowest 'cervical' count studied by Merriam (1908; UCMP 9154) was the smallest. Therefore, I do not consider the number of vertebrae bearing parapophyses as a good diagnostic character for *Cymbospondylus*. However, because of an apparently high ecological diversity of cymbospondylids (Chapter 5) from the Middle Triassic, detailed studies of postcranial anatomy of *Cymbospondylus* are required to fully resolve the taxonomic status of *Cy. nicholls*i.

The smaller size of FMNH PR 2251 compared to UCMP 9950 and UCMP 9913 suggests that FMNH PR 2251 might belong to a smaller, perhaps osteologically more immature, individual of *Cy. piscosus*. Although the degree of cranial bone co-ossification in FMNH PR 2251 is high and comparable

to those of UCMP 9950 and UCMP 9913, it was recently argued that at least in some groups the degree of co-ossification of cranial bones is not a good predictor of maturity (Bailleou et al., 2016). Furthermore, Ezcurra and Butler (2015) recently reported that the interdigitations of the fronto-parietal suture in the basal archosauromorph *Proterosuchus fergusi* became shallower throughout ontogeny. In FMNH PR 2251 the interdigitations of the fronto-parietal suture are comparably deep (Fig. 4.6), whereas the same interdigitations in UCMP 9950 and UCMP 9913 are much shallower. Even though the changes in the morphology of the fronto-parietal suture in ichthyosaurs have not been well studied, this nevertheless provides some limited evidence that FMNH PR 2251 could represent a growth stage of *Cy. piscosus*.

In summary, the cranial anatomy of FMNH PR 2251 bears no discrete character differences from the referred skulls of *Cy. piscosus* (UCMP 9950 and UCMP 9913), the differences in continuous characters between FMNH PR 2251 and *Cy. piscosus* are most likely influenced by deformation, and the postcranial characters used to differentiate FMNH PR 2251 from *Cy. petrinus* are unreliable and are most likely related with ontogeny and/or intraspecific variation. Therefore, I conclude that FMNH PR 2251 is not sufficiently different from the material described as *Cy. piscosus*, and that FMNH PR 2251 is referred to *Cy. piscosus* and *Cy. nicholllsi* becomes a subjective junior synonym of *Cy. piscosus*.

Taxonomic status of *Cy. buchseri* (Table 4.2). *Cy. buchseri* was originally diagnosed on the basis of the following characters: body size (estimated total body length) ~60% of *Cy. piscosus*; a postorbital region proportionally shorter than that of *Cy. piscosus*; a postfrontal not extending much beyond the posterior orbital margin; a scapula anteroposteriorly wider than that of *Cy. piscosus*; a humerus proximodistally shorter and anteroposteriorly wider than that of *Cy. piscosus*; and an ulna with a convex posterior margin (modified from Sander, 1989). However, McGowan and Motani (2003:66) raised the possibility that *Cy. buchseri* could potentially be an osteologically immature specimen of *Cy. piscosus*, based on the comparison of forefin elements between the two taxa (see below). Furthermore, Maisch and Matzke (2004:371) stated that the cranial anatomy of *Cy. buchseri* was indistinguishable from that of *Cy. piscosus*, raising further concerns about the validity of *Cy. buchseri*, but they did not provide any

evidence to support their claims. Here, I review the evidence supporting *Cy. buchseri* as a distinct taxon of *Cymbospondylus*, based mainly on new observations of its cranial osteology.

Re-examination of the skull of *Cy. buchseri* indicates that the cranial autapomorphies proposed to distinguish *Cy. buchseri* from *Cy. piscosus* by Sander (1989) are inapplicable. The skull of *Cy. buchseri* is broken posteriorly, so that the squamosal and anterior part of the quadratojugal are not preserved, while the quadrate, together with the posterior part of the quadratojugal, has been separated from the remainder of the skull and shifted anteriorly (Fig. 4.7). This gives the impression of a shorter postorbital region in *Cy. buchseri*, which in reality was probably not significantly shorter than that of *Cy. piscosus*. Furthermore, the bone identified as the postfrontal by Sander (1989) is here identified as the prefrontal, and its morphology does not differ from that of other specimens of *Cymbospondylus* (Fig. 4.7; see Prefrontal). Also, comparison of the type skull of *Cy. buchseri* with cranial material of other species of *Cymbospondylus* indicates that the cranial morphology of *Cy. buchseri* is almost identical to that of *Cy. piscosus* (UCMP 9950, UCMP 9913) and the holotype skull of *Cy. 'nicholllsi'* (FMNH PR 2251), as suggested by Maisch and Matzke (2004:371). The only difference in cranial morphology between *Cy. buchseri* and *Cy. piscosus* and *Cy. 'nicholllsi'* is that the posteroventral process of the jugal is absent in *Cy. buchseri*, while it is well developed in *Cy. petrinus* and *Cy. 'nicholllsi'* (compare Figs 4.3, 4.5, 4.7). A posteroventral process of the jugal is also known from the largest described specimen of the basal ichthyosaurian *Mixosaurus panxianensis*, while in smaller specimens of the same taxon this feature is absent (Jiang et al., 2005, 2006). This indicates that the presence of the posteroventral process of the jugal in basal ichthyosaurians could be related to ontogeny, therefore its absence in *Cy. buchseri* is not considered as a diagnostic character. The high degree of co-ossification of the cranial bones in the type of *Cy. buchseri* seems to indicate its osteological maturity. However, as mentioned above, the degree of co-ossification of cranial bones is not necessarily a reliable predictor of the ontogenetic stage at least in some taxa (Bailleul et al., 2016), so I consider that using the degree of suture closure to assess osteological maturity in *Cymbospondylus* is not reliable.

In the basal ichthyopterygian *Chaohusaurus chaoxianensis*, the length:width ratio of some forefin bones increases during ontogeny (Motani and You, 1998; McGowan and Motani, 2003:66). The scapula of *Cy. buchseri* is anteroposteriorly broader than that of *Cy. piscosus*, and the humerus of *Cy.*

buchseri is anteroposteriorly broader and proximodistally shorter than that of *Cy. piscosus*. Because the humerus morphologies of *Chaohusaurus* and *Cymbospondylus* are very similar, and because both taxa occupy a basal position within Ichthyopterygia, McGowan and Motani (2003:66) suggested that a similar length:width ratio increase of forefin elements during ontogeny could occur in *Cymbospondylus*. Although plausible, this ontogenetic change cannot be confirmed for *Cymbospondylus* at present, because of a low sample size of *Cymbospondylus* humeri and forefin elements. In conclusion, *Cy. buchseri* is retained as a distinct taxon, but it should be noted that the morphology of the type specimen indicates that it belongs to an osteologically immature individual. The hypothesis of *Cy. buchseri* being a taxon distinct from *Cy. piscosus* should be evaluated when more material of osteologically immature individuals of *Cymbospondylus*, in particular the cranium and forefins, become available.

FIGURES AND TABLES

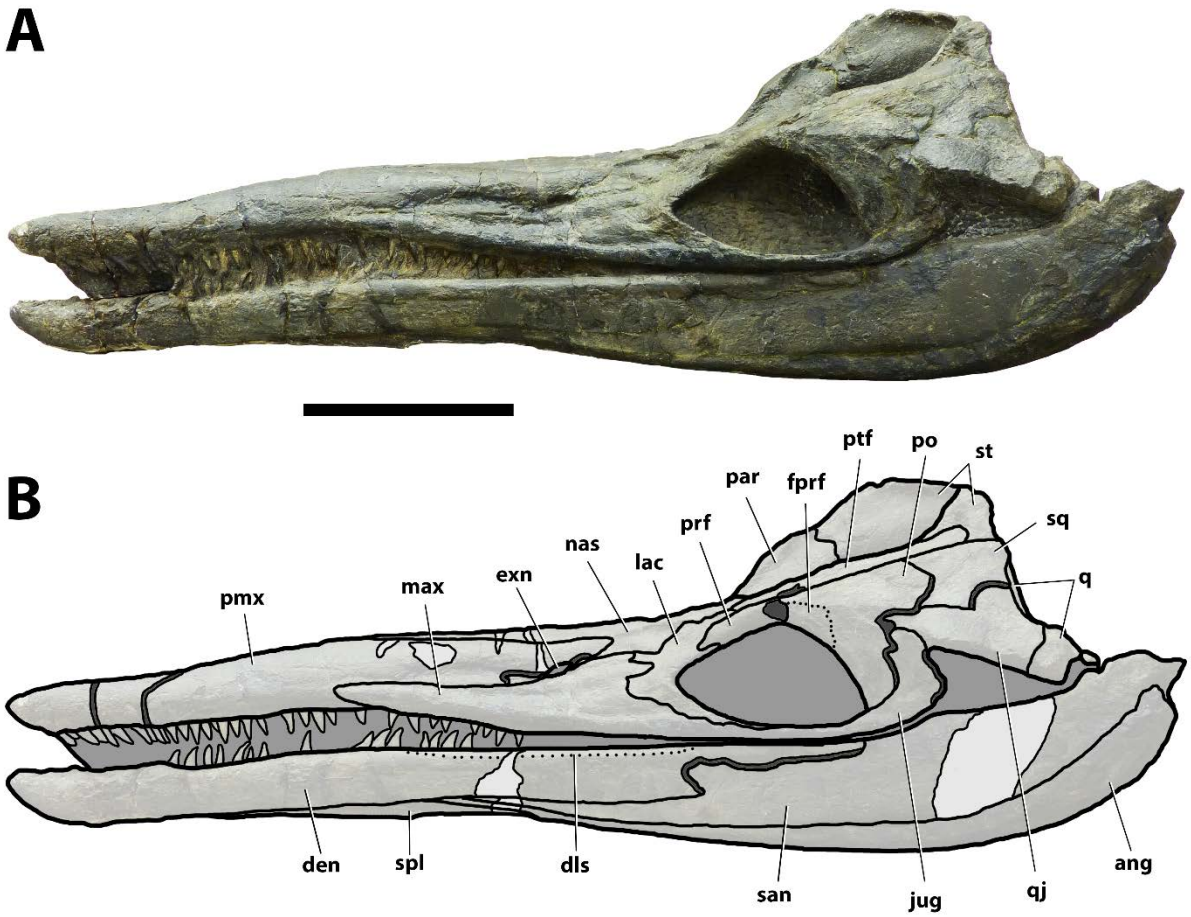

FIGURE 4.1. Referred skull of *Cymbospondylus piscosus* (UCMP 9950) in left lateral view (**A**). In line drawing (**B**), grey indicates rock matrix, light grey indicates reconstruction in plaster and dark grey indicates broken bone surface. Abbreviations: **ang**, angular; **den**, dentary; **dls**, dentary labial shelf; **exn**, external naris, **fprf**, facet for prefrontal; **jug**, jugal; **lac**, lacrimal; **max**, maxilla; **nas**, nasal; **par**, parietal; **prf**, prefrontal; **pmx**, premaxilla; **po**, postorbital; **ptf**, postfrontal; **q**, quadrate; **qj**, quadratojugal; **san**, surangular; **spl**, splenial; **sq**, squamosal; **st**, supratemporal. Scale bar equals 20 cm.

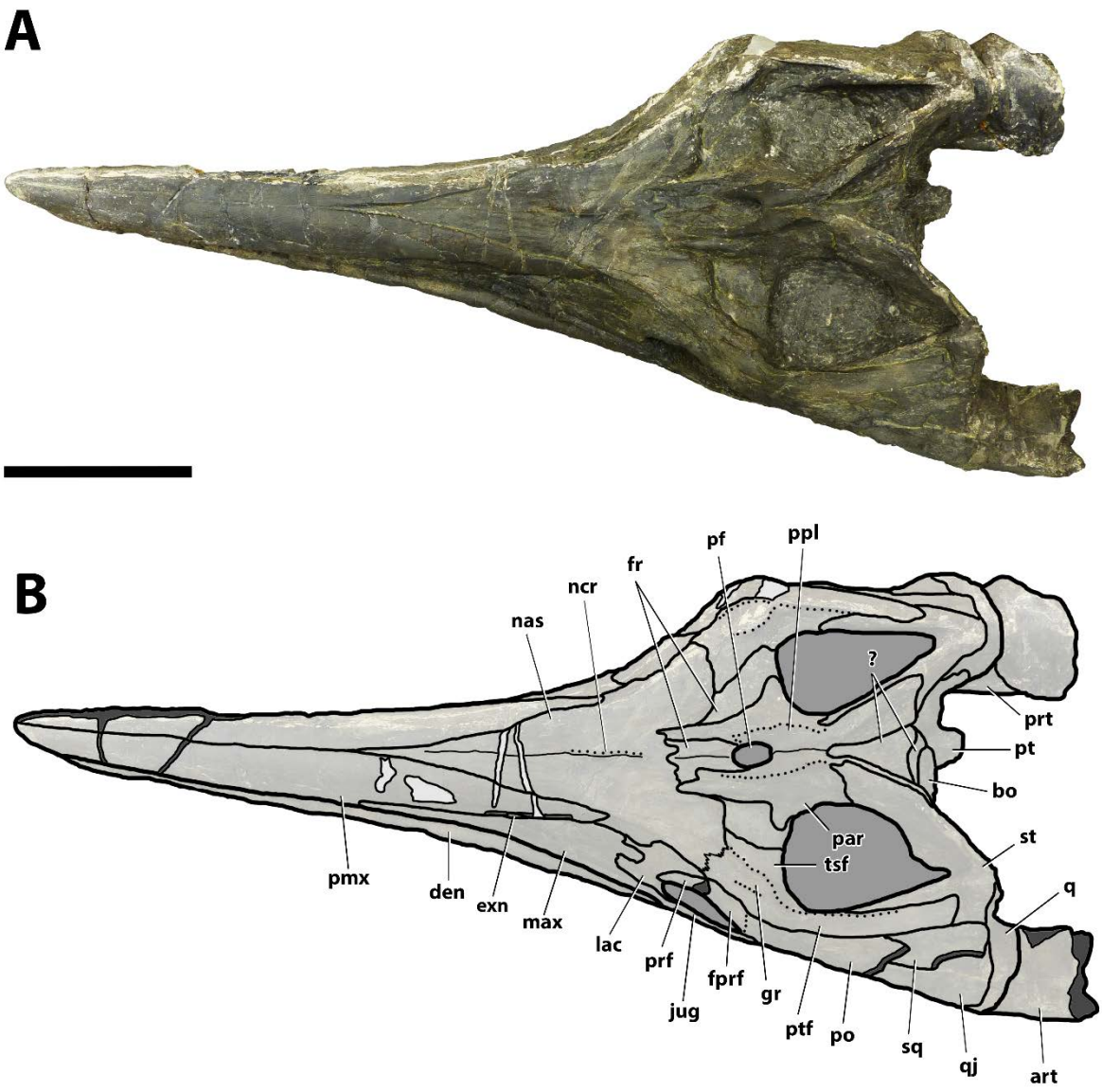

FIGURE 4.2. Referred skull of *Cymbospondylus piscosus* (UCMP 9950) in dorsal view (**A**). In line drawing (**B**), grey indicates rock matrix, light grey indicates reconstruction in plaster and dark grey indicates broken bone surface. Abbreviations: **art**, articular; **bo**, basioccipital; **den**, dentary; **exn**, external naris, **fprf**, facet for prefrontal; **fr**, frontal; **gr**, postfrontal lateral groove; **jug**, jugal; **lac**, lacrimal; **max**, maxilla; **nas**, nasal; **ncr**, nasal crest; **par**, parietal; **pf**, pineal foramen; **prf**, prefrontal; **pmx**, premaxilla; **po**, postorbital; **ppl**, parietal plateau; **pt**, pterygoid; **prt**, prearticular; **ptf**, postfrontal; **q**, quadrate; **qj**, quadratojugal; **sq**, squamosal; **st**, supratemporal; **tsf**, anterior terrace of supratemporal fenestra. Scale bar equals 20 cm.

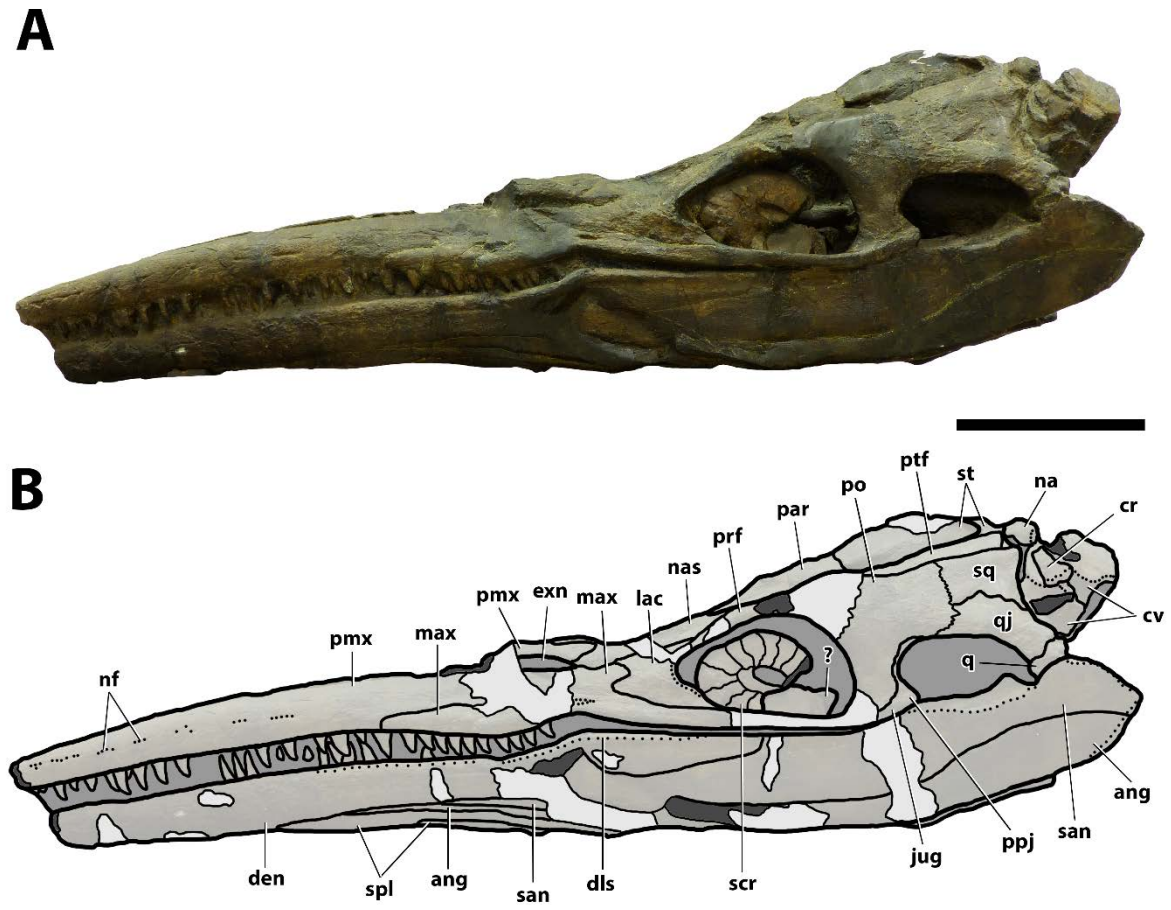

FIGURE 4.3. Referred skull of *Cymbospondylus piscosus* (UCMP 9913) in left lateral view (**A**). In line drawing (**B**), grey indicates rock matrix, light grey indicates reconstruction in plaster and dark grey indicates broken bone surface. Abbreviations: **ang**, angular; **cr**, cervical rib; **cv**, cervical vertebrae; **den**, dentary; **dls**, dentary labial shelf; **exn**, external naris; **jug**, jugal; **lac**, lacrimal; **max**, maxilla; **na**, neural arch; **nas**, nasal; **nf**, neurovascular foramina; **par**, parietal; **prf**, prefrontal; **pmx**, premaxilla; **po**, postorbital; **ppj**, posterior process of jugal; **ptf**, postfrontal; **q**, quadrate; **qj**, quadratojugal; **san**, surangular; **scr**, sclerotic ring; **spl**, splenial; **sq**, squamosal; **st**, supratemporal. Scale bar equals 20 cm.

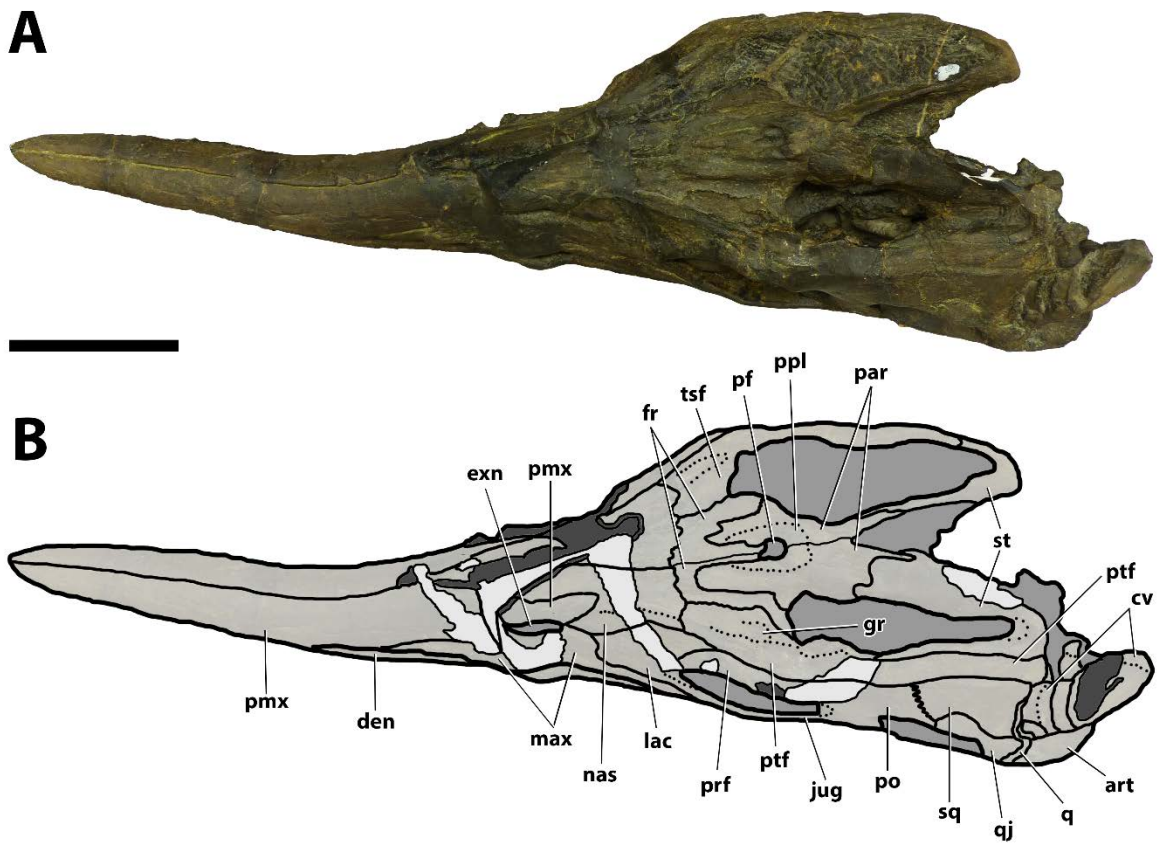

FIGURE 4.4. Referred skull of *Cymbospondylus piscosus* (UCMP 9950) in dorsal view (**A**). In line drawing (**B**), grey indicates rock matrix, light grey indicates reconstruction in plaster and dark grey indicates broken bone surface. Abbreviations: **art**, articular; **cv**, cervical vertebrae; **den**, dentary; **exn**, external naris; **fr**, frontal; **gr**, postfrontal lateral groove; **lac**, lacrimal; **max**, maxilla; **nas**, nasal; **par**, parietal; **pf**, pineal foramen; **pmx**, premaxilla; **po**, postorbital; **ppl**, parietal plateau; **prf**, prefrontal; **ptf**, postfrontal; **q**, quadrate; **qj**, quadratojugal; **sq**, squamosal; **st**, supratemporal; **tsf**, anterior terrace of supratemporal fenestra. Scale bar equals 20 cm.

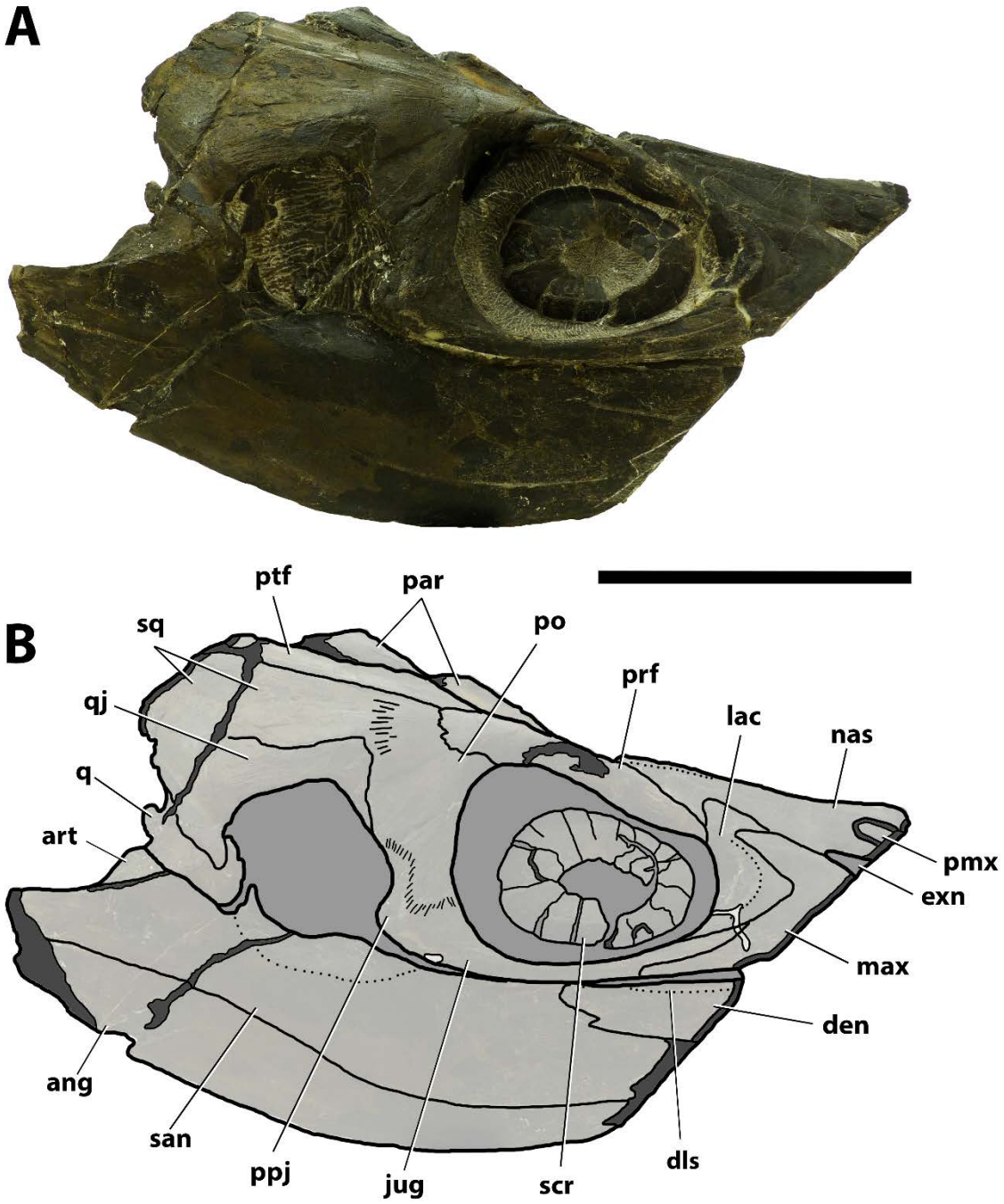

FIGURE 4.5. Referred skull of *Cymbospondylus piscosus* (FMNH PR 2251) in right lateral view (**A**). In line drawing (**B**), grey indicates rock matrix, light grey indicates reconstruction in plaster and dark grey indicates broken bone surface. Abbreviations: **ang**, angular; **art**, articular; **den**, dentary; **dls**, dentary labial shelf; **exn**, external naris, **jug**, jugal; **lac**, lacrimal; **max**, maxilla; **nas**, nasal; **par**, parietal; **prf**, prefrontal; **pmx**, premaxilla; **po**, postorbital; **ppj**, posterior process of jugal; **ptf**, postfrontal; **q**, quadrate; **qj**, quadratojugal; **san**, surangular; **scr**, sclerotic ring; **sq**, squamosal. Scale bar equals 20 cm.

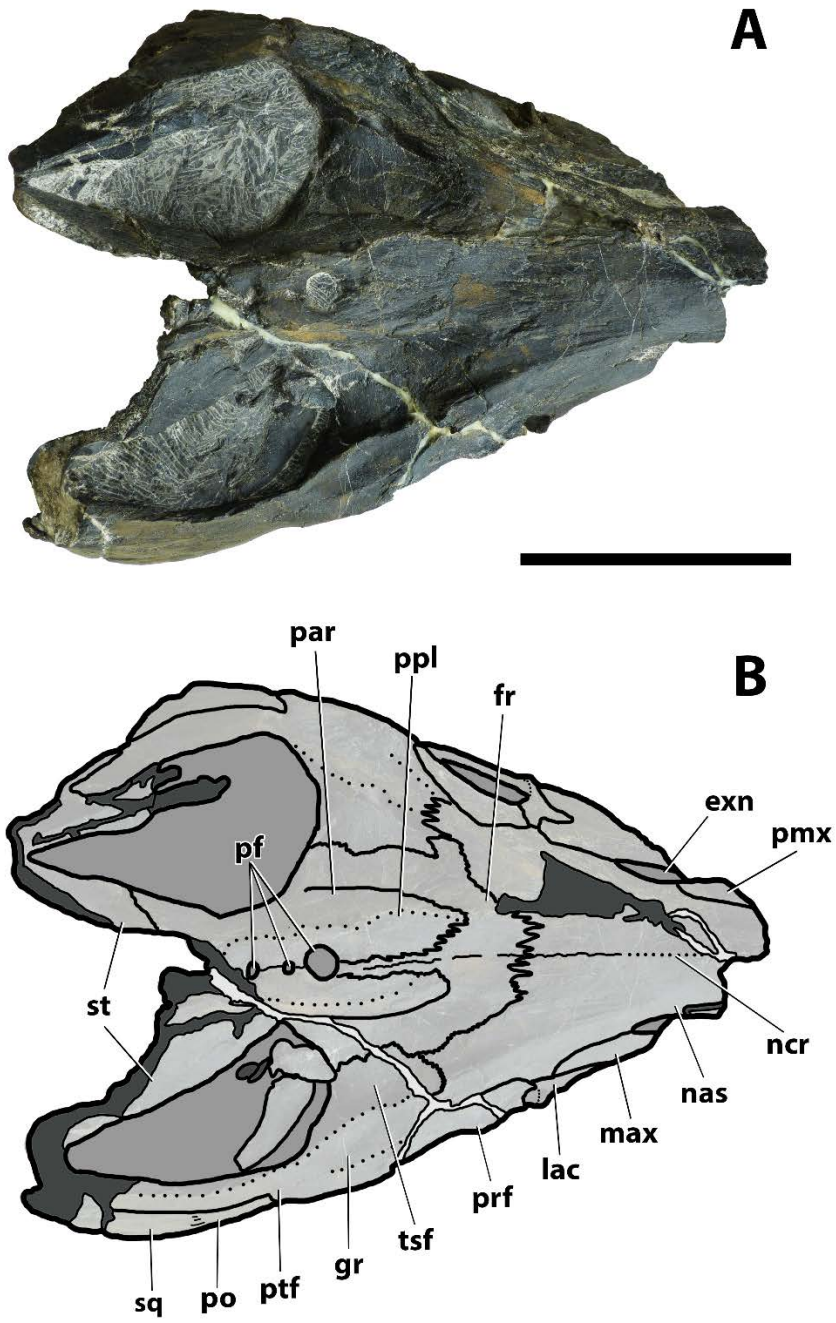

FIGURE 4.6. Referred skull of *Cymbospondylus piscosus* (FMNH PR 2251) in dorsal view (**A**). In line drawing (**B**), grey indicates rock matrix, light grey indicates reconstruction in plaster and dark grey indicates broken bone surface. Abbreviations: **den**, dentary; **exn**, external naris; **fr**, frontal; **gr**, postfrontal lateral groove; **lac**, lacrimal; **max**, maxilla; **nas**, nasal; **ncr**, nasal crest; **par**, parietal; **pf**, pineal foramen; **pmx**, premaxilla; **po**, postorbital; **ppl**, parietal plateau; **prf**, prefrontal; **ptf**, postfrontal; **sq**, quamosal; **st**, supratemporal; **tsf**, anterior terrace of supratemporal fenestra. Scale bar equals 20 cm.

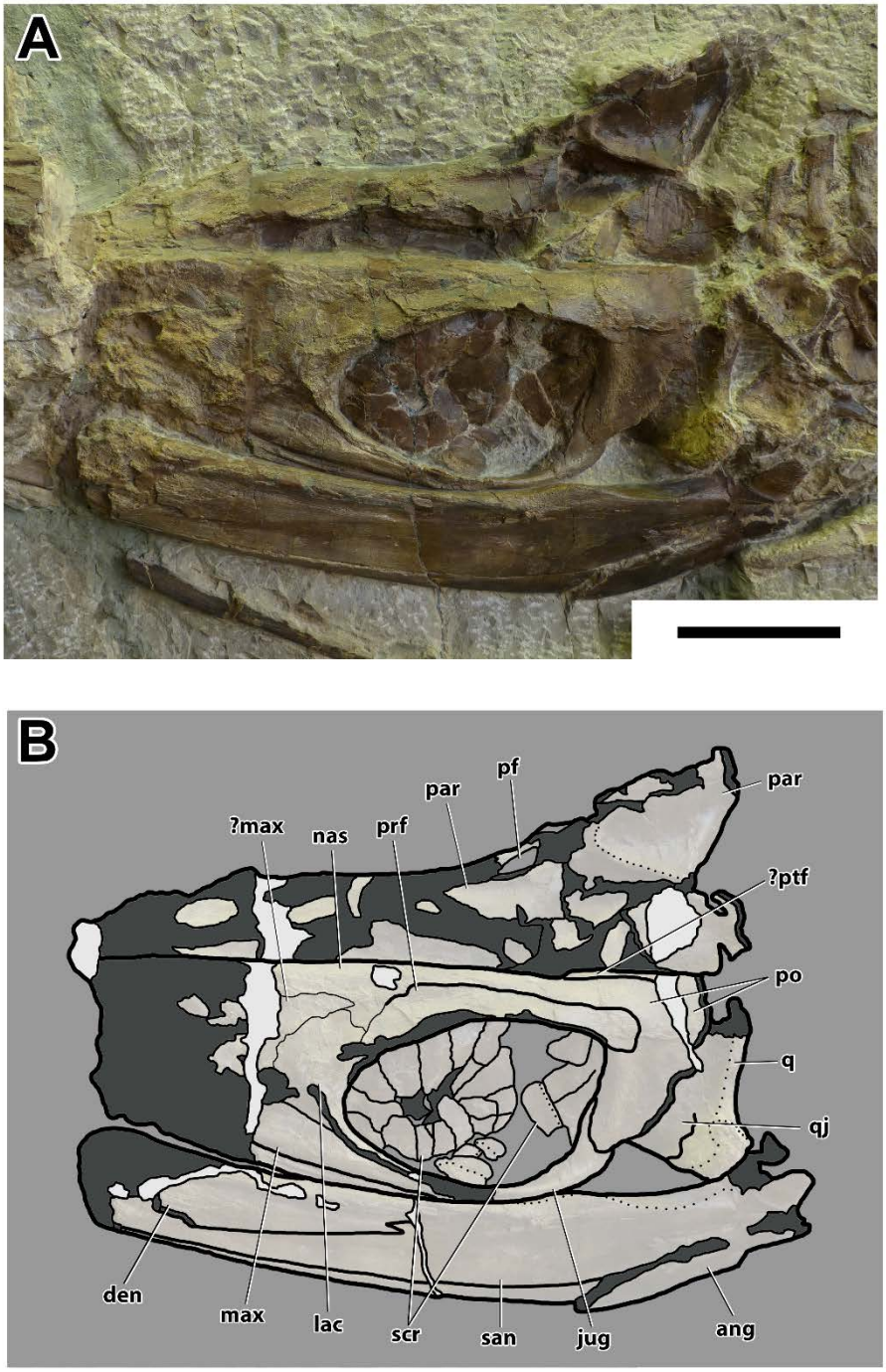

FIGURE 4.7. Type skull of *Cymbospondylus buchseri* (PIMUZ T 4351) in left lateral view (**A**). In line drawing (**B**), grey indicates rock matrix, light grey indicates reconstruction in plaster and dark grey indicates broken bone surface. Abbreviations: **ang**, angular; **den**, dentary; **jug**, jugal; **lac**, lacrimal; **max**, maxilla; **nas**, nasal; **par**, parietal; **prf**, prefrontal; **po**, postorbital; **?ptf**, ?postfrontal; **q**, quadrate; **qj**, quadratojugal; **san**, surangular; **scr**, sclerotic ring. Scale bar equals 10 cm.

FIGURE 4.8. Previous interpretations of the cranial anatomy of *Cymbospondylus piscosus* in left lateral view. (**A**) after Merriam, 1908; (**B**) after Huene, 1916; (**C**) after Camp, 1980 (inverted); (**D**) after Sander, 1989; (**E**) after Massare and Callaway, 1990 (inverted); (**F**) after Motani, 1999a; (**G**) after Maisch and Matzke, 2000, 2004; (**H**) after Fröbisch et al., 2006 (inverted); (**I**) after Ji et al., 2016. Grey indicates rock matrix, light grey indicates reconstruction in plaster. Abbreviations: **an**, angular; **d**, dentary; **j**, jugal; **l**, lacrimal; **m**, maxilla; **n**, nasal; **pf**, postfrontal; **pmx**, premaxilla; **?ppr**, postparietal; **pr**, parietal; **prf**, prefrontal; **pto**, postorbital; **q**, quadrate; **qj**, quadratojugal; **sa**, surangular; **sp**, splenial; **sq**, squamosal; **st**, supratemporal.

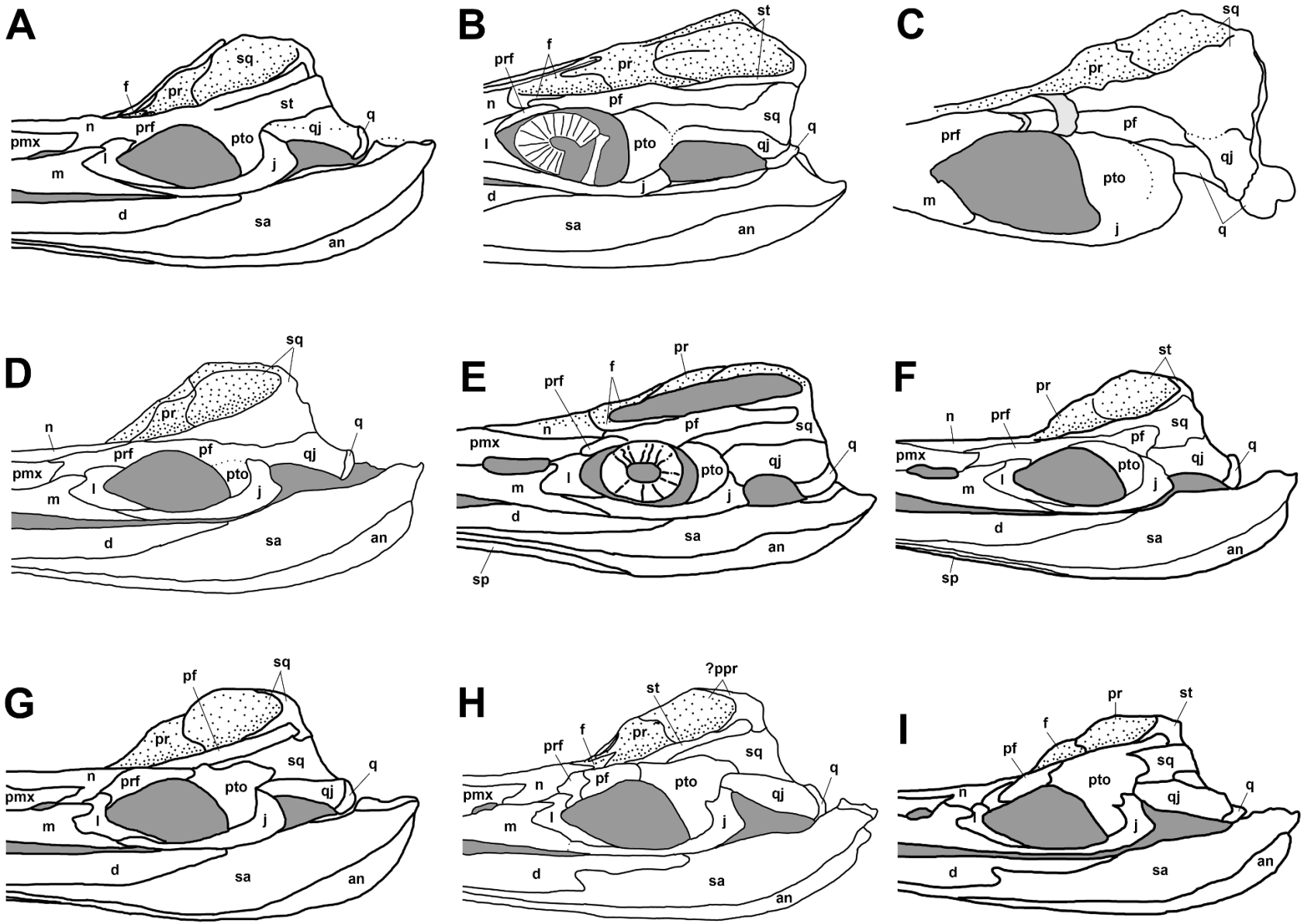
A
sq
f
pr
st
q
n
prf
pmx
pto
qj
l
j
m
d
sa
an
B
st
f
prf
pr
n
pf
sq
l
pto
qj
q
j
d
sa
an
C
sq
pr
prf
pf
qj
pto
m
j
q
D
sq
pr
n
q
prf
pf
qj
pmx
pto
l
j
m
d
sa
an
E
pr
f
prf
n
pf
sq
pmx
q
l
pto
qj
m
j
d
sa
an
sp
F
st
pr
n
prf
sq
pf
q
pmx
qj
l
pto
m
j
d
sa
an
sp
G
pf
sq
pr
n
sq
q
prf
pto
pmx
qj
l
m
j
d
sa
an
H
?ppr
st
f
prf
pr
sq
n
pf
pto
q
pmx
qj
l
m
j
d
sa
an
I
pr
st
f
pf
sq
pto
n
qj
q
l
j
d
sa
an

	UCMP 9950	UCMP 9913	PIMUZ T 4351
Skull maximum ap length	1110.0 (l), 1090.0 (r)	1200.0 (l), 1160 (r)	670.0i
Mandibular ramus maximum ap length	1220.0 (l), 1190 (r)	1260.0 (l), 1230.0 (r)	670.0i
Skull maximum ml width	470.0	370.0	N/A
Intramandibular maximum ml width	480.0	320.0	N/A
Preorbital maximum ap length	730.0 (l), 720.0 (r)	800.0 (l), ~730.0 (r)	435.0i
Premaxillary length	380.0 (l), 380 (r)	465.0 (l), 430 (r)	N/A
Prenarial length	575.0 (l), ~580.0 (r)	~620.0 (l), ~570.0 (r)	N/A
Postorbital length	190.0 (l), 200.0 (r)	220.0 (l), 240.0 (r)	90.0i
Orbit maximum ap length	190.0 (l), 175.0 (r)	183.0 (l), ~198.0 (r)	155.0
Orbit maximum dv height	98.0 (l), 104 (r)	107.0 (l), 126 (r)	101.8
Sclerotic ring maximum ap length	N/A	~150.0 mm (l)	105.4
Sclerotic ring maximum dv height	N/A	~100.0 (l)	96.9
Sclerotic ring aperture maximum ap length	N/A	~60.0 (l)	N/A
Sclerotic ring aperture maximum dv height	N/A	34.0 (l)	N/A
External naris maximum ap length	~45.0 mm (l)	~65.0 (l)	N/A
External naris maximum dv height	~10.0 mm (l)	16.0 (r)	N/A
Supratemporal fenestra maximum ap length	200.0 (l), 200.0 (r)	245.0 (l), 240 (r)	N/A
Supratemporal fenestra maximum ml width	125.0 (l), 125.0 (r)	70.0 (l), 94.0 (r)	N/A
Pineal foramen maximum ap length	35.8	27.3	28.4
Pineal foramen maximum ml width	27.7	21.1	11.6

TABLE 4.1. Selected cranial measurements of *Cymbospondylus piscosus* (UCMP 9950, UCMP 9913) and *Cy. buchseri* (PIMUZ T 4351) crania examined for this study. All measurements are given in mm. Abbreviations: ap, anteroposterior; dv, dorsoventral; i, incomplete; l, left; ml, mediolateral; r, right. Please refer to Fröbisch et al. (2006) for measurements of FMNH PR 2251.

Diagnostic character	*Cy. buchseri* (Sander, 1989)	*Cy. buchseri* (this study)	*Cy. nichollsi* (Fröbisch et al., 2006)	*Cy. nichollsi* (this study)	*Cy. piscosus* (this study)
Postorbital region	ap short	most likely ap long (posteriorly broken)	ap long, posnarial:postorbital ratio 1.85, compared with 2.11 in *Cy. piscosus*	ap long, postnarial:postorbital ratio 2.77	ap long, postorbital:postnarial ratio 2.58 (UCMP 9950) and 2.34 (UCMP 9913)
Postfrontal	extending posteriorly just beyond posterior orbital margin	most likely extending far posteriorly, along lateral margin of stf	extending posteriorly just beyond posterior orbital margin	extending far posteriorly, along lateral margin of stf	extending far posteriorly, along lateral margin of stf
Nasal	damaged posteriorly	damaged posteriorly	extending far posteriorly, to anterior margin of stf	separated from anterior margin of stf by postfrontal and frontal	separated from anterior margin of stf by postfrontal and frontal
Pineal foramen	enclosed entirely within frontals	enclosed mostly within parietals (frontals damaged)	enclosed entirely within parietals	enclosed mostly within parietals, anterior margin formed by frontals	enclosed mostly within parietals, anterior margin formed by frontals
Postorbital	triangular in outline	triangular in outline (damaged posteriorly), most likely eliminated from lateral margin of stf by ptf	triangular in outline, forms lateral margin of stf	triangular in outline, eliminated from lateral margin of stf by ptf	triangular in outline, eliminated from lateral margin of stf by ptf
Supratemporal	badly damaged (identified as squamosal)	badly damaged	small, ap elongate element, forms posterolateral margin of stf	massive, forms much of lateral and medial margins of stf	massive, forms much of lateral and medial margins of stf
Quadratojugal	not preserved	damaged, articulates with quadrate	excluded from contact with quadrate by squamosal	articulates with quadrate	articulates with quadrate
Clavicle	ap elongate and slender	most likely ap elongate (broken anteriorly, partially embedded in matrix)	ap elongate and slender, but more robust than in *Cy. piscosus*	ap elongate	not examined, illustrated in only one view by Merriam (1905, 1908)
No of centra with ossified parapophyses ('cervical' centra)	6	6	8–10	8–10	6–13 (Merriam, 1908)

Table 4.2. Revision of characters previously proposed as diagnostic for referred species of *Cymbospondylus*, and their comparison with the revised anatomy of the type species, *Cy. piscosus*. Abbreviations: **ap**, anteroposteriorly; **ptf**, postfrontal; **stf**, supratemporal fenestra.

CHAPTER 5: PHYLOGENY OF THE ICHTHYOPTERYGIA, INCORPORATING NEW DATA ON CYMBOSPONDYLIDAE AND BASAL PARVIPELVIA.

INTRODUCTION

Only four cladistic analyses of Ichthyopterygia, comprehensively sampling Triassic taxa, have been performed to date (Motani, 1999a; Maisch and Matzke, 2000a; Sander, 2000; Ji et al., 2016; Fig. 5.1–5.2). The studies of Motani (1999a), Maisch and Matzke (2000a) and Sander (2000) have helped to understand the basic phylogenetic relationships between major groups of ichthyosaurs and have remained the primary source of information on ichthyosaur evolution for 15 years. However, a significant advancement in our understanding of ichthyosaur evolution came from the study of Ji et al. (2016; expanded and modified by Jiang et al. [2016; Fig. 5.3]). This study incorporated information from the discoveries of Triassic ichthyosaurs from North America (Nicholls and Manabe, 2001, 2004; Fröbisch et al., 2006, 2013; Cuthbertson et al., 2013a, 2013b, 2014) and South China (Li, 1999; Yin et al., 2000; Li and You, 2002; Chen and Cheng, 2003; Nicholls et al, 2002; Pan et al., 2006; Jiang et al., 2006, 2007, 2008; Maisch et al., 2006, 2008; Chen et al., 2007; Shang and Li, 2009; Sander et al., 2011; Ji et al., 2013) made in the last 20 years. One of the more interesting results obtained by Ji et al. (2016) was the recovery of an expanded Cymbospondylidae, which, apart from the genus *Cymbospondylus*, included the small-bodied, durophagous *Xinminosaurus catactes* from the Middle Triassic (Anisian) of South China (Jiang et al., 2008) and the colossal apex predator *Thalattoarchon saurophagis* from the Middle Triassic (Anisian) of Nevada, USA (Fröbisch et al., 2013). Although nodal support recovered for this clade was weak (Bremer value = 1), it raised the possibility of the existence of a clade of ichthyosaurs that achieved high ecological diversity within only 4 million years of their first appearance in the fossil record (Motani et al., 2014). However, the phylogenetic analysis of Cuthbertson et al. (2013b) recovered *Xinminosaurus* in a more basal position within Ichthyopterygia, outside of Cymbospondylidae, and the analysis of Fröbisch et al. (2013) recovered *Thalattoarchon* as more

derived than *Cymbospondylus*, within a paraphyletic Shastasauridae. Therefore, a consensus on the phylogenetic position of these two taxa is yet to be established.

In recent years, the description and re-description of numerous derived parvipelvian ichthyosaurs has led to a significant increase in our knowledge of the evolution of ichthyosaurs from the Middle Jurassic–Late Cretaceous (e.g. Maxwell et al., 2012b; Roberts et al., 2014; Arkhangelsky and Zverkov, 2014; Fischer et al., 2016). However, the evolutionary history of basal parvipelvian ichthyosaurs from the Late Triassic–Early Jurassic interval has received far less attention. McGowan and Motani (2002) performed a phylogenetic analysis of Ichthyopterygia which incorporated two, then undescribed, ichthyosaur taxa from the Lower Jurassic of England, including Gen. at sp. nov. A, described in Chapter 2 of this thesis. Addition of these two taxa led to the loss of phylogenetic resolution within Parvipelvia, providing evidence that the evolutionary history of early Parvipelvia is more complex than previously thought. Furthermore, the discoveries of more complete specimens of *Macgowania janiceps*, the basalmost parvipelvian from the Pardonet Formation of British Columbia, Canada (Nicholls and Manabe, 2004; Henderson, 2015), and the description of a new genus of basal parvipelvian from the same stratigraphical unit (Chapter 3 of this thesis) allow for a more detailed investigation of the earliest evolutionary history of Parvipelvia.

The aims of this chapter are:

- to incorporate the new information obtained from a comprehensive re-description of the cranial anatomy of *Cymbospondylus* (Chapter 4 of this thesis) into a phylogenetic framework, in order to identify potential synapomorphies supporting an expanded, ecologically diverse Cymbospondylidae;
- to include two new taxa of parvipelvian ichthyosaurs from the Lower Jurassic of the United Kingdom (Chapter 2) and Late Triassic of British Columbia, Canada (Chapter 3) into a phylogenetic hypothesis of Ichthyopterygia, in order to investigate their effect on the topology of early diverging Parvipelvia.

METHODS

In order to test the phylogenetic relationships of Ichthyopterygia, incorporating the new data on Cymbospondylidae and basal Parvipelvia presented in this thesis, I used a modified version of the character-taxon matrix of Jiang et al. (2016). The data matrix of Jiang et al. (2016) is in itself a modified version of the data matrices of Motani et al. (2015a) and Ji et al. (2016), and is the most comprehensive data set published for Ichthyopterygia to date, including 73 taxa (12 outgroup and 61 ingroup) scored for 195 morphological characters (Fig. 5.3). The 12 outgroup taxa include two members of Nasorostra (*Cartorhynchus lenticarpus*, *Sclerocormus parviceps*), five representatives of Hupehsuchia (*Nanchangosaurus suni*, *Eohupehsuchus brevicollis*, *Hupehsuchus nanchangensis*, *Parahupehsuchus longus* and *Eretmorhipis carrolldongi*) and five diapsids of uncertain phylogenetic affinities (*Petrolacosaurus kansensis*, *Thadeosaurus colcanapi*, *Claudiosaurus germaini*, *Hovasaurus boulei* and *Wumengosaurus delicatomandibularis*). Nasorostrans were included as the outgroup taxa because they have recently been recovered as the sister taxon to Ichthyopterygia (both clades comprising Ichthyosauriformes; Motani et al., 2015a), and hupehsuchians were included because a growing number of evidence suggests that they are the sister group to Ichthyosauriformes (Hupehsuchia and Ichthyosauriformes comprising Ichthyosauromorpha; Motani et al., 2015a). *Wumengosaurus delicatomandibularis* is included because it was recently argued that it is the sister taxon to Ichthyosauromorpha (Chen et al., 2014a). However, because the exact phylogenetic position of Ichthyosauromorpha within Diapsida is still a matter of debate, four taxa widely regarded as very basal diapsids (*Petrolacosaurus kansensis*, *Thadeosaurus colcanapi*, *Claudiosaurus germaini*, *Hovasaurus boulei*) were also included, to provide a comprehensive sample of basal diapsid character states (Motani, 1999a). In addition to the 61 ingroup taxa included in the Jiang et al. (2016) dataset, two new ichthyosaur taxa were added to the matrix – *Gen. et sp. nov. A* (Chapter 2) and *Gen. et sp. nov. B* (Chapter 3).

A list of all ingroup and outgroup taxa included in the phylogenetic analysis, together with data sources used for character scoring and the proportion of missing data, is given in Appendix 1.

For this analysis, none of the original character definitions given by Jiang et al. (2016) were modified and four new characters were added (Fig. 5.4):

196. Nasal crest in posterior part of the internasal suture: (0) absent, (1) present;
197. Mediolaterally broad groove bordered by two, anterosposteriorly elongate ridges (a medial one and a lateral one), in the lateral part of the anteromedial process of the postfrontal: (0) absent, (1) present;
198. Parietal plateau surrounding the pineal foramen laterally and dorsally: (0) absent, (1) present; and
199. Dorsal orbital margin formed exclusively by the prefrontal, without a posterodorsal contribution from the frontal and/or postfrontal: (0) absent, (1) present.

A complete list of characters used in the phylogenetic analysis is provided in Appendix 2.

The new characters (196–199) were scored based on personal observation of fossil specimens and supplemented with relevant literature for all 75 taxa included in the analysis. In addition, 16 taxa were completely re-scored for the remaining characters (1–195). Within the 16 taxa that were re-scored, 5 were recovered in an expanded Cymbospondylidae in the original analysis of Jiang et al., (2016). *Cymbospondylus 'nichollsi'*, synonymised with *Cy. piscosus* in Chapter 4 of this thesis, was kept as a distinct taxon in this analysis. This was done in order to test whether *Cy. piscosus* and *Cy. 'nichollsi'* differ in any character scores, which were possible to score for both taxa. The remaining re-scored taxa include 10 early-diverging parvipelvians from the Late Triassic (*Macgowania janiceps*, *Hudsonelpidia brevirostris*) and Early Jurassic (*Temnodontosaurus*, *Leptonectes tenuirostris*, *Leptonectes solei*, *Leptonectes moorei*, *Excalibosaurus costini*, *Eurhinosaurus longirostris*, *Suevoleviathan disinteger*, *Hauffopteryx typicus*), and *Malawania anachronus*, a parvipelvian of uncertain phylogenetic affinities, recovered as the sister taxon to *Ichthyosaurus* by Fischer et al. (2013), but recovered in a more basal position by Jiang et al. (2016).

A full list of character scores for all 75 taxa included in the phylogenetic analysis is given in Appendix 3.

Parsimony analysis of the dataset was performed in TNT 1.5 (Goloboff et al., 2016). Memory was increased to allow for 10000 trees to be retained. All characters were treated as unordered and equally-weighted. The analysis involved New Technology Search options, including 1000 random addition sequences, combined sectorial-searches, drifting, ratcheting, and tree-fusing. Character fit was calculated using CI and RI (*Stats.run*) and nodal support was calculated as Bremer support (decay index) values (*Bremer.run*), including trees suboptimal by 10 steps.

Character optimization was performed using TNT 1.5 (Goloboff et al., 2016). TNT does not distinguish between ACCTRAN or DELTRAN transformations. Instead, it resolves ambiguous branches as such, and only the unambiguous character transformations are mapped on to the resultant trees.

RESULTS

The phylogenetic analysis produced 45 most parsimonious trees (MPTs) of 671 steps (CI = 0.359, RI = 0.788). A strict consensus of the MPTs is presented in Fig. 5.5. The obtained topology of the strict consensus cladogram is very similar to that recovered by Jiang et al. (2016; see Fig. 5.3), the only differences being: (1) the addition of *Gen. et sp. nov. A* and *Gen. et sp. nov. B*; (2) recovery of a monophyletic *Chaohusaurus*; (3) *Parvinatator wapitiensis* is recovered as the sister taxon to Ichthyosauria; (4) *Mixosaurus panxianensis* is recovered as the sister taxon to *Mixosaurus kuhnschnyderi*; (5) *Suevoleviathan disinteger* is recovered as the sister group to Thunnosauria; (6) *Eurhinosaurus*, *Excalibosaurus* and *Leptonectes* form a monophyletic clade; and (7) some of the relationship within Ophthalmosauridae are resolved. Only the topology and synapomorphies for Cymbospondylidae and early-diverging Parvipelvia are discussed, as these groups were the primary focus of the research presented in this thesis.

Cymbospondylidae. *Cymbospondylus*, *Xinminosaurus* and *Thalattoarchon* are recovered as members of an expanded Cymbospondylidae, but the nodal support for this clade (Bremer value = 1) is weak. This result is in accordance with Jiang et al. (2016) and Ji et al. (2016), who also recovered an expanded, but weakly-supported, Cymbospondylidae. No unambiguous synapomorphies supporting

Cymbospondylidae were recovered in the present analysis. This is likely the result of limited morphological overlap between the specimens of taxa comprising Cymbospondylidae – *Cymbospondylus* is known from well-preserved and mostly complete cranial and postcranial material, whereas *Xinminosaurus* is known primarily from the postcranial skeleton, with all available skull material being severely broken and incomplete (GMPKU-P-1071; GMPKU-P-1206; GMPKU uncatalogued). *Thalattoarchon*, on the other hand, is known most from its skull, with very few parts of the postcranial anatomy preserved (FMNH PR 3032; Fröbisch et al., 2013). Pruning of *Thalattoarchon* from the set of MPTs results in the recovery of two unambiguous synapomorphies for Cymbospondylidae, comprising *Cymbospondylus* and *Xinminosaurus*: coracoid foramen present (character 89:0) and coracoid anterior notch or concavity absent (character 90:0). After pruning *Cymbospondylus 'nichollsi'* from the set of MPTs, an additional unambiguous synapomorphy uniting *Xinminosaurus* and *Cymbospondylus* is recovered: a high presacral count of 55 or more vertebrae (character 166:2; *Cy.'nichollsi'* only preserves the anterior 28 presacral vertebrae [Fröbisch et al., 2006]). Ji et al. (2016) identified one additional synapomorphy uniting *Xinminosaurus* and *Cymbospondylus* – a short clavicle scapular process (character 77:0). This character state was confirmed in *Xinminosaurus* (GMPKU-P-1071), but personal examination of the clavicles of *Cymbospondylus buchseri* (PIMUZ T 4351) and *Cymbospondylus 'nichollsi'* (FMNH PR 2251) revealed that they are posteriorly elongate, much like in the basal ichthyopterygian *Utatsusaurus* (R. Motani, pers. comm., Nov 2016). Even though the clavicle figured by Merriam (1905, 1908) for *Cymbospondylus piscosus* (UCMP 9154) seems shortened posteriorly, it was not possible to locate this specimen in the collections of the UCMP during the preparation of this study (Nov 2014–Jun 2017), so this character state could not be confirmed for *Cy. piscosus*.

When *Xinminosaurus* is pruned from the set of MPTs, one unambiguous synapomorphy, supporting a clade consisting of *Thalattoarchon* + *Cymbospondylus*, is recovered – dorsal orbital margin formed exclusively by prefrontal, without a posterodorsal contribution from the frontal and/or postfrontal (character 199:1). After pruning *Cy. buchseri* (known from poorly preserved cranial material) from the set of MPTs, the clade comprising *Thalattoarchon* + *Cy. piscosus* + *Cy. 'nichollsi'*

is supported by three additional unambiguous synapomorphies: supratemporal anteromedial extension long (character 22:1); nasal crest in posterior part of the internasal suture present (character 196:1), mediolaterally broad groove bordered by two, anterosposteriorly elongate ridges (a medial one and a lateral one), in the lateral part of the anteromedial process of the postfrontal present (character 197:1); and parietal plateau surrounding the pineal foramen laterally and dorsally present (character 198:1).

It was possible to score 69 morphological characters for both *Cy. piscosus* and *Cy. 'nicholllsi'*. However, the only character which was possible to score for both *Cy. piscosus* and *Cy. 'nicholllsi'*, which was scored differently for both taxa, was character 41: parietal-frontal suture inter-digitation. This character was scored as absent (0) for *Cy. piscosus* and scored as present (1) for *Cy. 'nicholllsi'* (see Appendix 3).

Phylogenetic position of *Gen. et sp. nov. A* and *Gen. et sp. nov. B.* *Gen. et sp. nov. A* and *Gen. et sp. nov. B* are recovered as early diverging parvipelvians more derived than *Macgowania janiceps*, and as successive outgroups to the clade comprising (*Hudsonelipidia*, (*Malawania*, Neoichtyosauria)) (Fig. 5.5). The clade comprising *Gen. et sp. nov. A* and all other Parvipelvia, excluding *Macgowania* (node A in Fig. 5.5), receives weak nodal support (decay index = 1), but is supported by one unambiguous synapomorphy: maxilla dorsal lamina absent (character 4:0; the maxilla dorsal lamina is present in *Macgowania janiceps* [TMP 2009.121.1], contra character score in Jiang et al. [2016]). The clade comprising *Gen. et sp. nov. B* and (*Hudsonelpidia*, (*Malawania*, Neoichthyosauria)) (node B in Fig. 5.5) also receives weak nodal support (decay index = 1), but is supported by one unambiguous synapomorphy: humerus distal:proximal width ratio - wider distally (character 96:1).

DISCUSSION

Synapomorphies uniting *Cymbospondylus* and *Thalattoarchon*. Personal examination of all well-preserved cranial specimens of *Cymbospondylus* (Chapter 4) and comparisons with the type skull of *Thalattoarchon saurophagis* (FMNH PR 3032) have revealed that both taxa share a set of anatomical characters, to the exclusion of all other ichthyopterygians (characters 22:1, 196:1, 197:1, 198:1, 199:1;

see Results). This suggests a sister-group relationship between both taxa. However, because no well-preserved cranial material of *Xinminosaurus* has been described to date, it is not possible to determine whether the synapomorphies uniting *Cymbospondylus* and *Thallatoarchon* were also present in *Xinminosaurus*. As a result, I refrain from erecting a new systematic unit for the clade comprising *Cymbospondylus* + *Thalattoarchon*, until more complete cranial material of *Xinminosaurus* becomes available.

The results of the phylogenetic analysis provide additional support that Cymbospondylidae was an ecomorphologically diverse clade, comprising small-bodied (body length ~2.5 m), durophagous forms (*Xinminosaurus*), as well as colossal, apex predators (*Cymbospondylus*, *Thalattoarchon*; body length ~10 m). Because all currently known taxa comprising Cymbospondylidae are stratigraphically restricted to the middle Anisian (Middle Triassic), this indicates that early-diverging ichthyosaurs underwent a 10-fold increase in body size and became ecologically diverse in as many as three–four million years since their first appearance in the fossil record (Motani et al., 2014), which suggests rapid ecomorphological evolution in basal ichthyosaurs. This is in line with the results of a recent study, which proposed very high rates of morphological evolution in early-diverging ichthyosaurs, compared with those of derived members of the clade (Motani et al., 2017). However, because of a scarcity of ichthyosaurs fossils from the lower Anisian, it is not possible to determine whether ichthyosaurs achieved this high ecomorphological diversity in the middle Anisian or earlier. Further discoveries of ichthyosaurs from the early Anisian are needed to answer this question. Because ichthyosaurs were important predators in Mesozoic marine ecosystems and predator diversity is a good proxy for assessing ecosystem complexity (Scheyer et al., 2014), future studies of the tempo and mode of ecomorphological evolution in ichthyosaurs from the Early–Middle Triassic are encouraged in order to obtain a better understanding of the pattern and process of marine ecosystem recovery after the Permian–Triassic extinction event.

Taxonomic status of *Cy. 'nichollsi'*. Out of 69 characters that were possible to score for both *Cy. piscosus* and *Cy. 'nichollsi'*, only one character was scored differently for both taxa – the parietal-frontal suture interdigitation (character 41) was scored as absent for *Cy. piscosus* and as present for *Cy.*

'nichollsi'. However, as discussed in Chapter 4, the degree of suture interdigitation in the skull roof of some fossil reptiles has been demonstrated to decrease throughout ontogeny (Ezcurra et al., 2015). Because the holotype of *Cy. 'nichollsi'* (FMNH PR 2251) is smaller than the specimens of *Cy. piscosus*, in which the fronto-parietal suture does not interdigitate (UCMP 9950, UCMP 9913), this suggests that FMNH PR 2251 could be an osteologically immature specimen of *Cy. piscosus*. Therefore, in the absence of any other morphological characters differentiating FMNH PR 2251 from *Cy. piscosus* and taking into account the geographical and temporal proximity of FMNH PR 2251, UCMP 9950 and UCMP 9913, I designate FMNH PR 2251 as a referred specimen of *Cy. piscosus* (see Chapter 4).

Palaeoecology and early evolution of basal parvipelvian ichthyosaurs from Williston Lake. The Late Triassic Pardonet Formation outcrops of the Williston Lake area represent the stratigraphically oldest occurrences of parvipelvian ichthyosaurs in the world (McGowan, 1997; Motani, 1999a). Up until now, only two such parvipelvians were recognized from Williston Lake and nearby localities: *Macgowania janiceps* from the middle Norian (McGowan, 1996, 1997; Motani, 1999a) and *Hudsonelpidia brevirostris* from the lower Norian (McGowan, 1995a, 1997; Motani, 1999a). For two decades, these taxa have been the only source of information on the early evolution of Parvipelvia. In Chapter 3, I report a third parvipelvian from Williston Lake, *Gen. et sp. nov. B*. The large body size of *Gen. et sp. nov. B* (estimated body length exceeding 6.5 metres; see below) and bicarinate teeth suggest, for the first time, the presence of apex predators amongst basal representatives of Parvipelvia (discussed below).

The available material of Late Triassic basal parvipelvians is very incomplete and/or poorly preserved (McGowan, 1995a, 1996, 1997; Henderson, 2015; Chapter 3). Because of this, their ecology is poorly understood, and a comprehensive, quantitative palaeoecological analysis is not possible. However, some conclusions can be drawn from a qualitative assessment of their tooth morphology and body size. No dentition is preserved in the known specimens of *Hudsonelpidia brevirostris* (McGowan, 1995a, 1997), but teeth are preserved in two specimens of *Macgowania janiceps* (ROM 41992, TMP 2009.121.1) and the type specimen of *Gen. et sp. nov. B* (ROM 44295). The dentition of *Macgowania janiceps* resembles that of 'typical' ichthyosaurs (e.g. McGowan and Motani, 2003), in that the tooth

crowns are labiolingually recurved, conical, with a pointed apex. Similar dentition is present in *Stenopterygius*, an Early Jurassic ichthyosaur that is known from fossilised stomach contents to have preyed on cephalopods and fish (e.g. Böttcher, 1989; Dick et al., 2016). In contrast, *Gen. et sp. nov. B* has labiolingually flattened, bicarinate crowns, which have also been reported for other, large-bodied ichthyosaurs (*Cymbospondylus* sp. [e.g. PIMUZ T 39, UCMP 9950, UCMP 9913], *Thalattoarchon saurophagis* [FMNH PR 3032; Fröbisch et al., 2013], *Himalayasaurus tibetensis* [Motani et al., 1999a] and *Temnodontosaurus platyodon* [e.g. ROM 7972; McGowan, 1994]. These have generally been interpreted as indicating a macropredatory (apex predator) lifestyle (e.g. Massare, 1987). Such an interpretation is supported by the discovery of *Stenopterygius* remains in the gut contents of a specimen of a large-bodied ichthyosaur with bicarinate crowns, *Temnodontosaurus trigonodon* (SMNS 50000; Böttcher, 1989).

Body size is known to affect various aspects of organismal biology, including their metabolic rate, reproduction and feeding ecology (e.g. Brown, 1997; West et al., 2002), so studying the body size range of basal parvipelvians can provide additional information regarding their ecological diversity. *Hudsonelpidia brevisotris* was estimated to have a total body length of ~1 m (McGowan, 1995a), whereas *Macgowania janiceps* has an estimated body length of ~3 m (McGowan, 1996). Although the type specimen of *Gen. et sp. nov. B* is very incomplete, its body size can be estimated from the available forefin material. Martin et al. (2015) established a statistical relationship between radius size and fork length (length measured from tip of rostrum to the tail bend) for Late Triassic non-parvipelvian ichthyosaurs and Early Jurassic parvipelvians. Because the phylogenetic analysis recovered *Gen et sp. nov. B* as a basal parvipelvian, it is likely that its body proportions were similar to those of the majority of the ichthyosaurs covered by the dataset of Martin et al. (2015) and different to thunnosaurians, characterized by a shortened tail (e.g. Maisch and Matzke, 2000a). Using the equations of Martin et al., (2015) for both radius anteroposterior length and radius proximodistal height, a fork length of ~6.5 metres is obtained for ROM 44295. The estimated body size range of Late Triassic parvipelvians (1.5 metres in *Hudsonelpidia brevirostris* to 6.5 metres in *Gen. et sp. nov. B*) is therefore similar to that of parvipelvians from the earliest Jurassic (Hettangian–Pliensbachian) of the United Kingdom (1.5 metres

in *Ichthyosaurus breviceps* and *Ichthyosaurus conybeari* [e.g. McGowan and Motani, 2003] to up to 10 metres in *Temnodontosaurus platyodon* [NHMUK PV R2003; McGowan, 1996]).

At present, it is not clear whether attaining such a disparate morphological and body size range in basal parvipelvians occurred gradually or rapidly. None of the currently described basal parvipelvian taxa from Williston Lake co-occur in the same horizons, and there is a significant temporal gap of ~7 million years between the occurrence of the small-bodied *Hudsonelpidia brevirostris* (*quadrata* conodont biozone, lower Norian) and the occurrence of the large-bodied *Gen. et sp. nov. B* (*bidentata* conodont biozone, upper Norian; Gradstein et al., 2012). This seems to suggest prolonged evolution of large body size in basal parvipelvians. However, undocumented middle Norian horizons at Williston Lake, preserve medium-sized (cf. *Macgowania*) and large-bodied (cf. *Gen. et sp. nov. B*) ichthyosaurs together (R. Motani, pers. comm., Oct 2016). Furthermore, a recently explored Pardonet Formation outcrop, located on a steep slope in the southern bank of the Graham River in British Columbia, Canada, has yielded a referred specimen of *Macgowania janiceps* (TMP 2009.121.1) and the heavily eroded remains of another, large-bodied ichthyosaur (Henderson, 2015). This large ichthyosaur was tentatively assigned to *Shonisaurus* sp. by Henderson (2015), based on its large body size. However, cranial and jaw fragments found at the bottom of the same cliff, where both specimens were found, preserve dentition, which is strikingly similar to that described for *Gen et sp. nov. B* - the tooth crowns have a smooth or subtly ridged surface and possess mesial and distal carinae (Fig. 5.6). Furthermore, the teeth are closely packed, with no transverse alveolar walls separating the tooth bases. This is similar to the condition in parvipelvian ichthyosaurs, but different from shastasaurids (including *Shonisaurus*), where the teeth are set in sockets with clearly demarcated transverse walls (e.g. Ji et al., 2016: character 59). Even though no stratigraphic information was recorded for TMP 2009.121.1 or TMP 2009.121.2, the presence of *Macgowania janiceps* strongly indicates a middle Norian age (remains of *Macgowania janiceps* were recovered only from middle Norian horizons at Williston Lake; R. Motani, pers., comm., Oct 2016). This provides further evidence that the ecological diversity of basal parvipelvians was already high at least by the middle Norian. It is possible that basal parvipelvian ichthyosaurs underwent a Norian adaptive radiation soon after their first appearance in the fossil record, as a result of exploration

of new open-water habitats, devoid of other marine reptiles. However, this hypothesis needs to be corroborated by additional ichthyosaur fossils from the Norian, as well as model-based approaches to studying the tempo and mode of ichthyosaur morphological evolution.

Ichthyosaur turnover across the Triassic–Jurassic boundary. The Triassic–Jurassic extinction event is widely recognised as one of the 'big-five' extinction events in Earth's history (e.g. Hallam and Wignall, 1997). The end-Triassic extinction event is associated with major shifts in the faunal composition of both terrestrial and marine ecosystems. On land, crurotarsan-dominated faunas became extinct by the end of the Triassic, and were replaced by ornithodiran-dominated faunas in the earliest Jurassic (e.g. Irmis et al., 2011). In marine ecosystems, many groups of invertebrates show major turnovers at the end of the Triassic, and many groups of marine tetrapods, including placodonts and thalattosaurs became extinct by the end of the Triassic (e.g. Bardet, 1994; Hallam and Wignall, 1997). Recently, it was proposed that the Triassic–Jurassic extinction event had a particularly severe effect on the evolution of ichthyosaurs, causing a profound extinction of all groups of ichthyosaurs, except the Parvipelvia, which underwent an adaptive radiation at, or very close to, the Triassic–Jurassic boundary (Thorne et al., 2011; Fischer et al., 2013). However, little is directly known about the Triassic–Jurassic transition during ichthyosaur evolution. Although fragmentary remains from Rhaetian (Late Triassic) bonebeds in Europe indicate the survival of non-parvipelvian ichthyosaur lineages until the latest Triassic (e.g. Storrs, 1994; Fischer et al., 2014a), sampling of Late Triassic ichthyosaurs is dominated by occurrences from the Carnian.

The Late Triassic constitutes more than half of the total duration of the entire Triassic period (duration of ~35.7 million years, compared to a duration of ~50.6 million years for the entire Triassic; Cohen et al., 2013). However, the majority of Late Triassic ichthyosaur fossils come from horizons spanning the Carnian (~237–227 million years ago), with very few ichthyosaur fossils from the Norian–Rhaetian interval (~227–201.3 million years ago; McGowan and Motani, 2003). This incomplete sampling of the global Norian–Rhaetian fossil record of marine tetrapods hinders our understanding of ichthyosaur evolutionary dynamics at the Triassic–Jurassic boundary (e.g. Benson et al., 2010). Thorne et al., (2011) suggested that ichthyosaurs underwent a substantial decrease in morphological disparity

and taxonomic diversity at, or very close to, the Triassic–Jurassic boundary. However, this conclusion resulted from a direct comparison of diversity and disparity in an Early Jurassic time bin, represented by the diverse and well-sampled ichthyosaur faunas from the earliest Jurassic of England and Germany, to a Late Triassic time bin, which was heavily biased by data from the Carnian, so approximately 36 million years before the Triassic–Jurassic extinction event. Therefore, Thorne et al. (2011) do not provide conclusive evidence for a catastrophic turnover of ichthyosaurs during the end-Triassic extinction event, and additional data on Norian and Rhaetian ichthyosaurs are needed to understand the patterns of ichthyosaur extinction and diversification at the Triassic–Jurassic boundary.

The fossil record of Norian ichthyosaurs is very scarce. Ichthyosaurs currently recognized from Norian strata include the basal euichthyosaur or shastasaurid *Callawayia neoscapularis* and the colossal shastasaurid *Shonisaurus sikanniensis* (and likely closely related forms) from the middle Norian of the Pardonet Formation (McGowan, 1994, 1997; Nicholls and Manabe, 2001, 2004), the putative giant shastasaurid *Himalayasaurus tibetensis* from the lower–middle Norian of Tibet (Dong, 1972; Motani et al., 1999a) and the basal parvipelvians *Macgowania janiceps* and *Hudsonelpidia brevirostris* from the middle and lower Norian, respectively, of the Pardonet Formation (McGowan, 1995a, 1996, 1997; Motani, 1999a; Henderson, 2015). Previously, only fragmentary ichthyosaur remains have been reported from the upper Norian, both from the Kössen Formation - an isolated centrum of a giant shastasaurid from Bavaria, Germany (Karl et al., 2014) and a fragmentary skeleton of a giant shastasaurid from Graubünden, Switzerland (Callaway, 1989). *Gen. et sp. nov. B* is the first relatively complete ichthyosaur known from the upper Norian and helps bridge a ~16 million year gap between the middle Norian ichthyosaurs of the Pardonet Formation and the taxonomically and ecologically diverse ichthyosaur fauna from the Early Jurassic (Hettangian–Pliensbachian) of the United Kingdom, the first ichthyosaur fauna post-dating the Triassic–Jurassic boundary (Fig. 5.7). *Gen. et sp. nov. B* demonstrates that large-bodied parvipelvian ichthyosaurs were already present by the upper Norian (with their first occurrence probably extending at least to the middle Norian, as evidenced by TMP 2009.121.2; Fig. 5.6), and that the ecological diversity of parvipelvian ichthyosaurs in the middle and

upper Norian was comparable to that seen in the earliest Jurassic ichthyosaur faunas of the United Kingdom (see above).

Because the basal parvipelvians of the Pardonet Formation are not nested within Neoichthyosauria (last common ancestor of *Temnodontosaurus* and *Ophthalmosaurus icenicus*, and all its descendants [Sander, 2000; Maisch and Matzke, 2000a]), the possibility of a profound extinction of basal parvipelvians in the latest Triassic (upper Norian–Rhaetian), and a subsequent diversification of Neoichthyosauria in the aftermath of this extinction (Fischer et al., 2013), cannot be excluded. However, several lines of evidence suggest a different scenario for ichthyosaur turnover at the Triassic–Jurassic boundary. A recent re-description of historical ichthyosaur material from the Rhaetian of France (Fischer et al., 2014a), indicates that shastasaurid and possibly other non-parvipelvian ichthyosaur taxa were still present in the latest Triassic, co-occurring with parvipelvians (Mears et al., 2016) and the discovery of a putative giant shastasaurid radius from the Early Jurassic of the United Kingdom (Martin et al., 2015) shows that shastasaurids might have survived until the earliest Jurassic.

Furthermore, the phylogenetic analysis presented in this chapter recovers *Gen. et sp. nov. A* as an early-diverging parvipelvian, making it the only currently-known non-neoichthyosaurian from the Lower Jurassic (Fig. 5.7). This implies that an early-diverging parvipelvian ghost lineage extending from the Carnian–Norian, remains undetected in the Late Triassic fossil record. *Malawania anachronus* from the Hauterivian–Barremian (Early Cretaceous; Fischer et al., 2013), which was previously recovered as the sister taxon to *Ichthyosaurus*, is recovered as the sister taxon of Neoichthyosauria in the phylogenetic analysis presented here (Figs 5.5, 5.7; Jiang et al., [2016] recovered *M. anachornus* in the same position in their analysis). This suggests that lineages of early-diverging parvipelvians could have survived as late as the Early Cretaceous. However, the conflicting position recovered for *M. anachronus* by Fischer et al. (2013) and Jiang et al. (2016), and the low nodal support values recovered for the majority of nodes within Parvipelvia in the phylogenetic anaylsis presented in this chapter (Figs 5.5, 5.7) encourage further studies of ichthyosaur relationships, focusing on the Triassic–Jurassic boundary.

Together, these findings raise the possibility that ichthyosaur turnover across the Triassic–Jurassic boundary was not catastrophic, as suggested by Thorne et al. (2011) but rather mosaic, and more similar to the gradualistic or stepwise extinction pattern of other Late Triassic marine tetrapods and invertebrates (e.g. Benson et al., 2012; Fischer et al., 2014a). This hypothesis is in line with the hypothesis of Motani (2008), who suggested that the Triassic extinctions of some ichthyosaur lineages, adapted to shallow-water environments (e.g. durophagous forms), were likely related to falling sea levels, which reduced the availability of near-shore environments which these ichthyosaurs inhabited, and occurred over a prolonged period of time. Derived (parvipelvian) ichthyosaurs, adapted to life in the open ocean, remained unaffected by these changes in sea level. This hypothesis was recently supported by the studies of Benson and Butler (2011) and Kelley et al. (2014), who quantitatively determined that the diversity of shallow-marine tetrapods in the Late Triassic was largely determined by changes in sea level. The discovery of large-bodied, early-diverging parvipelvian ichthyosaurs from the latest Triassic (*Gen et sp. nov. B*; Chapter 3) and late-surviving basal parvipelvians from the Early Jurassic (*Gen. et sp. nov. A*; Chapter 1) provides additional evidence in support of this hypothesis. Further remains of Norian and Rhaetian ichthyosaur fossils, and a continued revision of the ichthyosaur faunas of the earliest Jurassic, will undoubtedly help to further elucidate the pattern and process of ichthyosaur turnover across the Triassic–Jurassic boundary.

FIGURES

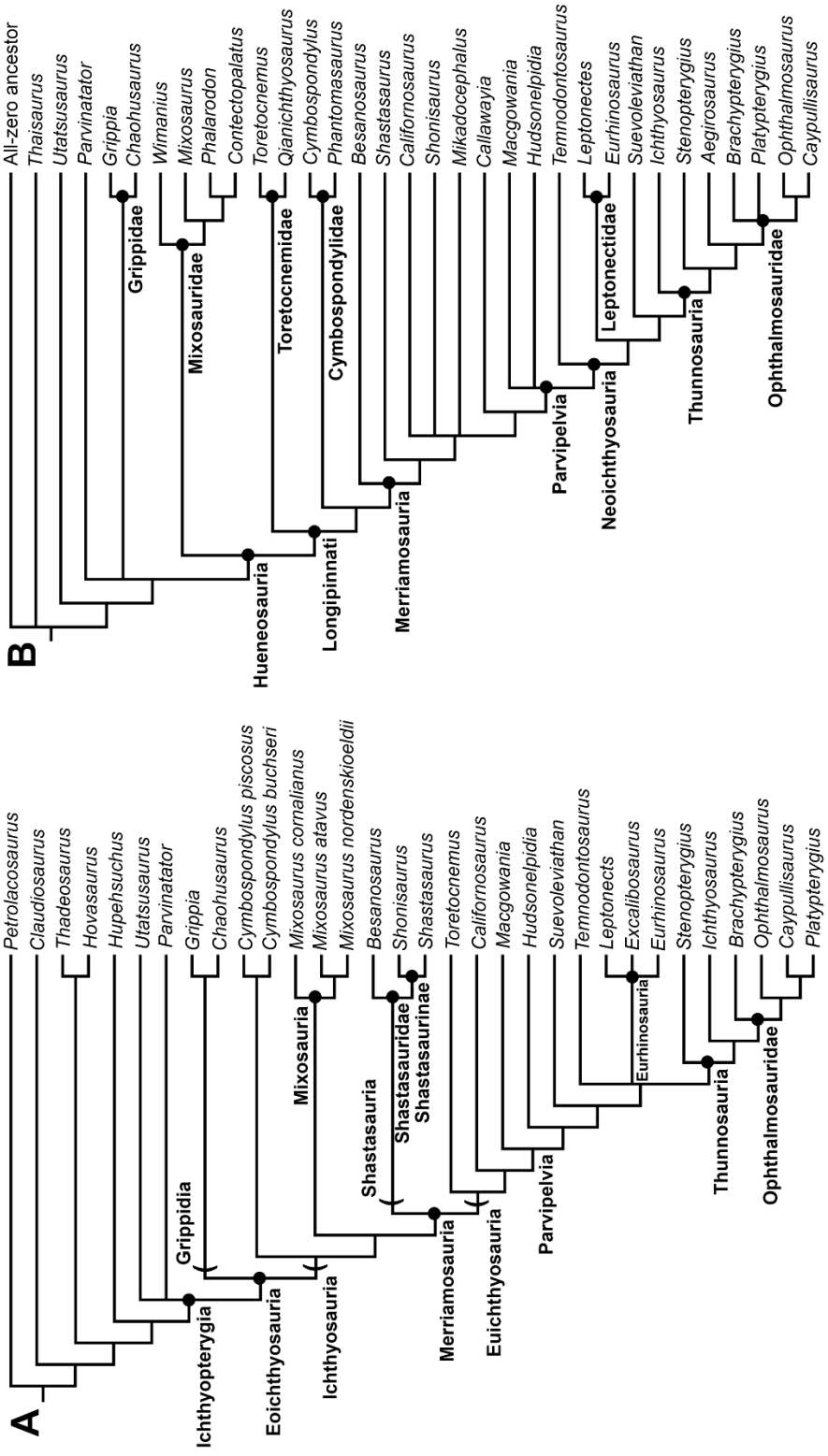

FIGURE 5.1. Results of previous, large-scale phylogenetic analyses of Ichthyopterygia. (**A**) after Motani, 1999a; (**B**) after Maisch and Matzke, 2000a.

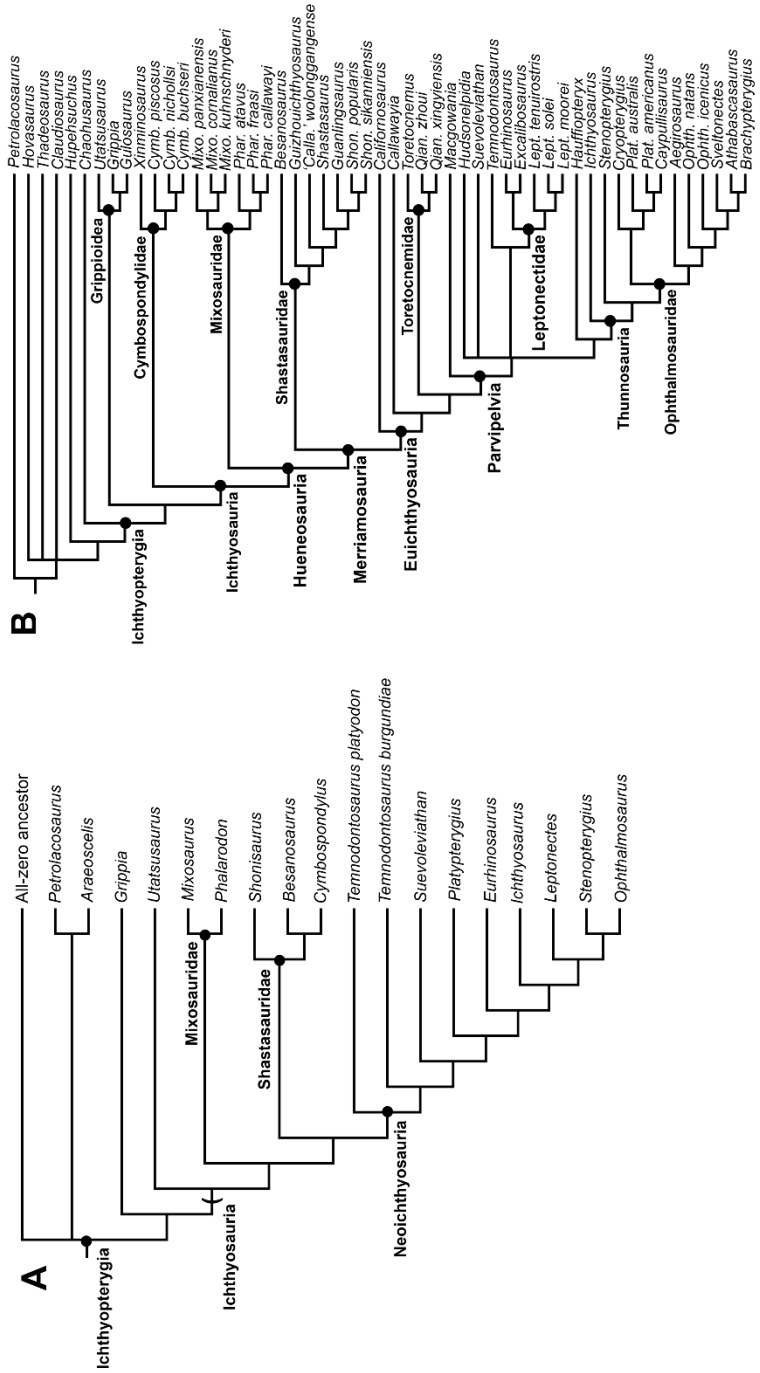

FIGURE 5.2. Results of previous, large-scale phylogenetic analyses of Ichthyopterygia. (**A**) after Sander, 2000; (**B**) after Ji et al., 2016. Abbreviations: *Calla.*, *Callawayia*; *Cymb.*, *Cymbospondylus*; *Lept.*, *Leptonectes*; *Mixo.*, *Mixosaurus*; *Ophth.*, *Ophthalmosarus*; *Phar.*, *Phalarodon*; *Plat.*, *Platypterygius*; *Qian.*, *Qianichthyosaurus*; *Shon.*, *Shonisaurus*.

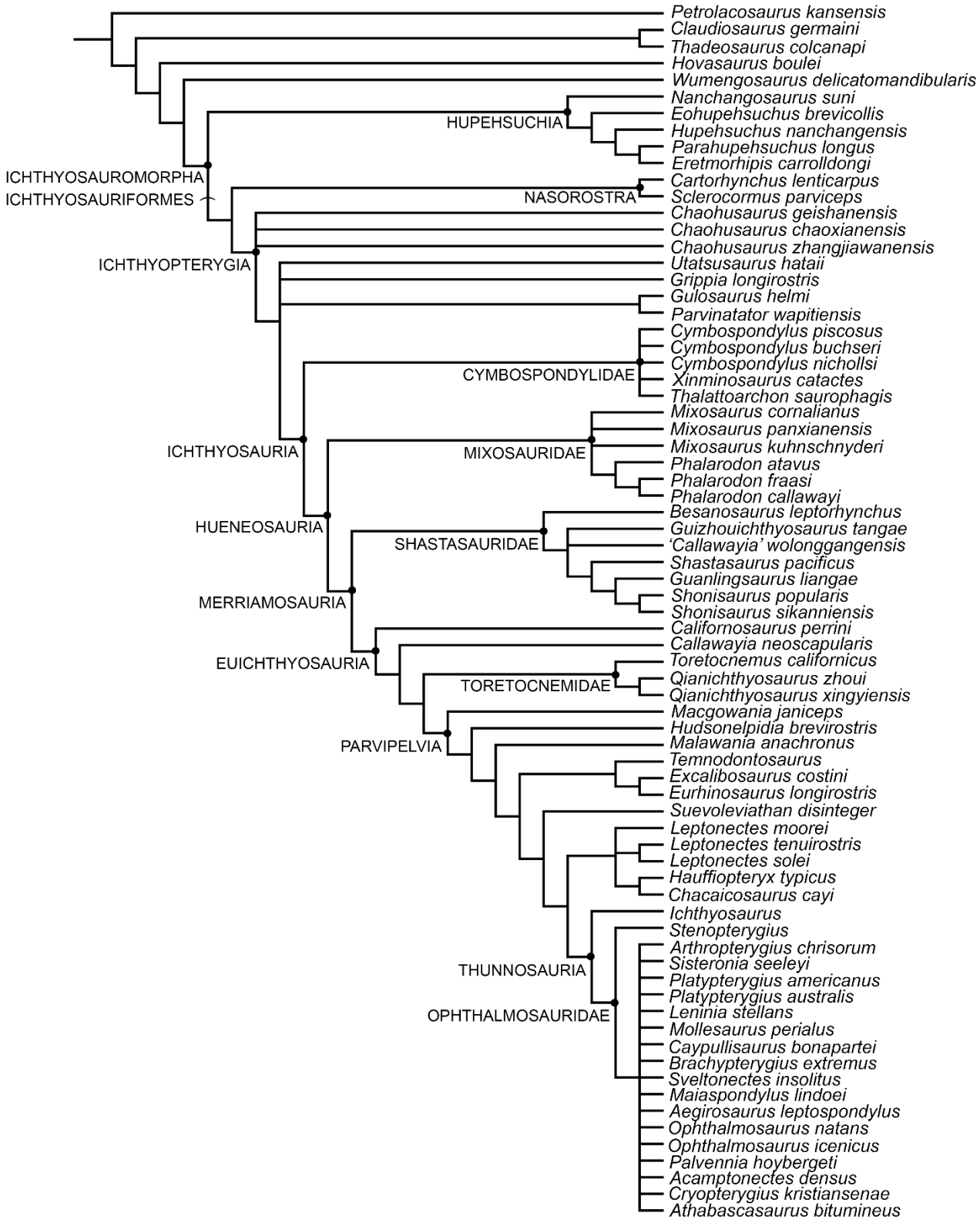

FIGURE 5.3. Strict consensus cladogram from the phylogenetic analysis of Ichthyopterygia performed by Jiang et al. (2016), based on an expanded and modified version the Ji et al. (2016) dataset (compare with Fig. 5.2B).

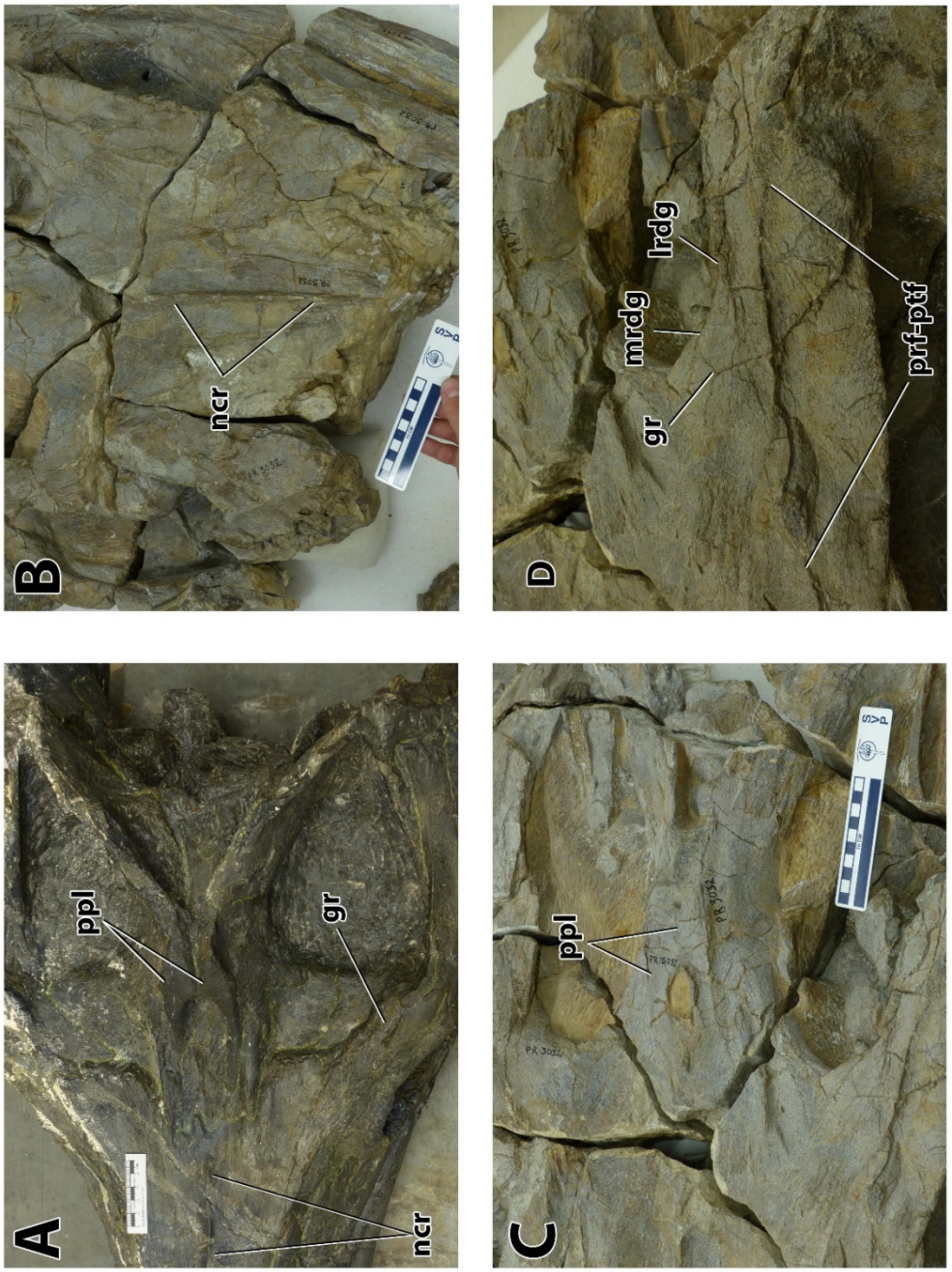

FIGURE 5.4. Comparison of skull roof anatomy of *Cymbospondylus piscosus* (**A**; UCMP 9950) and *Thalattoarchon saurophagis* (**B–D**; FMNH PR 3032), illustrating the new morphological characters incorporated into the Jiang et al. (2016) dataset. (**A)**, dorsal view; (**B)**, anterodorsal view; (**C)** and (**D)**, dorsolateral view. Abbreviations: **gr**, lateral groove on postfrontal; **lrdg**, lateral ridge; **mrdg**, medial ridge; **ncr**, nasal crest; **prf-ptf**, prefrontal-postfrontal suture; **ppl**, parietal plateau.

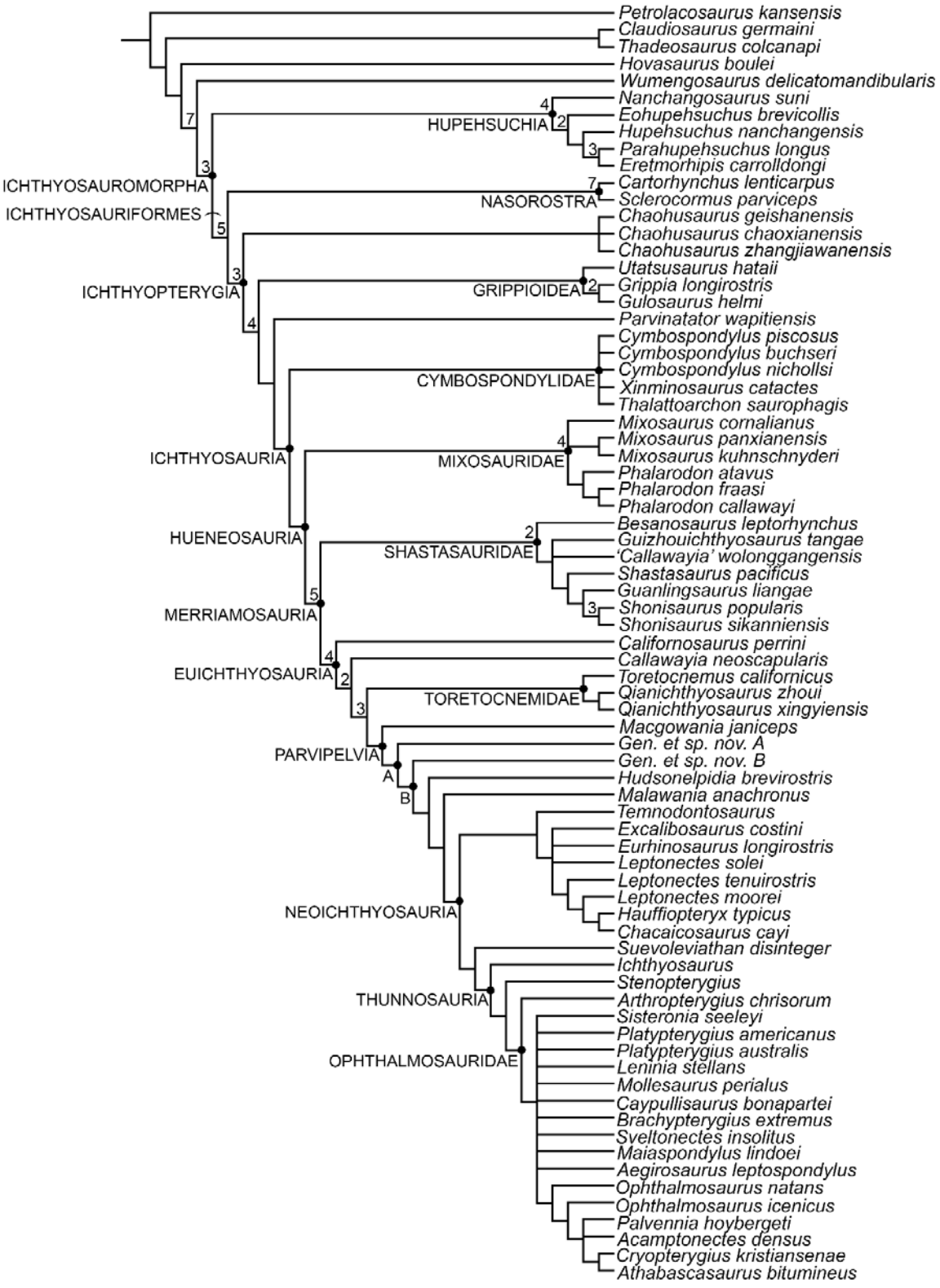

FIGURE 5.5. Strict consensus of 45 MPTs (671 steps, CI = 0.359, RI = 0.788) obtained from parsimony analysis of the modified data set of Jiang et al. (2016). Numbers above nodes indicate Bremer support values >1.

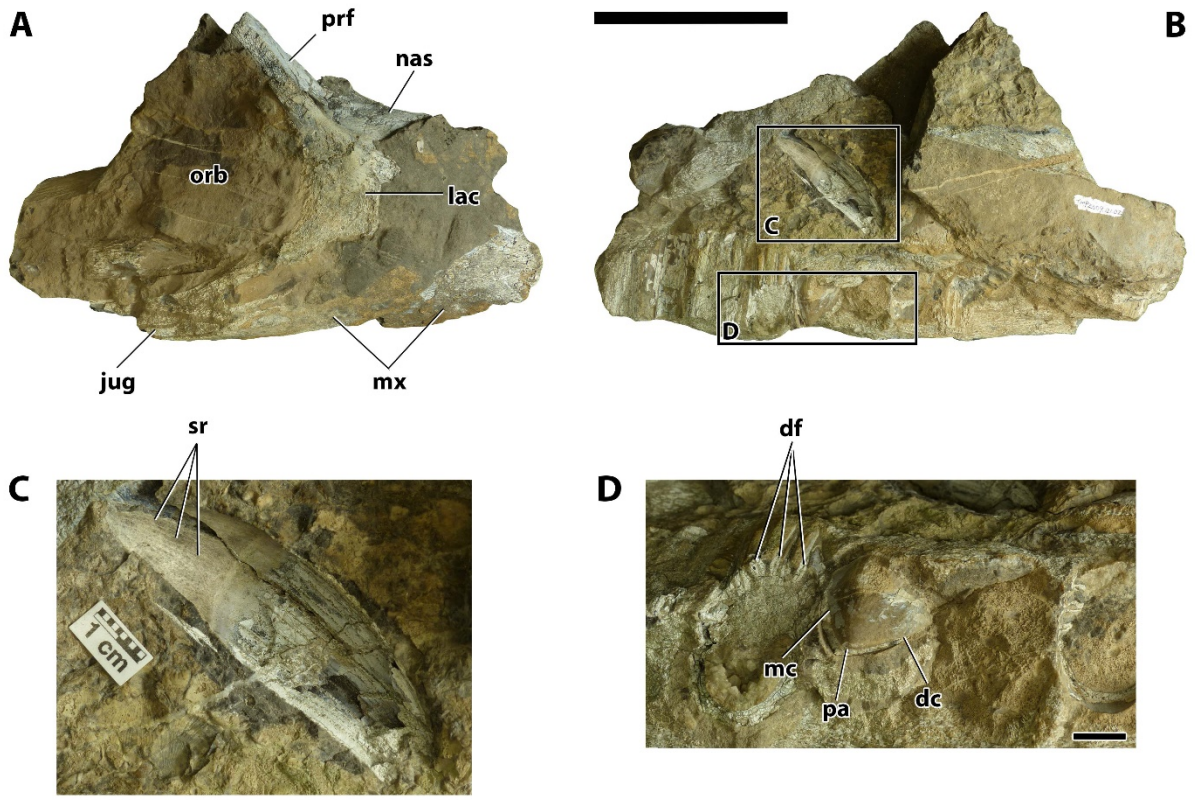

FIGURE 5.6. TMP 2009.121.2, a fragmentary antorbital region and associated teeth of cf. *Gen. et sp. nov. B* (compare with Fig. 3.2 in Chapter 3). **A**, right lateral view; **B**, medial view; **C**, close-up of one tooth impression; **D**, tooth in apical view. Abbreviations: **dc**, distal carina; **df**, dentine folds; **jug**, jugal; **lac**, lacrimal; **nas**, nasal; **mc**, mesial carina; **mx**, maxilla; **orb**, orbit; **prf**, prefrontal; **sr**, subtle ridges. Scale bar equals 10 cm in **A**, **B** and 10 mm in **C**, **D**.

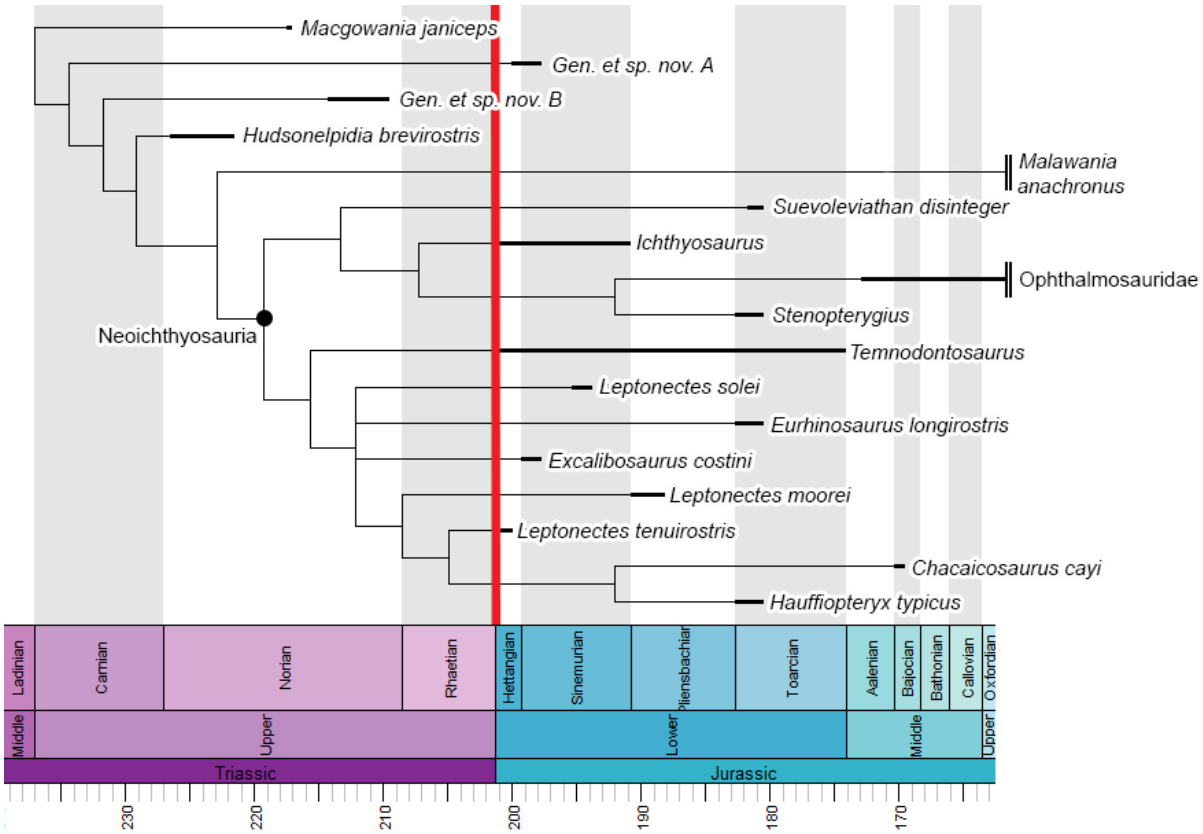

FIGURE 5.7. Time-calibrated part of the strict consensus cladogram resulting from the phylogenetic analysis of Ichthyopterygia (see Fig. 5.5), depicting phylogenetic relationships of parvipelvian ichthyosaurs and focused on the Late Triassic–Early Jurassic interval. Vertical red line indicates Triassic–Jurassic boundary. Note that *Gen. et sp. nov. B* bridges a nearly 16 million-year temporal gap between the middle Norian *Macgowania janiceps* and ichthyosaurs from the earliest Jurassic of the United Kingdom. *Gen. et sp. nov. A* is the only currently-known non-neoichthyosaurian from the Early Jurassic. All nodes depicted in this part of the cladogram are weakly supported (Bremer value = 1). The stratigraphic position of *Malawania anachronus* (Hauterivian–Barremian, Early Cretaceous) and derived ophthalmosaurids (extending to the upper Cenomanian, Late Cretaceous) were omitted for clarity. See Appendix 4 for details of time calibration method.

CHAPTER 6: CONCLUSIONS

- The true diversity of Lower Jurassic ichthyosaurs from the Blue Lias Formation (Hettangian–Sinemurian) of the United Kingdom is shown to have been underestimated, in concert with some previous studies. This is evidenced by the new genus and species of ichthyosaur described in Chapter 2. The new taxon is defined on the basis of well-defined, discrete character states, and encourages revision of other ichthyosaur taxa from the Lower Jurassic of England, in order to get a full appreciation of their taxonomic diversity. A phylogenetic analysis places the new taxon as an early-diverging parvipelvian outside of Neoichthyosauria, and suggests a mosaic, rather than the recently proposed catastrophic turnover of ichthyosaurs across the Triassic-Jurassic boundary. This stresses the need for detailed studies of Late Triassic and Early Jurassic ichthyosaur anatomy for a better understanding of their evolution during this time interval.

- A new taxon of basal parvipelvian ichthyosaur from the Late Triassic (upper Norian) of Williston Lake, British Columbia, Canada is described in Chapter 3. This specimen, which represents a large-bodied, macropredatory taxon, demonstrates that Parvipelvia were already ecologically diverse at the beginning of their evolutionary history. A fragmentary specimen of a similar taxon from the middle Norian of a nearby locality in British Columbia, Canada, indicates that large-bodied, macropredatory parvipelvians were already present in the middle Norian. This indicates that the high ecological diversity of parvipelvians was maintained throughout the Late Triassic, and does not agree with recently proposed scenarios of a severe effect of the end-Triassic extinction event on ichthyosaur evolution. Because of the incomplete sampling of the global Late Triassic marine fossil record, fieldwork in marine horizons of the Late Triassic is encouraged to provide new data on ichthyosaur evolution at the end of the Triassic.

- A re-examination of the cranial anatomy of *Cymbospondylus* (Chapter 4) resolves a nearly 100-year controversy surrounding the arrangemenet of cranial bones in this genus. This new information allows to determine that there are no significant differences in the cranial anatomy of the three species of *Cymbospondylus* erected on the basis of well-preserved material. Minor differences in the postcranial anatomy of the type species, *Cy. piscosus*, and *Cy. 'nicholllsi'* allow referral of the type specimen of *Cy. 'nicholllsi'* as a referred specimen of *Cy. piscosus*. Comparison of the cranial anatomy of *Cy. piscosus* with that of *Thalattoarchon saurophagis* leads to the identification of four features shared exclusively between the two taxa, and not present in any other ichthyosaurs: a posterior internasal crest; a parietal plateau; a groove on the dorsolateral surface of the anteromedial process of the postfrontal; and a prefrontal forming the entire dorsal margin of the orbit. These characters suggest a close phylogenetic relationship between the two taxa and indicate that Cymbospondylidae was the first diverse clade of ichthyosaurs, attaining great ecomorphological disparity by the Early Middle Triassic. This provides an interesting opportunity for future studies of the tempo and mode of body-size and ecomorphological evolution of ichthyosaurs throughout the Triassic, in order to establish the pattern and process of marine ecosystem regeneration after the end-Permian mass extinction.

- Incorporation of the new information on ichthyosaur anatomy obtained from description and re-description of important ichthyosaur taxa (Chapter 5) allows for a better understanding of ichthyosaur evolutionary dynamics in times of profound changes to the Earth system – in the aftermath of the end-Permian mass extinction and across the Triassic-Jurassic boundary. However, the low nodal support recovered in the phylogenetic analysis for parvipelvian clades necessitates further studies of their phylogenetic position, in order to obtain a better understanding of their evolution.

REFERENCES

ANDREWS, C. W. 1910. *A Descriptive Catalogue of the Marine Reptiles of the Oxford Clay. Part I.* Trustees of the British Museum, London, XXIV + 205 pp.

AMBROSE, K. 2001. The lithostratigraphy of the Blue Lias Formation (Late Rhaetian–Early Sinemurian) in the southern part of the English Midlands. *Proceedings of the Geologists' Association,* **112**(2), 97–110.

APPLEBY, R. M. 1956. The osteology and taxonomy of the fossil reptile *Ophthalmosaurus*. *Proceedings of the Zoological Society of London*, **126**, 403–447.

APPLEBY, R. M. 1979. The affinities of Liassic and other ichthyosaurs. *Palaeontology*, **22**, 921–946.

ARKHANGELSKY, M. S., and ZVERKOV, N. G. 2014. On a new ichthyosaur of the genus *Undorosaurus*. *Proceedings of the Zoological Institute of the Russian Academy of Sciences*, **318**, 187–196.

BAILLEUL, A. M., SCANELLA, J. B., HORNER, J. R., and EVANS, D. C. 2016. Fusion patterns in the skulls of modern archosaurs reveal that sutures are ambiguous maturity indicators for the Dinosauria. *PLoS ONE*, **11**(2), e0147687.

BARDET, N. 1994. Extinction events among Mesozoic marine reptiles. *Historical Biology*, **7**(4), 313–324.

BARDET, N., and FERNÁNDEZ, M. S. 2000. A new ichthyosaur from the Upper Jurassic lithographic limestones of Bavaria. *Journal of Paleontology*, **74**, 503–511.

BASSANI, F. 1886. Sui fossili e sull'eta degli schisti bituminosi triasici Besano in Lombardia. Communicazione preliminare. *Atti della Societa Italiana di Scienze Naturale del Museo Civili de Storia Naturale, Milano*, **29**, 15–17.

BELL, M. A., and LLOYD, G. T. 2015. strap: an R package for plotting phylogenies against stratigraphy and assessing their stratigraphic congruence. *Palaeontology*, **58**(2), 379–389.

BENSON, R. B. J. 2013. Marine Reptiles. 267–279. In MacLeod, N., Archibald, J. D., and Levin, P. S. (eds). *Grzimek's Animal Life Encyclopedia, Extinction.* Gale Cengage Learning, Farmington Hills, Michigan. 964 pp.

BENSON, R. B. J., and BUTLER, R. J. 2011. Uncovering the diversification history of marine tetrapods: ecology influences the effect of geological sampling biases. *Geological Society, London, Special Publications*, **358**(1), 191–208.

BENSON, R. B. J., BUTLER, R. J., LINDGREN, J., and SMITH, A. S. 2010. Mesozoic marine tetrapod diversity: mass extinctions and temporal heterogeneity in geological megabiases affecting vertebrates. *Proceedings of the Royal Society of London B: Biological Sciences*, **277**, 829–834.

BENTON, M., and SPENCER, P. S. 1995. *Fossil reptiles of Great Britain.* Geological Conservation Review Series. Chapman and Hall, London, UK, 386 pp.

BERNARD, A., LÉCUYER, C., VINCENT, P., AMIOT, R., BARDET, N., BUFFETAUT, E., CUNY, G., FOUREL, F., MARTINEAU, F., MAZIN, J. M. and PRIEUR, A. 2010. Regulation of body temperature by some Mesozoic marine reptiles. *Science*, **328**(5984), 1379–1382.

BESMER, A. 1947. Die Triasfauna der Tessiner Kalkalpen XVI. Beiträge zur Kenntnis des Ichthyosauriergebisses. *Schweizerische Palaeontologische Abhandlungen*, **65**, 1–21.

BLAINVILLE, H. M. D. DE. 1835. Description de quelques espèces de reptiles de la Californie, précedée de l'analyse d'un système général d'érpetologie et d'amphibiologie. *Nouvelles Annales du Muséum d 'Histoire Naturelle, Paris*, **4**, 233–296.

BLAKE, J. F. 1876. Order Ichthyopterygia. 253–254. In: TATE, R., and BLAKE, J. F. (eds). *The Yorkshire Lias.* J. Van Voorst, London, 475 pp.

BÖTTCHER, R. 1989. Über die Nahrung eines *Leptopterygius* (Ichthyosauria, Reptilia) aus dem süddeutschen Posidonienschiefer (Unterer Jura) mit Bemerkungen über den Magen der Ichthyosaurier. *Stuttgarter Beiträge für Naturkunde B*, **155**, 1–19.

BÖTTCHER, R. 1990. Neue Erkenntnisse über die Fortpflanzungsbiologie der Ichthyosaurier (Reptilia). *Stuttgarter Beiträge für Naturkunde B*, **164**, 1–51.

BOULENGER, G. A. 1904. On a new species of ichthyosaur from Bath. *Proceedings of the Zoological Society of London*, 1904 (**1**), 424–426.

BRINKMANN, W. 1998. Die Ichthyosaurier (Reptilia) aus der Grenzbitumenzone (Mitteltrias) des Monte San Giorgio (Tessin, Schweiz) - neue Ergebnisse. *Vierteljahrsschrift der Naturforschenden Gesellschaft in Zürich*, **143**, 165–177.

BRINKMANN, W. 2004. Mixosaurier (Reptilia, Ichthyosauria) mit Quetschzähnen aus der Grenzbitumenzone (Mitteltrias) des Monte San Giorgio (Schweiz, Kanton Tessin). *Schweizerische Paläontologische Abhandlungen*, **124**, 1–84.

BROWN, J. H. 1997. *Macroecology.* Chicago: University of Chicago Press, 269 pp.

BRUSATTE, S. L., BENTON, M. J., RUTA, M., and LLOYD, G. T. 2008. Superiority, competition, and opportunism in the evolutionary radiation of dinosaurs. *Science*, **321**(5895), 1485–1488.

CAINE, H., and BENTON, M. J. 2011. Ichthyosauria from the Upper Lias of Strawberry Bank, England. *Palaeontology*, **54**(5), 1069–1093.

CALLAWAY, J. M. 1989. *Systematics, Phylogeny, and Ancestry of Triassic Ichthyosaurs.* PhD dissertation, University of Rochester, Rochester, 204 pp.

CALLAWAY, J. M. 1997. Introduction. 3–16. In: CALLAWAY, J. M. and NICHOLLS, E. L. (eds). *Ancient marine reptiles.* Academic Press, 501 pp.

CALLAWAY, J. M., and MASSARE, J. A. 1989. *Shastasaurus altispinus* (Ichthyosauria, Shastasauridae) from the Upper Triassic of the El Antimonio district, northwestern Sonora, Mexico. *Journal of Paleontology*, **63**(6), 930–939.

CALDWELL, M. W. 1996. Ichthyosauria: A preliminary phylogenetic analysis of diapsid affinities. *Neues Jahrbuch für Geologie und Paläontologie-Abhandlungen*, **200**(3), 361–386.

CALDWELL, M. W. 1997. Modified perichondral ossification and the evolution of paddle-like limbs in ichthyosaurs and plesiosaurs. *Journal of Vertebrate Paleontology*, **17**(3), 534–547.

CAMP, C. L. 1980. Large ichthyosaurs from the Upper Triassic of Nevada. *Palaeontographica A*, **170**, 139–200.

CARROLL, R. L. 1981. Plesiosaur ancestors from the Upper Permian of Madagascar. *Philosophical Transanctions of the Royal Society of London B*, **293**(1066), 315–383.

CARROLL, R. L., and DONG, Z. 1991. *Hupehsuchus*, an enigmatic aquatic reptile from the Triassic of China, and the problem of establishing relationships. *Philosophical Transactions of the Royal Society of London B*, **331**(1260), 131–153.

CARTER, J. 1846a. On the occurrence of a new species of *Ichthyosaurus* in the Chalk in the neighbourhood of Cambridge [abstract]. *Report of the British Association for the Advancement of Science*, **15**, 60.

CARTER, J. 1846b. On the occurrence of a new species of *Ichthyosaurus* in the Chalk in the neighbourhood of Cambridge. *London Geological Journal*, **1**, 7–9.

CHEN L. 1985. [Ichthyosaurs from the Lower Triassic of Chao County, Anhui.] *Regional Geology of China*, **15**, 139–146 [in Chinese].

CHEN, X., and CHENG, L. 2003. A new species of large-sized and long-body ichthyosaur from the late Triassic Guanling biota, Guizhou, China. *Geological Bulletin of China*, **22**(4), 228–235 [in Chinese with English abstract].

CHEN, X., CHENG, L., and SANDER, P. M. 2007. A new species of *Callawayia* (Reptilia: Ichthyosauria) from the Late Triassic in Guanling, Guizhou. *Geology in China*, 34, 974–982 [in Chinese with English abstract].

CHEN, X., SANDER, P. M., CHENG, L., and WANG, X. 2013. A new Triassic primitive ichthyosaur from Yuanan, South China. *Acta Geologica Sinica (English Edition)*, **87**(3), 672–677.

CHEN, X., MOTANI, R., CHENG, L., JIANG, D., and RIEPPEL, O. 2014a. The enigmatic marine reptile *Nanchangosaurus* from the Lower Triassic of Hubei, China and the phylogenetic affinities of Hupehsuchia. *PLoS ONE*, **9**(7), e102361.

CHEN, G., JI, C., HUANG, J., ZHANG, R., SUN, Z., Li, Y., SUN, J., and JIANG, D. 2014b. Progress of the scientific excavation on the Early Triassic marine reptile fauna from Majiashan (Chaohu, Anhui Province) and its significance. *China Basic Science*, **5**, 8–14 [in Chinese with English abstract].

CHEN, X., MOTANI, R., CHENG, L., JIANG, D., and RIEPPEL, O. 2014c. A small short-necked hupehsuchian from the Lower Triassic of Hubei Province, China. *PLoS ONE*, **9**(12), e115244.

CHEN, X., MOTANI, R., CHENG, L., JIANG, D., and RIEPPEL, O. 2014d. A carapace-like bony 'body tube' in an Early Triassic marine reptile and the onset of marine tetrapod predation. *PLoS ONE*, **9**(4), e94396.

CHEN, X., MOTANI, R., CHENG, L., JIANG, D., and Rieppel, O. 2015. A new specimen of Carroll's mystery hupehsuchian from the Lower Triassic of China. *PLoS ONE*, **10**(5), e0126024.

CONYBEARE, W. D. 1822. Additional notices on the fossil genera Ichthyosaurus and *Plesiosaurus*. *Transactions of the Geological Society of London*, **1**, 103–123.

COPE, J. C. W., GETTY, T. A., HOWARTH, M. K., MORTON, N., and TORRENS, H. S. 1980. A correlation of Jurassic rocks in the British Isles. Part One: Introduction and Lower Jurassic. *Special Report of the Geological Society of London*, **14**, 1–73.

CURRIE, P. J. 1981. *Hovasaurus boulei*, an aquatic eosuchian from the Upper Permian of Madagascar. *Palaeontologia Africana*, **24**, 99–168.

CUTHBERTSON, R. S., RUSSELL, A. P., and ANDERSON, J. S. 2013a. Reinterpretation of the cranial morphology of *Utatsusaurus hataii* (Ichthyopterygia) (Osawa Formation, Lower Triassic, Miyagi, Japan) and its systematic implications. *Journal of Vertebrate Paleontology*, **33**(4), 817–830.

CUTHBERTSON, R. S., RUSSELL, A. P., and ANDERSON, J. S. 2013b. Cranial morphology and relationships of a new grippidian (Ichthyopterygia) from the Vega-Phroso Siltstone Member (Lower Triassic) of British Columbia, Canada. *Journal of Vertebrate Paleontology*, **33**(4), 831–847.

CUTHBERTSON, R. S., RUSSELL, A. P., and ANDERSON, J. S. 2014. The first substantive evidence of *Utatsusaurus* (Ichthyopterygia) from the Sulphur Mountain Formation (Lower–Middle Triassic) of British Columbia, Canada: a skull roof description in comparison with other early taxa. *Canadian Journal of Earth Sciences*, **51**(2), 180–185.

DAL SASSO, C., and PINNA, G. 1996. *Besanosaurus leptorhynchus* n. gen. n. sp., a new shastasaurid ichthyosaur from the Middle Triassic of Besano (Lombardy, N. Italy). *Paleontologia Lombarda, Nuova Serie*, **4**, 3–23.

DE LA BECHE, H. T., and CONYBEARE, W. D. 1821. Notice of the discovery of a new fossil animal, forming a link between the *Ichthyosaurus* and Crocodile, together with general remarks on the Osteology of the *Ichthyosaurus*. *Transactions of the Geological Society of London*, **5**, 559–594.

DEEMING, D. C., HALSTEAD, L. B., MANABE, M., and UNWIN, D. M. 1993. An ichthyosaur embryo from the Lower Lias (Jurassic: Hettangian) of Somerset, England, with comments on the reproductive biology of ichthyosaurs. *Modern Geology*, **18**, 423–442.

DELAIR, J. B. 1969. A history of the early discoveries of Liassic ichthyosaurs in Dorset and Somerset (1779–1835). *Proceedings of the Dorset Natural History and Archaeological Society*, **90**, 1–9.

DICK, D. G., and MAXWELL, E. E. 2015. The evolution and extinction of the ichthyosaurs from the perspective of quantitative ecospace modelling. *Biology Letters*, **11**(7), 20150339.

DONG Z. 1972. [An ichthyosaur fossil from the Qomolangma Feng region]. 7–10. In YANG, Z., and DONG, Z. (eds.). [Aquatic Reptiles from the Triassic of China.] *Academia Sinica, Institute of Vertebrate Paleontology and Palaeoanthropology, Memoir 9* [in Chinese].

DRUCKENMILLER, P. S., and MAXWELL, E. E. 2010. A new lower Cretaceous (lower Albian) ichthyosaur genus from the Clearwater Formation, Alberta, Canada. *Canadian Journal of Earth Sciences*, **47**(8), 1037–1053.

DRUCKENMILLER, P. S., HURUM, J. H., KNUTSEN, E. M. and NAKREM, H. A. 2012. Two new ophthalmosaurids (Reptilia: Ichthyosauria) from the Agardhfjellet Formation (Upper Jurassic: Volgian/Tithonian), Svalbard, Norway. *Norwegian Journal of Geology*, **92**, 311–339.

EZCURRA, M. D., and BUTLER, R. J. 2015. Post-hatchling cranial ontogeny in the Early Triassic diapsid reptile *Proterosuchus fergusi*. *Journal of Anatomy*, **226**(5), 387–402.

FERNÁNDEZ, M. S. 1994. A new long-snouted ichthyosaur from the Early Bajocian of Neuquén Basin (Argentina). *Ameghiniana*, **31**, 291 – 297.

FERNÁNDEZ, M. S. 1997. A new ichthyosaur from the Tithonian (Late Jurassic) of the Neuquén Basin (Argentina). *Journal of Paleontology*, **71**, 479–484.

FERNÁNDEZ, M. S. 1999. A new ichthyosaur from the Los Molles Formation (Early Bajocian), Neuquén basin, Argentina. *Journal of Paleontology*, **73**, 677–681.

FERNÁNDEZ, M. S. 2007. Redescription and phylogenetic position of *Caypullisaurus* (Ichthyosauria: Ophthalmosauridae). *Journal of Paleontology*, **81**, 368–375.

FERNÁNDEZ, M. S., and MAXWELL, E. E. 2012. The genus *Arthropterygius* Maxwell (Ichthyosauria: Ophthalmosauridae) in the Late Jurassic of the Neuquén Basin, Argentina. *Geobios*, **45**, 535–540.

FERNÁNDEZ, M. S., ARCHUBY, F., TALEVI, M., and EBNER, R. 2005. Ichthyosaurian eyes: paleobiological information content in the sclerotic ring of *Caypullisaurus* (Ichthyosauria, Ophthalmosauria). *Journal of Vertebrate Paleontology*, **25**(2), 330 – 337.

FISCHER, V. 2016. Taxonomy of *Platypterygius campylodon* and the diversity of the last ichthyosaurs. PeerJ, **4**, e2604.

FISCHER, V., GUIOMAR, M., and GODEFROIT, P. 2011a. New data on the palaeobiogeography of Early Jurassic marine reptiles: the Toarcian ichthyosaur fauna of the Vocontian Basin (SE France). Neues Jahrbuch für Geologie und Paläontologie-Abhandlungen, 261(1), 111–127.

FISCHER, V., MASURE, E., ARKHANGELSKY, M. S., and GODEFROIT, P. 2011b. A new Barremian (Early Cretaceous) ichthyosaur from western Russia. *Journal of Vertebrate Paleontology*, **31**(5), 1010–1025.

FISCHER, V., MAISCH, M. W., NAISH, D., KOSMA, R., LISTON, J., JOGER, U., KRÜGER, F. J., PÉREZ, J. P., TAINSH, J. and APPLEBY, R. M. 2012. New ophthalmosaurid ichthyosaurs from the European Lower Cretaceous demonstrate extensive ichthyosaur survival across the Jurassic–Cretaceous boundary. *PLoS ONE*, **7**(1), e29234.

FISCHER, V., APPLEBY, R. M., NAISH, D., LISTON, J., RIDING, J. B., BRINDLEY, S., and GODEFROIT, P. 2013. A basal thunnosaurian from Iraq reveals disparate phylogenetic origins for Cretaceous ichthyosaurs. *Biology Letters*, **9**(4), 20130021.

FISCHER, V., CAPETTA, H., VINCENT, P., GARCIA, G., GOOLAERTS, S., MARTIN, J. E., ROGGERO, D. and VALENTIN, X. 2014a. Ichthyosaurs from the French Rhaetian indicate a severe turnover across the Triassic–Jurassic boundary. *Naturwissenschaften*, **101**(12), 1027–1040.

FISCHER, V., ARKHANGELSKY, M. S., USPENSKY, G. N., STENSHIN, I. M. and GODEFROIT, P. 2014b. A new Lower Cretaceous ichthyosaur from Russia reveals skull shape conservatism within Ophthalmosaurinae. *Geological Magazine*, **151**(1), 60–70.

FISCHER, V., BARDET, N., GUIOMAR, M. and GODEFROIT, P., 2014c. High diversity in Cretaceous ichthyosaurs from Europe prior to their extinction. *PLoS ONE*, **9**(1), p.e84709.

FISCHER, V., BARDET, N., BENSON, R. B. J., ARKHANGLESKY, M. S., and FRIEDMAN, M. 2016. Extinction of fish-shaped marine reptiles associated with reduced evolutionary rates and global environmental volatility. Nature Communications, 7, 10825.

FRAAS, E. 1891. *Ichthyosaurier der süddeutschen Trias- und Jura-Ablagerungen*. H. Laupp, Tübingen, 81 pp.

FRÖBISCH, N. B., SANDER, P. M., and RIEPPEL, O. 2006. A new species of *Cymbospondylus* (Diapsida, Ichthyosauria) from the Middle Triassic of Nevada and a re-evaluation of the skull osteology of the genus. *Zoological Journal of the Linnean Society*, **147**(4), 515–538.

FRÖBISCH, N. B., FRÖBISCH, J., SANDER, P. M., SCHMITZ, L., and RIEPPEL, O. 2013. Macropredatory ichthyosaur from the Middle Triassic and the origin of modern trophic networks. *Proceedings of the National Academy of Sciences*, **110**(4), 1393–1397.

GILMORE, C. W. 1905. Osteology of *Baptanodon* (Marsh). *Memoirs of the Carnegie Museum*, **2**(2), 77–129.

GODEFROIT, P. 1993. The skull of *Stenopterygius longifrons* (Owen, 1881). *Revue de Paléobiologie, Genève, Volume Spéciale*, **7**, 67–84.

GOLOBOFF, P. A., and CATALANO, S. A. 2016. TNT version 1.5, including a full implementation of phylogenetic morphometrics. *Cladistics*, **32**(3), 221–238.

GRADSTEIN, F. M., OGG, J. G., SCHMITZ, M., and OGG, G. (eds.). 2012. *The geologic time scale*. Elsevier, 1176 pp.

HALLAM, A., and WIGNALL, P. B. 1997. *Mass extinctions and their aftermath.* Oxford University Press, UK, 324 pp.

HAUFF, B., and HAUFF R. B. 1981. *Das Holzmadenbuch.* Repro-Druck GmbH, Fellbach, Germany, 136 pp.

HAWKINS, T. 1834. *Memoirs of Ichthyosauri and Plesiosauri, Extinct Monsters of the Ancient Earth.* Rolfe and Fletcher, London, XI + 58 pp.

HENDERSON, D. M. 2015. A new, nearly three-dimensional specimen of the skull and anterior body of the Late Triassic ichthyosaur *Macgowania janiceps* (McGowan 1996) from northeastern British Columbia, Canada. 121–149. In: BININDA-EMONDS, O. R. P., POWELL, G. L., JAMNICZKY, H. A., BAUER, A. M., and THEODOR, J. *All animals are interesting: a Festschrift in honour of Anthony P. Russell.* BIS Verlag, Oldenberg, Germany, 521 pp.

HOME, E. 1814. Some account of the fossil remains of an animal more nearly allied to fishes than any other classes of animals. *Philosophical Transactions of the Royal Society of London*, **101**, 571–577.

HUENE, F. VON. 1916. Beiträge zur Kenntnis der Ichthyosaurier im deutschen Muschelkalk. *Palaeontographica*, **62**, 1–68.

HUENE, F. VON. 1922. Die Ichthyosaurier des Lias und ihre Zusammenhänge. *Monographien für Mineralogie, Geologie un Paläontologie*, 1, Verlag von Gebrüder Bornträger, Berlin, VIII + 114 pp.

HUENE, F. VON. 1926. Neue Ichthyosaurierfunde aus dem schwäbischen Lias. *Neues Jahrbuch für Mineralogie, Geologie und Paläontologie, Beilage-Band, B*, **55**, 66–86.

HUENE, F. VON. 1948. Short review of the lower tetrapods. 65 – 106. In: Du TOIT, A. L. (ed.). Robert Broom Commemorative Volume. *Special Publication of the Royal Society of South Africa*, Cape Town.

HULL, D. L. 2010. *Science as a Process: an Evolutionary Account of the Social and Conceptual Development of Science.* University of Chicago Press, 600 pp.

IRMIS, R. B., MUNDIL, R., MARTZ, J. W., and PARKER, W. G. 2011. High-resolution U–Pb ages from the Upper Triassic Chinle Formation (New Mexico, USA) support a diachronous rise of dinosaurs. *Earth and Planetary Science Letters*, **309**(3), 258–267.

JAEKEL, O. 1904. Eine neue Darstellung von *Ichthyosaurus*. *Zeitschrift der Deutschen Geologischen Gesellschaft*, **56**, 26–34.

JI, C., JIANG, D., HAO, W., SUN, Z., and SUN Y. 2010. True tailbend occurred in the Late Triassic – evidence from ichthyosaur skeletons of South China. *Acta Scientiarum Naturalium Universitatis Pekinensis*, **47**(2), 309 – 314 [in Chinese with English abstract].

JI, C., JIANG, D., MOTANI, R., HAO, W., SUN, Z., and CAI, T. 2013. A new juvenile specimen of *Guanlingsaurus* (Ichthyosauria, Shastasauridae) from the Upper Triassic of Southwestern China. *Journal of Vertebrate Paleontology*, **33**, 340–348.

JI, C., JIANG, D., MOTANI, R., RIEPPEL, O., HAO, W. and SUN, Z. 2016. Phylogeny of the Ichthyopterygia incorporating recent discoveries from South China. *Journal of Vertebrate Paleontology*, **36**(1), e1025956.

JIANG, D., SCHMITZ, L., HAO, W. and SUN, Y. 2006. A new mixosaurid ichthyosaur from the Middle Triassic of China. *Journal of Vertebrate Paleontology*, **26**(1), 60–69.

JIANG, D., SCHMITZ, L., MOTANI, R., HAO, W. and SUN, Y. L. 2007. The mixosaurid ichthyosaur *Phalarodon* cf. *P. fraasi* from the Middle Triassic of Guizhou Province, China. *Journal of Paleontology*, **81**(3), 602–605.

JIANG, D., MOTANI, R., HAO, W., SCHMITZ, L., RIEPPEL, O., SUN, Y., and SUN, Z. 2008a. New primitive ichthyosaurian (Reptilia, Diapsida) from the Middle Triassic of Panxian, Guizhou, southwestern China and its position in the Triassic biotic recovery. *Progress in Natural Science*, **18**(10), 1315–1319.

JIANG, D., RIEPPEL, O., MOTANI, R., HAO, W., SUN, Y., SCHMITZ, L., and SUN, Z. 2008b. A new middle Triassic eosauropterygian (Reptilia, Sauropterygia) from southwestern China. *Journal of Vertebrate Paleontology*, **28**, 1055–1062.

JIANG, D., MOTANI, R., HUANG, J., TINTORI, A., HU, Y., RIEPPEL, O., FRASER, N. C., JI, C., KELLEY, N. P., FU, W. and ZHANG, R. 2016. A large aberrant stem ichthyosauriform indicating early rise and demise of ichthyosauromorphs in the wake of the end-Permian extinction. *Scientific reports*, **6**, 26232.

JOHNSON, R. 1977. Size independent criteria for estimating relative age and the relationships among growth parameters in a group of fossil reptiles (Reptilia: Ichthyosauria). *Canadian Journal of Earth Sciences*, **14**(8), 1916–1924.

KARL, H. V., ARP, G., SIEDERSBECK, E., and REITNER, J., 2014. A large ichthyosaur vertebra from the lower Kössen Formation (upper Norian) of the Lahnewiesgraben near Garmisch-Partenkirchen, Germany. *Göttingen Contributions to Geosciences*, **77**, 191–197.

KEAR, B. P. 2005. Cranial morphology of *Platypterygius longmani* Wade, 1990 (Reptilia: Ichthyosauria) from the Lower Cretaceous of Australia. *Zoological Journal of the Linnean Society*, **145**(4), 583–622.

KEAR, B. P., and ZAMMIT, M. 2014. In utero foetal remains of the Cretaceous ichthyosaurian *Platypterygius*: ontogenetic implications for character state efficacy. *Geological Magazine*, **151**(1), 71–86.

KELLER, T. 1976. Magen- und Darminhalte von Ichthyosauriern des süddeutschen Posidonienschiefers. *Neues Jahrbuch für Geologie und Paläontologie. Monatshefte*, **5**, 266–283.

KELLEY, N. P., MOTANI, R., JIANG, D., RIEPPEL, O. and SCHMITZ, L. 2014. Selective extinction of Triassic marine reptiles during long-term sea-level changes illuminated by seawater strontium isotopes. Palaeogeography, Palaeoclimatology, Palaeoecology, **400**, 9–16.

KIRTON, A. M. 1983. *A review of British Upper Jurassic ichthyosaurs*. PhD dissertation, University of Newcastle-upon-Tyne, 239 pp.

LANE, H. H. 1945. New Mid-Pennsylvanian reptiles from Kansas. *Transactions of the Kansas Academy of Sciences*, **47**, 381–390.

LANG, W. D. 1959. Mary Anning's escape from lightening. *Proceedings of the Dorset Natural History and Archaeology Society*, **80**, 91–93.

LEIDY, J. 1868. Notice of some reptilian remains from Nevada. *Proceedings of the Academy of Natural Sciences, Philadelphia*, **20**, 177–178.

LI, C. 1999. [A preliminary study of a new ichthyosaur from the Triassic of Guizhou.] *Chinese Science Bulletin*, **44**, 1318–1321 [in Chinese].

LI, C., and YOU, H. *Cymbospondylus* from the Upper Triassic of Guizhou, China. *Vertebrata Palasiatica*, **40**(3), 9–16.

LIU, J., AITCHISON, J. C., SUN, Y., ZHANG, Q., ZHOU, C., and LY, T. 2011. A new mixosaurid ichthyosaur specimen from the Middle Triassic of SW China: further evidence for the diapsid origin of ichthyosaurs. *Journal of Paleontology*, **85**(1), 32 – 36.

LIU, J., MOTANI, R., JIANG, D., HU, S., AITCHISON, J., RIEPPEL, O., BENTON, M., ZHANG, Q., and ZHOU, C. 2013. The first specimen of the Middle Triassic *Phalarodon atavus* (Ichthyosauria: Mixosauridae) from South China, showing postcranial anatomy and peri-Tethyan distribution. *Palaeontology*, **56**(4), 849–886.

LOMAX, D. R. 2017. A new leptonectid ichthyosaur from the Lower Jurassic (Hettangian) of Nottinghamshire, England, UK, and the taxonomic usefulness of the ichthyosaurian coracoid. *Journal of Systematic Palaeontology*, **15**(5), 387–401.

LOMAX, D. R., and MASSARE, J. A. 2015. A new species of *Ichthyosaurus* from the Lower Jurassic of West Dorset, England, UK. *Journal of Vertebrate Paleontology*, **35**(2), e903260.

LOMAX, D. R., and MASSARE, J. A. 2016. Two new species of *Ichthyosaurus* from the lowermost Jurassic (Hettangian) of Somerset, England. *Papers in Palaeontology*, **3**, 1–20.

LOMAX, D. R., MASSARE, J. A., and MISTRY, R. T. 2017. The taxonomic utility of forefin morphology in Lower Jurassic ichthyosaurs: *Protoichthyosaurus* and *Ichthyosaurus*. *Journal of Vertebrate Paleontology*, **37**(5), e1361433.

LYDEKKER, R. 1888. Note on the classification of the Ichthyopterygia with a notice of two new species. *Geological Magazine*, **5**(7), 309–314.

MAISCH, M. W. 1997. A case against a diapsid origin of the Ichthyosauria. *Neues Jahrbuch für Geologie und Paläontologie-Abhandlungen*, **205**, 111–127.

MAISCH, M. W., and MATZKE, A. T. 1997. Observations on Triassic ichthyosaurs. Part I: Structure of the palate and mode of tooth implantation in *Mixosaurus cornalianus* (BASSANI, 1886). *Neues Jahrbuch für Geologie und Paläontologie, Monatshefte*, **1997**, 717–732.

MAISCH, M. 1998. A new ichthyosaur genus from the Posidonia Shale (Lower Toarcian, Jurassic) of Holzmaden, SW-Germany with comments on the phylogeny of post-Triassic ichthyosaurs. *Neues Jahrbuch für Geologie und Paläontologie-Abhandlungen*, **209**, 47–78.

MAISCH, M. W. 2008. Revision der Gattung *Stenopterygius* Jaekel, 1904 emend, von Huene, 1922 (Reptilia: Ichthyosauria) aus dem unteren Jura Westeuropas. *Palaeodiversity*, **1**, 227–271.

MAISCH, M. W. 2010. Phylogeny, systematics, and origin of the Ichthyosauria – the state of the art. *Palaeodiversity*, **3**, 151–214.

MAISCH, M. W. and MATZKE, A. T. 2000a. The Ichthyosauria. *Stuttgarter Beitrage zur Naturkunde, Serie B*, **298**, 1–159.

MAISCH, M. W., and MATZKE, A. T. 2000b. New data on the cranial ostelogy of *Ichthyosaurus communis* Conybeare, 1822 (Ichthyosauria, Lower Jurassic). *Geologica et Palaeontologica*, **34**, 137–143.

MAISCH, M. W., and MATZKE, A. T. 2001. Observations on Triassic ichthyosaurs. Part VIII: a redescription of *Phalarodon major* (von Huene, 1916) and the composition and phylogeny of the Mixosauridae. *Neues Jahrbuch für Geologie und Paläontologie-Abhandlungen*, **220**, 431–447.

MAISCH, M. W., and MATZKE, A. T. 2004. Observations on Triassic ichthyosaurs. Part XIII: New data on the cranial osteology of *Cymbospondylus petrinus* (Leidy, 1868) from the Middle Triassic Prida Formation of Nevada. *Neues Jahrbuch für Geologie und Paläontologie, Monatshefte*, **6**, 370–384.

MAISCH, M. W., PAN, X., SUN, Z., CAI, T., ZHANG, D., and XIE, J. 2006. Cranial osteology of *Guizhouichthyosaurus tangae* (Reptilia: Ichthyosauria) from the Upper Triassic of China. *Journal of Vertebrate Paleontology*, **26**, 588–597.

MAISCH, M. W., JIANG, D., HAO, W., SUN, Y., SUN, Z., and STÖHR, H. 2008. A well-preserved skull of *Qianichthyosaurus zhoui* Li, 1999 (Reptilia: Ichthyosauria) from the Upper Triassic of China and the phylogenetic position of the Toretocnemidae. *Neues Jahrbuch für Geologie und Paläontologie-Abhandlungen*, **248**(3), 257–266.

MANTELL, G. A. 1851. *Petrifactions and their Teachings or a Handbook to the Gallery of Organic Remains of the British Museum.* H. G. Bohn, London, XII + 496 pp.

MAREK, R. D., MOON, B. C., WILLIAMS, M., and BENTON, M. J. 2015. The skull and endocranium of a Lower Jurassic ichthyosaur based on digital reconstructions. *Palaeontology*, **58**(4), 723–742.

MARSH, O. C. 1879. A new order of extinct reptiles (Sauranodonta), from the Jurassic Formation of the Rocky Mountains. *American Journal of Science*, (**3**)17: 85–86.

MARTILL, D. 1995. An ichthyosaur with preserved soft tissue from the Sinemurian of southern England. *Palaeontology*, **38**(4), 897–903.

MARTIN, J. E., FISCHER, V., VINCENT, P. and SUAN, G. 2012. A longirostrine *Temnodontosaurus* (Ichthyosauria) with comments on Early Jurassic ichthyosaur niche partitioning and disparity. *Palaeontology*, **55**(5), 995–1005.

MARTIN, J. E., VINCENT, P., SUAN, G., SHARPE, T., HODGES, P., WILLIAMS, M., HOWELLS, C., and FISCHER, V. 2015. A mysterious giant ichthyosaur from the lowermost Jurassic of Wales. *Acta Palaeontologica Polonica*, **60**(4), 837–842.

MASSARE, J. A. 1987. Tooth morphology and prey preference of Mesozoic marine reptiles. *Journal of Vertebrate Paleontology*, **7**(2), 121–137.

MASSARE, J. A. 1988. Swimming capabilities of Mesozoic marine reptiles: implications for method of predation. *Palaeobiology*, **14**(2), 187–205.

MASSARE, J. A., and CALLAWAY, J. M. 1990. The affinities and ecology of Triassic ichthyosaurs. *Geological Society of America Bulletin*, **102**, 409–416.

MASSARE, J. A., and LOMAX, D. R. 2016a. Composite skeletons of Ichthyosaurus in historic collections. *Paludicola*, **10**, 207–250.

MASSARE, J. A., and LOMAX, D. R. 2016b. A new specimen of *Ichthyosaurus conybeari* (Reptilia, Ichthyosauria) from Watchet, Somerset, England, UK, and a re-examination of the species. *Journal of Vertebrate Paleontology*, **36**(5), e1163264.

MASSARE, J. A., and LOMAX, D. R. 2018. A taxonomic reassessment of *Ichthyosaurus communis* and *I. intermedius* and a revised diagnosis for the genus. *Journal of Systematic Palaeontology*, **16**(3), 263–277.

MAXWELL, E. E. 2010. Generic reassignment of an ichthyosaur from the Queen Elizabeth Islands, Northwest Territories, Canada. *Journal of Vertebrate Paleontology*, **30**(2), 403–415.

MAXWELL, E. E., and CALDWELL, M. W. 2006 A new genus of ichthyosaur from the Lower Cretaceous of Western Canada. *Palaeontology*, **49**, 1043–1052.

MAXWELL, E. E., ZAMMIT, M., and DRUCKENMILLER, P. S. 2012a. Morphology and orientation of the ichthyosaurian femur. *Journal of Vertebrate Paleontology*, **32**(5), 1207–1211.

MAXWELL, E. E., FERNÁNDEZ, M. S., and SCHOCH, R. R. 2012b. First diagnostic marine reptile remains from the Aalenian (Middle Jurassic): a new ichthyosaur from southwestern Germany. *PLoS ONE*, **7**(8), e41692.

MAZIN, J.-M. 1982. Affinités et phylogénie des Ichthyopterygia. *Géobios, Mémoire Spécial*, **6**, 85–98.

MCCOY, F. 1867. On the occurrence of *Ichthyosaurus* and *Plesiosaurus* in Australia. *The Annals and Magazine of Natural History, Series 3*, **19**, 355–356.

MCGOWAN, C. 1973. The cranial morphology of the Lower Liassic latipinnate ichthyosaurs of England. *Bulletin of the British Museum (Natural History), Geology*, **24**, 1–109.

MCGOWAN, C. 1974a. A revision of the longipinnate ichthyosaurs of the Lower Jurassic of England, with descriptions of two new species (Reptilia: Ichthyosauria). *Life Sciences Contributions, Royal Ontario Museum*, **97**, 1–37.

MCGOWAN, C. 1974b. A revision of the latipinnate ichthyosaurs of the Lower Jurassic of England (Reptilia: Ichthyosauria). *Life Sciences Contributions, Royal Ontario Museum*, **100**, 1–30.

MCGOWAN, C. 1976. The description and phenetic relationships of a new ichthyosaur genus from the Upper Jurassic of England. *Canadian Journal of Earth Sciences*, **13**, 668–683.

MCGOWAN, C. 1979. A revision of the Lower Jurassic ichthyosaurs of Germany with descriptions of two new species. *Palaeontographica Abteilung A*, **166**, 93–135.

MCGOWAN, C. 1986. A putative ancestor for the swordfish-like ichthyosaur *Eurhinosaurus*. *Nature*, **322**, 454–456.

MCGOWAN, C. 1989. *Leptopterygius tenuirostris* and other long-snouted ichthyosaurs from the English Lower Lias. *Palaeontology*, **32**(2), 409–427.

MCGOWAN, C. 1990. Problematic ichthyosaurs from southwest England: a question of authenticity. *Journal of Vertebrate Paleontology*, **10**(1), 72–79.

MCGOWAN, C. 1991. An ichthyosaur forefin from the Triassic of British Columbia exemplifying Jurassic features. *Canadian Journal of Earth Sciences*, **28**(10), 1553–1560.

MCGOWAN, C. 1993. A new species of large, long-snouted ichthyosaur from the English lower Lias. *Canadian Journal of Earth Sciences*, **30**(6), 1197–1204.

MCGOWAN, C. 1994. A new species of *Shastasaurus* (Reptilia: Ichthyosauria) from the Triassic of British Columbia: the most complete exemplar of the genus. *Journal of Vertebrate Paleontology*, **14**(2), 168–179.

MCGOWAN, C. 1995a. A remarkable small ichthyosaur from the Upper Triassic of British Columbia, representing a new genus and species. *Canadian Journal of Earth Sciences*, **32**(3), 292–303.

MCGOWAN, C. 1995b. *Temnodontosaurus risor* is a juvenile of *T. platyodon* (Reptilia: Ichthyosauria). *Journal of Vertebrate Paleontology*, **14**(4), 472–479.

MCGOWAN, C. 1996. A new and typically Jurassic ichthyosaur from the Upper Triassic of British Columbia. *Canadian Journal of Earth Sciences*, **33**(1), 24–32.

MCGOWAN, C. 1997. A transitional ichthyosaur fauna. 61–80. In: CALLAWAY, J. M., and NICHOLLS, E. L. (eds). *Ancient marine reptiles.* Academic Press, 501 pp.

MCGOWAN, 2001. *The Dragon Seekers: How an Extraordinary Circle of Fossilists Discovered the Dinosaurs and Paved the Way for Darwin.* Cambridge (Massachusetts), Perseus Publishing, XVI + 254 pp.

MCGOWAN, C. 2003. A new specimen of *Excalibosaurus* from the English Lower Jurassic. *Journal of Vertebrate Paleontology*, **23**(4), 950–956.

MCGOWAN, C., and MILNER, A. C. 1999. A new Pliensbachian ichthyosaur from Dorset, England. *Palaeontology*, **42**(5), 761–768.

MCGOWAN, C., and MOTANI, R. 2002. Two new ichthyosaurs from English Lias causing a polytomy. *Journal of Vertebrate Paleontology*, **22**, 86A.

MCGOWAN, C., and MOTANI, R. 2003. Part 8: Ichthyopterygia. 1–175. In: SUES, H.-D. (ed.). *Handbook of Paleoherpetology.* Verlag Dr. Friedrich Pfeil, Munich.

MCROBERTS, C. A. 2011. Late Triassic Bivalvia (Chiefly Halobiidae and Monotidae) from the Pardonet Formation, Williston Lake Area, Northeastern British Columbia, Canada. *Journal of Paleontology*, **85**(4), 613–664.

MEARS, E. M., ROSSI, V., MACDONALD, E., COLEMAN, G., DAVIES, T. G., ARIAS-RIESGO, C., HILDEBRANDT, C., THIEL, H., DUFFIN, C. J., WHITESIDE, D. I., and BENTON, M. J. 2016. The Rhaetian (Late Triassic) vertebrates of Hampstead Farm Quarry, Gloucestershire, UK. Proceedings of the Geologists' Association, 127(4), 478–505.

MERRIAM, J. C. 1895. On some reptilian remains from the Triassic of northern California. *American Journal of Science*, (**3**)50, 55–57.

MERRIAM, J. C. 1902. Triassic Ichthyopterygia from California and Nevada. *University of California Publications, Bulletin of the Department of Geology*, **3**(4), 63–108.

MERRIAM, J. C. 1903. New Ichthyosauria from the Upper Triassic of California. *University of California Publications, Bulletin of the Department of Geology*, **3**(12), 249–263.

MERRIAM, J. C. 1905. The types of limb-structure in the Triassic Ichthyosauria. *American Journal of Science*, **19**(4), 23–30.

MERRIAM, J. C. 1908. Triassic Ichthyosauria, with special reference to the American forms. *Memoirs of the University of California*, **1**, 1–252.

MERRIAM, J. C. 1910. The skull and dentition of a primitive ichthyosaurian from the Middle Triassic. *University of California Publications, Bulletin of the Department of Geology*, **5**(24), 381–390.

MOON, B. C., and KIRTON, A. M. 2016. Ichthyosaurs of the British Middle and Upper Jurassic. Part 1 – *Ophthalmosaurus*. *Monograph of the Palaeontographical Society*, **170**(647), 1–84.

MOTANI, R. 1996. Redescription of the dental features of an Early Triassic ichthyosaur *Utatsusaurus hataii*. *Journal of Vertebrate Paleontology*, **16**, 396–402.

MOTANI, R. 1997a. Phylogeny of the Ichthyosauria (Amniota: Reptilia) with special reference to Triassic forms. PhD dissertation, University of Toronto, Toronto, Ontario, Canada, xxiv + 384 pp.

MOTANI, R. 1997b. Redescription of the dentition of *Grippia longirostris* (Ichthyosauria) with a comparison with *Utatsusaurus hataii*. *Journal of Vertebrate Paleontology*, **17**, 39–44.

MOTANI, R. 1997c. New information on the forefin of *Utatsusaurus hataii* (Ichthyosauria). *Journal of Paleontology*, **71**, 475–479.

MOTANI, R. 1998a. Ichthyosaurian swimming revisited: implications from the vertebral column and phylogeny. *Journal of Vertebrate Paleontology*, **18**, 65A.

MOTANI, R. 1998b. First complete forefin of the ichthyosaur *Grippia longirostris* discovered from the Triassic of Spitsbergen. *Palaeontology*, **41**, 591–600.

MOTANI, R. 1999a. Phylogeny of the Ichthyopterygia. *Journal of Vertebrate Paleontology*, **19**(3), 473–496.

MOTANI, R., 1999b. The skull and taxonomy of *Mixosaurus* (Ichthyopterygia). *Journal of Paleontology*, **73**(5), 924–935.

MOTANI, R. 1999c. On the evolution and homologies of ichthyopterygian forefins. *Journal of Vertebrate Paleontology*, **19**(1), 28–41.

MOTANI, R. 2000. Skull of *Grippia longirostris*: no contradiction with a diapsid affinity for the Ichthyopterygia. *Palaeontology*, **43**, 1–14.

MOTANI, R. 2002a. Scaling effects in caudal fin propulsion and the speed of ichthyosaurs. *Nature*, **415**, 309–312.

MOTANI, R. 2002b. Swimming speed estimation of extinct marine reptiles: energetic approach revisited. *Palaeobiology*, **28**(2), 251–262.

MOTANI, R. 2005a. Evolution of fish-shaped reptiles (Reptilia: Ichthyopterygia) in their physical environments and constraints. *Annual Reviews in Earth and Planetary Sciences*, **33**, 395–420.

MOTANI, R. 2005b. Detailed tooth morphology in a durophagous ichthyosaur captured by 3D laser scanner. *Journal of Vertebrate Paleontology*, **25**(2), 462–465.

MOTANI, R. 2005c. True skull roof configuration of *Ichthyosaurus* and *Stenopterygius* and its implications. *Journal of Vertebrate Paleontology*, **25**(2), 338–342.

MOTANI, R. 2008. Combining uniformitarian and historical data to interpret how Earth environment influenced the evolution of Ichthyopterygia. *The Paleontological Society Papers*, **14**, 147–164.

MOTANI, R. 2009. The evolution of marine reptiles. *Evolution: Education and Outreach*, **2**(2), 224–235.

MOTANI, R. 2010. Warm-blooded 'sea dragons'? *Science*, **328** (5984), 1361–1362.

MOTANI, R. 2016. Palaeobiology: born and gone in global warming. *Current Biology*, **26**(11), R466–R468.

MOTANI, R., and YOU, H. 1998. Taxonomy and limb ontogeny of Chaohusaurus geishanensis (Ichthyosauria), with a note on the allometric equation. Journal of Vertebrate Paleontology, 18(3), 533–540.

MOTANI, R., YOU, H., and MCGOWAN, C. 1996. Eel-like swimming in the earliest ichthyosaurs. Nature, 382, 347–348.

MOTANI, R., MINOURA, N., and ANDO, T. 1998. Ichthyosaurian relationships illuminated by new primitive skeletons from Japan. Nature, 393, 255–257.

MOTANI, R., MANABE, M., and DONG, Z. 1999a. The status of Himalayasaurus tibetensis (Ichthyopterygia). Paludicola, 2(2), 174–181.

MOTANI, R., ROTHSCHILD, B. M., and WAHL, W. 1999b. Large eyeballs in diving ichthyosaurs. Nature, 402, 747-747.

MOTANI, R., JI, C., TOMITA, T., KELLEY, N. P., MAXWELL, E. E., Jiang, D., and Sander, P. M. 2013. Absence of suction feeding ichthyosaurs and its implications for Triassic mesopelagic paleoecology. *PLoS ONE*, **8**(12), e66075.

MOTANI, R., JIANG, D., TINTORI, A., RIEPPEL, O. and CHEN, G. 2014. Terrestrial origin of viviparity in Mesozoic marine reptiles indicated by Early Triassic embryonic fossils. *PLoS ONE*, **9**(2), e88640.

MOTANI, R., JIANG, D., CHEN, G., TINTORI, A., RIEPPEL, O., JI, C. and HUANG, J. D. 2015a. A basal ichthyosauriform with a short snout from the Lower Triassic of China. *Nature*, **517**, 485–488.

MOTANI, R., JIANG, D., TINTORI, A., RIEPPEL, O., CHEN, G., and YOU, H. 2015b. Status of *Chaohusaurus chaoxianensis* (Chen, 1985). *Journal of Vertebrate Paleontology*, **35**(1), e892011.

MOTANI, R., JIANG, D., TINTORI, A., RIEPPEL, O., CHEN, G., and YOU, H. 2015c. First evidence of centralia in Ichthyopterygia reiterating bias from paedomorphic characters on marine reptile phylogenetic reconstruction. *Journal of Vertebrate Paleontology*, **35**(4), e948547.

MOTANI, R., JIANG, D., TINTORI, A., JI, C., and HUANG, J. D. 2017. Pre-versus post-mass extinction divergence of Mesozoic marine reptiles dictated by time-scale dependence of evolutionary rates. *Proceedings of the Royal Society B*, **284**(1854), 20170241.

NACE, R. L. 1939. A new ichthyosaur from the Upper Cretaceous Mowry Formation of Wyoming. *American Journal of Science*, **237**, 673–686.

NEENAN, J. M., KLEIN, N., and SCHEYER, T. M. 2013. European origin of placodont marine reptiles and the evolution of crushing dentition in Placodontia. *Nature Communications*, **4**, 1621.

NEENAN, J. M., LI, C., RIEPPEL, O. and SCHEYER, T. M. 2015. The cranial anatomy of Chinese placodonts and the phylogeny of Placodontia (Diapsida: Sauropterygia). *Zoological Journal of the Linnean Society*, **175**(2), 415–428.

NICHOLLS, E. L., and BRINKMAN, D. B. 1995. A new ichthyosaur from the Triassic of Sulphur Mountain Formation of British Columbia. 521–535. In: SARJEANT W. A. S. (ed.). *Vertebrate Fossils and the Evolution of Scientific Concepts*. Gordon and Breach, Switzerland, 622 pp.

NICHOLLS, E. L., and MANABE, M. 2001. A new genus of ichthyosaur from the Late Triassic Pardonet Formation of British Columbia: bridging the Triassic Jurassic gap. *Canadian Journal of Earth Sciences*, **38**(6), 983–1002.

NICHOLLS, E. L., and MANABE, M. 2004. Giant ichthyosaurs of the Triassic—a new species of *Shonisaurus* from the Pardonet Formation (Norian: Late Triassic) of British Columbia. *Journal of Vertebrate Paleontology*, **24**(4), 838–849.

NICHOLLS, E. L., BRINKMAN, D. B., and CALLAWAY, J. M. 1999. New material of Phalarodon (Reptilia, Ichthyosauria) from the Triassic of British Columbia and its bearing on the interrelationships of mixosaurs. Palaeontographica A, 252, 1–22.

NICHOLLS, E. L., WEI, C., and MANABE, M. 2002. New material of *Qianichthyosaurus* Li, 1999 (Reptilia, Ichthyosauria) from the Late Triassic of southern China, and implications for the distribution of Triassic ichthyosaurs. *Journal of Vertebrate Paleontology*, **22**(4), 759–765.

ORCHARD, M. J., and TOZER, E. T. 1997. Triassic conodont biochronology, its calibration with the ammonoid standard, and a biostratigraphic summary for the Western Canada Sedimentary Basin. *Bulletin of Canadian Petroleum Geology*, **45**(4), 675–692.

OWEN, R. 1840. Report on British fossil reptiles. Part I. *Report of the British Association for the Advancement of Science, Plymouth*, **9**, 43–126.

OWEN, R. 1849–1884. *A History of British Fossil Reptiles. Volumes I–IV*. Cassell & Company Limited, London.

OWEN, R. 1851. The Fossil Reptiles of the Cretaceous Formations. *Palaeontographical Society Monographs*, **5**, 1-118.

OWEN, R. 1881. A monograph on the fossil Reptilia of the Liassic formations. Part III. *Plesiosaurus, Dimorphodon,* and *Ichthyosaurus*. *Monograph of the Palaeontographical Society*, **35**(166), 1–134.

PAN, X., JIANG, D., SUN, Z., CAI, T., ZHANG, D., and XIE, J. 2004. Discussion on *Guizhouichthyosaurus tangae* Cao and Luo in Yin et al., 2000 (Reptilia, Ichthyosauria) from the Late Triassic of Guanling County, Guizhou. *Acta Scientiarum Naturalium Universitatis Pekinensis*, **42**, 697–703.

PARADIS, E., CLAUDE, J. and STRIMMER, K. 2004. APE: analyses of phylogenetics and evolution in R language. *Bioinformatics*, **20**(2), 289–290.

PIVETEAU, J. 1926. Paléontologie de Madagascar XIII. Amphibiens et reptiles Permiens. *Annales de Paléonlologie*, **15**, 55–179.

POLLARD, J. E. 1968. The gastric contents of an ichthyosaur from the Lower Lias of Lyme Regis, Dorset. *Palaeontology*, **11**, 376–388.

QUENSTEDT, F. A. 1852. *Handbuch der Petrefaktenkunde.* H. Laupp, Tübingen, IV + 792 pp.

R CORE TEAM. 2017. *R: A language and environment for statistical computing.* Vienna.

REISZ, R. R. 1981. A diapsid reptile from the Pennsylvanian of Kansas. *University of Kansas Publications of the Museum of Natural History*, **7**, 1–74.

RIESS, J. 1986. Fortbewegungsweise, Schwimmbiophysik, und Phylogenie der Ichthyosaurier. *Palaeontographica A*, **192**, 93–155.

ROBERTS, A. J., DRUCKENMILLER, P. S., SÆTRE, G. P., and HURUM, J. H. 2014. A new Upper Jurassic ophthalmosaurid ichthyosaur from the Slottsmøya Member, Agardhfjellet Formation of central Spitsbergen. *PloS ONE*, **9**(8), e103152.

ROMER, A. S. 1968. An ichthyosaur skull from the Cretaceous of Wyoming. *Contributions to Geology, University of Wyoming*, **7**, 27–41.

RUSSELL, D. A. 1993. Jurassic marine reptiles from Cape Grassy, Melville Island, Arctic Canada. 195–201. In: Christie, R. L., and McMillan, N. J. (eds). The Geology of Melville Island, Arctic Canada. *Geological Survey of Canada Bulletin* **450**.

SANDER, P. M. 1989. The large ichthyosaur *Cymbospondylus buchseri*, sp. nov., from the Middle Triassic of Monte San Giorgio (Switzerland), with a survey of the genus in Europe. *Journal of Vertebrate Paleontology*, **9**(2), 163–173.

SANDER, P. M., 2000. Ichthyosauria: their diversity, distribution, and phylogeny. *Paläontologische Zeitschrift*, **74**(1–2), 1–35.

SANDER, P. M., CHEN, X., CHENG, L., and WANG, X. 2011. Short-snouted toothless ichthyosaur from China suggests Late Triassic diversification of suction feeding ichthyosaurs. *PLoS ONE*, **6**(5), e19480.

SCHEYER, T. M., NEENAN, J. M., BODOGAN, T., FURRER, H., OBRIST, C., and PLAMONDON, M. 2017. A new, exceptionally preserved juvenile specimen of *Eusaurosphargis dalsassoi* (Diapsida) and implications for Mesozoic marine diapsid phylogeny. *Scientific reports*, **7**(1), 4406.

SCHEYER, T. M., ROMANO, C., JENKS, J., and BUCHER, H. 2014. Early Triassic marine biotic recovery: the predators' perspective. *PLoS ONE*, **9**(3), e88987.

SEELEY, H. G. 1874. On the pectoral arch and fore limb of *Ophthalmosaurus*, a new ichthyosaurian genus from the Oxford Clay. *Quarterly Journal of the Geological Society of London*, 30, 696–707.

SHANG, Q., and LI, C. 2009. On the occurrence of the ichthyosaur *Shastasaurus* in the Guanling Biota (Late Triassic), Guizhou, China. *Vertebrata PalAsiatica*, **47**, 178–193.

SHIKAMA, T., KAMEI, T. and MURATA, M. 1978. Early Triassic Ichthyosaurus, *Utatsusaurus hataii* gen. et sp. nov., from the Kitakami Massif, northeast Japan. *Science Reports of the Tohoku University, Second Series (Geology)*, **48**(2), 77–97.

SCHMITZ, L., 2005. The taxonomic status of *Mixosaurus nordenskioeldii* (Ichthyosauria). *Journal of Vertebrate Paleontology*, **25**(4), 983–985.

SCHMITZ, L., SANDER, P. M., STORRS, G. W., and RIEPPEL, O. 2004. New Mixosauridae (Ichthyosauria) from the Middle Triassic of the Augusta Mountains (Nevada, USA) and their implications for mixosaur taxonomy. *Palaeontographica, Abteilung A*, **270**, 133–162.

STANLEY, G. D., and SENOWBARI-DARYAN, B. 1999. Upper Triassic reef fauna from the Quesnel terrane, central British Columbia, Canada. *Journal of Paleontology*, **73**(5), 787–802.

STORRS, G. W. 1994. Fossil vertebrate faunas of the British Rhaetian (latest Triassic). *Zoological Journal of the Linnean Society*, **112**(1–2), 217–259.

THORNE, P. M., RUTA, M., and BENTON, M. J. 2011. Resetting the evolution of marine reptiles at the Triassic-Jurassic boundary. *Proceedings of the National Academy of Sciences*, **108**(20), 8339–8344.

WADE, M., 1984. *Platypterygius australis*, an Australian Cretaceous ichthyosaur. *Lethaia*, **17**(2), 99–113.

WAGNER, J. A. 1853. Die Charakteristik einer neuen Art von *Ichthyosaurus* aus den lithographischen Schiefern und eines Zahnes von *Polyptychodon* aus dem Grünsandsteine von Kehlheim. *Gelehrte Anzeigen der Koeniglich Bayerischen Akademie der Wissenschaften*, **36**, 25–32.

WANG, K. 1959. Über eine neue fossile Reptiliform von Provinz Hupeh, China. *Acta Palaeontologica Sinica*, **7**, 367–373.

WEST, G. B., WOODRUFF, W. H., and BROWN, J. H. 2002. Allometric scaling of metabolic rate from molecules and mitochondria to cells and mammals. *Proceedings of the National Academy of Sciences, USA*, **99**, 2473–2478.

WIMAN, C. 1910. Ichthyosaurier aus der Trias Spitzbergens. *Bulletin of the Geological Institution of the University of Upsala*, **10**, 124–148.

WIMAN, C. 1929. Eine neue Reptilien-Ordnung aus der Trias Spitzbergens. *Bulletin of the Geological Institution of the University of Uppsala*, **22**, 183–196.

WOODWARD, A. S. 1906. On two specimens of *Ichthyosaurus* showing contained embryos. *Geological Magazine, Decade 5*, **3**, 443–444.

WU, X., CHENG, Y., LI, C., ZHAO, L., and SATO, T. 2011. New information on *Wumengosaurus delicatomandibularis* Jiang et al., 2008 (Diapsida: Sauropterygia), with a revision of the osteology and phylogeny of the taxon. *Journal of Vertebrate Paleontology*, **31**(1), 70–83.

WU, X., ZHAO, L. J., SATO, T., GU, S., and JIN, X. 2016. A new specimen of *Hupehsuchus nanchangensis* Young, 1972 (Diapsida, Hupehsuchia) from the Triassic of Hubei, China. *Historical Biology*, **28**(1–2), 43 – 52.

YANG P., JI, C., JIANG D., MOTANI, R., TINTORI, A., SUN Y., and SUN Z. 2013. A New Species of *Qianichthyosaurus* (Reptilia: Ichthyosauria) from Xingyi Fauna (Ladinian, Middle Triassic) of Guizhou. *Acta Scientiarum Naturalium Universitatis Pekinensis*, **49**(6), 1002–1008.

YIN, G., X. ZHOU, Z. CAO, Y. YU & Y. LUO. 2000. [A preliminary study on the early Late Triassic marine reptiles from Guanling, Guizhou, China.] *Geology-Geochemistry*, **28**(3), 1–23 [in Chinese].

YOUNG, C. 1972. *Hupehsuchus nanchangensis*. 28–34. In: YOUNG C, and DONG, Z. (eds). [Aquatic reptiles from the Triassic of China]. *Academia Sinica, Institute of Vertebrate Paleontology and Palaeoanthropology, Memoir 9* [in Chinese].

YOUNG, C., and DONG, Z. 1972. [Chaohusaurus geishanensis from Anhui Province]. 11–14. In: YOUNG, C., and DONG, Z. (eds.). [Aquatic Reptiles from the Triassic of China.] *Academia Sinica, Institute of Vertebrate Paleontology and Palaeoanthropology, Memoir 9* [in Chinese].

ZHOU, M., JIANG, D., MOTANI, R., TINTORI, A., JI, C., SUN, Z., NI, P., and LU, H. 2017. The cranial osteology revealed by three-dimensionally preserved skulls of the Early Triassic ichthyosauriform *Chaohusaurus chaoxianensis* (Reptilia: Ichthyosauromorpha) from Anhui, China. *Journal of Vertebrate Paleontology*, **37**(4), e1343831.

APPENDIX 1

List of taxa included in the phylogenetic analysis, with information on locality, stratigraphic horizon, data sources used for character scoring and the proportion of missing data.

Outgroup

1. ***Petrolacosaurus kansensis*** Lane, 1945
   Locality: Garnett Quarry, Missourian Series, Anderson County, Kansas, USA.
   Horizon: Rock Lake Member, Stanton Formation, Lansing Group, Kasimovian–Gzhelian, Upper Pennsylvanian, upper Carboniferous.
   Data sources (for characters 196–199): Reisz (1977).
   Missing data: 4%.

2. ***Claudiosaurus germaini*** Carroll, 1981
   Locality: Leoposa, Benenitra and Ranohira, southwestern Madagascar.
   Horizon: Lower Sakamena Formation, Sakamena Group, Lopingian, upper Permian.
   Data sources (for characters 196–199): Carroll (1981).
   Missing data: 10.6%.

3. ***Thadeosaurus colcanapi*** Carroll, 1981
   Locality: Sakamena River Valley, Mount Eliva, southwestern Madagascar.
   Horizon: Lower Sakamena Formation, Sakamena Group, Lopingian, upper Permian.
   Data sources (for characters 196–199): Carroll (1981).
   Missing data: 43.1%.

4. ***Hovasaurus boulei*** Piveteau, 1926
   Locality: Sakamena River Valley, southwestern Madagascar.
   Horizon: Lower Sakamena Formation, Sakamena Group, Lopingian, upper Permian.
   Data sources (for characters 196–199): Currie (1981).
   Missing data: 28.1%.

5. ***Wumengosaurus delicatomandibularis*** Jiang et al., 2008b
   Locality: Yanjuan, Xinmin District, Panxian County, China.
   Horizon: *kockeli* biozone, Upper Member of Guanling Formation, middle Anisian, Middle Triassic.
   Data sources (for characters 196–199): Jiang et al. (2008b), Wu et al. (2011).
   Missing data: 9%.

6. ***Nanchangosaurus suni*** Wang, 1959

   Locality: Yuan’an and Nanzhang counties, Hubei Province, China.

   Horizon: uppermost part of Jialingjiang Formation, Spathian, Olenekian, Lower Triassic.

   Data sources (for characters 196–199): Chen et al. (2014a).

   Missing data: 64.3%.

7. ***Eohupehsuchus brevicollis*** Chen et al., 2014c

   Locality: Yangping, Yuan’an County, Hubei Province, China.

   Horizon: Jialingjiang Formation, upper Spathian, Olenekian, Lower Triassic.

   Data sources (for characters 196–199): Chen et al. (2014c).

   Missing data: 35.7%.

8. ***Hupehsuchus nanchangensis*** Young, 1972

   Locality: Xunjian, Nanzhang County and Mingfeng, Yuan’an County, Hubei Province, China.

   Horizon: Jialingjiang Formation, upper Spathian, Olenekian, Lower Triassic.

   Data sources (for characters 196–199): Carroll and Dong (1991), Wu et al. (2015).

   Missing data: 24.1%.

9. ***Parahupehsuchus longus*** Chen et al., 2014d

   Locality: Yuan’an County, Hubei Province, China.

   Horizon: Jialingjiang Formation, upper Spathian, Olenekian, Lower Triassic.

   Data sources (for characters 196–199): Chen et al. (2014d).

   Missing data: 61.8%.

10. ***Eretmorhipis carrolldongi*** Chen et al., 2015

    Locality: Tuling, Baihechuan, Xunjian District, Nanzhang County and Yingzhishan, Yuan'an County, Hubei Province, China.

    Horizon: Jialingjiang Formation, upper Spathian, Olenekian, Lower Triassic.

    Data sources (for characters 196–199): Chen et al. (2015).

    Missing data: 56.3%.

11. ***Cartorhynchus lenticarpus*** Motani et al., 2015a

    Locality: second level of Majiashan Quarry, Chaohu, Hefei, Anhui Province, China.

    Horizon: *subcolumbites* zone, Upper Member of Nanlinghu Formation, Spathian, Olenekian, Lower Triassic.

    Data sources (for characters 196–199): Motani et al. (2015a).

Missing data: 30.7%.

12. ***Sclerocormus parviceps*** Jiang et al., 2016
    Locality: first level of Majiashan Quarry, Chaohu, Hefei, Anhui Province, China.
    Horizon: *subcolumbites* zone, Upper Member of Nanlinghu Formation, Spathian, Olenekian, Lower Triassic.
    Data sources (for characters 196–199): Jiang et al. (2016).
    Missing data: 25.6%.

Ingroup

13. ***Chaohusaurus geishanensis*** Young and Dong, 1972
    Locality: Guishan and Majiashan, Chaohu, Anhui Province, China.
    Horizon: Upper Member of Nanlinghu Formation, Spathian, Olenekian, Lower Triassic.
    Data sources (for characters 196–199): GMPKU-P-1118, Young and Dong (1972).
    Missing data: 54.3%.

14. ***Chaohusaurus chaoxianensis*** (Chen, 1985)
    Locality: Majiashan, Chaohu, Anhui Province, China.
    Horizon: Upper Member of Nanlinghu Formation, Spathian, Olenekian, Lower Triassic.
    Data sources (for characters 196–199): Zhou et al. (2017).
    Missing data: 6.0%.

15. ***Chaohusaurus zhangjiawanensis***, Chen et al., 2013
    Locality: Zhangjiawan, Yangping, Yuan'an Province, China.
    Horizon: Jialingjiang Formation, Spathian, Olenekian, Lower Triassic.
    Data sources (for characters 196–199): Chen et al. (2013).
    Missing data: 54.3%.

16. ***Utatsusaurus hataii***, Shikama et al., 1978
    Locality: Miyagi, Hokkaido, Japan
    Horizon: Middle–Upper Osawa Formation, Spathian, Olenekian, Lower Triassic.
    Data sources (for characteres 196–199): Cuthbertson et al., 2013a.
    Missing data: 7.0%.

17. ***Grippia longirostris*** Wiman, 1929
    Locality: Agardh Range and Mt. Milne Edwards, Spitsbergen, Svalbard.

Horizon: Upper Sticky Keep Formation, Spathian, Olenekian, Lower Triassic.

Data sources (for characters 196–199): Motani (2000).

Missing data: 33.7%.

18. ***Gulosaurus helmi*** Cuthbertson et al., 2013b

Locality: Wapiti Lake area, British Columbia, Canada.

Horizon: Vega-Phroso Siltstone Member, Sulphur Mountain Formation, Lower–Middle Triassic.

Data sources (for characters 196–199): TMP 89.127.3 (holotype), Cuthbertson et al. (2013b).

Missing data: 43.7%.

19. ***Parvinatator wapitiensis*** Brinkman and Nicholls, 1995

Locality: Wapiti Lake area, British Columbia, Canada.

Horizon: Vega-Phroso Siltstone Member, Sulphur Mountain Formation, Lower–Middle Triassic.

Data sources (for characters 196 – 199): TMP 89.127.8 (holotype), Brinkman and Nicholls (1995), Motani (1997).

Missing data: 63.8%.

20. ***Cymbospondylus piscosus*** Leidy, 1868

Locality: Humboldt Range and New Pass Range, northern Nevada, USA.

Horizon: Prida Formation, Anisian, Middle Triassic.

Data sources (for all characters): UCMP 9950 (skull only; cast of complete specimen displayed in the Natural History Museum, Sierra College, Rocklin, CA, USA, was also examined); UCMP 9913; UCMP 9154 (humerus, coracoid and gastral basket only); Merriam (1908).

Missing data: 20.6%.

21. ***Cymbospondylus buchseri*** Sander, 1989

Locality: Cava Tre Fontane, Monte San Giorgio, Ticino (Tessin), Switzerland.

Horizon: Grenzbitumenzone, Anisian–Ladinian, Middle Triassic.

Data sources (for all characters): PIMUZ T 4351 (holotype); Sander (1989).

Missing data: 63.8%.

22. ***Cymbospondylus nichollsi*** Fröbisch, et al., 2006

Locality: Augusta Mountains, Pershing County, Nevada, USA.

Horizon: Fossil Hill Member, Favret Formation, Anisian, Middle Triassic.

Data sources (for all characters): FMNH PR 2251 (holotype); Fröbisch et al. (2006).
Missing data: 64.3 %.

23. ***Xinminosaurus catactes*** Jiang et al., 2008a
Locality: vicinity of Yangjuan Village, Xinmin District, Panxian County, Guizhou Province, China.
Horizon: *Nicoraella kockeli* conodont biozone, Upper Member of the Guanling Formation, Anisian, Middle Triassic.
Data sources (for all characters): GMPKU-P-1071 (holotype); GMPKU-P-1206; GMPKU uncatalogued; Jiang et al. (2008a).
Missing data: 39.2 %.

24. ***Thalattoarchon saurophagis*** Fröbisch, et al., 2013
Locality: Favret Canyon, Augusta Mountains, Pershing County, Nevada, USA.
Horizon: *Nevadisculites taylori* ammonoid biozone, Fossil Hill Member, Favret Formation, Anisian, Middle Triassic.
Data sources (for all characters): FMNH PR 3032 (holotype); Fröbisch et al. (2013).
Missing data: 65.32 %.

25. ***Mixosaurus panxianensis*** Jiang et al., 2006
Locality: Yangjuan Village, Xinmin District, Panxian County, Guizhou Province, China.
Horizon: Upper Member of Guanling Formation, Anisian, Middle Triassic.
Data sources (for characters 196–199): GMPKU-P-1033 (holotype), GMPKU-P-1039 (paratype), GMPKU-P-1008, GMPKU-P-1009, Jiang et al. (2006), Ji et al. (2016).
Missing data: 10.0%.

26. ***Mixosaurus cornalianus*** (Bassani, 1886)
Locality: Besano, Italy and Monte San Giorgio, Ticino (Tessin), Switzerland.
Horizon: Grenzbitumenzone, Anisian–Ladinian, Middle Triassic.
Data sources (for characters 196–199): PIMUZ T4848, PIMUZ T2420.
Missing data: 11%.

27. ***Mixosaurus kuhnschnyderi*** (Brinkmann, 1998)
Locality: Monte San Giorgio, Ticino (Tessin), Switzerland.
Horizon: Grenzbitumenzone, Anisian–Ladinian, Middle Triassic.
Data sources (for characters 196–199): Brinkmann (1998, 2004).
Missing data: 64.3%.

28. ***Phalarodon atavus*** (Quenstedt, 1852)

Locality and horizon: Muschelkalk (Anisian–Ladinian, Middle Triassic) of Germany and Poland; Upper Member of Guanling Formation, Anisian, Middle Triassic of Luoping County, Yunnan Province, China.

Data sources (for characters 196–199): Motani (1999c), Liu et al. (2013).

Missing data: 38.2%.

29. ***Phalarodon fraasi*** Merriam, 1910

Locality and horizon: West Humboldt Range, Prida Formation (holotype) and Augusta Mountains, Fossil Hill Member, Favret Formation (Anisian, Middle Triassic) of Nevada, USA; Botneheia Formation–Tschermakfjellet Formation (Ladinian–Carnian, Middle–Late Triassic) of Spitzbergen, Svalbard; Vega-Phroso Siltstone Member, Whistler Member and Llana Member, Sulphur Mountain Formation (Lower–Middle Triassic) of Wapiti Lake area, British Columbia, Canada.

Data sources (for characters 196–199): UCMP 9863 (holotype).

Missing data: 55.8%.

30. ***Phalarodon callwayi*** Schmitz et al., 2004

Locality and horizon: Fossil Hill Member, Favret Formation (Anisian, Middle Triassic) of Muller Canyon, Augusta Mountains, Pershing County (holotype) and Prida Formation (Anisian, Middle Triassic) of Humboldt Range, Nevada, USA; Botneheia Formation–Tschermakfjellet Formation (Ladinian–Carnian, Middle–Late Triassic) of Spitzbergen, Svalbard; Vega-Phroso Siltstone Member, Whistler Member and Llana Member, Sulphur Mountain Formation (Lower–Middle Triassic) of Wapiti Lake area, British Columbia, Canada.

Data sources (for characters 196–199): Nicholls et al. (1999), Schmitz et al. (2004).

Missing data: 59.5%.

31. ***Besanosaurus leptorhynchus*** Dal Sasso and Pinna, 1996

Locality: Sasso Caldo Quarry, Besano, Varese Province, Lombardy, Italy.

Horizon: *nevadites zone*, Besano Formation, uppermost Anisian, Middle Triassic.

Data sources (for characters 196–199): Dal Sasso and Pinna (1996).

Missing data: 50.3%.

32. ***Guizhouichthyosaurus tangae*** Cao and Lu in Yin et al., 2000

Locality: Guizhou Province, China.

Horizon: Lower Xiaowa Formation, Carnian, Upper Triassic.

Data sources (for characters 196 – 199): IVPP V11865, IVPP V11869.

Missing data: 13.1%.

33. ***'Callawayia' wolonggangensis*** Chen et al., 2007

Locality: Xinpu Village, Guanling County, Guizhou Province, China.

Horizon: Lower Xiaowa Formation, Carnian, Upper Triassic.

Data sources (for characters 196–199): SPCV 10306 (holotype), SPCV 10305.

Missing data: 45.7%.

34. ***Guanlingsaurus liangae*** Cao and Lu in Yin et al., 2000

Locality: Guizhou Province, China.

Horizon: Lower Xiaowa Formation, Carnian, Upper Triassic.

Data sources (for characters 196–199): SPCV 03107, Sander et al. (2011).

Missing data: 17.6%.

35. ***Shastasaurus pacificus*** Merriam, 1895

Locality: Redding, Shasta County, California, USA.

Horizon: Hosselkus Limestone, upper Carnian, Upper Triassic.

Data sources (for characters 196–199): UCMP 9017.

Missing data: 43.7%.

36. ***Shonisaurus popularis*** Camp, 1980

Locality: Gabbs, Nye County, Nevada, USA.

Horizon: Luning Formation, upper Carnian, Upper Triassic.

Data sources (for characters 196–199): uncatalogued specimens in NSM (including holotype).

Missing data: 51.8%.

37. ***Shonisaurus sikanniensis*** Nicholls and Manabe, 2004

Locality: Sikanni Chief River area, British Columbia, Canada.

Horizon: *postera* zone, Pardonet Formation, middle Norian, Upper Triassic.

Data sources (for characters 196–199): TMP 94.378.2 (holotype).

Missing data: 73.4%.

38. ***Californosaurus perrini*** (Merriam, 1902)

Locality: Redding, Shasta County, California, USA.

Horizon: Hosselkus Limestone, upper Carnian, Upper Triassic.

Data sources (for characters 196–199): UCMP 9119 (holotype), UCMP 9082.
Missing data: 58.3%.

39. ***Toretocnemus californicus*** Merriam, 1903
Locality: Brock Mountain and Smith's Cove, Shasta County, California, USA.
Horizon: Hosselkus Limestone, upper Carnian, Upper Triassic.
Data sources (for characters 196–199): UCMP 8100 (holotype), UCMP 8099.
Missing data: 51.8%.

40. ***Qianichthyosaurus zhoui*** Li, 1999
Locality: Guizhou Province, China.
Horizon: Lower Xiaowa Formation, Carnian, Upper Triassic.
Data sources (for characters 196–199): GMPKU-P-1208, Maisch et al. (2008).
Missing data: 15.1%.

41. ***Qianichthyosaurus xingyiensis*** Yang et al., 2013
Locality: Wusha Town, Xingyi City, Guizhou Province, China.
Horizon: Zhuganpo Member, Falang Formation, Ladinian, Middle Triassic.
Data sources (for characters 196–199): Yang et al. (2013).
Missing data: 39.2%.

42. ***Callawayia neoscapularis*** (McGowan, 1994)
Locality: Williston Lake and Chicken Creek, British Columbia, Canada.
Horizon: *triangularis* conodont biozone, Pardonet Formation, lower Norian, Upper Triassic.
Data sources (for characters 196–199): ROM 41993 (holotype), TMP 94.380.11, TMP 94.382.2.
Missing data: 20.1%.

43. ***Hudsonelpidia brevirostris*** McGowan, 1995a
Locality: Brown Hill, Peace Reach, Williston Lake, British Columbia, Canada.
Horizon: *quadrata* conodont biozone, Pardonet Formation, lower Norian, Upper Triassic.
Data sources (for all characters): ROM 44629 (holotype); ROM 44633; McGowan (1995, 1997).
Missing data: 69.8%.

44. ***Macgowania janiceps*** McGowan, 1996

Locality: Jewitt Spur, Peace Reach, Williston Lake; Sikanni Chief River and Graham River, British Columbia, Canada.

Horizon: *multidentata* conodont biozone (type specimen only; horizon of origin of referred specimens was not recorded), Pardonet Formation, middle Norian, Upper Triassic.

Data sources (for all characters): ROM 41992 (holotype); ROM 41991; ROM uncatalogued; TMP 98.77.7; TMP 2009.121.1; McGowan (1991, 1996, 1997); Nicholls and Manabe (2004); Henderson (2015).

Missing data: 34.2%.

45. ***Gen. et sp. nov. B***

Locality: Pardonet Hill, Peace Reach, Williston Lake, British Columbia, Canada.

Horizon: *bidentata* conodont biozone, Pardonet Formation, upper Norian, Upper Triassic.

Data sources (for all characters): ROM 44295 (holotype); McGowan (1997); McGowan and Motani (2003).

Missing data: 66.3%.

46. ***Gen. et sp. nov. A***

Locality: Stockton, Warwickshire (holotype) and Lyme Regis, Dorset (referred specimen), England, United Kingdom.

Horizon: Rugby Limestone Member, upper Hettangian–lower Sinemurian (holotype); *angulata* biozone, Hettangian (referred specimen), Blue Lias Formation, Lias Group, Lower Jurassic.

Data sources (for all characters): NHMUK PV R3000 (holotype); ROM 28964.

Missing data: 59.8%.

47. ***Temnodontosaurus sp.*** Lydekker, 1888

Locality: Lyme Regis, Dorset and Whitby, Yorkshire, England, United Kingdom; Banz, Bavaria and Baden-Württemberg, Germany; Arlon, Belgium; Yonne, Millau, and Belmont areas, France.

Horizon: Hettangian–Toarcian, Lower Jurassic.

Data sources (for characters 196–199): NHMUK PV R1158, ROM 7972 (*T. platyodon*); SMNS 15950, SMNS 13128 (*T. trigonodon*).

Missing data: 2.5%.

48. ***Leptonectes tenuirostris*** (Conybeare, 1822)

Locality: Street, Somerset, England, United Kingdom.

Horizon: pre-*Planorbis* beds, lowermost Hettangian, Lower Jurassic.
Data sources (for all characters): NHMUK PV R498; NHMUK PV R2009; BGS 51236; OUMNH J.10305; OUMNH J.10319; McGowan (1974b), McGowan (1989).
Missing data: 14.1%.

49. ***Leptonectes solei*** McGowan, 1993
Locality: Stonebarrow, Charmouth, Dorset, England, United Kingdom.
Horizon: *stellare* subzone, *obtusum* zone, upper Sinemurian, Lower Jurassic.
Data sources (for all characters): photos of BRSMG Ce 9856 provided by Nick Pope; photos of MHN 96270 provided by Dylan Bastiaans; McGowan (1993).
Missing data: 51.3%.

50. ***Leptonectes moorei*** McGowan and Milner, 1999
Locality: Seatown, Dorset, England, United Kingdom.
Horizon: uppermost part of the Belemnite Marls, 1 m below the Belemnite Stone band, lower Pliensbachian, Lower Jurassic.
Data sources (for all characters): NHMUK PV R14370 (holotype); McGowan and Milner (1999).
Missing data: 46.7%.

51. ***Excalibosaurus costini*** McGowan, 1986
Locality: Lilstock and Watchet, Somerset, England, United Kingdom.
Horizon: Sinemurian, Lower Jurassic.
Data sources (for all characters): ROM 47697; McGowan (1986, 2003).
Missing data: 21.1%.

52. ***Eurhinosaurus longirostris*** (Mantell, 1851)
Locality: Banz, Bavaria and multiple localities in Baden-Württemberg, Germany; Whitby, Yorkshire, England, United Kingdom; Dudelange, Luxembourg; Staffelegg, Aargau, Switzerland; Pic-Saint-Loup (Montagne Noire), Noirefontaine (Franche-Comté), and Marcoux (Vocontian Basin), France.
Horizon: lower–middle Toarcian, Lower Jurassic.
Data sources (for all characters): SMNS 14931, SMNS R4085, NHMUK PV R5465, ROM 55094, Huene (1922); Hauff and Hauff (1981), Maisch and Matzke (2000a).
Missing data: 5.0%.

53. ***Suevoleviathan disinteger*** (Huene, 1926)

Locality: Holzmaden, Baden-Württemberg, Germany.

Horizon: *exaratum* subzone, *falcifer* zone, Lias epsilon II-6 (Steinplatte & Wolke), lower Toarcian, Lower Jurassic.

Data sources (for all characters): SMNS 15390 (holotype); Maisch (1998).

Missing data: 15.6%.

54. ***Ichthyosaurus sp.*** De la Beche and Conybeare, 1821

Locality: Street, Somerset and Lyme Regis, Dorset, UK; Lorraine, Belgium.

Horizon: Hettangian–Sinemurian, Lower Jurassic.

Data sources (for characters 196–199): NHMUK PV R8177, NHMUK PV R6697, NHMUK PV R49203, NHMUK PV R10021, NHMUK PV R15943.

Missing data: 0.5%.

55. ***Malawania anachronus*** Fischer et al., 2013

Locality: Chia Gara, Amaria, Kurdistan, Iraq.

Horizon: late Hauterivian–Barremian, Early Cretaceous.

Data sources (for all characters): NHMUK PV R6682 (holotype); Fischer et al. (2013).

Missing data: 74.9%.

56. ***Hauffiopteryx typicus*** Maisch, 2008

Locality: Holzmaden, Baden-Württemberg, Germany; Dudelange, Luxemburg; and Ilminster, Somerset, UK.

Horizon: Toarcian, Lower Jurassic.

Data sources (for all characters): SMNS 51552; SMNS 80225; SMNS 81965; SMNS 81367; SMNS 81962; Maisch, 2008; Caine and Benton, 2011; Marek et al., 2015.

Missing data: 6.5%.

57. ***Stenopterygius sp.*** Jaekel, 1904

Locality: Holzmaden, Baden-Württemberg and Dobbertin, Germany; Dudelange, Luxembourg.

Horizon: Toarcian, Lower Jurassic.

Data sources (for characters 196–199): NHMUK PV R33157, NHMUK PV R32681.

Missing data: 1%.

58. ***Aegirosaurus leptospondylus*** (Wagner, 1853)

Locality: Solnhofen and Eichstätt, Bavaria, Germany.

Horizon: Malm ζ2b, Solnhofen Formation, lowermost Tithonian, Upper Jurassic.
Data sources (for characters 196–199): SMNS 54607, Bardet and Fernández (2000).
Missing data: 27.6%.

59. ***Acamptonectes densus*** Fischer et al., 2012
Locality: Speeton and Filey, Yorkshire, England, UK; Cremlingen, Germany.
Horizon: Hauterivian, Lower Cretaceous.
Data sources (for characters 196–199): Fischer et al. (2012).
Missing data: 73.4%.

60. ***Maiaspondylus lindoei*** Maxwell and Caldwell, 2006
Locality: Hay River, Northwest Territories, Canada.
Horizon: Loon River Formation, Albian, Lower Cretaceous.
Data sources (for characters 196–199): Maxwell and Caldwell (2006).
Missing data: 79.9%.

61. ***Arthropterygius chrisorum*** (Russell, 1993)
Locality: Melville Island, Northwest Territories, Canada (type locality); Pampa Tril, Neuquén province, Argentina; Porozhsk village, Sosnogorsk District, Komi Republic, Russia.
Horizon: Oxfordian–Tithonian, Upper Jurassic.
Data sources (for characters 196–199): Maxwell (2010), Fernández and Maxwell (2012).
Missing data: 77.9%.

62. ***Athabascasaurus bitumineus*** Druckenmiller and Maxwell, 2010
Locality: Fort McMurray area, Alberta, Canada.
Horizon: Wabiskaw Member, Clearwater Formation, lowermost Albian, Lower Cretaceous.
Data sources (for characters 196–199): TMP 2000.29.01 (holotype), Druckenmiller and Maxwell (2010).
Missing data: 62.8%.

63. ***Sveltonectes insolitus*** Fischer et al., 2011b
Locality: upper Barremian, Lower Cretaceous.
Horizon: Ulyanovsk area, Ulyanovsk region, Russia.
Data sources (for characters 196–199): Fischer et al. (2011b).
Missing data: 32.7%.

64. ***Brachypterygius extremus*** (Boulenger, 1904)

Locality: Weymouth, Dorset and Stowbridge, Norfolk, England, United Kingdom.

Horizon: Kimmeridge Clay Formation, middle Kimmeridgian–lower Tithonian, Upper Jurassic.

Data sources (for characters 196–199): McGowan (1976), Kirton (1983).

Missing data: 57.3%.

65. ***Caypullisaurus bonapartei*** Fernández, 1997

Locality: Neuquén Basin (Neuquén and Mendoza Provinces), Argentina.

Horizon: Vaca Muerta Formation, lower Tithonian–lower Berriasian, Upper Jurassic–Lower Cretaceous.

Data sources (for characters 196–199): Fernández (2007).

Missing data: 39.7%.

66. ***Mollesaurus perialus*** Fernández, 1999

Locality: Chacaico Sur, Neuquén Basin, Argentina.

Horizon: *giebeli* biozone of the Los Molles Formation, lower Bajocian, Middle Jurassic.

Data sources (for characters 196–199): Fernández (1999).

Missing data: 80.9%.

67. ***Leninia stellans*** Fischer et al., 2014b

Locality: Kriushi, Sengiley district, Ulyanovsk Region, Russia.

Horizon: *volgensis* biozone, Lower Aptian, Lower Cretaceous.

Data sources (for characters 196–199): Fischer et al. (2014b).

Missing data: 82.9%.

68. ***Chacaicosaurus cayi*** Fernández, 1994

Locality: Chacaico Sur, Neuquén Basin, Argentina.

Horizon: *giebeli* subzone, *multiformis* zone of the Los Molles Formation, lower Bajocian, Middle Jurassic.

Data sources (for characters 196–199): Fernández (1994).

Missing data: 74.4%.

69. ***Platypterygius australis*** (McCoy, 1867)

Locality: Australia.

Horizon: Aptian–Cenomanian, Lower–Upper Cretaceous.

Data sources (for characters 196–199): Kear (2005).

Missing data: 12%.

70. ***Platypterygius americanus*** (Nace, 1939)
Locality: Crook County, Wyoming; Southern Saskatchewan, Canada.
Horizon: Albian–Cenomanian, Lower Cretaceous.
Data sources (for characters 196–199): TMP 72.06.01 (cast of holotype).
Missing data: 43.7%.

71. ***Cryopterygius kristiansenae*** Druckenmiller et al., 2012
Locality: Janusfjellet, Spitsbergen, Norway.
Horizon: *ilovaiskyi*–maximus biozones, Slottsmøya Member, Agardhfjellet Formation, Tithonian, Upper Jurassic.
Data sources (for characters 196–199): Druckenmiller et al. (2012).
Missing data: 34.2%.

72. ***Ophthalmosaurus icenicus*** Seeley, 1874
Locality: England, United Kingdom.
Horizon: Oxford Clay Formation, middle Callovian, Middle Jurassic and Kimmeridge Clay Formation, lower Kimmeridgian–lower Tithonian, Upper Jurassic.
Data sources (for characters 196–199): Andrews (1910), Appleby (1956), Moon and Kirton (2016).
Missing data: 3%.

73. ***Ophthalmosaurus natans*** (Marsh, 1879)
Locality: Wyoming, USA.
Horizon: Red Water Shale Member, Sundance Formation, upper Callovian–middle Oxfordian, Middle–Upper Jurassic.
Data sources: CM 878, CM 603.
Missing data: 27.1%.

74. ***Palvennia hoybergeti*** Druckenmiller et al., 2012
Locality: Janusfjellet, Spitsbergen, Norway.
Horizon: *ilovaiskyi*–maximus biozones, Slottsmøya Member, Agardhfjellet Formation, Tithonian, Upper Jurassic.
Data sources (for characters 196–199): Druckenmiller et al. (2012).
Missing data: 79.9%.

75. ***Sisteronia seeleyi*** Fischer et al., 2014c

Locality: Sisteron and Bevons, Vocontian Basin, France; Cambridgeshire, UK.

Horizon: Albian–Cenomanian, Upper Cretaceous.

Data sources (for characters 196–199): Fischer et al. (2014c).

Missing data: 89.4%.

APPENDIX 2

Character list used for the phylogenetic analysis. Characters 1–195 are the original characters of Jiang et al. (2016), characters 196–199 are new characters.

1. Premaxilla dorsal process: (0) long; (1) short (modified from Maisch and Matzke, 2000a:10).

2. Premaxilla ventral process: (0) long; (1) short (modified from Maisch and Matzke, 2000a:9).

3. Maxilla anterior process: (0) reduced; (1) extending anteriorly as far as nasal or further anteriorly (Fischer et al., 2011:7).

4. Maxilla dorsal lamina: (0) absent; (1) present (Motani, 1999a:2).

5. Maxilla prefrontal contact: (0) absent; (1) present (Maisch and Matzke, 2000a:12).

6. Maxilla external naris contact: (0) present; (1) absent (Motani, 1999a:3).

7. Maxilla longer than premaxilla: (0) true; (1) false.

8. External naris orientation: (0) lateral; (1) dorsal (Motani, 1999a:4).

9. Shallow groove anterior to the external naris: (0) absent; (1) present.

10. Narial shelf: (0) absent; (1) present (Jiang et al., 2006:4).

11. Nasal anteriorly extending beyond external naris: (0) false; (1) true.

12. Nasal parietal contact lateral to frontal: (0) absent; (1) present (Motani, 1999a:7).

13. Nasal postfrontal contact: (0) no contact; (1) contact extensive, posterior extension of nasal separates frontal from prefrontal in dorsal view; (2) eliminated by prefrontal medially extension (modified from Motani, 1999a:6).

14. Descending process of the nasal on the dorsal border of the nares: (0) absent; (1) present (Fernández, 2007:2).

15. Nasals rostrally reaching snout tip: (0) false; (1) true.

16. Processus narialis of prefrontal: (0) absent; (1) present (Fischer et al., 2011a:11).

17. Supraorbital crest on prefrontal and postfrontal: (0) absent; (1) present (Maisch and Matzke, 2000a:22).

18. Prefrontal–postfrontal contact: (0) absent; (1) present (Motani, 1999a:8).

19. Prefrontal exposure in upper temporal fenestra: (0) absent; (1) present.

20. Anterior orbital margin: (0) of regular rounded shape; (1) irregular (Maisch and Matzke, 2000a:23).

21. Postfrontal medially extension: (0) over the anteriormost margin of upper temporal fenestra; (1) not over the anteriormost margin of upper temporal fenestra.

22. Supratemporal antero-medial extension: (0) short; (1) long.

23. Supratemporal-postorbital contact: (0) absent; (1) present (Fischer et al., 2013:15).

24. Supratemporal/squamosal relative size: (0) equal or st smaller; (1) st clearly larger.

25. Sagittal eminence: (0) absent; (1) present but small, involving only the parietal; (2) present and large, involving the parietal, frontal and nasal (Motani, 1999a:16).

26. Frontal dorsal exposure: (0) clearly present; (1) nearly absent.

27. Frontal participation in upper temporal fenestra: (0) absent; (1) present.

28. Squamosal triangular shape: (0) false; (1) true; (2) squamosal absent (Fischer et al., 2013:16).

29. Squamosal participation in upper temporal fenestra: (0) present; (1) absent; (2) squamosal absent (Motani, 1999a:13).

30. Squamosal-quadrate articulation: (0) present; (1) absent.

31. Postorbital postero-dorsal corner: (0) narrow, giving triradiate shape; (1) broad and triangular; (2) absent or round.

32. Postorbital participation in upper temporal fenestra: (0) present; (1) absent (Motani, 1999a:12).

33. Jugal anterior margin: (0) tapering, between lacrimal and maxilla; (1) broad and fan-like, covering ma.

34. Jugal/quadratojugal lateral contact: (0) present; (1) absent (Motani, 1999a:23).

35. Lower temporal arch between jugal and quadratojugal: (0) present; (1) lost (Fisher et al., 2013:18).

36. Quadratojugal: (0) longer than tall; (1) taller than long.

37. Quadratojugal exposure: (0) quadratojugal small; (1) extensive; (2) small, largely covered by squamosal and postorbital (Fischer et al., 2013:17).

38. Parietal ridge: (0) absent; (1) present (Motani, 1999a:17).

39. Parietal supratemporal process: (0) short; (1) long (Motani, 1999a:18).

40. Parietals' anterior processes: (0) contacting each other anteriorly, eliminating frontal from pineal foramen; (1) narrowly separated anteriorly, forming parietal fork, and frontal dorsally visible along the pineal foramen; (2) widely open, resulting in absence of clear fork (Motani, 1999a:19).

41. Parietal-frontal suture inter-digitation: (0) absent; (1) present.

42. Anterior terrace of upper temporal fenestra: (0) absent; (1) present but small; (2) present and large (Motani, 1999a:14).

43. Basioccipital peg: (0) clearly present; (1) absent or extremely reduced (Motani, 1999a:29).

44. Basioccipital extracondylar area: (0) wide; (1) reduced to a narrow band of concavity (Motani, 1999a:30).

45. Basioccipital/atlas articulation convexity: (0) flat or anterior; (1) posterior.

46. Ventral notch in the extracondylar area of the basioccipital: (0) present; (1) absent (Fischer et al., 2012:19).

47. Pterygoid, transverse flange: (0) antero-lateral; (1) not well defined; (2) postero-lateral (Motani, 1999a:26).

48. Basipterygoid processes: (0) short, giving basisphenoid a square outline in dorsal view; (1) markedly expanded laterally, being wing-like, giving basisphenoid a marked pentagonal shape in dorsal view (Fischer et al., 2011:18).

49. Interpterygoid vacuity: (0) present; (1) absent or extremely reduced (Maisch and Matzke, 1997:22).

50. Ectopterygoid: (0) present; (1) absent (Callaway, 1989:9).

51. Shape of the paroccipital process of the opisthotic: (0) short and robust; (1) elongated and slender (Fischer et al., 2012:20).

52. Stapes proximal head: (0) slender, much smaller than opisthotic proximal head; (1) massive, as large or larger than opisthotic (Fischer et al., 2013:24).

53. Cheek orientation: (0) lateral; (1) posterior (Motani, 1999a:25).

54. Overbite: (0) absent or very slightly; (1) present (Motani, 1999a:33).

55. Prenarial snout longer than the postorbital skull: (0) false; (1) true.

56. Snout extremely slender: (0) no; (1) yes (Motani, 1999a:34).

57. Snout, constriction: (0) absent; (1) present.

58. Snout flattened: (0) false; (1) true.

59. Scleral ring extensively ossified, filling or almost filling the orbit: (0) false; (1) true.

60. Pineal foramen posterior to or between orbits: (0) posterior; (1) between.

61. Angular lateral exposure at its maximum depth: (0) semi-equal to surangular; (1) clearly shallower than surangular; (2) much deeper than surangular (Motani, 1999a:32).

62. Coronoid region: (0) slightly elevated or high; (1) flat (Jiang et al., 2006:13).

63. Root striations: (0) present; (1) absent (Fischer et al., 2013:4).

64. Plicidentine: (0) absent; (1) at least partly present (Motani, 1999a:36).

65. Bony fixation of teeth: (0) present; (1) absent (Motani, 1999a:43).

66. Tooth horizontal section: (0) circular; (1) disto-medially compressed; (2) lateral compressed (Motani, 1999a:37).

67. Tooth size relative to the skull width: (0) over 0.1; (1) below 0.05 (Motani, 1999a:39).

68. Dentigerous region in adult: (0) complete; (1) largely reduced; (2) edentulous.

69. Dental groove: (0) present throughout jaw margin; (1) only present anteriorly; (2) absent (Motani, 1999a:41, 42).

70. Anterior sockets: (0) present; (1) absent.

71. Maxilla multiple tooth row: (0) absent; (1) present (Motani, 1999a:40).

72. Dentary labial shelf: (0) present; (1) absent (Jiang et al., 2006: char14).

73. Posterior tooth crown: (0) conical; (1) rounded; (2) flat (Motani, 1999a:38).

74. Tooth crown surface of at least one maxillary tooth with mesiodistal ridge: (0) false; (1) true (Jiang et al., 2006:18).

75. Ossified sternum: (0) absent; (1) present (Motani, 1999a:50).

76. Ossified cleithrum: (0) present; (1) absent (Motani, 1999a:51).

77. Clavicle orientation at proximal end: (0) oblique to sagittal plane; (1) transverse.

78. Clavicle scapular process length distal to clavicular main body: (0) short; (1) long.

79. Interclavicle anterior process separating clavicles: (0) present; (1) absent.

80. Interclavicle posterior process: (0) rod-like; (1) triangular; (2) absent.

81. Scapular blade shaft: (0) absent; (1) present at least proximally (Motani, 1999a:47).

82. Scapula anterior flange: (0) complete; (1) emarginated; (2) absent (modified from Maisch and Matzke, 2000a:70).

83. Scapula antero-proximal extension toward clavicle: (0) absent; (1) present.

84. Prominent acromion process of scapula: (0) absent; (1) present (Fischer et al., 2011:28).

85. Scapula posterior extension: (0) present; (1) absent (modified from Maisch and Matzke, 2000a:71).

86. Scapular axis and glenoid facet orientations: (0) nearly parallel; (1) at 60 degrees or more (Motani, 1999a:48).

87. Coracoid facet on scapula: (0) fused scapulocoracoid; (1) absent; (2) equal or smaller than glenoid facet of scapula; (3) twice as large as glenoid facet (Motani, 1999a:49).

88. Coracoid parasagittal length vs. transverse width: (0) semi-equal or longer than wide; (1) clearly wider than long.

89. Coracoid foramen: (0) present; (1) absent.

90. Coracoid anterior notch or concavity: (0) absent; (1) present.

91. Coracoid posterior notch or concavity: (0) absent; (1) present.

92. Intercoracoid facet: (0) short, medial margin round shaped; (1) long, medial margin relatively straight (modified from Maisch and Matzke, 2000a:73).

93. Humerus anterior flange: (0) absent; (1) present and complete; (2) present but reduced proximally, leaving leading edge tuberosity (Callaway, 1989:29).

94. Plate-like dorsal ridge on humerus: (0) absent; (1) present (Motani, 1999a:56).

95. Protruding triangular deltopectoral crest on humerus: (0) present but small; (1) present and very large, bordered by concave areas (Fischer et al., 2013:39).

96. Humerus distal proximal width ratio: (0) nearly equal; (1) distal wider (Motani, 1999a:55).

97. Humerus with posterodistally deflected ulnar facet and distally facing radial facet: (0) ulnar facet contains convexity in lateral view; (1) absent; (2) present (modified from Fischer et al., 2013:42).

98. Humerus distal articular facets: (0) not terminal; (1) radial facet larger than ulna facet; (2) two facet nearly equal; (3) three facets (Motani, 1999a:52).

99. Humerus anterodistal facet for accessory zeugopodial element anterior to radius: (0) absent; (1) present (Fischer et al., 2013:41).

100. Humerus/intermedium contact: (0) absent; (1) present (Fernández, 2007:15).

101. Radius peripheral shaft: (0) complete or nearly complete; (1) notch or absent (modified from Motani, 1999a:59).

102. Radius contiguous shaft: (0) about half or more of radial length; (1) notch or absent (modified from Motani, 1999a:60).

103. Ulna peripheral shaft: (0) complete or nearly complete; (1) notch or absent (modified from Motani, 1999a:62).

104. Ulna contiguous shaft: (0) complete or nearly complete; (1) notch or absent (modified from Motani, 1999a:63).

105. Shape of the posterior surface of the ulna: (0) radius not discoidal; (1) rounded or straight and nearly as thick as the rest of the element; (2) concave with a thin, blade-like margin (Fischer et al., 2012:36).

106. Radius/ulna relative size: (0) nearly equal; (1) radius much larger than ulna; (2) ulna larger than radius (Motani, 1999a:64).

107. Radio-ulnar foramen: (0) present; (1) absent (Fischer et al., 2013:46).

108. Radiale, anterior notch: (0) absent; (1) present (Motani, 1999a:65).

109. Manual pisiform: (0) present; (1) absent (Motani, 1999a:67).

110. Manual pisiform 2 (neomorph): (0) absent; (1) present (Jiang et al., 2006:20).

111. Intermedium: (0) longer than wide; (1) as wide as long or wider than long (Jiang et al.,2006).

112. Proximal carpals: (0) packed; (1) small, round and separated.

113. Distal carpal 1: (0) ossified; (1) unossified; (2) absent.

114. Distal carpal 2: (0) ossified; (1) unossified; (2) absent.

115. Manual centralia: (0) present; (1) absent.

116. Metacarpal I peripheral shaft: (0) complete; (1) notch or largely reduced; (2) absent; (3) mc 1 not ossified (Motani, 1999a:68).

117. Metacarpal III shaft: (0) present; (1) absent (Motani, 1999a:69).

118. Metacarpal V: (0) present; (1) not ossified (Motani, 1999a:70).

119. Manual digit 2 distal elements peripheral shaft: (0) complete; (1) notch or absent; (Motani, 1999a:71).

120. Forelimb hyperphalangy with more than five phalanges ossified in longest digit: (0) absent; (1) present (Motani, 1999a:77).

121. Notching of anterior facet of leading edge elements of forefin in adults: (0) elements not discoidal; (1) present; (2) absent (Fischer et al., 2013:48).

122. First preaxial accessory digits on forelimb: (0) absent; (1) present (Maisch and Matzke, 2000a:91).

123. Postaxial accessory digit on forelimb: (0) absent; (1) only one; (2) more than one (Motani, 1999a:72).

124. Proximal manual phalanges proximo-distal packing: (0) well-packed; (1) not packed.

125. Manual digit between 4th and 5th digits: (0) absent; (1) present (Motani, 1999a:73).

126. Propodial + epipodial versus manus length: (0) propodial + epipodial longer; (1) manus longer (Motani, 1999a:58).

127. Forelimb/hindlimb ratio: (0) nearly equal or hind longer; (1) forelimb longer but less than twice as hindlimb; (2) forelimb longer twice as much as hindlimb (Motani, 1999a:79).

128. Zeugopodium flattened: (0) false; (1) true.

129. Manual anterior sesamoid: (0) absent; (1) present.

130. Second preaxial accessory digit of forelimb: (0) absent; (1) present.

131. Delayed mesopodial ossification: (0) present; (1) absent.

132. Forelimb hypophalangy with less than five digits ossified in longest digit: (0) absent; (1) present.

133. Carpus elongated, as long as the more distal forelimb part or longer: (0) false; (1) true.

134. Extra proximal carpal preaxially: (0) absent; (1) present.

135. Interdigital separation: (0) present; (1) absent (Motani, 1999a:78).

136. Iliac blade shape: (0) with thick shaft; (1) plate-like; (2) narrow and styloidal (Motani, 1999a:80).

137. Iliac antero-medial prominence: (0) absent; (1) present (Motani, 1999a:81).

138. Ilium-pubis relative proximo-distal length: (0) semi-equal; (1) ilium clearly shorter.

139. Pubis, styloidal or plate-like: (0) plate-like; (1) styloidal (Motani, 1999a:85).

140. Pubis obturator foramen: (0) completely enclosed in pubis; (1) mostly in pubis but open on one side; (2) part of obturator fossa (Motani, 1999a:84).

141. Pubis and ischium median symphysis: (0) present; (1) not well defined (modified from Maisch and Matzke, 2000a:108).

142. Pubis and ischium fused in adult: (0) complete; (1) absent; (2) present only medially; (3) present medially and distally (Motani, 1999a:83).

143. Pubis ischium relative size: (0) nearly equal or ischium slightly larger; (1) pubis twice as large as ischium (Motani, 1999a:86).

144. Ischium, styloidal or plate-like: (0) plate-like, longer sagittally than wide transversely; (1) plate-like, wider transversely than long sagittally; (2) styloidal (modified from Motani, 1999a:87).

145. Thyroid fenestra: (0) absent; (1) one median opening; (2) two openings, being medially separated (Motani, 1999a:82).

146. Femur strongly constricted medially, forming a slender shaft region, proximal width remarkably larger than medial width: (0) present; (1) absent.

147. Femur antero-distal expansion, forming a distinctive structure at the distal end: (0) absent; (1) present.

148. Prominent, ridge-like dorsal and ventral processes demarcated from the head of the femur and extending up to mid-shaft: (0) absent; (1) present (Fischer et al., 2011:46).

149. Wide distal femur blade: (0) absent, the proximal and distal extremity of the femur being sub-equal in dorsal view; (1) present (Fischer et al., 2013:61).

150. Femur distal facets: (0) two; (1) three (Maxwell, 2010:32).

151. Astragalus/femoral contact: (0) absent; (1) present (Maxwell, 2010:33).

152. Femur anterodistal facet for accessory zeugopodial element anterior to tibia: (0) absent; (1) present (Fischer et al., 2011:48).

153. Tibia contiguous shaft: (0) complete or nearly complete; (1) notch or absent (Motani, 1999:91).

154. Tibia peripheral shaft: (0) complete or nearly complete; (1) notch or absent (modified from Motani, 1999:92).

155. Tibia antero-proximal end nearly rectangular, forming a deep notch on the anterior margin: (0) absent; (1) present.

156. Fibula posterior extent: (0) not fixed, fibula being mobile relative to femur; (1) much posterior to femur; (2) about the same level as femur (Motani, 1999a:93).

157. Fibula contiguous margin: (0) concave; (1) nearly straight or convex.

158. Fibula posterior flange: (0) absent; (1) present.

159. Tibia and fibula: (0) in contact or closely placed with each other; (1) widely separated from each other (Motani, 1999a:88).

160. Spatium interosseum between tibia and fibula: (0) present; (1) absent (Fischer et al., 2013:64).

161. Hind fin leading edge element in adults: (0) elements not discoidal; (1) notched; (2) straight (Fischer et al., 2013:65).

162. Postaxial accessory digit in hind limb: (0) absent; (1) present (Fischer et al., 2011:50).

163. Pes digit 1: (0) present; (1) absent (Motani, 1999:89).

164. Distal tarsal 2 in line with distal tarsals 3 and 4: (0) true; (1) false, distal tarsal 2 in line with calcaneum.

165. Atlas/axis fusion: (0) absent; (1) present (Motani, 1999a:94).

166. Presacral count: (0) less than 30; (1) between 40-52; (2) 55 or more (Motani, 1999a:95).

167. Vertebra count between sacral and apical about: (0) tail stem not well defined; (1) 1/2 of the prepelvic count; (2) 2/3 of the prepelvic count or more.

168. Posterior dorsal centra shape: (0) cylindrical; (1) discoidal (Motani, 1999a:97).

169. Posterior dorsal/anterior caudal centra degree of shortening: (0) 3.5 times or less as high as long; (1) four times or more as high as long (Fischer et al., 2013:26).

170. Cervical bicipital rib facet: (0) absent; (1) present (Motani, 1999a:99).

171. Rib articulation in thoracic region: (0) predominantly unicapitate; (1) exclusively bicapitate (Maisch and Matzke, 2000a:53).

172. Antero-dorsal rib facets: (0) confluent with anterior facet in at least near pelvic girdle; (1) not confluent in any of the centra (Motani, 1999a:101).

173. Posterior-dorsal bicipital rib facet: (0) absent; (1) present, might be resulted from the split of diapophysis (Motani, 1999a:100).

174. Last caudal rib facet reaching the caudal peak area: (0) false; (1) true.

175. Rib mid-shaft broadening rostro-caudally: (0) absent; (1) present.

176. Sacral ribs: (0) at least two, distinguishable; (1) absent (Motani, 1999a:104).

177. Anterior dorsal neural spine: (0) normal; (1) narrow (Motani, 1999a:102).

178. Neural spines of atlas-axis: (0) functionally separate, never fused; (1) completely overlapping, may be fused (Druckenmiller and Maxwell, 2010:26).

179. Neural spine anticlination in tail: (0) absent; (1) present (Motani, 1999a: 103).

180. Dorsal neural arch, transverse process: (0) present; (1) absent.

181. Second dorsal segment on dorsal neural spines: (0) absent; (1) present.

182. Anterior dorsal neural spines with thickened central axis and rostral and caudal median ridges or flanges: (0) absent; (1) present.

183. Caudal peak with curved vertebral column, near anticlination of neural spine: (0) absent; (1) present (Motani, 1999:96).

184. Anterior caudal vertebral size about 1/2 of the largest dorsal vertebrae or less: (0) false; (1) true.

185. Mid-caudal vertebrae height change: (0) gradually decrease; (1) increase; (2) sudden decrease (Motani, 1999a:98).

186. Pre-flexural wedge-shaped centra: (0) absent; (1) present.

187. Tail: (0) as long or longer than the rest of the body; (1) distinctly shorter (modified from Maisch and Matzke, 2000a:65).

188. Lunate tailfin: (0) absent; (1) well developed lunate tailfin (modified from Maisch and Matzke, 2000a:66).

189. Chevrons in apical region: (0) present; (1) absent (Sander, 2000:72).

190. Fluke vertebrae, laterally flattened and packed: (0) absent; (1) present.

191. Posterior gastralia immediately craniad of pelvic girdle: (0) present; (1) absent (Motani, 1999a:105).

192. Flat gastral elements with caudad one outlying the craniad one: (0) absent; (1) present.

193. Dermal ossicle: (0) absent; (1) present.

194. Dermal armour above caudal vertebrae with hemal arches: (0) absent; (1) present.

195. Dermal armour above dorsal neural spines, first layer: (0) absent; (1) present.

196. Nasal crest in posterior part of the internasal suture: (0) absent, (1) present (NEW CHARACTER).

197. Mediolaterally broad groove bordered by two, anteroposteriorly elongate ridges (a medial one and a lateral one), in the lateral part of the anteromedial process of the postfrontal: (0) absent, (1) present (NEW CHARACTER).

198. Parietal plateau surrounding the pineal foramen laterally and dorsally: (0) absent, (1) present (NEW CHARACTER).

199. Dorsal orbital margin formed exclusively by the prefrontal, without a posterodorsal contribution from the frontal and/or postfrontal: (0) absent, (1) present (NEW CHARACTER).

APPENDIX 3

Character scores for the taxa used in the phylogenetic analysis.

Petrolacosaurus kansensis

000000000000000000000000000000000000000?00?0?00??000000?000?000000000000000000
0000000000000000000000000000000000000000000000000000000000000000000000000000000
0000000000000000000000000?00000000

Claudiosaurus germaini

000100010000??00000000?000000000?101001010??0?0?10??0000000000?000000?010001000000?
?0000000000?1000000000000001000000000000000000000000?0000100100000000000000000000
0000?0?00000?00000000?0?0000000000

Thadeosaurus colcanapi

??????0???0????????????110??00000000000
0000??00000000000000000000000000000000000000000001001000000000000000000?0000?00
00000?00000000?0?0?0000????

Hovasaurus boulei

?????????????????0??00?000000000??0?0000?0?01?1?0?0???0????0?0????????????100?100000000
00000001?00000000000000000000000000000000000000000011000000000000000000000000000
10?00000?0001000000?000000?0??

Wumengosaurus delicatomandibularis

0011001010000000000000???0000000001010000010??0?1?010?001010100??0??100?0110010001121
000201110000002000000000010011110000000000001000000000100011000000000000000000200??
100000??000000000000000?0000000000

Nanchangosaurus suni

0??100?????0010000??000?000000000?010?1000??????????0????1?0???????2??????????????????0
100?10?0?20?0000000????????????????????1????0????????????????????????????????1?0?00?0?000
??010?????????11010000

Eohupehsuchus brevicollis

01110010000000000?10100000000000001????0000??????????0?1001?0?0?????2????????00?000001
0?0000?10?0120000000000001000001000??000????1001?00000?0??????10010?000010000?????1?0?
0?01?0?0???10????????011110000

Hupehsuchus nanchangensis

01?1?0?00000000?0{01}?10???0?0?0??0???1?000?0??0?2?0???0010010000?????2????????00??00?
?0020000010?01200000000000100000100000000000111001000010000?10011001000010100002000
1000?00001?00001{01}0000?0?00111100?0

Parahupehsuchus longus

???1???????????????????????????????????
1??012000000000001000001000000100001100100010??????????10?000000001000000000?1?0??00??10
0?0?10????????01111????

Eretmorhipis carrolldongi

??
1??11200000000000000001000000100001110100100000 1?100110?00000001000000000?1?0??000?100?00100????0??01111????

Cartorhynchus lenticaprus

11010000001000100000000?00000?00?1010010?1????????0?0000101100?????2???1???1000000000????????20?011001010000010111 1????10000101110000101001???????1001?000001000020?0?0?0?00???100??100????????000000000

Sclerocormus parviceps

00111010001001100100111000000?000????01200??????????0000101100????????????01000000001 1??????????????????1?1???10111101001010010111000010100001110001001000000100002000?0200?0??0100101010000000011000000

Chaohusaurus geishanensis

??0???1???1??000?1?0??0????0??1?00010??????????????10111011111??110??1110?11???00?0002?????10?0110000000000101010110000000001?1000100????????????01?00???????020??????0?0??0??0?100????0????0000????

Chaohusaurus chaoxianensis

11010010001000000100000100000110000100000 10?0?1?01??10111011111??1100?011001111200000020110010?1110000000000010111101000000010111000100100001110011001000000100002000?1100000000000110010000??1000000000

Chaohusaurus zhangjiawanensis

???????????00????1??00??000?0??0?????000?1??0??????????1???1??????????????01?1??000000??????10?0110000000000?01?10??00??0?????????????00?00?100?10010?0000?00?0?????110?00?0?100?11001?0?????000000000

Utatsusaurus hataii

01110011001000000001100100001110011010100 1????0?11??00101011 11??011000010001010000000010111010000100000000000010001100000000000100100010000001001100100000010000000001100 0?000000?1100100000?100000???0

Grippia longirostris

011100?1001000?0000110110000 0?100110101 0?1????0?????0?101??111?10110001110?1????0000001011101000010000000000001000110000000000010010001000000100110010000001000000000 11000?000000?1100100000?100000???0

Gulosaurus helmi

00?1001100?0000000?10011000?1??0?????01001????0?????00101011?1?1??10??1?10??????00001 01011101?0?0100000000000000001000??0001???1001?001????????????????????????????????0010?0?0?0??100?????????00000000

Parvinatator wapitiensis

???1?0?000?????0?0?0??11???011100?1?????????????????????1?10?110?1?000?00100?????????????????????0100000000000000001100010000 0??10010001???000

Cymbospondylus piscosus

01110010001010000100010110101111000010110 1??0?2?11??00101011 10?10000?00000010???010000100010100001000010000??11?????0??????????1???????10000110011001000000100000????021101000?0?001100100000?1000001111

Cymbospondylus buchseri

??????????????????100????1??????10?????110???????????0?10?01110???00???????010???0100001?00?010?0010000100000??11????????000??1?1?0??????????????????????????????????????02?101000?0?0??100?????????00?0???1

Cymbospondylus nichollsi

0??100?0?0?01??00100?10110101111 0?00101111??0?2?11??0??0101110????????????0101????????00010??0??1?1000?0?0??100???????????0?01111

Xinminosaurus catactes

??????????????????????????????????0??????????????????????1??00?0?00?01?2001?0??000000?00010101000010000100000000010100001000001110010001100 0?1100110010000001000000000221010???000?110?10000001?0000????

Thalattoarchon saurophagis

???1???????01??0?100?10110101111 0?101011?1??0?2?????0??01011?0010200??00?0??10000?????10010?0??????????????101011???0??100?????????????1111

Mixosaurus panxianensis

11111010001000001100101120001 12?011?110102??????????0010101111??0?000001100111110000001011101001010010100000001100012000100000111001000110000011011001000000100000000?111010?1?011?1100101000010000000000

Mixosaurus cornalianus

11111010001000001100 1?1120??1121000?110102??1???11??0010101111??00100?0110011111000000010111010010100010000001100012000100000111001000110?000011011001000000100000000?111010011011?1100101000010000 0????

Mixosaurus kuhnschnyderi

1???1?1??01?????11?010??20??????1?00??101?2???????????01?101111???200000110?????1000000 1011?01001010?1010000?????00?????????????????1??0??00???1???????1????1?0???????

Phalarodon atavus

111110?0011000?0110010112000112100001101 02????2?11??0?101??1??110200{12}00?00?????1?00000??????1001?3000010000000010001200010000 0??1001???1??????????10?00??????00??000??1?1????????1?1???1???0?0?0????0000

Phalarodon fraasi

11?110?0011????111?01??????????2?????????????????????????1?1?1?1??1?20010002 1?1??????00???0????1?0101??0010?0?00100001????????0???10010001?0???011??00?????000100????00??????????0???11001??????1??0000000

Phalarodon callawayi

11111011011??00011?0??1120????2100011????2??????????0010101?1????0?0110021????????????
1?????????????????????????0?????????????????????????1???00011???0?1000000100000000???000???
??10?????????????????0000

Besanosaurus leptorhunchus

???11?1???1?????01?0????????????0?????????????????????01110???1?1?0?0??0100?????02000020
1110100001001111110101???????1?112????1?????????100011100110000000001000??????2?10100?
?010??100????0?0100000????

Guizhouichthyosaurus tangae

01110010{01}010100001000?01100011210??11??101??????????0010101111?1?0000001000111100
2000121111010000100111111101010201310112001011100100011000111001100000000010000101
0?2?1010?0?010?11001???0001?00000000

‘Callawayia’ wolonggangensis

011100101010100001?000011010112{01}00012011?1????2?1???001{01}101111?1?000000100????
?0????0??011101?0001001?11111?101????31011100101??????0?1?????????????????????????????
2?10?0?0?????????????????0???0000

Guanlingsaurus liangae

011110100010100001?000111010112{01}0????01001??????????0010101111?????2??????011????2
0001?1111?10000100111111101011201311102001010100111011000211001100000000010100101002
02110?00?1010?1100100000110000000000

Shastasaurus pacificus

????0?1???100???01?0000110100?2100?1101101?01?2011??0?1?????11?1?0????????011???120001
211111100001001 1?11111???0??1?????1??????1001????100011100110000000010000???0???101?
????1??????1????????????0000

Shonisaurus popularis

??????1?????1???????????1????????????????1???01???????00??????11?1?0?1200???????10120001211
1111000010010101100???????311111????111???????10?0111001100000000?10100??1??2?101??0?
010??10?1??????100000????

Shonisaurus sikanniensis

??????????1???0???111???0?12001?0?????0120?0???11
1?1000010010101 10???00000????01?0??????2?1010?0???0?
???????????10?0??????

Californosaurus perrini

??2000030110
?1000020010101001101???1????????1???1001???111002110011000000001100 00?????1210?01?10
10?1100112????1?0600????

Toretocnemus californicus

??????????????????????????????0?????????????????001?1?1?10?110?0010100?????????????0
011?0?1200101010011010201311111100001?10010001200001100101010001112000010 11???10?0?
1??1???1?0?????????????????

Qianichthyosaurus zhoui

1101001000100000001?0??1110?1111{01}0???2????0?01???????001010111001?0?0??0100011111??
2000??011011000120010101001101020131111101001110010001200001100101010000112000020 1
1?111010?11010?110011210?11000000000

Qianichthyosaurus xingyiensis

10?100?00??0000011?0??1??0??????0??????????????????????010101?1??????00?0?00???????20000?
0??0?10001100101010001 00????31111100001?????000120?011101?01010?00?120000?????111000
01?0?0?110010210?1?00000?000

Callawayia neoscapularis

11???01000101?0?01?00?01101?1121?????11101?01?2?????001010?111?1100000010001??????0?0
??1111010001100111011010010201 31?11100101110010001 20?021100110010001{01}1210001?10
022101000?0101?100?12?0??1?00000000

Hudsonelpidia brevirostris

??????????????????0?????????????????????????????????010?????0????????????????????????????
?2??1120011111000??10??131011?0100??10010001 21????10??10?10?0101???101?1???????????0?
1???0????????????00????

Macgowania janiceps

100100100010100011000001100?1121010111021 1??1???????00101011100??000??0100011010121
?10301111??00120011111001101020131011101001?10010001??????????????????????????????????
10???0?0??100??????????0000000

Gen. et sp. nov. B

??0112000 1??????????????????
?2??11?0011?1??01101020131?11101001110010001???121?012?1?10001112001010 10???????????
??????????????????????????

Gen. et sp. nov. A

10000110001?10000100000111 01?1210001210101????2001??0110101110011000010100?????????
????????2000120??
?0??1?0?????????????0000

Temnodontosaurus

10100110001110000110000111011121001111{01}1000010200100001010110101100001010001111
012?010301101{02}00112001111101010102013111110{01}0011100100012 0?121{12}0121101000
11021010101111210101?10101?10011210001?00000000

Leptonectes tenuirostris

10000?10001?110??10000?1?10?1121001??10110?01???????10111011011??0100100000111101210
103011??2001120011111000101020131011100{01}0111001000120012 1{23}022000100110021010
1011?1210?01?1010??10011210??1100000000

Leptonectes solei

??0???1???????0????0??????????????????????????01?????0??01110??????????????????????12??1??011
0120?11200111110 10?01020131?11?0?10?110010001200??11012100100011021010??1111?1010??
?0?0??100?1????????000????

Leptonectes moorei

10000010001??00?1100???????1112100111???????1???????1011?01?2?0??0??01010001111012111
030110?200112001111101010102013101120000 1?10010001?????????????????????????????1??????
???0??????????????????????0

Excalibosaurus costini

10000010001??00????0???????111210?????????001??????1111101?01????00101??011110121110
3011012001120011111011101020131111101001110010001 2????11???10010001102101 01?11?1210
?01?1010?110011210??110000???0

Eurhinosaurus longirostris

10000010001110001100 00?1?10111210011200100?0102?0?00111110110101101001010001111012
10103011012001120011111 01{01}001020131011{12}011011100100012001211012100100011021 0
10{01}01111210?011?010?110011210??1100000000

Suevoleviathan disinteger

10000010001010 00?1000011?00111210010110210?????????00101010110?0??0000?01000111??1210
1030???120?1120011111010?010201310112010111100100011101211012100100011021011111 1?1
21000101010??100112?0??1??0000000

Ichthyosaurus

10000110001020000110001 1000{12}212100112102100010200100001010111101100001010001111
012101030111100001200111 1010{01}010201310112011012100100012001 21{12}0221000000110
21001101111?101111101{01}1{01}1001121110110000000 0

Malawania anachronus

??1?????????????????????12??10?????
???0112001111101 0?0102013101110?001?10010001?????????????????????????????1??1???0??0?0
???0?????????????0????

Hauffiopteryx typicus

10000010001?2001110000?1?10111210011110 1?00010????00101110112 10?1010010100011110121
11030110120011200111110111010201310111000012100100012001212022100100011021011101111
12101111?010??10011211?11000000000

Stenopterygius

10000{01}10001{01}2000011000111001112100112102 10?0102001010010101111111000010100011
11101211103011010001120011111011001020131011 1000{01}1{01}12100100012011213022 10?0000
11021001101111211111110100{01}1{01}011211111100000000

Aegirosaurus leptospondylus

10000110001011011 1?00?01?0111121101?2???2?0???????????0111011201????00?0?0?00?1?0?????
??0100?01?113011111121000002013101121100111111000120?1213?1210?0000110210012111?12
1??????0?0??1001???11?1?00000?00

Acamptonectes densus

???0?????????1?????????????????????????0?????111?1??11?0?0?0????11?0??0????0??????121110201
10101012310??112?1?0????????????1???1??10???1?0?0?
??00??????1?????0????

Maiaspondylus lindoei

?10001?0???????????????????????0??????????????0??????????????01?0?00?0?00???????????????
??01?01301??111?1?00??????10?????0??????????1????????????????????????????????1??111?0????
?00?????????????????

Arthropterygius chrisorum

???110?0??????????????1????????????????????????0110
10100231011111010??1?????????21??????1???????????????100000?????????????1??111?1???????
?00??????1??????????

Athabascasaurus bituminous

1111?0?00010?0??11?00?01010011211??01002?0?11??????10??0?011??11??0?0?0?00???1????????
??20?121302210?????????????????11?10?????0?
00??00???????????000000

Sveltonectes insolitus

1?000110001011?111?0????001???2?1?1??01????11120???1?01010??0111?0?0??0?00?????012111
03011010110120011????100?10201310112110 01?110?0?01???12130121010000110210012111?121
0???1?0?0??1001?2???1????00????

Brachypterygius extremus

11100110?????1???1?0???1???????1111??????11111?1????0010101?0?1110000?0?00?????????1???
?????01?01301111110100?10201310112110 01?11010001???????????????????????????????1??????
?????1???????????00??????

Caypullisaurus bonapartei

00100{01}100?1??100???0??11???0?12???111??????1?????????010101101?????1?????????1101211
1030?1??0110131011111010101020131111212001?11110001??????????10100001102100121?11??
1??????0?0??100?????????00000000

Mollesaurus perialus

10?000?0????11?011?0???????0????1?112?????1110?10?010???????????1???00?0?00???1??????????
???1??10???1?0????
????????????????????

Leninia stellans

???00??0????11?111?00?01?00?111110???01110?110??????0???????1???????????????????????????
???
???????????????0000

Chacaicosaurus cayi

??????10????????????????????????????????1011???????011101??????????????????????????????
???1???2001111101110101013101110000 1?100?0?01???????????1?????????????????1????1???????
??????????????????????

Platypterygius australis

1011101000101100110010 1?10122?2110111102000111210101001010112011100001 0?00??????121
1103011012110131011111010001020131111212001?10111001???121302?1010101110110012{01}
1111?101111?0?00??001??11?1??00000000

Platypterygius americanus

101001100010?10011?0??0??0?22?21?0111??????????????10010101101?1??00010?00??????12111
0??????2110130011111010001020?31??????????10?1?001???121302?1011100????????????1??1011
?1?0?0???00???????????000000

Cryopterygius kristiansenae

1011001000???1?0?1?0????????????1011????????????????0010?01?20?1?000??0?000111?0121110
2011012?1022001111?010101020131011211001?10011?0120112120221010000110?10?1????1121?
11?1?010??100??2?1?1????00???0

Ophthalmosaurus icenicus

110001100010110011?0001100011121101021020011102{01}011100101011001110?0010?0001111
01211103011012110231011112010001020131011211001210011?0120112130221010000110210012
0111121{01}11111010{01}?10011211111?00000000

Ophthalmosaurus natans

110000100010110??1?0001?1001102110112?0200111?2101??00101011?011?0000?0?00011110121
11030110121?113101111?01?001020?310?????0???1??11001??????????10?11101102100120111??1
?11?1?0?01?100?????????0000000

Palvennia hoybergeti

??0?0?10??101?0??1?000??000????1??????020?1?11???????010101?0??1??00??0?00??????????????
?????????31???1???????????????
?????????????00????

Sisteronia seeleyi

??1???111?0??0????????????11?0??????0???????12011?????
????1??300???11??????????
??????????????????

APPENDIX 4

Time-calibration of cladogram depicted in Figure 5.7.

Time calibration was performed in R v. 3.5.0 using the packages ape v. 5.1 and strap v. 1.4 (Paradis et al., 2004; Bell and Lloyd, 2015). Taxon age ranges were taken from the relevant literature, to ammonite/conodont biozone level where possible, and converted into absolute ages based on Gradstein et al. (2012). The time-calibrated tree was created with the DatePhylo function of strap, with node ages calculated using the equal-age method of Brusatte et al. (2008). A root length of 10.5 Ma was used as this is the smallest age difference between *Macgowania janiceps* and its temporally nearest outgroup (*Qianichthyosaurus xingyiensis*, late Ladinian). The obtained time-scaled tree was then plotted against a geological timescale with the geoscalePhylo function of strap. The R code used is presented below.

```
#set working directory
setwd()
#upload packages
library(ape)
library(strap)
#import tree
tree<-read.nexus("tree.nex")
#import taxon ranges table
times<-read.table("ages.txt", row.names=1)
#calibrate tree
timeTree<-DatePhylo(tree, times, rlen=10.5, method="equal", add.terminal=FALSE)
#plot tree against time scale
geoscalePhylo(ladderize(timeTree), times, direction="rightwards", units=c("Period", "Epoch", "Age"), boxes ="Age", tick.scale="myr", cex.age=0.7, cex.ts=0.85, cex.tip=0.5, width=1.9, ts.col=TRUE, vers="ICS2013")
```